Angle Rigidity Graph Theory and Multi-agent Formations

Liangming Chen

university of groningen

The research described in this dissertation has been carried out at the Faculty of Science and Engineering, University of Groningen, The Netherlands.

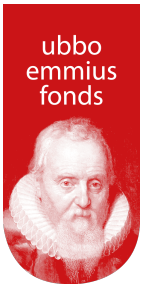

This work was supported by the Ubbo Emmius Scholarship.

Printed by Ipskamp Printing
Enschede, The Netherlands

university of groningen

Angle Rigidity Graph Theory and Multi-agent Formations

PhD thesis

to obtain the degree of PhD at the
University of Groningen
on the authority of the
Rector Magnificus, Prof. C. Wijmenga
and in accordance with
the decision by the College of Deans.

This thesis will be defended in public on

Friday 21 May 2021 at 9.00 hours

by

Liangming Chen

born on 22 April 1993
in Hunan, China

Supervisors
Prof. M. Cao
Prof. J.M.A. Scherpen

Assessment Committee
Prof. H.S. Ahn
Prof. C. De Persis
Prof. I. Shames

I would like to dedicate this thesis to my loving parents.

Acknowledgments

My journey in Groningen is coming to an end soon, which could not have been so memorable without the support and help from my colleagues, friends, and family. First, I would like to express my sincerest gratitude to my supervisor, Prof. Ming Cao, for giving me this opportunity to conduct the Ph.D. program in Groningen. I still remember that when I was first at his office discussing future research, he drew a geometric shape with many interior angles, which guides me to think deeper and deeper about formation control and finally comes to the contents of this thesis. I really appreciate his patient guidance, strict criticism and high standard on writing and publishing. I also wish to show my great thanks to him for the career suggestions and the numerous effects of revising papers and this thesis. Then, I want to thank my second supervisor Prof. Jacquelien M.A. Scherpen who provided a very pleasant and nice research environment for our group. I appreciate her reading and commenting on this thesis and providing support when I was looking for a postdoc position.

I would like to give my special thanks to Prof. Brian D. O. Anderson from Australia National University. I really appreciate the opportunities of talking with him and his help in many aspects. Sincere thanks to Prof. Chuanjiang Li from Harbin Institute of Technology who is always there when I meet some difficulty. I want to thank Dr. Hector G. de Marina, Dr. Zhiyong Sun and Dr. Qingkai Yang for many discussions about formation control problems. I also want to express my thanks for the helpful discussion with my collaborators Dr. Yuri Kapitanyuk, Dr. Xiaodong Cheng, and Dr. Mingming Shi.

My sincere thanks also go to all my dear colleagues. I gratefully thank Prof. Bayu Jayawardhana for our academic discussions, his delightful humor in our group activities, and his organization of the Nexus meetings. I would like to thank Dr. Ashish Cherukuri for the nice talking and travelling together to attend American Control Conference. Thank Prof. Claudio De Persis for the short time but very nice talking many times in the lunch time. I also want to thank Simon Busman

and Martin Stokroos for the experimental support in the development of robotic formation platforms. I am grateful to our secretary Frederika Fokkens for countless help in many aspects. Thanks also go to my officemates and all colleagues in DTPA, SMS, ODS, and SCAA groups.

Special thanks to my reading committee members, Prof. Hyo-Sung Ahn, Prof. Claudio De Persis, and Prof. Iman Shames, for spending time reading and commenting this thesis.

I thank Weijia Yao and Ningbo Li for being my paranymphs. Also, many thanks go to Nelson Chan for translating the summary of this thesis into Dutch and Matthijs de Jong for proofreading it. I also want to thank so many of my friends in Groningen and my life in Groningen could not have been so joyful without you. Last but not least, I would like to thank my parents for the endless love and support. I also thank my girlfriend for her support and care.

Liangming Chen
Groningen
27-01-2021

Contents

Chapter 1

Introduction

Motivated by the challenging formation control problem for a team of mobile vehicles in which each vehicle can only measure some of the angles towards its neighbors in its local coordinate frame, this thesis develops angle rigidity graph theory in both 2D and 3D. The angle rigidity graph theory is developed for a class of multi-point frameworks, called "angularity", consisting of a set of nodes embedded in a Euclidean space and a set of angle constraints among them. Here angle rigidity refers to the property specifying that under proper angle constraints, the angularity can only translate, rotate or scale as a whole when one or more of its nodes are perturbed locally. Using the developed angle rigidity theory, angle-only formation control algorithms are designed for the team of mobile vehicles to achieve a desired angle rigid formation, in which only local angle measurements[1] are needed for each vehicle. Before proceeding to the specific results, I will briefly introduce the background, problem statement and structure of this thesis.

1.1 Background

In this chapter, the background of multi-agent formation control is introduced, in order to motivate the need to develop angle rigidity graph theory and the corresponding angle-only formation control algorithms. The detailed literature review will be provided at the beginning of each chapter for the corresponding topics.

1.1.1 Multi-agent formation control

Multi-agent formation control has recently attracted great attention due to its broad applications in, e.g., search and rescue of unmanned aerial vehicles [35, 48, 78], deep-sea exploration of multiple autonomous underwater vehicles [69, 81], coordination of mobile robots [19, 74], and Earth observation of satellite formation flying [12, 53]. In Fig. 1.1, several application examples of multi-agent formations are provided, in which the agent represents robot, drone, autonomous underwater

[1] Also referred to as direction measurements or local bearing measurements in some literature.

vehicle and satellite, respectively. Generally speaking, multi-agent formation control aims at achieving a prescribed geometric shape for a group of agents [32, 80, 94]. The geometric shape, e.g., triangle, rectangle or polyhedron, can be described by a set of agent absolute positions, inter-agent relative positions, distances, bearings or triple-agent angles [3, 60, 86, 95].

(a) Robotic formation for object transportation

(b) Drone swarm for forest rescue[2]

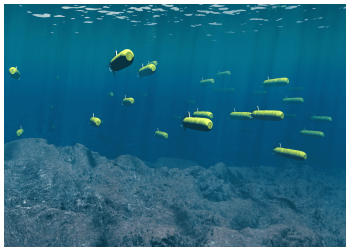

(c) AUV formation for deep-sea exploration[1]

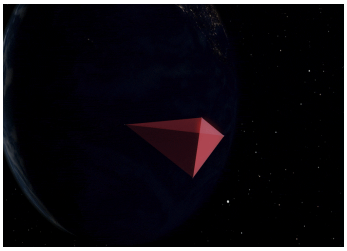

(d) Satellite formation flying for magnetic measurement[47]

Figure 1.1: *Applications of multi-agent formations*

To achieve the desired geometric shape for a group of agents, some researchers have proposed various formation control approaches towards the different combinations of formation shape descriptions and available sensing information [19, 20, 83, 84], see Table 1.1. It is worth mentioning that most of these approaches require

Property / Approach	Shape description	Measurement	Coordinate-dependence
Position-based	A	A	Yes
Displacement-based	R	R, A	Yes
Distance-based	D	D, R	No

In the table, A refers to absolution positions, R to relative positions and D to distances.

Table 1.1: *The comparison of several formation approaches.*

the measurements of absolute positions in a global coordinate frame, inter-agent distance or relative positions [19, 70]. However, the following two factors limit the

application of those formation control approaches into engineering practices.

(i) The common knowledge of a global coordinate frame is sometimes unavailable. For example, in Fig. 1.1(a),(b),(c),(d), the GPS receiver, as the main type of the provider of global positioning information, becomes imprecise or even unavailable in indoor space, forest, deep sea and deep space.

(ii) As a low-cost, lightweight and low-power sensor for ground, aerial and aerospace vehicles to achieve various sensing tasks, optical camera/sensor array/passive radar can easily produce bearing measurements but comparatively difficult to generate precise distance information [14, 33, 103, 104].

To tackle these limitations, a new formation control approach, bearing-only formation control, has been proposed in [101] which only relies on inter-agent bearing measurements. However, the proposed bearing-only formation control approach in [101] requires that all the agents have the same orientation of their coordinate frames, which is a coordinate-dependent property, as shown in Table 1.1. This is because the bearings used in [101] are vectors whose description always depends on a common coordinate frame orientation. However, it is technically hard to guarantee the perfect alignment of all agents' coordinate frames due to the existence of measurement noise and undesired measurement bias in sensors [59, 79, 82]. When a small degree of misalignment exists among agents' coordinate frames, it can be shown that a distorted formation shape and nonzero translational and scaling velocity can be generated, which may cause the formation to collide into one point or grow disproportionately in size. In other words, the formation described by relative positions or bearing vectors, can be sensitive to the misalignment of agents' coordinate frames [65, 105].

As a consequence, it is crucial to develop a new formation control approach which makes use of cheap and reliable angle measurements, while at the same time allowing the agents to have their own different orientations of coordinate frames. Even after the formation shape is described by bearings in $\mathrm{SE}(2)$ or $\mathrm{SE}(3)$, which allows the agents to have different orientations of frames, the corresponding formation control law may still not be robust against orientation bias in agents' coordinate frames because the description of each desired bearing in $\mathrm{SE}(2)$ or $\mathrm{SE}(3)$ still relies on a predetermined coordinate frame. We show that a promising way is to choose a set of interior angles to describe the desired formation shape, because an interior angle can be calculated through inter-agent bearings and is independent of the orientation of agent's coordinate frame. Thus, we propose to use triple-agent angles to describe the formation shape. The next natural question to address is how to properly choose angle constraints to construct the desired formation shape and develop a theoretical framework to check which geometric shapes can be uniquely determined by angle constraints. Towards this end, we propose angle rigidity to determine the uniqueness of the formation shape under angle constraints. It is worth noting that the formation shape in [52] is described by angles, in which,

however, the designed formation control algorithm still requires each agent to be able to sense the real-time relative positions with respect to its neighbors. Table 1.2 summarizes the differences between bearing-based and angle-based formation control approaches.

Property / Approach	Shape description	Measurement	Coordinate-dependence
Bearing-based	Bearing vectors	B [101], R [98]	Yes
Angle-based	Interior angles	A [22], R [52]	No

In the table, B refers to bearings, R to relative positions and A to angles.

Table 1.2: *The difference between bearing-based and angle-based formation control approaches.*

1.1.2 Rigidity graph theory

Rigidity graph theory has been studied for centuries, dating back to the works of Euler [76] and Cauchy [4], which is mainly used to describe the stiffness of a structure. Over the past decades, *distance rigidity* has been intensively investigated both as a mathematical topic in graph theory [43, 77] and an engineering problem in applications including formations of multi-agent systems [7], mechanical structures [49] and biological materials [67]. Distance rigidity [10] is defined for a framework based on the definition that when the only allowed smooth motions are those that preserve the distance between every pair of joints, the framework is said to be rigid. To determine whether a given framework is distance rigid, two methods have been reported. The first is to test the rank of the distance rigidity matrix which is derived from the infinitesimal distance rigid motions [9]. The second is enabled by Laman's theorem, which is a combinatorial test and works only for generic frameworks. More recently, *bearing rigidity* has been investigated, in which the shape of a framework is prescribed when inter-point bearing or direction constraints are satisfied [37, 101]. Here bearing is defined as a unit vector in a given global coordinate frame, and bearing rigidity can be defined accordingly [36, 101]. To check whether a framework is bearing rigid, conditions similar to those for distance rigidity have been discussed [15, 36, 101, 103]. Distance constraints in determining distance rigidity are in general quadratic in the associated end points' positions. While a bearing constraint is always linear in the associated end point's position, the description of bearings directly depends on the existence of a global coordinate frame or a coordinate frame in $\mathrm{SE}(2)$ or $\mathrm{SE}(3)$ [39, 68, 97].

Different from distance and bearing constraints, angle constraint is also one of the fundamental elements in discrete geometry [37]. It is of interest to describe a geometric shape using angle constraints, which is the main research subject in

angle rigidity theory. Note that graphs have been used dominantly in rigidity theory for multi-point frameworks under distance or bearing constraints since an edge of a graph can be naturally used to denote the existence of a distance or bearing constraint between the two points corresponding to the vertices associated with this edge [73]. However, when describing angles formed by rays connecting points, to use edges of a graph becomes inefficient because an angle constraint always involves three points. Thus, instead of using graphs that relate pairs of vertices as the main tool to define rigidity, we have to define a new combinatorial structure which is able to relate triples of vertices to develop the theory of angle rigidity. It is worth mentioning that in [52], by using the cosine of each triple-agent angle as the constraint, the planar angle rigidity has been defined, in which, however, flip and flex ambiguity exists. Since a globally rigid framework is of great importance in rigidity theory, it is crucial to define angle rigidity which may easily distinguish global rigidity from local rigidity.

Various fundamental results in distance rigidity have been developed by Euler [38], Cauchy [18], Alexandrov [5], Dehn [34], Henneberg [44], Laman [58], Connelly [25], Whiteley [93], and other researchers. Three seminal results are Cauchy's Arm Lemma [18], Henneberg's construction [45], and Laman's combinatorial condition [58]. Cauchy's Arm Lemma together with the related works by Liebmann [62], Alexandrov [5], Dehn [34] and Connelly [24], leads to the result that any convex triangulated polytope is distance rigid, see Fig. 1.2(a). Henneberg's construction approach can be efficiently used to generate or trim a distance rigid framework, see Fig. 1.2(b). Without using the embedding information, a generic and planar framework's distance rigidity can be checked by Laman's combinatorial condition, see Fig. 1.2(c). However, it is still an open question to find how these construction approaches or conditions work for a multi-point framework with angle constraints. Therefore, in this thesis, we will investigate these fundamental problems when the constraints among agents are given using triple-agent angles.

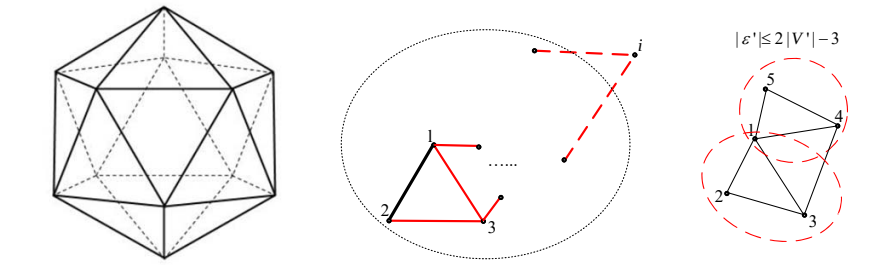

(a) Cauchy's Arm Lemma on convex polytope (b) Henneberg's construction (c) Lamman's condition

Figure 1.2: *Three seminal results in distance rigidity.*

Also note that the property of rigidity depends on its embedding space of the configuration. The necessary and sufficient condition of a generic framework's rigidity is closely related to the dimension d of the underlying embedding space [9]. For the necessary and sufficient condition of global rigidity, it has been proved that Hendrickson's conjecture is true for $d = 1, 2$ but false for $d \geqslant 3$ [26, 50]. Different from distance rigidity, bearing rigidity has been established by using bearing constraints which give direction information instead of range information [97, 101]. When all bearings are described in the coordinate frames with the same orientation, it has been shown that local bearing rigidity implies global bearing rigidity in an arbitrary dimension d [101]. Therefore, it is interesting to investigate the difference between 2D angle rigidity and 3D angle rigidity. Table 1.3 compares these three types of rigidity theory.

Rigidity / Property	Distance rigidity	Bearing rigidity	Angle rigidity
Constraints	distances	bearings	angles
Order of constraints as polynomials	quadratic	linear	quadratic or linear
Coordinate-dependence	no	yes	no
Global and local	different	same	different
Dimension invariance	no	yes	no

Table 1.3: *The comparison of three types of rigidity theory.*

1.2 Problem statement

The aim of this thesis is to address the following problems which have not been adequately investigated in the existing literature.

(i) Angle rigidity: Under which angle constraints, is a multi-point framework angle rigid or globally angle rigid? For a given multi-point framework with angle constraints, how to check whether it is angle rigid?

(ii) Formation stabilization: How to design an angle-only formation control law such that the desired angle rigid formation can be achieved, in which all agents are allowed to have different orientation of coordinate frames?

(iii) Formation maneuvering: How to design an angle-only formation maneuvering law such that all the agents can move collectively with the desired translating, rotating and scaling motions?

1.3 Outline and main contributions of this thesis

The main results of this thesis are split into two parts, which correspond to 2D and 3D cases respectively. Part I focuses on the problems given in Section 1.2 in 2D. Chapter 2 first answers the problem (i) in 2D. To describe the angle constraints, a new multi-point framework is defined, called "angularity". By defining signed angles, a sufficient condition for global angle rigidity is proposed in Chapter 2 based on the developed vertex addition operations. Later on, a necessary and sufficient condition is proposed for infinitesimal angle rigidity to check whether a given angularity is angle rigid.

Chapter 3 deals with the problem (ii) in 2D in which the agents are modeled by single-integrators or double-integrators. We show that by controlling each agent to move along the bisector of its measured interior angle, the desired angle rigid formation can be achieved without requiring the alignment of the agents' coordinate frames. In this chapter, the formula to calculate the dynamics of angle errors is explicitly derived.

The problem (iii) for the agents with single-integrator or double-integrator dynamics in 2D has been addressed in Chapter 4. By introducing a pair of mismatches into each desired angle, the collective motions in terms of translation, rotation and scaling are achieved by the proposed formation maneuvering law.

In Part II, Chapter 5 answers the problem (i) in 3D, in which the main difference of angle rigidity theory between 2D and 3D has been emphasized and the notion of angularity has been extended to 3D. Based on the angle constraints, the angle rigidity matrix in 3D have been defined. In addition, the merging of two 3D angle rigid angularities has been investigated and special attention has also been paid to angle rigidity of convex polyhedra. In Chapter 6, the problem (ii) in 3D has been investigated, in which another formation controller with a simpler form is proposed. Both the cases of sequential formations and convex polyhedral formations have been studied.

1.4 List of publications

Journal papers

[1] L. Chen, M. Cao, and C. Li. Angle rigidity and its usage to stabilize multiagent formations in 2-D. To appear in IEEE Transactions on Automatic Control, 2021, DOI: 10.1109/TAC.2020.3025539.

[2] L. Chen, H.G. De Marina, and M. Cao. Maneuvering formations of mobile agents using designed mismatched angles. To appear in IEEE Transactions on

Automatic Control, 2022, DOI: 10.1109/TAC.2021.3066388.

[3] L. Chen, and M. Cao. Angle rigidity for multiagent formations in 3-D. Submitted, 2021.

[4] L. Chen, M. Shi, H.G. De Marina, and M. Cao. Stabilizing and maneuvering angle rigid formations with double-integrator dynamics. Submitted, 2021.

Conference papers

[1] L. Chen, M. Cao, Z. Sun, B.D.O. Anderson, and C. Li. Angle-based formation shape control with velocity alignment, in Proceedings of the 21th IFAC World Congress, Berlin, Germany, 2020.

[2] L. Chen, M. Cao, C. Li, X. Cheng, and Y. Kapitanyuk. Multi-agent formation control using angle measurements, in Proceedings of American Control Conference, Philadelphia, USA, 2019, pp. 59-64.

[3] L. Chen, M. Cao, H.G. De Marina, and Y. Guo. Triangular formation maneuver using designed mismatched angles, in Proceedings of IEEE European Control Conference, Naples, Italy , 2019, pp. 1544-1549.

[4] L. Chen, M. Cao, B. Jayawardhana, Q. Yang, C. Li. Stabilizing a mobile agent under two angle constraints, in Proceedings of IEEE International Conference on Control and Automation, Edinburgh, Scotland, 2019, pp. 758-763.

[5] Y. Lin, M. Cao, Z. Lin, Q. Yang, L. Chen. Global stabilization for triangular formations under mixed distance and bearing constraints, in Proceedings of IEEE International Conference on Control and Automation, Edinburgh, Scotland, 2019, pp. 1545-1550.

Part I

Angle rigidity and formation control in 2D

Chapter 2

Angle rigidity in 2D

In this chapter, we develop the notion of "angle rigidity" for a multi-point framework, called "angularity", consisting of a set of nodes embedded in a Euclidean space and a set of angle constraints among them. Different from bearings or angles defined in a global frame, the angles we use do not rely on the knowledge of a global frame and have positive signs in the counterclockwise direction. Here *angle rigidity* refers to the property specifying that under proper angle constraints, the angularity can only translate, rotate or scale as a whole when one or more of its nodes are perturbed locally. We first demonstrate that this angle rigidity property, in sharp comparison to bearing rigidity or other reported rigidity related to angles of frameworks in the literature, is *not* a global property since an angle rigid angularity may allow flex ambiguity. We then construct necessary and sufficient conditions for *infinitesimal* angle rigidity by checking the rank of an angularity's rigidity matrix. We develop a combinatorial necessary condition for infinitesimal minimal angle rigidity. These results will be used as a theoretical foundation for the formation control task.

2.1 Introduction

Distance constraints in determining distance rigidity are in general quadratic in the associated end points' positions. While a bearing constraint is always linear in the associated end point's position, the description of bearings directly depends on the availability of a global coordinate frame or a coordinate frame in $\mathrm{SE}(2)$ or $\mathrm{SE}(3)$ [68, 97]. Different from distance or bearing rigidity, in this chapter we aim at presenting *angle rigidity* theory for multi-point frameworks with angle constraints as either linear or quadratic constraints on the end points' positions without relying on a global coordinate frame. Different from the usual definition for an angle [52, 88], the angle defined in this thesis has signs, for which we take the counterclockwise direction to be each angle's positive direction. Angle rigidity is defined for an *angularity* which consists of vertices and angle constraints among them. We show that the planar angle rigidity is a local property because of the existence of flex ambiguity. To check whether an angularity is angle rigid, angle rigidity matrix is derived based on the infinitesimally angle rigid motions. Then,

the angle rigidity of an angularity can be determined by testing the rank of its angle rigidity matrix. Also, we develop a combinatorial necessary condition to test the angle rigidity of an angularity. We underline that the Laman's theorem and Henneberg's construction method do not apply directly to angle rigidity, which makes our results important. Using the defined signed angles, we further propose the construction methods for angle rigid and globally angle rigid angularities.

2.2 Angularity and its angle rigidity

Graphs have been used dominantly in rigidity theory for multi-point frameworks under distance constraints since an edge of a graph can be naturally used to denote the existence of a distance constraint between the two points corresponding to the vertices associated with this edge. However, when describing angles formed by rays connecting points, to use edges of a graph becomes cumbersome and even illogical because an angle constraint always involves three points. For this reason, instead of using graphs that relate pairs of vertices as the main tool to define rigidity, we define a new combinatorial structure "angularity" that relates triples of vertices to develop the theory of angle rigidity. In all the following discussions we confine ourselves to the plane.

2.2.1 Angularity

We use the vertex set $\mathcal{V} = \{1, 2, \cdots, N\}$ to denote the set of indices of the $N \geqslant 3$ points of a framework in the plane. As shown in Fig. 2.1, to describe the *signed* angle from the ray j-i to ray j-k, one needs to use the ordered triplet (i, j, k), and obviously the two angles corresponding to (i, j, k) and (k, j, i) are different, and in fact are called explementary or conjugate angles. Here, following convention, the angle $\measuredangle ijk$ for each triplet (i, j, k) is measured counterclockwise in the range $[0, 2\pi)$. We use $\mathcal{A} \subset \mathcal{V} \times \mathcal{V} \times \mathcal{V} = \{(i, j, k), i, j, k \in \mathcal{V}, i \neq j \neq k\}$ to denote the *angle set*, each element of which is an ordered triplet. We denote the number of elements $|\mathcal{A}|$ of the angle set $\mathcal{A}$ by M. Throughout this chapter, we assume that no pair of triplets in $\mathcal{A}$ are explementary to each other. Now consider the embedding of the vertex set $\mathcal{V}$ in the plane $\mathbb{R}^2$ through which each vertex i is associated with a distinct position $p_i \in \mathbb{R}^2$ and let $p = [p_1^{\mathrm{T}}, \cdots, p_N^{\mathrm{T}}]^{\mathrm{T}} \in \mathbb{R}^{2N}$. We assume there is no overlapping points in p, i.e., $p_i \neq p_j$ for $i \neq j$ and $i, j = 1, 2, \cdots, N$. Then the combination of the vertex set $\mathcal{V}$, the angle set $\mathcal{A}$ and the position vector p is called an *angularity*, which we denote by $\mathbb{A}(\mathcal{V}, \mathcal{A}, p)$. In fact, given non-overlapping

positions p_i, p_j, p_k, the angle $\measuredangle ijk \in [0, 2\pi)$ can be uniquely calculated by

$$\measuredangle ijk = \begin{cases} \arccos(z_{ji}^{\mathsf{T}} z_{jk}) & \text{if } z_{ji}^{\perp} \cdot z_{jk} \geqslant 0, \\ 2\pi - \arccos(z_{ji}^{\mathsf{T}} z_{jk}) & \text{otherwise,} \end{cases} \tag{2.1}$$

where $z_{ji} = \frac{p_i - p_j}{\|p_i - p_j\|}$, $z_{jk} = \frac{p_k - p_j}{\|p_k - p_j\|}$, $z_{ji}^{\perp} = Q_0 z_{ji} = \begin{bmatrix} 0 & -1 \\ 1 & 0 \end{bmatrix} z_{ji}$ is the vector obtained by rotating z_{ji} counterclockwise by $\frac{\pi}{2}$, and $\cdot$ denotes the dot product.

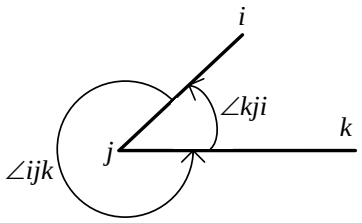

Figure 2.1: *Signed angle used in defining angle rigidity.*

2.2.2 Angle rigidity

We first define what we mean by two equivalent or congruent angularities.

Definition 2.1 (Equivalency and congruency)**.** *We say two angularities $\mathbb{A}(\mathcal{V}, \mathcal{A}, p)$ and $\mathbb{A}'(\mathcal{V}, \mathcal{A}, p')$ with the same $\mathcal{V}$ and $\mathcal{A}$ are* equivalent *if*

$$\measuredangle ijk(p_i, p_j, p_k) = \measuredangle ijk(p'_i, p'_j, p'_k) \text{ for all } (i, j, k) \in \mathcal{A}. \tag{2.2}$$

We say they are congruent *if*

$$\measuredangle ijk(p_i, p_j, p_k) = \measuredangle ijk(p'_i, p'_j, p'_k) \text{ for all } i, j, k \in \mathcal{V}. \tag{2.3}$$

From the equivalent and congruent relationships, it is easy to define global angle rigidity.

Definition 2.2 (Global angle rigidity)**.** *An angularity $\mathbb{A}(\mathcal{V}, \mathcal{A}, p)$ is* globally angle rigid *if every angularity that is equivalent to it is also congruent to it.*

When such a rigidity property holds only locally, one has angle rigidity.

Definition 2.3 (Angle rigidity)**.** *An angularity $\mathbb{A}(\mathcal{V}, \mathcal{A}, p)$ is angle rigid if there exists an $\epsilon > 0$ such that every angularity $\mathbb{A}'(\mathcal{V}, \mathcal{A}, p')$ that is equivalent to it and satisfies $\|p' - p\| < \epsilon$, is congruent to it.*

Definition 2.3 implies that every configuration which is sufficiently close to p and satisfies all the angle constraints formed by $\mathcal{A}$, has the same magnitudes of the angles formed by any three vertices in $\mathcal{V}$ as the original configuration at p.

As is clear from Definitions 2.2 and 2.3, global angle rigidity always implies angle rigidity. A natural question to ask is whether angle rigidity also implies global angle rigidity. In fact, for bearing rigidity, it has been shown that indeed global bearing rigidity and bearing rigidity are equivalent [36, 101]. However, this is *not* the case for angle rigidity.

Theorem 2.4 (Non-equivalence between angle rigidity and global angle rigidity)**.** *An angle rigid angularity $\mathbb{A}(\mathcal{V}, \mathcal{A}, p)$ is not necessarily globally angle rigid.*

We prove this theorem by providing the following example. Fig. 2.2 shows an an-

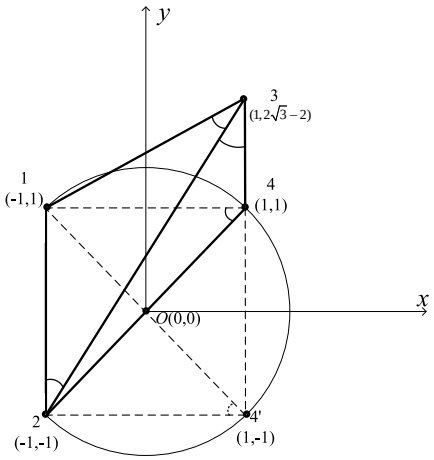

Figure 2.2: *Flex ambiguity in angle rigid angularity*

gularity with $\mathcal{V} = \{1, 2, 3, 4\}$, and its elements in the set $\mathcal{A} = \{(3, 2, 1), (1, 3, 2), (2, 3, 4), (1, 4, 2)\}$ take the values

$$\measuredangle 321 = \arccos\left(\frac{4\sqrt{3} - 2}{2\sqrt{17 - 4\sqrt{3}}}\right) \approx 39.07^\circ, \tag{2.4}$$

$$\measuredangle 132 = \arccos\left(\frac{19 - 8\sqrt{3}}{\sqrt{25 - 12\sqrt{3}}\sqrt{17 - 4\sqrt{3}}}\right) \approx 37.88^\circ, \tag{2.5}$$

$$\measuredangle 234 = 30^\circ, \tag{2.6}$$

$$\measuredangle 142 = 45^\circ, \tag{2.7}$$

and its p is shown as in the coordinates of the vertices. We first show $\mathbb{A}(\mathcal{V}, \mathcal{A}, p)$ is angle rigid, then show $\mathbb{A}(\mathcal{V}, \mathcal{A}, p)$ is not globally angle rigid.

Now first look at the triangle formed by 1, 2 and 3. Since two of its angles $\measuredangle 321$ and $\measuredangle 132$ have been constrained, the remaining $\measuredangle 213$ is uniquely determined to be $\pi - \measuredangle 321 - \measuredangle 132$ no matter how p is locally perturbed. The constraint on $\measuredangle 234$ requires 4 must lie in the ray starting from 3 and rotating from the ray 32 counterclockwise by $30°$; at the same time, the constraint on $\measuredangle 142$ requires 4 must lie on the arc passing through 1 and 2 such that the inscribed angle $\measuredangle 142$ is $45°$. No matter how p is locally perturbed there is only one unique position for 4 in the neighborhood of its current given coordinates because the two intersection points between the ray and the arc are not in the same local neighborhood. This local uniqueness implies that this four-vertex angularity is angle rigid (when 4's position is uniquely determined, any angle associated with it is also uniquely determined).

Now we show $\mathbb{A}(\mathcal{V}, \mathcal{A}, p)$ is not globally angle rigid. Note that there is the other intersection point $4'$ as shown in Fig. 2.2 satisfying the angle constraints given in $\mathcal{A}$, which implies that this angularity is not globally angle rigid because $\mathbb{A}'(\mathcal{V}, \mathcal{A}, p')$ is equivalent to $\mathbb{A}(\mathcal{V}, \mathcal{A}, p)$, but they are not congruent.

We provide the following further insight to explain this sharp difference between the angle rigidity that we have defined and the bearing rigidity that has been reported in the literature. Bearing rigidity as defined in [36, 101] is a global property because the bearing constraints always represent linear constraints in the end point's position (similar to the angle constraint $\measuredangle 234 = 30°$ in the form of the ray from 3 to 4 in the above example) and two non-collinear rays have at most one intersection. In contrast, our angle constraints can be either linear constraint in p when it requires the corresponding vertex to be on a ray or quadratic in p when it restricts the corresponding vertex to be on an arc passing through other vertices. The possible nonlinearity in the angle constraints gives rise to potential ambiguity of the vertices' positions under the given angle constraints.

Note that the embedding of p in the plane may affect the rigidity of $\mathbb{A}$. Consider the 3-vertex angularity as embedded in the following three different situations when its angle set $\mathcal{A}$ contains only one element $(2, 1, 3)$. Fig. 2.3(a) shows that 1,

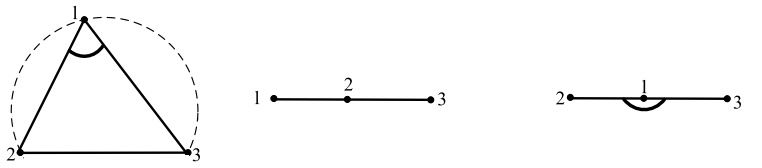

(a) Not rigid when $\measuredangle 213 = \frac{\pi}{3}$ (b) Angle rigid when $\measuredangle 213 = 0$ (c) Globally angle rigid when $\measuredangle 213 = \pi$

Figure 2.3: *Non-generic p changes rigidity*

2, 3 are not collinear, and then this angularity is in general not rigid since if we perturb point 1 in an arc with 2 and 3 as the arc's ending points, $\measuredangle 213$ can be the same while angles $\measuredangle 123$ and $\measuredangle 132$ change. In Fig. 2.3(b), 1, 2, 3 are collinear and 1 is on one side; in this case if the angle constraint happens to be $\measuredangle 213 = 0$, then one can check the angularity becomes angle rigid, although it is not globally rigid since the angle of $\measuredangle 132$ changes by 180 degree if we swap 2 and 3. In Fig. 2.3(c), 1, 2, 3 are collinear and 1 is in the middle, when the constraint becomes $\measuredangle 213 = \pi$, one can check that the angularity is not only rigid, but also globally rigid (swapping of 2 and 3 in this case does not change the resulting angles $\measuredangle 132, \measuredangle 123$ being zero). So the angularity $\mathbb{A}(\{1,2,3\},\{(2,1,3)\},p)$ is generically not rigid, but rarely rigid depending on p. To clearly describe this relationship between angle rigidity and p, like in standard rigidity theory, we define what we mean by generic positions.

Definition 2.5 (Generic position)**.** *The position vector p is said to be* generic *if its components are algebraically independent [28]. Then we say an angularity is* generically (resp. globally) angle rigid *if its p is generic and it is (resp. globally) angle rigid.*

An example for non-generic positions is the case when three points are collinearly positioned. Note that angle rigidity for $\mathbb{A}(\mathcal{V},\mathcal{A},p)$ with generic p represents the common property of the combination $(\mathcal{V},\mathcal{A})$ from a topological perspective, which is also referred to as *generic angle rigidity*. For convenience, we also say an angularity is generic if its p is generic. Now we provide some sufficient conditions for an angularity to be globally angle rigid. Towards this end, we need to introduce some concepts and operations. For two angularities $\mathbb{A}(\mathcal{V},\mathcal{A},p)$ and $\mathbb{A}'(\mathcal{V}',\mathcal{A}',p')$, we say $\mathbb{A}$ is a *sub-angularity* of $\mathbb{A}'$ if $\mathcal{V}\subset\mathcal{V}'$, $\mathcal{A}\subset\mathcal{A}'$ and p is the corresponding sub-vector of p'. We first clarify that for the smallest angularities, namely those contains only three vertices, there is no gap between global and local angle rigidity assuming generic positions.

Lemma 2.6. *For a 3-vertex angularity, if it is generically angle rigid, it is also generically globally angle rigid.*

Proof. For this 3-vertex angularity $\mathbb{A}(\mathcal{V},\mathcal{A},p)$, since it is angle rigid and p is generic, $\mathcal{A}$ must contain at least two elements, or said differently, two of the interior angles of the triangle formed by the three vertices are constrained. Again since p is generic, the sum of the three interior angles in this triangle has to be π, and thus the magnitude of this triangle's remaining interior angle is uniquely determined too. Therefore, $\mathbb{A}$ is generically globally angle rigid. □

Now, we define linear and quadratic constraints.

Definition 2.7 (Linear and quadratic constraints)**.** *For a given angularity $\mathbb{A}(\mathcal{V},\mathcal{A},p)$, a new vertex i positioned at p_i is* linearly constrained *with respect to $\mathbb{A}$ if there is*

$j \in \mathcal{V}$ such that $p_i \neq p_j$ and p_i is constrained to be on a ray starting from p_j; we also say i is quadratically constrained *with respect to $\mathbb{A}$ if there are $j, k \in \mathcal{V}$ such that $\{p_i, p_j, p_k\}$ is generic and p_i is constrained to be on an arc with p_j and p_k being the arc's two ending points. Correspondingly, we call i's constraint in the former case a* linear constraint *and in the latter case a* quadratic constraint *with respect to $\mathbb{A}$.*

As shown in Fig. 2.2, $\angle 234 = 30°$ is a linear constraint for the end vertex 4 since p_4 is constrained to be on a ray starting from p_3 and rotating from the ray 32 counterclockwise by $30°$, while $\angle 142 = 45°$ is a quadratic constraint for 4 because p_4 is constrained to be on the major arc $\overset{\frown}{12}$.

Similar to Henneberg's construction in distance rigidity, in the following we define two types of vertex addition operations to demonstrate how a bigger angularity might grow from a smaller one, which are shown in Fig. 2.4.

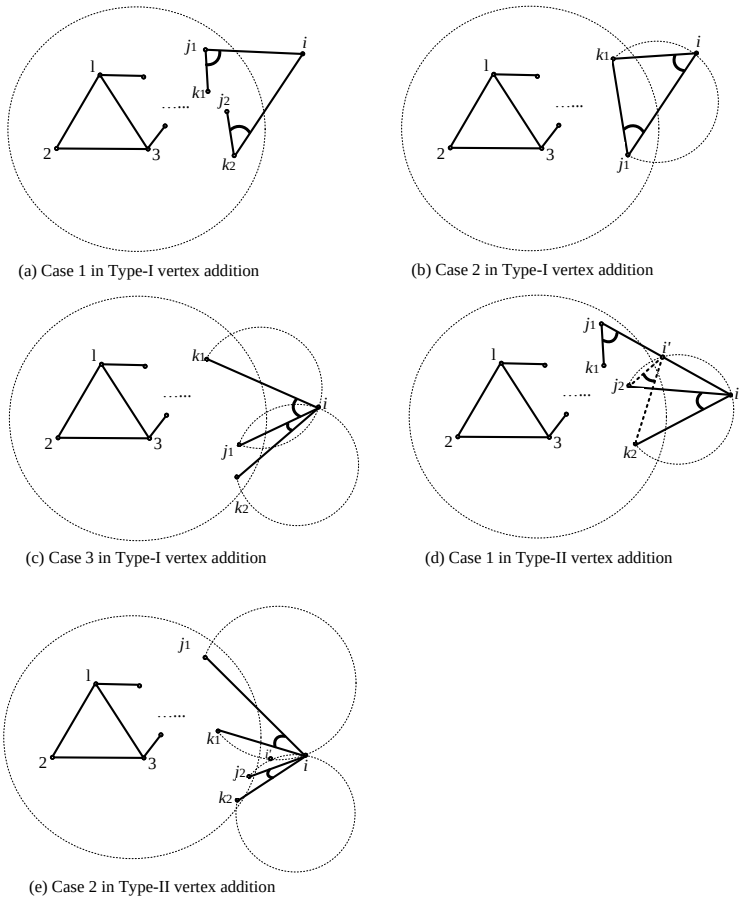

(a) Case 1 in Type-I vertex addition

(b) Case 2 in Type-I vertex addition

(c) Case 3 in Type-I vertex addition

(d) Case 1 in Type-II vertex addition

(e) Case 2 in Type-II vertex addition

Figure 2.4: *Type-I vertex addition and Type-II vertex addition*

Definition 2.8 (Type-I vertex addition)**.** *For a given angularity $\mathbb{A}(\mathcal{V}, \mathcal{A}, p)$, we say the angularity $\mathbb{A}'$ with the augmented vertex set $\{\mathcal{V} \cup \{i\}\}$ is obtained from $\mathbb{A}$ through a* Type-I vertex addition *if the new vertex i's constraints with respect to $\mathbb{A}$ contain at least one of the following:*

Case 1) two linear constraints, not aligned, associated with two distinct vertices in $\mathcal{V}$ (one vertex for one constraint and the other vertex for the other constraint);

Case 2) one linear constraint and one quadratic constraint associated with two distinct vertices in $\mathcal{V}$ (one for the former and both for the latter);

Case 3) two quadratic constraints associated with three vertices in $\mathcal{V}$ (two for each and one is shared by both), and the positions of i and these three vertices are generic.

Definition 2.9 (Type-II vertex addition)**.** *For a given angularity $\mathbb{A}(\mathcal{V}, \mathcal{A}, p)$, we say the angularity $\mathbb{A}'$ with the augmented vertex set $\{\mathcal{V} \cup \{i\}\}$ is obtained from $\mathbb{A}$ through a* Type-II vertex addition *if the new vertex i's constraints with respect to $\mathbb{A}$ contain at least one of the following:*

Case 1) one linear constraint and one quadratic constraint associated with three distinct vertices in $\mathcal{V}$ (one for the former and the other two for the latter);

Case 2) two different quadratic constraints associated with four vertices in $\mathcal{V}$ (two for the former and the other two for the latter), and the positions of i and these four vertices are generic.

Remark 2.10. Although the types of constraints are similar between Case 2 of Definition 2.8 and Case 1 of Definition 2.9, the numbers of vertices involved in Case 2 of Definition 2.8 and Case 1 of Definition 2.9 differ in these two types of vertex addition operations. Similarly, those in Case 3 of Definition 2.8 and Case 2 of Definition 2.9 are also different.

Remark 2.11. Note that in these two vertex addition operations, the involved vertices are required to be in generic positions. However, the overall angle rigid angularity $\mathbb{A}'$ constructed through a sequence of vertex addition operations is *not* necessarily generic, and an example is given in Fig. 2.5.

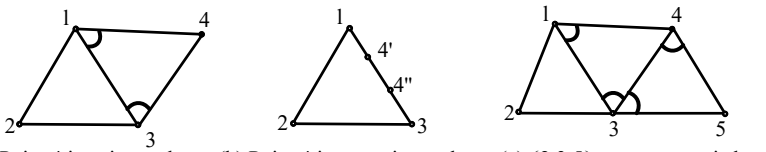

(a) Point 4 is unique when {1,3,4} are generic (b) Point 4 is not unique when {1,3,4} are not generic (c) {2,3,5} are not generic but the angularity is rigid

Figure 2.5: *The overall angularity is not necessarily generic*

Now we are ready to present a sufficient condition for global angle rigidity using Type-I vertex addition.

Proposition 2.12 (Sufficient condition for global angle rigidity)**.** *An angularity is globally angle rigid if it can be obtained through a sequence of Type-I vertex additions from a generically angle rigid 3-vertex angularity.*

Proof. According to Lemma 2.6, the generically angle rigid 3-vertex angularity is globally angle rigid. Consider the three conditions in the Type-I vertex addition. If 1) applies, then the position p_i of the newly added vertex i is unique since two rays, not aligned, starting from two different points may intersect only at one point; if 2) applies, p_i is again unique since a ray starting from the end point of an arc may intersect with the arc at most at one other point; and if 3) applies, p_i is unique since two arcs sharing one end point on different circles can only intersect at most at one other point. Therefore, p_i is always globally uniquely determined. After p_i is globally uniquely determined, all the angles associated with p_i are also globally uniquely determined. Because each Type-I vertex addition operation can guarantee a unique adding point p_i, we conclude that the obtained angularity after a sequence of Type-I vertex additions is globally angle rigid. □

In comparison, Type-II vertex additions can only guarantee angle rigidity, but not global angle rigidity.

Proposition 2.13 (Sufficient condition for angle rigidity)**.** *An angularity is angle rigid if it can be obtained through a sequence of Type-II vertex additions from a generically angle rigid 3-vertex angularity.*

The proof can be easily constructed following similar arguments as those for Proposition 2.12. The only difference is that p_i now may have two solutions and is only unique locally.

After having presented our results on angularity and generic angle rigidity, in the following section, we discuss infinitesimal angle rigidity, which relates closely to infinitesimal motion.

2.3 Infinitesimal angle rigidity

Analogous to distance rigidity, infinitesimal angle rigidity can be characterized by the kernel of a properly defined rigidity matrix. Towards this end, we first introduce the following angle function. For each angularity $\mathbb{A}(\mathcal{V}, \mathcal{A}, p)$, we define the *angle function* $f_{\mathcal{A}}(p) : \mathbb{R}^{2N} \to \mathbb{R}^M$ by

$$f_{\mathcal{A}}(p) := [f_1, \cdots, f_M]^{\mathrm{T}}, \tag{2.8}$$

where $f_m : \mathbb{R}^6 \to [0, 2\pi)$, $m = 1, \cdots, M$, is the mapping from the position vector $[p_i^{\mathrm{T}}, p_j^{\mathrm{T}}, p_k^{\mathrm{T}}]^{\mathrm{T}}$ of the mth element (i, j, k) in $\mathcal{A}$ to the signed angle $\measuredangle ijk \in [0, 2\pi)$. Using this angle function, one can define $\mathbb{A}$'s angle rigidity matrix.

2.3.1 Angle rigidity matrix

We consider an arbitrary element (i, j, k) in $\mathbb{A}$ and denote the corresponding angle constraint by $\measuredangle ijk(p_i, p_j, p_k) = \beta \in [0, 2\pi)$, or in shorthand $\measuredangle ijk = \beta$. From the definition of the dot product, one has

$$\cos\beta = \frac{(p_i - p_j)^{\mathrm{T}}}{\|p_i - p_j\|}\frac{(p_k - p_j)}{\|p_k - p_j\|} = z_{ji}^{\mathrm{T}} z_{jk}, \tag{2.9}$$

where $\|\cdot\|$ denotes the Euclidean vector norm and we have used $\cos\beta = \cos(2\pi - \beta)$ according to (2.1). Differentiating both sides of (2.9) with respect to time leads to

$$\begin{aligned}(-\sin\beta)\dot{\beta} &= \dot{z}_{ji}^{\mathrm{T}} z_{jk} + z_{ji}^{\mathrm{T}}\dot{z}_{jk} \\ &= [\frac{P_{z_{ji}}}{l_{ji}}(\dot{p}_i - \dot{p}_j)]^{\mathrm{T}} z_{jk} + z_{ji}^{\mathrm{T}}\frac{P_{z_{jk}}}{l_{jk}}(\dot{p}_k - \dot{p}_j),\end{aligned} \tag{2.10}$$

where $l_{jk} = \|p_j - p_k\|$, $P_{z_{ji}} = I_2 - z_{ji}z_{ji}^{\mathrm{T}}$, I_2 denotes the 2×2 identity matrix, and we have used the fact that for $x \in \mathbb{R}^2, x \neq 0$, $\frac{\mathrm{d}}{\mathrm{d}t}(\frac{x}{\|x\|}) = \frac{P_{x/\|x\|}}{\|x\|}\dot{x}$. By rearranging (2.10), one obtains

$$\begin{aligned}\frac{\mathrm{d}\beta}{\mathrm{d}t} &= \frac{\partial\beta}{\partial p_i}\dot{p}_i + \frac{\partial\beta}{\partial p_j}\dot{p}_j + \frac{\partial\beta}{\partial p_k}\dot{p}_k \\ &= N_{kji}\dot{p}_i - (N_{kji} + N_{ijk})\dot{p}_j + N_{ijk}\dot{p}_k,\end{aligned} \tag{2.11}$$

where $N_{kji} = -\frac{z_{jk}^{\mathrm{T}} P_{z_{ji}}}{l_{ji}\sin\beta} \in \mathbb{R}^{1\times 2}$, $N_{ijk} = -\frac{z_{ji}^{\mathrm{T}} P_{z_{jk}}}{l_{jk}\sin\beta} \in \mathbb{R}^{1\times 2}$, and we have assumed $\sin\beta \neq 0$, i.e., no collinearity among p_i, p_j, p_k. For each (i, j, k) in $\mathcal{A}$ we obtain an equation in the form of (2.11), and then one can write such M equations into the matrix form

$$\frac{\mathrm{d}f_{\mathcal{A}}(p)}{\mathrm{d}t} = \frac{\partial f_{\mathcal{A}}(p)}{\partial p}\dot{p} = R_a(p)\dot{p}, \tag{2.12}$$

where $R_a(p) \in \mathbb{R}^{M\times 2N}$ is called the *angle rigidity matrix*, whose rows are indexed by the elements of $\mathcal{A}$ and columns the coordinates of the vertices:

$$R_a(p) = \begin{bmatrix} & \cdots & \text{Vertex } i & \cdots & \text{Vertex } j & \cdots & \text{Vertex } k & \cdots \\ \text{Angle } 1 & \cdots & \cdots & \cdots & \cdots & \cdots & \cdots & \cdots \\ \cdots & \cdots & \cdots & \cdots & \cdots & \cdots & \cdots & \cdots \\ \measuredangle ijk & 0 & N_{kji} & 0 & -N_{kji} - N_{ijk} & 0 & N_{ijk} & 0 \\ \cdots & \cdots & \cdots & \cdots & \cdots & \cdots & \cdots & \cdots \\ \text{Angle } M & \cdots & \cdots & \cdots & \cdots & \cdots & \cdots & \cdots \end{bmatrix} \tag{2.13}$$

For an angularity, its angle preservation motions satisfy $\dot{f}_{\mathcal{A}} = R_a(p)\dot{p} = 0$ which include translation, rotation and scaling. One may rightfully expect that such motions are captured by the null space of the angle rigidity matrix, which always contains the following four linearly independent vectors

$$q_1 = 1_N \otimes \begin{bmatrix} 1 \\ 0 \end{bmatrix}, \quad q_2 = 1_N \otimes \begin{bmatrix} 0 \\ 1 \end{bmatrix}, \tag{2.14}$$

$$q_3 = \begin{bmatrix} (Q_0 p_1)^{\mathrm{T}}, & (Q_0 p_2)^{\mathrm{T}}, & \cdots, & (Q_0 p_N)^{\mathrm{T}} \end{bmatrix}^{\mathrm{T}}, \tag{2.15}$$

$$q_4 = \begin{bmatrix} (\kappa p_1)^{\mathrm{T}}, & (\kappa p_2)^{\mathrm{T}}, & \cdots, & (\kappa p_N)^{\mathrm{T}} \end{bmatrix}^{\mathrm{T}}, \tag{2.16}$$

where $\kappa \in \mathbb{R}$ is a nonzero scaling factor, $\otimes$ represents Kronecker product and 1_N denotes the $N \times 1$ column vector of all ones. Note that q_1 and q_2 correspond to translation, q_3 rotation, and q_4 scaling. We state this fact as a lemma.

Lemma 2.14 (Rank of angle rigidity matrix)**.** *For an angle rigidity matrix $R_a(p)$, it always holds that* Span$\{q_1, q_2, q_3, q_4\} \subseteq$ Null$(R_a(p))$ *and correspondingly* Rank$(R_a(p)) \leqslant 2N - 4$.

Proof. Because each row sum of $R_a(p)$ equals zero, one has $R_a(p)q_1 = 0$ and $R_a(p)q_2 = 0$. Taking an arbitrary row $\measuredangle ijk$ in $R_a(p)$ as an example, one has the corresponding row in $R_a(p)q_3$

$$\begin{aligned} & N_{kji}Q_0(p_i - p_j) + N_{ijk}Q_0(p_k - p_j) \\ =& \frac{z_{jk}^{\mathrm{T}} P_{z_{ji}} Q_0 z_{ji} + z_{ji}^{\mathrm{T}} P_{z_{jk}} Q_0 z_{jk}}{-\sin\beta} \\ =& \frac{z_{jk}^{\mathrm{T}} Q_0 z_{ji} + z_{ji}^{\mathrm{T}} Q_0 z_{jk}}{-\sin\beta} = 0, \end{aligned} \tag{2.17}$$

where we have used the fact that $Q_0^{\mathrm{T}} = -Q_0$ and $z_{ji}^{\mathrm{T}} Q_0 z_{ji} = 0$. Similarly, for $R_a(p)q_4$, one has

$$\kappa N_{kji}(p_i - p_j) + \kappa N_{ijk}(p_k - p_j) = \kappa \frac{z_{jk}^{\mathrm{T}} P_{z_{ji}} z_{ji} + z_{ji}^{\mathrm{T}} P_{z_{jk}} z_{jk}}{-\sin\beta} = 0, \tag{2.18}$$

where we have used the fact that $P_{z_{ji}} z_{ji} = 0$. Therefore, Span$\{q_1, q_2, q_3, q_4\} \subseteq$ Null$(R_a(p))$.

Since p has no overlapping elements, one has that q_3, q_4 are linearly independent to q_1 and q_2. Because $q_1^{\mathrm{T}} q_2 = 0$ and $q_3^{\mathrm{T}} q_4 = 0$, one has that q_1, q_2, q_3, q_4 are linearly independent. □

Obviously the row rank of the angle rigidity matrix, or equivalently its row

linear dependency, is a critical property of an angularity. We describe this property by using the notion of "independent" angles.

Definition 2.15 (Independent angles)**.** *For an angularity $\mathbb{A}(\mathcal{V},\mathcal{A},p)$, we say its angles in $f_{\mathcal{A}}(p)$ are* independent *if its angle rigidity matrix $R_a(p)$ has full row rank.*

Since rank is a generic property of a matrix, one may wonder whether it is possible to disregard p of $\mathbb{A}$ and define generic angle rigidity only using $(\mathcal{V},\mathcal{A})$. This is indeed doable as what we will show in the following subsection. Note that $2N-4$ is the maximum rank that $R_a(p)$ can have. When p is generic, the exact realization of p is not important for $(\mathcal{V},\mathcal{A})$, and when checking the angle rigidity matrix's rank, one can replace p by a random generic realization.

Using the notion of infinitesimal motion, checking the rank of the rigidity matrix can also enable us to check "infinitesimal" angle rigidity.

2.3.2 Infinitesimal angle rigidity

To consider infinitesimal motion, suppose that each $p_i,\forall i\in\mathcal{V}$ of $\mathbb{A}(\mathcal{V},\mathcal{A},p)$ is on a differentiable smooth path. We say the whole path $p(t)$ is generated by an *infinitesimally angle rigid motion* of $\mathbb{A}$ if on the path $f_{\mathcal{A}}(p)$ remains constant, i.e., $\dot{f}_{\mathcal{A}}=R_a(p)\dot{p}\equiv 0$. We say such an infinitesimally angle rigid motion $p(t)$ is *trivial* if it can be given by [23]

$$p_i(t)=\kappa(t)\mathcal{Q}(t)p_i(t_0)+\mathcal{W}(t),\forall i\in\mathcal{V},t\geqslant t_0, \tag{2.19}$$

where $\kappa(t)\neq 0$ is a scalar scaling factor, $\mathcal{Q}(t)\in\mathbb{R}^{2\times 2}$ is a rotation matrix, $\mathcal{W}(t)\in\mathbb{R}^2$ is a translation vector, and $\kappa(t),\mathcal{Q}(t),\mathcal{W}(t)$ are all differentiable smooth functions. Since all $p_i(t),\forall i\in\mathcal{V}$, share the same $\kappa(t),\mathcal{Q}(t),\mathcal{W}(t)$, it follows

$$p(t)=\{I_N\otimes[\kappa(t)\mathcal{Q}(t)]\}p(t_0)+1_N\otimes\mathcal{W}(t),t\geqslant t_0. \tag{2.20}$$

Now we are ready to define infinitesimal angle rigidity.

Definition 2.16 (Infinitesimal angle rigidity)**.** *An angularity $\mathbb{A}(\mathcal{V},\mathcal{A},p)$ is infinitesimally angle rigid if all its continuous infinitesimally angle rigid motion $p(t)$ are trivial.*

In fact, a motion satisfying (2.20) is always an infinitesimally angle rigid motion because the combination of translation, rotation and scaling preserves all the angle constraints. However, the converse does not necessarily hold, e.g., non-trivial infinitesimally angle rigid motion exists when only point 1 moves along the line 12 in Fig. 2.3(b). We formalize these remarks in the following theorem.

Theorem 2.17 (Sufficient and necessary condition for infinitesimal angle rigidity)**.** *An angularity $\mathbb{A}(\mathcal{V}, \mathcal{A}, p)$ is infinitesimally angle rigid if and only if the rank of its angle rigidity matrix $R_a(p)$ is $2N-4$.*

Proof. In view of the definition, $\mathbb{A}$ is infinitesimally angle rigid if and only if all its infinitesimally angle rigid motions are trivial. That is to say, these infinitesimally angle rigid motions $p(t), t \in [t_0, t_1]$ maintaining the angle constraints are exactly the combination of translation, rotation, and scaling with respect to the initial configuration $p(t_0)$, which are precisely captured by the four linearly independent vectors q_1, q_2, q_3, and q_4, which in turn is equivalent to the fact that the rigidity matrix's null space is precisely the span of $\{q_1, q_2, q_3, q_4\}$. The conclusion then follows from the fact that such a specification of the null space holds if and only if the rank of the rigidity matrix reaches its maximum $2N-4$. □

Note that this theorem implies that $\mathbb{A}(\mathcal{V}, \mathcal{A}, p)$ is infinitesimally angle rigid if and only if there are $2N-4$ independent angles in $f_{\mathcal{A}}(p)$. We want to further remark that no matter what p is if one of the following three combinatorial structures appears, then the angles are always dependent.
(1) A cycle formed by the triplets in $\mathcal{A}$. For example, $\mathcal{A} = \{(i,j,k),(j,k,m),$ $(k,m,n),(m,n,l),(n,l,i),(l,i,j)\}$, see Fig. 2.6(a).
(2) Angles around a vertex. For example, $\mathcal{A} = \{(i,m,j),(j,m,k),(k,m,i)\}$, see Fig. 2.6(b).
(3) A nonempty subset $\mathcal{A}' \subset \mathcal{A}$ such that the number N' of the involved vertices in $\mathcal{A}'$ satisfies $|\mathcal{A}'| > 2N'-4$. For example, $\mathcal{A} = \{(i,m,j),(m,j,i),(i,k,j),(i,j,k),$ $(k,m,j),(n,i,m),(n,m,i)\}$ and $\mathcal{A}' = \{(i,m,j),(m,j,i),(i,k,j),(i,j,k),(k,m,j)\}$, and thus $N'=4$, $|\mathcal{A}'|=5$ in Fig. 2.6(c).

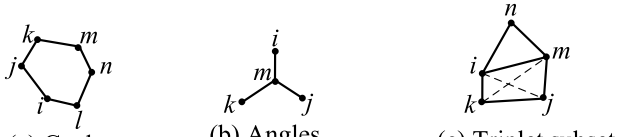

(a) Cycle (b) Angles around a vertex (c) Triplet subset

Figure 2.6: *Types of dependent triplet elements*

If $\mathcal{A}$ contains one of the above three combinatorial structures, we say the triplet elements in $\mathcal{A}$ are dependent; otherwise, they are independent. One can further quantify the number of triplet elements such that the angularity is infinitesimally angle rigid.

Theorem 2.18 (Combinatoral necessary condition for infinitesimal angle rigidity)**.** *For an angularity $\mathbb{A}(\mathcal{V}, \mathcal{A}, p)$, if it is infinitesimally angle rigid, then it has $2N-4$ independent triplet elements in $\mathcal{A}$.*

Proof. From Theorem 2.17, we know $\mathbb{A}$ has $2N-4$ independent angles in $f_{\mathcal{A}}(p)$. First, we prove that dependent triplet elements in $\mathcal{A}$ imply dependent angles in $f_{\mathcal{A}}(p)$. Note that $N_{kji}^{\mathrm{T}} = \frac{(l_{jk}\cos\angle ijk)z_{ji}-(p_k-p_j)}{l_{ji}l_{jk}\sin\angle ijk} = -\frac{(p_i-p_j)^{\perp}}{l_{ij}^2}$. Then, by taking the dependent triplet elements in Fig. 2.6(a) as an example, it can be verified that

$$\begin{bmatrix}1 & 1 & 1 & 1 & 1 & 1\end{bmatrix} R_a(p) = 0, \tag{2.21}$$

which implies the row dependence in $R_a(p)$ and dependent angles in $f_{\mathcal{A}}(p)$. The cases in Fig. 2.6 (b), (c) can be similarly obtained. Now, one has that dependent triplet elements in $\mathcal{A} \Rightarrow$ dependent angles in $f_{\mathcal{A}}(p)$, which implies that independent angles in $f_{\mathcal{A}}(p) \Rightarrow$ independent triplet elements in $\mathcal{A}$. So its angle set $\mathcal{A}$ has $2N-4$ independent triplet elements. □

Now we show the relationship between angle rigidity and infinitesimal angle rigidity.

Theorem 2.19 (Relationship between infinitsimal angle rigidity and angle rigidity)**.** *If an angularity $\mathbb{A}(\mathcal{V},\mathcal{A},p)$ is infinitesimally angle rigid, then it is angle rigid.*

Proof. From Definition 2.16, we know that if $\mathbb{A}(\mathcal{V},\mathcal{A},p)$ is infinitesimally angle rigid, then all the continuous infinitesimally angle rigid motion $p(t)$ are trivial, which are the combination of translation, rotation and scaling of $\mathbb{A}$. Consider another angularity $\mathbb{A}(\mathcal{V},\mathcal{A},p')$ with $\varepsilon > 0$ and $\|p'-p\| < \varepsilon$, which is equivalent to $\mathbb{A}(\mathcal{V},\mathcal{A},p)$. Then, the continuous motion from p to p' maintaining $f_{\mathcal{A}}(p)$ are the combination of translation, rotation and scaling of $\mathbb{A}(\mathcal{V},\mathcal{A},p)$, which are angle-preserving motions, i.e., (2.3) holds. Therefore, $\mathbb{A}(\mathcal{V},\mathcal{A},p')$ is congruent to $\mathbb{A}(\mathcal{V},\mathcal{A},p)$, which implies that $\mathbb{A}(\mathcal{V},\mathcal{A},p)$ is angle rigid. □

For infinitesimally angle rigid angularities, we now discuss when its number of angles in $\mathcal{A}$ becomes the minimum. Towards this end, we need to clarify what we mean by minimal angle rigidity.

Definition 2.20 (Minimal angle rigidity)**.** *An angularity $\mathbb{A}(\mathcal{V},\mathcal{A},p)$ is* minimally angle rigid *if it is angle rigid and fails to remain so after removing any element in $\mathcal{A}$, and is* infinitesimally minimally angle rigid *if it is infinitesimally angle rigid and minimally angle rigid.*

Since $\mathrm{Rank}[R_a(p)] \leqslant 2N-4$, the minimum number of angle constraints in $f_{\mathcal{A}}(p)$ to maintain infinitesimal angle rigidity is exactly $2N-4$. So we immediately have the following lemma.

Lemma 2.21. *An angularity $\mathbb{A}(\mathcal{V},\mathcal{A},p)$ is infinitesimally minimally angle rigid if and only if it is infinitesimally angle rigid and $|\mathcal{A}| = 2N-4$.*

For an infinitesimally minimally distance rigid framework, there must exist a vertex associated with fewer than 4 distance constraints [87, 92]; otherwise, the total number of distance constraints will be at least $2N$ and thus greater than the minimum number $2N-3$. This property is critical for the success of the Henneberg construction method in order to generate an arbitrary infinitesimally minimally distance rigid framework [58, 87]. However, for an infinitesimally minimally angle rigid angularity, the situation is more challenging, which in fact prevents drawing similar conclusions as the Henneberg construction does for distance rigidity. To be more precise, we have the following lemma.

Lemma 2.22. *For an infinitesimally minimally angle rigid angularity $\mathbb{A}(\mathcal{V}, \mathcal{A}, p)$ with $|\mathcal{A}| = 2N-4$, it must have a vertex involved in more than one but fewer than 6 angle constraints.*

Proof. If every vertex is involved in at least 6 angle constraints, then the total number of angle constraints is at least $|\mathcal{A}| \geqslant \frac{6N}{3} = 2N$, which contradicts Lemma 2.21. Then for that vertex, which has fewer than 6 angle constraints, if it is involved in only one angle constraint, then it is not rigid with respect to the rest of the angularity, which contradicts the property of angle rigidity. So there must be at least one vertex that is involved in 2, 3, 4 or 5 angle constraints. □

In the following example, we show an infinitesimally minimally angle rigid angularity in Fig. 2.7, whose vertices are all involved in 5 angle constraints. Note

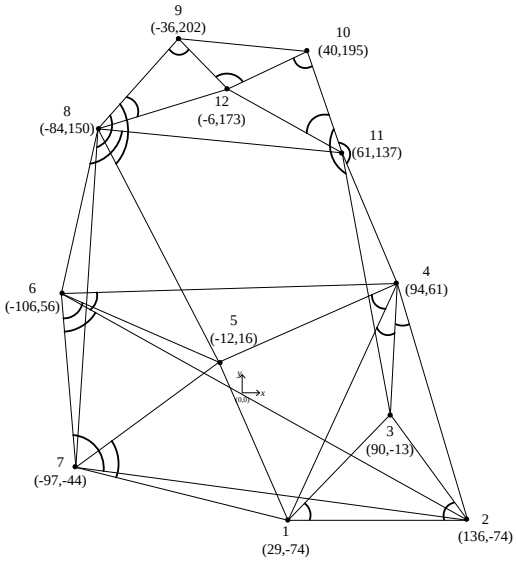

Figure 2.7: *All vertices are involved in 5 angle constraints.*

that if an angularity $\mathbb{A}(\mathcal{V}, \mathcal{A}, p)$ is infinitesimally minimally angle rigid, then $|\mathcal{A}| = 2N - 4$, and more importantly, the triplet elements in $\mathcal{A}$ need to be independent; this also implies that those situations listed in Fig. 2.6, namely cyclic angles, angles around a vertex, and overly constrained angle subsets, cannot show up in $\mathcal{A}$, which is a necessary combinatorial condition for infinitesimal minimal angle rigidity. In the following section, we show how to apply the angle rigidity theory we have developed for multi-agent formation control.

2.4 Concluding remarks

In this chapter, we have proposed the angle rigidity theory in 2D. The notion of angularity has been defined to describe the multi-point framework with angle constraints. The established angle rigidity has shown to be a local property because of the existence of flex ambiguity. The infinitesimal angle rigidity has been developed based on the trivial motions of the angularity. A sufficient and necessary condition for infinitesimal angle rigidity has been investigated by checking the rank of the angle rigidity matrix.

Chapter 3

Formation stabilization in 2D

This chapter shows how to achieve an angle rigid formation in 2D for a group of mobile agents. Many formation control algorithms have been designed by using the measurement of relative positions [8, 52, 63] or aligned bearings [89, 101], or using the information acquired through communication [52, 96]. Note that in [52] a gradient-based formation stabilization control law is designed to achieve an infinitesimally angle rigid formation, which utilizes the measurements of relative positions, and the received information through communication of the neighbors' angle errors. In this chapter we demonstrate how to stabilize a multi-agent planar formation using only local angle measurements with the help of the angle rigidity theory that we have developed in the last chapter.

3.1 Introduction

Multi-agent formation control has been extensively studied due to its wide applications in, e.g., robotic transportation [30] and search and rescue of mobile robots [51]. Sensors used in formation stabilization mainly include GPS receivers, radars and cameras, which can acquire absolute positions, inter-agent relative positions, or angles/bearings [7, 71]. In particular, angle measurements are becoming cheaper, more reliable and accessible than absolute or relative position measurements [71, 103]. Angle information can be easily obtained from a camera or a sensor array in their local coordinate frames [30]. Using 2D angle rigidity developed in Chapter 2, we show in this chapter how to stabilize a planar formation by using only local angle measurements. Different from the designed bearing-based formation control algorithms in [99, 101] where all agents' local coordinate systems are required to be aligned, the proposed angle-only formation control algorithm does not require the alignment of agents' coordinate frames since the angle described in different planar coordinate frames remains the same. Note that in [52], planar angle rigidity is established by specifying the cosine of an angle formed by two jointed edges as the angle constraint. The formation stabilization algorithm constructed in [52] requires that each agent can sense the real-time relative positions with respect to its neighbors. Different from [52], in this chapter the desired formation shape is realized using only angle measurements.

In addition, other rigidity notions with mixed distance and angle constraints have been investigated in [56, 57, 73], under which the formation control algorithms are also designed for agents by using the measurements of relative positions.

3.2 Angle-only formation control for single-integrators

For an agent i moving in the plane, in this subsection we consider its dynamics are modeled by single-integrators

$$\dot{p}_i = u_i, i = 1, \cdots, N, \tag{3.1}$$

where $p_i \in \mathbb{R}^2$ denotes agent i's position, $u_i \in \mathbb{R}^2$ is the control input to be designed, and N is the number of agents in the group. Agent i can only measure angles; to be more specific, it can only measure the angle $\phi_{ij} \in [0, 2\pi)$ with respect to another agent j evaluated counterclockwise from the X-axis of its own local coordinate frame of choice that is fixed to the ground.

To avoid confusion in the stability analysis, we first describe all variables in a global coordinate frame and in the end we demonstrate that this global coordinate frame is only needed for analysis purposes and not needed in the control implementation. Now we define the bearing $z_{ij} \in \mathbb{R}^2$ to be the unit vector pointing from agent i to a non-coincident j, i.e.,

$$z_{ij} = \frac{p_j - p_i}{\|p_j - p_i\|} = \begin{bmatrix} \cos\phi_{ij} \\ \sin\phi_{ij} \end{bmatrix}, \tag{3.2}$$

where ϕ_{ij} determines uniquely z_{ij} when $p_i \neq p_j$. Therefore, when ϕ_{ij} can be measured, z_{ij} is known. In the triangle $\triangle ijk$ shown in Fig. 3.1, the interior angle α_i can be computed by

$$\alpha_i = \measuredangle kij = \arccos(z_{ij}^{\mathrm{T}} z_{ik}), \tag{3.3}$$

using bearings z_{ij} and z_{ik}. Note that the X-axes of agents i, j and k do not need to align, and the angle α_i to be controlled is not the measured angle ϕ_{ij}, but the relative measured angle $\alpha_i = [(\phi_{ij} - \phi_{ik}) \bmod 2\pi]$.

We construct the desired planar formation through a sequence of Type-I vertex additions (Case 3) from a generically angle rigid 3-vertex angularity, which is globally angle rigid according to Proposition 2.12. First, in an N-agent formation, we label the agents by 1 to N. Then agents 1, 2, 3 aim at forming the first triangular shape, and each of agents 4 to N aims at achieving two desired angles formed with other three agents, see Fig. 3.2. Therefore, the construction process can be summarized as follows:

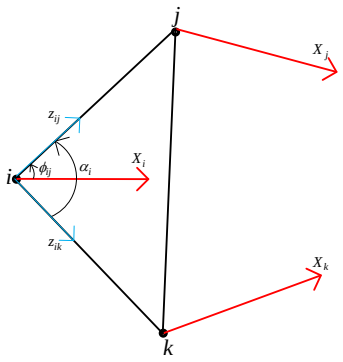

Figure 3.1: *The angle measurements.*

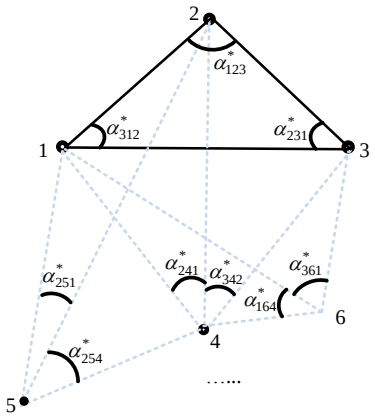

Figure 3.2: *Constructing desired formation by using Case 3 of Type-I vertex addition.*

Step 1: One constructs the first triangular formation $\triangle 123$ using three angle constraints: $\measuredangle 123, \measuredangle 231, \measuredangle 312$.

Step 2: One adds agent 4 under the two angle constraints: $\measuredangle 142$ and $\measuredangle 243$.

...

Step $k-2$: One adds agent k under the two angle constraints: $\measuredangle j_1 k j_2$ and $\measuredangle j_2 k j_3$, $j_1, j_2, j_3 \in \{1, ..., k-1\}$.

...

Step $N-2$: One adds agent N under the two angle constraints: $\measuredangle i_1 N i_2$ and $\measuredangle i_2 N i_3$, for some distinct $i_1, i_2, i_3 \in \{1, ..., N-1\}$.

To guarantee the uniqueness of each agent's position in these steps under the given two angle constraints, the following assumption is needed.

Assumption 3.1. In the aforementioned Step $k, k = 2, \cdots, N-2$ with the cor-

responding newly added agent i and its angle constraints $\measuredangle j_1ij_2$ and $\measuredangle j_2ij_3$, we assume that $\{p_i, p_{j_1}, p_{j_2}, p_{j_3}\}$ is generic and no collinearity occurs, namely $\measuredangle j_1ij_2 \neq 0, \measuredangle j_1ij_2 \neq \pi$ and $\measuredangle j_2ij_3 \neq 0, \measuredangle j_2ij_3 \neq \pi$.

Remark 3.2. According to Proposition 2.13 in Chapter 2, when $\{p_i, p_{j_1}, p_{j_2}, p_{j_3}\}$ is generic, j_1, i, j_2 are not collinear and j_2, i, j_3 are not collinear as stipulated in Assumption 3.1, the position of each newly added agent $i, i = 2, \cdots, N$ is locally uniquely determined by $\measuredangle j_1ij_2$ and $\measuredangle j_2ij_3$, which implies the angle rigidity of the constructed formation.

Based on the above construction process, the aim is to achieve the desired angle rigid formation specified as follows. For agents 1 to 3

$$\lim_{t\to\infty} e_1(t) = \lim_{t\to\infty}(\alpha_{312}(t) - \alpha^*_{312}) = 0, \tag{3.4}$$
$$\lim_{t\to\infty} e_2(t) = \lim_{t\to\infty}(\alpha_{123}(t) - \alpha^*_{123}) = 0, \tag{3.5}$$
$$\lim_{t\to\infty} e_3(t) = \lim_{t\to\infty}(\alpha_{231}(t) - \alpha^*_{231}) = 0, \tag{3.6}$$

where $\alpha^*_{jik} \in (0, \pi), i, j, k \in \{1, 2, 3\}$ denote agent i's desired angle formed with agents j, k. For agents 4 to N

$$\lim_{t\to\infty} e_{i1}(t) = \lim_{t\to\infty}(\alpha_{j_1ij_2}(t) - \alpha^*_{j_1ij_2}) = 0, \tag{3.7}$$
$$\lim_{t\to\infty} e_{i2}(t) = \lim_{t\to\infty}(\alpha_{j_2ij_3}(t) - \alpha^*_{j_2ij_3}) = 0, \tag{3.8}$$

where $i = 4, \cdots, N$, $j_1 < i, j_2 < i, j_3 < i$, and $\alpha^*_{j_1ij_2} \in (0, \pi), \alpha^*_{j_2ij_3} \in (0, \pi)$ denote agent i's two desired angles formed with agents $j_1, j_2, j_3 \in \{1, 2, ..., i-1\}, j_1 \neq j_2 \neq j_3$. Therefore, the angle-only formation control problem to be solved in this section is formally described below.

Problem 1 Given feasible desired angles $f_{\mathcal{A}}(p) = \{\alpha^*_{312}, \alpha^*_{123}, \alpha^*_{231}, \alpha^*_{241}, \alpha^*_{342}, .. ., \alpha^*_{i_1Ni_2}, \alpha^*_{i_2Ni_3}\}$, design control law u_i for each agent i by only using angle measurements ϕ_{ij} with respect to agent i's neighboring agent j to achieve (3.4)-(3.8).

Remark 3.3. One may also choose other cases in Type-I and Type-II vertex addition operations to construct the desired formations. However, the constructed formations are not globally angle rigid or the realization depends on the knowledge of the neighbors' angle error, which are the drawbacks of the other cases when they are applied to formation control. For example, in Case 1 of Type-II vertex addition (Fig. 2.4(d)), Proposition 2.13 shows that the constructed formation is only angle rigid which may cause ambiguity; moreover, the angle $\alpha_{k_1j_1i}$ cannot be obtained by agent i's local angle measurements.

3.2.1 Triangular formation control for agents 1 to 3

To achieve the desired angles for agents 1 to 3, we design their formation control laws

$$u_i = -(\alpha_i - \alpha_i^*)(z_{i(i+1)} + z_{i(i-1)}), \tag{3.9}$$

where $i \in \{1,2,3\}$, $z_{i(i+1)} = z_{31}$ when $i = 3$ and $z_{i(i-1)} = z_{13}$ when $i = 1$, and α_i represents $\alpha_{(i-1)i(i+1)}$ for conciseness.

To obtain the convergence of the angle errors, we first analyze the dynamics of the angle errors $e_i(t), i = 1,2,3$. Different from [11], we use the dot product of two bearings to obtain the angle error dynamics. According to (2.10), agent 1's angle dynamics can be obtained by

$$\dot{\alpha}_1 = -[\frac{P_{z_{13}}}{l_{13}\sin\alpha_1}(\dot{p}_3 - \dot{p}_1)]^{\mathrm{T}} z_{12} - z_{13}^{\mathrm{T}} \frac{P_{z_{12}}}{l_{12}\sin\alpha_1}(\dot{p}_2 - \dot{p}_1). \tag{3.10}$$

By following the calculation in Appendix A, one has the first three agents' angle dynamics

$$\begin{aligned} \dot{e}_f &= [\dot{\alpha}_1 \;\; \dot{\alpha}_2 \;\; \dot{\alpha}_3]^{\mathrm{T}} = F(e_f)e_f \\ &= \begin{bmatrix} -g_1 & f_{12} & f_{13} \\ f_{21} & -g_2 & f_{23} \\ f_{31} & f_{32} & -g_3 \end{bmatrix} \begin{bmatrix} \alpha_1 - \alpha_1^* \\ \alpha_2 - \alpha_2^* \\ \alpha_3 - \alpha_3^* \end{bmatrix}, \end{aligned} \tag{3.11}$$

where $e_f = \begin{bmatrix} \alpha_1 - \alpha_1^* & \alpha_2 - \alpha_2^* & \alpha_3 - \alpha_3^* \end{bmatrix}^{\mathrm{T}}$, $g_i = (\sin\alpha_i)(1/l_{i(i+1)} + 1/l_{i(i-1)})$, $f_{ij} = (\sin\alpha_j)/l_{ij}$.

To guarantee that the triangular formation system under the control law (3.9) is well defined, we first prove that no collinearity and collision will take place under (3.11) if the formation is not collinear initially.

Lemma 3.4 (No collinearity)**.** *For the three-agent formation, if the initial formation is not collinear, it will not become collinear for $t > 0$ under the angle dynamics (3.11).*

Proof. Consider the manifold $\mathcal{M}_a = \{(\alpha_1,\alpha_2,\alpha_3) | \alpha_1 + \alpha_2 + \alpha_3 = \pi, 0 < \alpha_1 < \pi, 0 < \alpha_2 < \pi, \text{and } 0 < \alpha_3 < \pi\}$ which is an open set. To show $\mathcal{M}_a$ is positively invariant, we show that for any $(\alpha_1,\alpha_2,\alpha_3) \in \mathcal{M}_a$, it is impossible for α_i to escape $\mathcal{M}_a$. Consider the boundary states $\alpha_i(t) = \pi - \varepsilon_1$ with $\varepsilon_1 = 0^+$, $\alpha_{i+1}(t) = \varepsilon_2 = 0^+$, $\alpha_{i-1}(t) = \varepsilon_3 = 0^+$, $\varepsilon_1 = \varepsilon_2 + \varepsilon_3$.

According to (3.11), one has

$$\dot{e}_i = -g_i e_i + f_{i(i+1)} e_{i+1} + f_{i(i-1)} e_{i-1}. \tag{3.12}$$

Since $0 < \alpha_i^* < \pi$ and α_i^* is bounded away from 0 and π, one has

$$g_i e_i = g_i(\alpha_i - \alpha_i^*) > 0, \tag{3.13}$$

$$f_{i(i+1)} e_{i+1} = f_{i(i+1)}(\alpha_{i+1} - \alpha_{i+1}^*) < 0, \tag{3.14}$$

$$f_{i(i-1)} e_{i-1} = f_{i(i-1)}(\alpha_{i-1} - \alpha_{i-1}^*) < 0, \tag{3.15}$$

which implies that $\dot{e}_i(t) < 0$. Thus when $\alpha_i(t)$ is close to π, $\alpha_i(t)$ will decrease, which implies that $\mathcal{M}_a$ is positively invariant, i.e. trajectories starting from $\mathcal{M}_a$ remains in $\mathcal{M}_a$. □

Lemma 3.5 (No collision). *For the three-agent formation, if the initial angles $\alpha_i \neq 0, i = 1, 2, 3$, no collision will take place for $t > 0$ under the formation control law (3.9).*

Proof. Suppose on the contrary that collision may happen between agents i and j at $t = t_1$. Then one of the following two cases shown in Fig. 3.3 will take place.

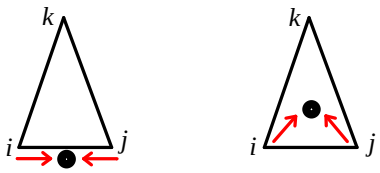

Figure 3.3: *Collision cases.*

For the first case, $\dot{p}_i(t_1) = -\gamma \dot{p}_j(t_1)$ where γ is a positive constant. Note that the moving direction of agent i under the control law (3.9) is always the bisector of the interior angle α_i. According to Lemma 3.4, no collinearity will happen for $t > 0$ which implies that $z_{ik}(t) \neq -z_{jk}(t)$ for $t > 0$. According to the control law (3.9), $\dot{p}_i(t_1) = -\gamma \dot{p}_j(t_1)$ requires $z_{ik}(t_1) = -z_{jk}(t_1)$ which is impossible for $t > 0$.

For the second case, since agents i and j move towards the inside of the triangle, it follows from the control law (3.9) that $\frac{\pi}{2} - \varepsilon_1 = \alpha_i(t_1^-) < \alpha_i^*$ and $\frac{\pi}{2} - \varepsilon_2 = \alpha_j(t_1^-) < \alpha_j^*$, where $\varepsilon_1 = 0^+$ and $\varepsilon_2 = 0^+$. Then, $\alpha_i^* + \alpha_j^* + \alpha_k^* = \pi > \pi + \alpha_k^* - \varepsilon_1 - \varepsilon_2$, which contradicts the fact that α_k^* is bounded away from 0. □

Now, we give the main result for the convergence of the triangular formation.

Theorem 3.6 (Stability of the first three agents). *For the triangular formation under the control law (3.9), if $\alpha_i(0) \neq 0$ and the initial angle errors $e_i(0), i = 1, 2, 3$*

are sufficiently small, the angle errors e_i and agents' control input $u_i(t)$ converge exponentially to zero.

Proof. From Lemmas 3.4 and 3.5, no collinearity and collision will take place since $\sin\alpha_i \neq 0, l_{ij} \neq 0, \forall i,j = 1,2,3$, which guarantees that the closed-loop system under the control law (3.9) is well defined. Since $e_1+e_2+e_3 = \sum_{i=1}^{3}\alpha_i - \sum_{i=1}^{3}\alpha_i^* \equiv 0$, the angle dynamics (3.11) can be reduced to

$$\dot{e}_s = \begin{bmatrix}\dot{e}_1\\ \dot{e}_2\end{bmatrix} = \begin{bmatrix}-(g_1+f_{13}) & f_{12}-f_{13}\\ f_{21}-f_{23} & -(g_2+f_{23})\end{bmatrix}\begin{bmatrix}e_1\\ e_2\end{bmatrix} = F_s(e_s)e_s. \tag{3.16}$$

Let $\mathbb{U}_2 \in \mathbb{R}^2$ denote a neighborhood of the origin $\{e_1 = e_2 = 0\}$, in which we investigate the local stability of (3.16). Linearizing (3.16) around the origin, we obtain

$$\dot{e}_s = L_1(\alpha^*)e_s, \tag{3.17}$$

where $L_1(\alpha^*) = F_s(e_s)|_{e_s=0}$. Then, one has

$$\text{tr}(L_1(\alpha^*)) = -g_1^* - f_{13}^* - g_2^* - f_{23}^* < 0, \tag{3.18}$$

$$\begin{aligned}\det(L_1(\alpha^*)) =& (g_1^*+f_{13}^*)(g_2^*+f_{23}^*) - (f_{21}^*-f_{23}^*)(f_{12}^*-f_{13}^*)\\ >& g_1^*f_{23}^* + g_2^*f_{13}^* + f_{21}^*f_{13}^* + f_{12}^*f_{23}^* > 0,\end{aligned} \tag{3.19}$$

where we have used the fact that $g_1^*g_2^* > f_{21}^*f_{12}^*$, $g_i^* = g_i|_{e_s=0}$, $f_{ij}^* = f_{ij}|_{e_s=0}$, and tr() and det() denote the trace and determinant of a square matrix, respectively. According to (3.18) and (3.19), one has that $L_1(\alpha^*)$ is Hurwitz. According to the Lyapunov Theorem [54, Theorem 4.6], there always exists positive definite matrices $P_1 \in \mathbb{R}^{2\times2}$ and $Q_1 \in \mathbb{R}^{2\times2}$ such that $-Q_1 = P_1L_1(\alpha^*) + L_1^{\mathrm{T}}(\alpha^*)P_1$. Design the Lyapunov function candidate as

$$V_1 = e_s^{\mathrm{T}}P_1e_s. \tag{3.20}$$

Taking the time-derivative of V_1 yields

$$\dot{V}_1 = -e_s^{\mathrm{T}}Q_1e_s \leqslant -\frac{\lambda_{\min}(Q_1)}{\lambda_{\max}(P_1)}V_1, \tag{3.21}$$

which implies that $V_1(t) \leqslant V_1(0)e^{-\frac{\lambda_{\min}(Q_1)}{\lambda_{\max}(P_1)}t}$. Since $P_1 > 0$, one has

$$e_1^2 + e_2^2 = \|e_s\|^2 \leqslant \frac{V_1}{\lambda_{\min}(P_1)} \leqslant \frac{V_1(0)}{\lambda_{\min}(P_1)}e^{-\frac{\lambda_{\min}(Q_1)}{\lambda_{\max}(P_1)}t}. \tag{3.22}$$

Also, one has

$$e_3^2 = e_1^2 + e_2^2 + 2e_1e_2 \leqslant 2(e_1^2 + e_2^2) \leqslant \frac{2V_1(0)}{\lambda_{\min}(P_1)} e^{-\frac{\lambda_{\min}(Q_1)}{\lambda_{\max}(P_1)}t}$$

which implies that e_i under the dynamics (3.11) is exponentially stable when the initial states lie in $\mathbb{U}_2$. According to (3.9), $\|u_i\| \leqslant 2|e_i|$ also converge to zero at an exponential rate. □

Remark 3.7. With non-collinear initial positions, the first three agents' angle dynamics $\dot{e}_s = F_s(e_s)e_s$ are globally stable, as a consequence of the Poincare-Bendixson theorem [54, Lemma 2.1] employed in [11, Theorem 6]. The difference between the angle dynamics $\dot{e}_s = F_s(e_s)e_s$ and the angle dynamics given in [11] is that $\sin\alpha_i$ shown in g_i, f_{ij} in (3.11) is replaced by $\sin\frac{\alpha_i}{2}$ in [11]. However, for a triangular formation, it holds that $\sin\frac{\alpha_i}{2} > 0$ and $\sin\alpha_i > 0$ for all $\alpha_i \in (0, \pi)$. Therefore, one can similarly obtain the almost global stability of $\dot{e}_s = F_s(e_s)e_s$ by following [11, Theorem 6].

After proving that the first three agents converge to the desired formation, we now look at the remaining agents.

3.2.2 Adding agents 4 to N in sequence

In this subsection, we consider that agent $i, i = 4, ..., N$, are added to the formation through the Type-I vertex addition operation with two desired angles. For agents $i = 4, ..., N$, the control algorithm is designed to be

$$u_i = -(\alpha_{j_1ij_2} - \alpha^*_{j_1ij_2})(z_{ij_1} + z_{ij_2}) - (\alpha_{j_2ij_3} - \alpha^*_{j_2ij_3})(z_{ij_2} + z_{ij_3}), \tag{3.23}$$

where $\alpha^*_{j_1ij_2} \in (0, \pi)$ and $\alpha^*_{j_2ij_3} \in (0, \pi)$, $j_1 < i, j_2 < i, j_3 < i$, $j_1 \neq j_2 \neq j_3$ are the two desired angles. Different from the first three agents, the bearing measurement topology from agents 4 to N becomes directed, which is also similarly employed in [88].

To prove the stability from agents 4 to N, we use induction. Towards this end, we need to first prove that the 4-agent formation of 1 to 4 converges to the desired shape exponentially. For the 4-agent formation, the control algorithm (3.23) can be written as

$$u_4 = -(\alpha_{241} - \alpha^*_{241})(z_{41} + z_{42}) - (\alpha_{342} - \alpha^*_{342})(z_{42} + z_{43}). \tag{3.24}$$

Then, one has the following result.

Lemma 3.8 (Stability of agent 4)**.** *Suppose $e_i(0), i = 1, 2, 3$ are sufficiently small and the sub-formation of 1, 2, 3 is governed by (3.9). Under the control algorithm (3.24)*

for agent 4, if the initial distances $l_{4i}(0)$ are sufficiently bounded away from zero, the initial angle errors $e_{41}(0)$ and $e_{42}(0)$ are sufficiently small and $\alpha^*_{341} = \alpha^*_{241} + \alpha^*_{342}$, $\sin\alpha^*_{124} > \sin\alpha^*_{412}$, $\sin\alpha^*_{423} > \sin\alpha^*_{234}$, then $e_{41}(t)$ and $e_{42}(t)$ converge to zero exponentially fast.

Proof. To analyze the stability of the angle errors e_{41} and e_{42} under the control algorithm (3.24), we first calculate the error dynamics of e_{41} and e_{42}. According to the calculation in Appendix B, one has the following angle dynamics

$$\begin{aligned}\dot{e}_4 &= [\dot{\alpha}_{241} \;\; \dot{\alpha}_{342}]^{\mathrm{T}} = F_4(e_4)e_4 + W(e_4)e_s \\ &= \begin{bmatrix} j_{11} & j_{12} \\ j_{21} & j_{22} \end{bmatrix} \begin{bmatrix} e_{41} \\ e_{42} \end{bmatrix} + \begin{bmatrix} w_{11} & w_{12} \\ w_{21} & w_{22} \end{bmatrix} \begin{bmatrix} e_1 \\ e_2 \end{bmatrix}, \end{aligned} \tag{3.25}$$

where $j_{11} = -\frac{\sin\alpha_{241}}{l_{41}} - \frac{\sin\alpha_{241}}{l_{42}}$, $j_{22} = -\frac{\sin\alpha_{342}}{l_{43}} - \frac{\sin\alpha_{342}}{l_{42}}$, $j_{12} = -\frac{(\sin\alpha_{241})+(\sin\alpha_{341})}{l_{41}} + \frac{\sin\alpha_{342}}{l_{42}}$, $j_{21} = -\frac{(\sin\alpha_{342})+(\sin\alpha_{341})}{l_{43}} + \frac{\sin\alpha_{241}}{l_{42}}$, $w_{11} = \frac{z_{42}^{\mathrm{T}} P_{z_{41}}(z_{12}+z_{13})}{l_{41}\sin\alpha_{241}}$, $w_{12} = \frac{z_{41}^{\mathrm{T}} P_{z_{42}}(z_{21}+z_{23})}{l_{42}\sin\alpha_{241}}$, $w_{21} = -\frac{z_{42}^{\mathrm{T}} P_{z_{43}}(z_{31}+z_{32})}{l_{43}\sin\alpha_{342}}$, $w_{22} = \frac{z_{43}^{\mathrm{T}} P_{z_{42}}(z_{21}+z_{23})}{l_{42}\sin\alpha_{342}} - \frac{z_{42}^{\mathrm{T}} P_{z_{43}}(z_{31}+z_{32})}{l_{43}\sin\alpha_{342}}$.

Now, by conducting linearization towards (3.25) in a small neighborhood of the origin $\{e_1 = 0, e_2 = 0, e_{41} = 0, e_{42} = 0\}$, one has

$$\dot{e}_4 = L_2(\alpha^*)e_4 + \bar{W}e_s, \tag{3.26}$$

where $L_2(\alpha^*) = F_4(e_4)|_{e_s=0,e_4=0}$ and $\bar{W} = W(e_4)|_{e_s=0,e_4=0}$. Then, one has

$$\mathrm{tr}(L_2(\alpha^*)) = (j_{11} + j_{22})|_{e_s=0,e_4=0} < 0, \tag{3.27}$$

$$\begin{aligned}&\det(L_2(\alpha^*)) = (j_{11}j_{22} - j_{12}j_{21})|_{e_s=0,e_4=0} \\ =&\frac{l^*_{41}(\sin\alpha^*_{241}\sin\alpha^*_{342} + \sin^2\alpha^*_{342} + \sin\alpha^*_{342}\sin\alpha^*_{341})}{l^*_{41}l^*_{42}l^*_{43}} \\ &+ \frac{l^*_{43}(\sin\alpha^*_{241}\sin\alpha^*_{342} + \sin^2\alpha^*_{241} + \sin\alpha^*_{241}\sin\alpha^*_{341})}{l^*_{42}l^*_{41}l^*_{43}} \\ &- \frac{l^*_{42}(\sin\alpha^*_{241}\sin\alpha^*_{341} + \sin\alpha^*_{341}\sin\alpha^*_{342} + \sin^2\alpha^*_{341})}{l^*_{41}l^*_{42}l^*_{43}}.\end{aligned}$$

where l^*_{ij} is the distance between agents i and j in the desired formation. Therefore, if $\det(L_2(\alpha^*)) > 0$, one has that $L_2(\alpha^*)$ is Hurwitz. By using the law of sines, $\sin\alpha^*_{124} > \sin\alpha^*_{412}$ and $\sin\alpha^*_{423} > \sin\alpha^*_{234}$ imply $l^*_{41} > l^*_{42}$ and $l^*_{43} > l^*_{42}$, respectively. Then, one can check that $\det(L_2(\alpha^*)) > 0$ if $l^*_{41} > l^*_{42}$ and $l^*_{43} > l^*_{42}$ hold because on the one hand

$$l^*_{43}\sin\alpha^*_{241}\sin\alpha^*_{341} > l^*_{42}\sin\alpha^*_{241}\sin\alpha^*_{341}, \tag{3.28}$$

$$l_{41}^* \sin\alpha_{341}^* \sin\alpha_{342}^* > l_{42}^* \sin\alpha_{341}^* \sin\alpha_{342}^*, \tag{3.29}$$

and on the other hand

$$\begin{aligned}\sin^2\alpha_{341}^* =& [\sin\alpha_{241}^*\cos\alpha_{342}^* + \cos\alpha_{241}^*\sin\alpha_{342}^*]^2 \\ =& \sin^2\alpha_{241}^*\cos^2\alpha_{342}^* + \cos^2\alpha_{241}^*\sin^2\alpha_{342}^* \\ &+ 2\sin\alpha_{241}^*\cos\alpha_{342}^*\cos\alpha_{241}^*\sin\alpha_{342}^*,\end{aligned} \tag{3.30}$$

and $l_{41}^*\sin^2\alpha_{342}^* > l_{42}^*\sin^2\alpha_{342}^*\cos^2\alpha_{241}^*$, $l_{43}^*\sin^2\alpha_{241}^* > l_{42}^*\sin^2\alpha_{241}^*\cos^2\alpha_{342}^*$ and

$$\begin{aligned}&l_{41}^*\sin\alpha_{241}^*\sin\alpha_{342}^* + l_{43}^*\sin\alpha_{241}^*\sin\alpha_{342}^* > 2l_{42}^*\sin\alpha_{241}^*\sin\alpha_{342}^* \\ &> 2l_{42}^*\sin\alpha_{241}^*\cos\alpha_{342}^*\cos\alpha_{241}^*\sin\alpha_{342}^*.\end{aligned}$$

By combining (3.17) and (3.26) together, one has the overall linearized 4-agent angle error dynamics

$$\dot{\bar{e}}_4 = \begin{bmatrix}\dot{e}_s \\ \dot{e}_4\end{bmatrix} = L_4(\alpha^*)\bar{e}_4 = \begin{bmatrix}L_1(\alpha^*) & 0 \\ \bar{W} & L_2(\alpha^*)\end{bmatrix}\begin{bmatrix}e_s \\ e_4\end{bmatrix} \tag{3.31}$$

When $L_1(\alpha^*)$ and $L_2(\alpha^*)$ are Hurwitz, one has that $L_4(\alpha^*)$ is also Hurwitz. When $L_4(\alpha^*)$ is Hurwitz, for an arbitrary positive definite matrix $Q_2 \in \mathbb{R}^{4\times4}$, there always exists positive definite matrix $P_2 \in \mathbb{R}^{4\times4}$ such that $-Q_2 = P_2L_4(\alpha^*) + L_4^{\mathrm{T}}(\alpha^*)P_2$. Design the Lyapunov function candidate as

$$V_2 = \bar{e}_4^{\mathrm{T}}P_2\bar{e}_4. \tag{3.32}$$

Taking the time-derivative of V_2 along (3.25) yields

$$\dot{V}_2 = -\bar{e}_4^{\mathrm{T}}Q_2\bar{e}_4 \leqslant -\lambda_{\min}(Q_2)\|\bar{e}_4\|^2 \leqslant -\frac{\lambda_{\min}(Q_2)}{\lambda_{\max}(P_2)}V_2. \tag{3.33}$$

Then, one has

$$\|e_4\|^2 \leqslant \|\bar{e}_4\|^2 \leqslant \frac{V_2}{\lambda_{\min}(P_2)} \leqslant \frac{V_2(0)}{\lambda_{\min}(P_2)}e^{-(\frac{\lambda_{\min}(Q_2)}{\lambda_{\max}(P_2)})t}, \tag{3.34}$$

which implies that the agent 4's angle error e_4 also converges to zero at an exponential rate. To guarantee that $\|W(e_4)\|$ is bounded and control law (3.24) is well defined, the collision between agent 4 and agents 1 to 3 should be avoided. Take

agent 1 as an example, one has

$$\begin{aligned}
&\|p_4(t)-p_1(t)\| = \|p_4(0)+\int_0^t u_4(s)\mathrm{d}s - p_1(0) - \int_0^t u_1(s)\mathrm{d}s\| \\
\geqslant &\|p_4(0)-p_1(0)\| - \int_0^t \|u_1(s)-u_4(s)\|\mathrm{d}s \\
\geqslant &l_{14}(0) - 2\int_0^t (|e_1(s)|+|e_{41}(s)|+|e_{42}(s)|)\mathrm{d}s.
\end{aligned}$$

Since $l_{14}(0)$ is sufficiently bounded away from zero, there always exists a finite time T such that in the time interval $[0,T)$ there is no collision between agent 4 and agent 1. Then, according to (3.22) and (3.34), one has

$$\begin{aligned}
&\|p_4(T)-p_1(T)\| \geqslant l_{14}(0) - 2\int_0^T (|e_1(s)|+|e_{41}(s)|+|e_{42}(s)|)\mathrm{d}s \\
\geqslant &l_{14}(0) - 4[\frac{\lambda_{\max}(P_1)}{\lambda_{\min}(Q_1)}\sqrt{\frac{V_1(0)}{\lambda_{\min}(P_1)}}(1-e^{-\frac{\lambda_{\min}(Q_1)}{2\lambda_{\max}(P_1)}T}) \\
&+ \frac{\lambda_{\max}(P_2)}{\lambda_{\min}(Q_2)}\sqrt{\frac{2V_2(0)}{\lambda_{\min}(P_2)}}(1-e^{-(\frac{\lambda_{\min}(Q_2)}{2\lambda_{\max}(P_2)})T})],
\end{aligned} \tag{3.35}$$

where we have used the fact that $|e_{41}|+|e_{42}| \leqslant \sqrt{2(e_{41}^2+e_{42}^2)} = \sqrt{2}\|e_4\|$. Since $V_1(0)$ and $V_2(0)$ are sufficiently small and $l_{14}(0)$ is sufficiently bounded away from zero, one has $\|p_4(T)-p_1(T)\| > 0$ since $l_{14}(0) > 4[\frac{\lambda_{\max}(P_1)}{\lambda_{\min}(Q_1)}\sqrt{\frac{V_1(0)}{\lambda_{\min}(P_1)}} + \frac{\lambda_{\max}(P_2)}{\lambda_{\min}(Q_2)}\sqrt{\frac{2V_2(0)}{\lambda_{\min}(P_2)}}]$. Then, we extend T to infinity. Because $e^{-\frac{\lambda_{\min}(Q_1)}{2\lambda_{\max}(P_1)}t} > 0$ and $e^{-(\frac{\lambda_{\min}(Q_2)}{2\lambda_{\max}(P_2)})t} > 0, \forall t > 0$, one has that $l_{41}(t) = \|p_4(t)-p_1(t)\| > 0$ for $t > 0$. On the other hand, since the initial angle errors $e_{41}(0)$ and $e_{42}(0)$ are sufficiently small and $e_1(t)$, $e_2(t)$, $e_{41}(t)$ and $e_{42}(t)$ converge at an exponential speed, $\alpha_{241}(t)$ and $\alpha_{342}(t)$ will be bounded away from 0 and π. Therefore, $\|W(e_4)\|$ is bounded and (3.25) is well defined. The proof for 4-agent formation is completed. □

Now, we present the main result for agents 4 to N.

Theorem 3.9 (Stability of all the agents)**.** *Consider a formation of $N > 3$ agents, each of which is governed by (3.1). Suppose $e_i(0), i = 1,2,3$ are sufficiently small and the sub-formation of 1, 2, 3 is governed by (3.9). For agent $i, 4 \leqslant i \leqslant N$, if the initial distances $l_{ij_1}(0)$, $l_{ij_2}(0)$, $l_{ij_3}(0)$ are sufficiently bounded away from zero, the initial angle errors $e_{i1}(0)$ and $e_{i2}(0)$ are sufficiently small and $\alpha^*_{j_3ij_1} = \alpha^*_{j_2ij_1} + \alpha^*_{j_3ij_2}$, $\sin\alpha^*_{j_1j_2i} > \sin\alpha^*_{ij_1j_2}$, $\sin\alpha^*_{ij_2j_3} > \sin\alpha^*_{j_2j_3i}$, then under (3.23), the formation achieves its desired shape exponentially.*

Proof. From Lemma 3.8, 4-agent formation achieves the desired shape exponen-

tially. Suppose for a $4 < k < N$, the k-agent formation converges to the desired shape exponentially. We need to prove that for $(k+1)$-agent formation, the relative angle errors $e_{(k+1)1} = \alpha_{j_1(k+1)j_2} - \alpha^*_{j_1(k+1)j_2}$ and $e_{(k+1)2} = \alpha_{j_2(k+1)j_3} - \alpha^*_{j_2(k+1)j_3}$ converges to zero exponentially. Similar to the proof from (3.24) to (3.33), one has that the angle errors $e_{(k+1)1}$ and $e_{(k+1)2}$ exponentially converge to zero. Therefore, the control algorithm (3.23) can locally stabilize agent $k+1$, i.e., the $(k+1)$-agent formation converge to the desired shape exponentially. So, from induction, N-agent formation converges to the desired formation shape exponentially. The proof for Theorem 3.9 is completed. □

Remark 3.10. Note that the control laws (3.9) and (3.23) can be described by a unified form

$$u_i = -\sum\nolimits_{(j,i,k)\in\mathcal{A}} (\alpha_{jik} - \alpha^*_{jik})(z_{ij} + z_{ik}), \tag{3.36}$$

where $\mathcal{A} = \{(1,2,3),(2,3,1),(3,1,2),(1,4,2),(2,4,3),\cdots,(j_1,k,j_2),(j_2,k,j_3),\cdots,(i_1,N,i_2),(i_2,N,i_3)\}, j_1 < k, j_2 < k, j_3 < k, j_1 \neq j_2 \neq j_3$. Therefore, the unified control algorithm (3.36) can locally stabilize the angle rigid formation constructed through a sequence of Type-I vertex additions (Case 3) from a generically angle rigid 3-vertex angularity. Because we aim at obtaining local stability for multi-agent formations in Section IV, we only consider the range of the desired angles belonging to $(0,\pi)$ in (3.4)-(3.8), and the case of $\alpha_i(0) \in (\pi, 2\pi), \alpha^*_i \in (\pi, 2\pi)$ can be similarly obtained. However, to achieve a general infinitesimally and minimally angle rigid formation, one can use the gradient-based control law

$$\dot{p} = u = -\left(\frac{\partial V_3}{\partial p}\right)^\top = -R_a^\top(p)(\alpha - \alpha^*), \tag{3.37}$$

where $V_3 = 0.5(\alpha-\alpha^*)^\top(\alpha-\alpha^*)$, p, u, α are the stack vectors of p_i, u_i, α_{jik}, respectively. It follows that $\dot{V}_3 = -(\alpha-\alpha^*)^\top R_a(p) R_a^\top(p)(\alpha-\alpha^*)$. Because $R_a(p)R_a^\top(p)$ is positive definite when p is in a small neighborhood of the desired formation, one has the local convergence of $(\alpha - \alpha^*)$.

Remark 3.11. Although each agent's position in (3.1) is described in the global coordinate system, it is not used in the control algorithm (3.36). The control algorithm (3.36) can be realized in each agent's local coordinate system since (3.36) can be equivalently written in agent i's local coordinate frame

$$R_g^b u_i = -\sum\nolimits_{(j,i,k)\in\mathcal{A}} (\alpha_{jik} - \alpha^*_{jik}) R_g^b (z_{ij} + z_{ik}), \tag{3.38}$$

where $R_g^b \in SO(2)$ is the rotation matrix from the global coordinate frame to agent i's local coordinate frame, $R_g^b u_i$ is the controller input in agent i's local coordinate frame, and $R_g^b z_{ij}, R_g^b z_{ik}$ are the local bearings measured in agent i's local coordinate frame. Since $(\alpha_{jik} - \alpha^*_{jik})$ is a scalar and α_{jik} is the same under

different coordinate frames, (3.38) and (3.36) are equivalent.

Now we have studied the formation for single-integrator formations, in the following section, we look at double-integrator formations.

3.3 Angle-only formation control for double-integrators

Consider N mobile agents moving in the plane. Agents are labeled from 1 to N and $\mathcal{V} = \{1, 2, \cdots, N\}$ is the index set. The dynamics of each agent $i, i \in \mathcal{V}$ are modeled by

$$\begin{aligned} \dot{p}_i &= v_i, \\ \dot{v}_i &= u_i, \end{aligned} \tag{3.39}$$

where $p_i \in \mathbb{R}^2$ denotes the position of agent i with respect to a fixed global coordinate frame, $v_i \in \mathbb{R}^2$ is its velocity in the same frame, and $u_i \in \mathbb{R}^2$ is its control input to be determined. In this section, we discuss formation stabilization using identical and distinct control gains, respectively.

3.3.1 The case of identical control gains

We first consider the situation when all agents have the same velocity feedback gain. Specifically, we design the formation stabilization law as

$$u_i = -k_s v_i - \sum\nolimits_{(j,i,k)\in\mathcal{A}} (\alpha_{jik} - \alpha^*_{jik})(z_{ij} + z_{ik}), \tag{3.40}$$

where the gain $k_s > 0$ is identical for all the agents. To obtain the convergence of angle errors under (3.40), we need to analyze their dynamics. First, we assume that $l_{ij}(0), l_{ik}(0)$ and $\sin\alpha_{jik}(0), \forall(j,i,k) \in \mathcal{A}$ are bounded away from zero where $l_{ij}(t) = \|p_i(t) - p_j(t)\|$. According to (3.40), when the initial velocity $v_i(0)$ is bounded and $l_{ij}(0) \neq 0, l_{ik}(0) \neq 0$, the control input $u_i(0)$ will be bounded. Therefore, $\exists T_1 > 0$ such that for $t \in [0, T_1)$, $l_{ij}(t), l_{ik}(t)$ and $\sin\alpha_{jik}(t), \forall(j,i,k) \in \mathcal{A}$ are bounded away from zero. We now analyze the angle error dynamics for $t \in [0, T_1)$ and the extension of T_1 to infinity will be discussed later. Since $\frac{\mathrm{d}(\cos\alpha_{jik})}{\mathrm{d}t} = -(\sin\alpha_{jik})\dot{\alpha}_{jik}$, one has

$$\dot{\alpha}_{jik} = \left(\frac{\mathrm{d}(\cos\alpha_{jik})}{\mathrm{d}t}\right) / (-\sin\alpha_{jik}). \tag{3.41}$$

Also, one has

$$\begin{aligned}\frac{\mathrm{d}(\cos\alpha_{jik})}{\mathrm{d}t} =& \frac{\mathrm{d}(z_{ij}^T z_{ik})}{\mathrm{d}t} = \dot{z}_{ij}^T z_{ik} + z_{ij}^T \dot{z}_{ik} \\ =& z_{ik}^T \frac{P_{z_{ij}}}{l_{ij}}(v_j - v_i) + z_{ij}^T \frac{P_{z_{ik}}}{l_{ik}}(v_k - v_i),\end{aligned} \tag{3.42}$$

where $P_{z_{ij}} = I_2 - z_{ij} z_{ij}^T$, $I_2 \in \mathbb{R}^{2\times 2}$ is the 2×2 identity matrix. Substituting (3.42) into (3.41) yields

$$\begin{aligned}\dot{\alpha}_{jik} =& - z_{ik}^T \frac{P_{z_{ij}}}{l_{ij}\sin\alpha_{jik}} v_j - z_{ij}^T \frac{P_{z_{ik}}}{l_{ik}\sin\alpha_{jik}} v_k \\ &+ (z_{ik}^T \frac{P_{z_{ij}}}{l_{ij}\sin\alpha_{jik}} + z_{ij}^T \frac{P_{z_{ik}}}{l_{ik}\sin\alpha_{jik}}) v_i.\end{aligned} \tag{3.43}$$

Let us choose the following error variables as the system state

$$X = [e_1, e_2, e_{41}, e_{42}, \cdots, e_{N1}, e_{N2}, v_1^T, \cdots, v_N^T]^T \in \mathbb{R}^{4N-4} \tag{3.44}$$

which consists of $2N-4$ independent angle errors and all agents' velocities. Then, from (3.40) and (3.43), one can check that the closed-loop dynamics satisfy

$$\dot{X} = \begin{bmatrix} 0_{(2N-4)\times(2N-4)} & R(X) \\ B(X) & -k_s \otimes I_{2N} \end{bmatrix} X = D_1(X) X, \tag{3.45}$$

where $R(X) \in \mathbb{R}^{(2N-4)\times 2N}$, $B(X) \in \mathbb{R}^{2N\times(2N-4)}$ and

$$R(X) = \begin{bmatrix} N_{213}+N_{312} & -N_{312} & -N_{213} & 0 & \cdots & 0 \\ -N_{321} & N_{321}+N_{123} & -N_{123} & 0 & \cdots & 0 \\ \cdots & \cdots & \cdots & \cdots & \ddots & \cdots \\ -N_{j_1 i j_2} & N_{j_1 i j_2} + N_{j_2 i j_1} & -N_{j_2 i j_1} & \cdots & \cdots & \cdots \end{bmatrix} \tag{3.46}$$

with $N_{jik} = z_{ij}^T \frac{P_{z_{ik}}}{l_{ik}\sin\alpha_{jik}} \in \mathbb{R}^{1\times 2}, j, i, k \in \mathcal{V}$, and

$$B(X) = \begin{bmatrix} -z_{12}-z_{13} & 0 & 0 & 0 & \ldots & 0 \\ 0 & -z_{21}-z_{23} & 0 & 0 & \ldots & 0 \\ z_{31}+z_{32} & z_{31}+z_{32} & 0 & 0 & \ldots & 0 \\ 0 & 0 & -z_{41}-z_{42} & -z_{42}-z_{43} & \ldots & 0 \\ \ldots & \ldots & \ldots & \ldots & \ldots & \ldots \end{bmatrix}. \tag{3.47}$$

Now, we linearize (3.45) around the desired equilibrium $X = 0$ to study its local stability. By linearizing (3.45) around $X = 0$ for $t \in [0, T_1)$, one has

$$\begin{aligned}\dot{X} &= [\frac{\partial [D_1(X)X]}{\partial X}|_{X=0}]X = [D_1(X)|_{X=0}]X \\ &= \begin{bmatrix} 0_{(2N-4)\times(2N-4)} & R(X)|_{X=0} \\ B(X)|_{X=0} & -k_s \otimes I_{2N} \end{bmatrix} X = D_1^* X. \end{aligned} \tag{3.48}$$

For notation conciseness in the following analysis, a quantity with the superscript $*$ means that it is evaluated at $X = 0$. We then show that system (3.48) is stable by checking that $D_1^* \in \mathbb{R}^{4N-4}$ is Hurwitz through examining its eigenvalues. Consider the characteristic polynomial of D_1^*

$$|\lambda I_{4N-4} - D_1^*| = \begin{vmatrix} \lambda I_{2N-4} & -R^* \\ -B^* & (\lambda + k_s) \otimes I_{2N} \end{vmatrix}, \tag{3.49}$$

where $\lambda \in \mathbb{C}$ is an eigenvalue of D_1^*. According to the Schur complement theorem[46], one has

$$\begin{aligned} &|\lambda I_{4N-4} - D_1^*| \\ =&(\lambda + k_s)^{2N} \text{det}[\lambda I_{2N-4} - \frac{R^* B^*}{\lambda + k_s}] \\ =&(\lambda + k_s)^{2N} \text{det}[\frac{\lambda(\lambda + k_s) I_{2N-4} - R^* B^*}{\lambda + k_s}] \\ =&(\lambda + k_s)^{4} \text{det}[\lambda(\lambda + k_s) I_{2N-4} - R^* B^*]. \end{aligned} \tag{3.50}$$

Hence, $-k_s$ is a stable eigenvalue of geometric multiplicity at least 4. To find the other eigenvalues, we now analyze the structure of the matrix $R^* B^*$. For the first three-agent case, one has the corresponding sub-matrix

$$[RB]_{(1:2,1:2)} = \tilde{F}_1 = \begin{bmatrix} a_{11} & a_{12} \\ a_{21} & a_{22} \end{bmatrix}, \tag{3.51}$$

where $[RB]_{(i:j,k:m)}$ is the sub-matrix selecting rows from i to j and columns from k to m from the matrix RB. Therefore, it follows that

$$a_{11} = (N_{213} + N_{312})(-z_{12} - z_{13}) - N_{213}(z_{31} + z_{32}),$$

$$a_{12} = N_{312}(z_{21} + z_{23}) - N_{213}(z_{31} + z_{32}),$$

$$a_{21} = N_{321}(z_{12} + z_{13}) - N_{123}(z_{31} + z_{32}),$$

$$a_{22} = (N_{321} + N_{123})(-z_{21} - z_{23}) - N_{123}(z_{31} + z_{32}).$$

Since $P_{z_{ij}} z_{ij} = 0$ and $N_{312} z_{12} = 0$, one obtains

$$\tilde{F}_1 = \begin{bmatrix} N_{213}(z_{21} + z_{23}) - N_{312} z_{13} & (N_{312} + N_{213}) z_{23} \\ (N_{321} + N_{123}) z_{13} & N_{123}(z_{13} + z_{12}) - N_{321} z_{23} \end{bmatrix}. \tag{3.52}$$

Substituting the definition of N_{jik} given after (3.46) into a_{11} yields

$$\begin{aligned} a_{11} &= \frac{z_{12}^T P_{z_{13}} (z_{21} + z_{23})}{l_{13} \sin\alpha_1} - \frac{z_{13}^T P_{z_{12}} z_{13}}{l_{12} \sin\alpha_1} \\ &= \frac{p_{12}^T P_{z_{13}}}{l_{12} l_{13} \sin\alpha_1} (\frac{p_{21}}{l_{21}} + \frac{p_{13} - p_{12}}{l_{23}}) - \frac{p_{13}^T P_{z_{12}} p_{13}}{l_{12} l_{13}^2 \sin\alpha_1} \\ &= \frac{1}{\sin\alpha_1} (-\frac{p_{12}^T P_{z_{13}} p_{12}}{l_{12} l_{13} l_{23}} - \frac{p_{12}^T P_{z_{13}} p_{12}}{l_{12}^2 l_{13}} - \frac{p_{13}^T P_{z_{12}} p_{13}}{l_{12} l_{13}^2}) \\ &= -\frac{\sin\alpha_1}{l_{12} l_{13} l_{23}} (l_{12}^2 + l_{12} l_{23} + l_{13} l_{23}), \end{aligned} \tag{3.53}$$

where $p_{ij} = p_j - p_i, i, j \in \mathcal{V}$. By using the law of sines $\frac{\sin\alpha_1}{l_{23}} = \frac{\sin\alpha_2}{l_{13}} = \frac{\sin\alpha_3}{l_{21}}$, one has

$$a_{11} = -(\frac{\sin\alpha_1}{l_{12}} + \frac{\sin\alpha_1}{l_{13}} + \frac{\sin\alpha_3}{l_{13}}) = -(g_1 + f_{13}), \tag{3.54}$$

where we define $f_{ij} = \frac{\sin\alpha_j}{l_{ij}}, g_i = (\sin\alpha_i)(\frac{1}{l_{i(i+1)}} + \frac{1}{l_{i(i-1)}}), i, j \in \{1, 2, 3\}$, and $(i-1) \in \mathcal{N}_i$, $(i+1) \in \mathcal{N}_i$. Similarly, by using simplification and the law of sines, one also has

$$a_{22} = -\frac{\sin\alpha_2}{l_{12} l_{13} l_{23}} (l_{12}^2 + l_{12} l_{13} + l_{23} l_{13}) = -(g_2 + f_{23}). \tag{3.55}$$

Then, we calculate

$$\begin{aligned} a_{12} &= (\frac{p_{13}^T P_{z_{12}}}{l_{12} l_{13} \sin\alpha_1} + \frac{p_{12}^T P_{z_{13}}}{l_{12} l_{13} \sin\alpha_1}) \frac{p_{21} + p_{13}}{l_{23}} \\ &= \frac{l_{13}^2 - l_{12}^2 - \frac{p_{13}^T p_{12} p_{12}^T p_{13}}{l_{12}^2} + \frac{p_{12}^T p_{13} p_{13}^T p_{12}}{l_{13}^2}}{l_{12} l_{13} l_{23} \sin\alpha_1} \\ &= \frac{(l_{13}^2 - l_{12}^2) \sin\alpha_1}{l_{12} l_{13} l_{23}}. \end{aligned} \tag{3.56}$$

By using the law of sines $\frac{\sin\alpha_1}{l_{23}} = \frac{\sin\alpha_2}{l_{13}} = \frac{\sin\alpha_3}{l_{21}}$, one has

$$a_{12} = f_{12} - f_{13}. \tag{3.57}$$

Similarly, one has

$$a_{21} = \frac{(l_{23}^2 - l_{21}^2)\sin\alpha_2}{l_{12}l_{13}l_{23}} = f_{21} - f_{23}. \tag{3.58}$$

Note that the matrix $\tilde{F}_1$ is equal to F_s defined in Subsection 3.2. Then, writing down all the other elements in matrix RB, one finds that RB has a block lower triangular structure. Consider that for agent $i, i \geqslant 4$, there are two desired angles $\alpha^*_{j_1ij_2}$ and $\alpha^*_{j_2ij_3}$ where $j_1, j_2, j_3 < i$ are the three neighboring agents whom the agent i will measure the directions with respect to. Then, one has

$$[RB]_{(2i-3:2i-4,2i-3:2i-4)} = \tilde{F}_i = \tag{3.59}$$
$$\begin{bmatrix} -(N_{j_1ij_2} + N_{j_2ij_1})(z_{ij_1} + z_{ij_2}) & -(N_{j_1ij_2} + N_{j_2ij_1})(z_{ij_2} + z_{ij_3}) \\ -(N_{j_2ij_3} + N_{j_3ij_2})(z_{ij_1} + z_{ij_2}) & -(N_{j_2ij_3} + N_{j_3ij_2})(z_{ij_2} + z_{ij_3}) \end{bmatrix}.$$

By using similar simplification as for the first three agents, one also has

$$\tilde{F}_i = \begin{bmatrix} \bar{\omega}_1 & \bar{r}_{12} \\ \bar{r}_{21} & \bar{\omega}_2 \end{bmatrix} = \tag{3.60}$$
$$\begin{bmatrix} -\sin\alpha_{j_1ij_2}(\frac{1}{l_{ij_1}} + \frac{1}{l_{ij_2}}) & \frac{\sin\alpha_{j_2ij_3}}{l_{ij_2}} - \frac{\sin\alpha_{j_1ij_2} + \sin\alpha_{j_1ij_3}}{l_{ij_1}} \\ \frac{\sin\alpha_{j_1ij_2}}{l_{ij_2}} - \frac{\sin\alpha_{j_2ij_3} + \sin\alpha_{j_1ij_3}}{l_{ij_3}} & -\sin\alpha_{j_2ij_3}(\frac{1}{l_{ij_3}} + \frac{1}{l_{ij_2}}) \end{bmatrix}.$$

Now, we find that $\tilde{F}_i, 4 \leqslant i \leqslant N$ in (3.60) is equal to F_i defined in Subsection 3.2. By checking other matrix elements, one obtains that the matrix $R(X)B(X)$ in the closed-loop error dynamics (3.45) of double-integrators is the same as the system matrix $A(e_a)$ in the angle dynamics $\dot{e}_a = A(e_a)e_a$ of single-integrators (e_a denotes the column vector consisting of all the $2N-4$ independent angle errors), i.e.,

$$R(X)B(X) = A(e_a) = \begin{bmatrix} \tilde{F}_1 & 0 & 0 & \cdots & 0 \\ ** & \tilde{F}_4 & 0 & \cdots & 0 \\ ** & ** & \tilde{F}_5 & \cdots & 0 \\ \cdots & \cdots & \cdots & \ddots & \vdots \\ ** & ** & ** & ** & \tilde{F}_N \end{bmatrix}, \tag{3.61}$$

which is an important and convenient fact for the later analysis. We summarize this using the following remark about matrices $\tilde{F}_i, i = 1, 4, ..., N$.

Remark 3.12. Under the angle set $\mathcal{A}$ and control law (3.40), $R(X)B(X)$ in the closed-loop error dynamics (3.45) of double-integrators is the same as the system matrix $A(e_a)$ in the angle dynamics $\dot{e}_a = A(e_a)e_a$ of single-integrators. Therefore, according to [22, Theorems 7 and 8], the matrix $\tilde{F}_1^*$ is always Hurwitz and $\tilde{F}_i^*, \forall 4 \leqslant i \leqslant N$ are Hurwitz if $\alpha^*_{j_1ij_3} = \alpha^*_{j_1ij_2} + \alpha^*_{j_2ij_3}$, $\sin\alpha^*_{j_1j_2i} > \sin\alpha^*_{ij_1j_2}$ and $\sin\alpha^*_{ij_2j_3} > \sin\alpha^*_{j_2j_3i}$.

In the case of single-integrators, $A(e_a)|_{e_a=0}$ being Hurwitz is sufficient to make the angle-based formation system $e_a = A(e_a)e_a$ locally and exponentially stable. However, this is not sufficient for double-integrators due to (3.50). Note that in the case of double-integrators, according to (3.50) and (3.61), the necessary and sufficient condition to make (3.48) exponentially stable is that the solutions of

$$\det[\lambda(\lambda + k_s)I_2 - \tilde{F}_i^*] = 0, i = 1, 4, 5, \cdots, N, \tag{3.62}$$

have negative real parts. Before presenting the main result, we provide an example to illustrate that improper selection of gain k_s will make a stable angle-controlled single-integrator system become unstable in angle-controlled double-integrator system.

Example 3.1. The desired angles: $\alpha_{123}^* = \pi/2, \alpha_{312}^* = \pi/4, \alpha_{231}^* = \pi/4, \alpha_{142}^* = \arctan(1.2), \alpha_{243}^* = \arctan(0.3), \alpha_{251}^* = \arctan(3/\sqrt{10}), \alpha_{452}^* = \arctan(1.2)$. The initial states: $p_1(0) = [0.5, 0.1]^T, p_2(0) = [0.1, 1.2]^T, p_3(0) = [-1.2, 0.2]^T, p_4(0) = [0.1, 2.0]^T, p_5(0) = [-1.4, 1.2]^T, \dot{p}_1(0) = [-0.1, -0.2]^T, \dot{p}_2(0) = [0.2, -0.1]^T, \dot{p}_3(0) = [-0.1, -0.1]^T$, $\dot{p}_4(0) = [-0.1, 0.4]^T, \dot{p}_5(0) = [0.1, 0.1]^T$.

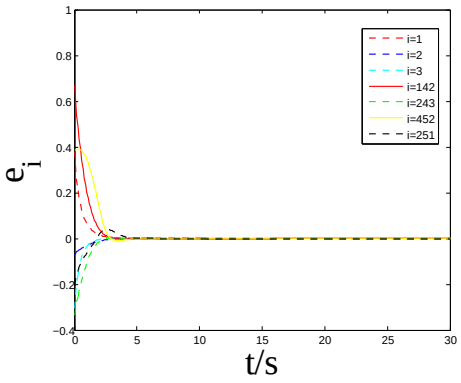

Figure 3.4: *Evolution of angle errors for single-integrator dynamics with Hurwitz matrices* $\tilde{F}_i^*, i = 1, 4, 5$.

This example illustrates that the proper selection of velocity damping gain k_s in angle-controlled double-integrator system is important. Now, we present the remaining results.

Lemma 3.13. *The dynamical system (3.48) is asymptotically stable if and only if*

$$k_s^2 \mathrm{Re}(\lambda_{ij}) + (\mathrm{Im}(\lambda_{ij}))^2 < 0, j = 1, 2 \tag{3.63}$$

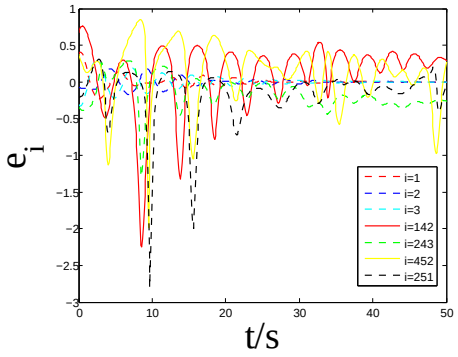

Figure 3.5: *Evolution of angle errors for double-integrator dynamics with gain* $k_s = 0.2$.

holds for $\forall i = 1, 4, \cdots, N$, *where* λ_{i1} *and* λ_{i2} *are the two conjugated eigenvalues of the matrix* $\tilde{F}_i^*$, *and* Re() *and* Im() *denote the real and imaginary parts of a complex number, respectively.*

Proof. Note that one can always find a nonsingular matrix $\bar{P} \in \mathbb{C}^{2\times 2}$ such that

$$\tilde{F}_i^* = \bar{P} \begin{bmatrix} \lambda_{i1} & ** \\ 0 & \lambda_{i2} \end{bmatrix} \bar{P}^{-1}, \tag{3.64}$$

where $**$ represents an element which does not affect the following analysis. Then, (3.62) can be written into

$$\begin{aligned} &\det[\lambda(\lambda + k_s)I_2 - \tilde{F}_i^*] \\ &= \det\{\bar{P} \begin{bmatrix} \lambda(\lambda + k_s) - \lambda_{i1} & ** \\ 0 & \lambda(\lambda + k_s) - \lambda_{i2} \end{bmatrix} \bar{P}^{-1}\} \\ &= [\lambda(\lambda + k_s) - \lambda_{i1}][\lambda(\lambda + k_s) - \lambda_{i2}], \end{aligned} \tag{3.65}$$

which implies that the stability of (3.48) depends on the solutions of $\lambda(\lambda + k_s) - \lambda_{ij} = 0, i = 1, 4, \cdots, N, j = 1, 2$. Note that λ_{ij} can be a complex number. According to [66, Theorem 40.1], (3.63) is the necessary and sufficient condition to guarantee that the two solutions of $\lambda(\lambda + k_s) - \lambda_{ij} = 0$ have negative real parts. □

Now, we further explore the condition (3.63) by calculating λ_{i1} and λ_{i2}. According to Lemma 1, we have that $A(e_a)|_{e_a=0} = R^*B^*$ is Hurwitz which implies that $\mathrm{Re}(\lambda_{ij}) < 0, \forall i = 1, 4, \cdots, N, j = 1, 2$. According to Lemma 3.13, when $\mathrm{Im}(\lambda_{ij}) = 0$, $\lambda(\lambda + k_s) - \lambda_{ij} = 0$ will always have two solutions with negative real parts.

• For the case of $\text{Im}(\lambda_{i1}) = \text{Im}(\lambda_{i2}) = 0$ in the first three agents, we require for $\tilde{F}_1^*$ in (3.51) that

$$\begin{aligned}\Delta_1^* &= (a_{11}^* - a_{22}^*)^2 + 4a_{12}^* a_{21}^* \\ &= (g_1^* + f_{13}^* - g_2^* - f_{23}^*)^2 + 4(f_{12}^* - f_{13}^*)(f_{21}^* - f_{23}^*) \geqslant 0.\end{aligned} \tag{3.66}$$

By using law of sines $\frac{\sin\alpha_1^*}{l_{23}^*} = \frac{\sin\alpha_2^*}{l_{13}^*} = \frac{\sin\alpha_3^*}{l_{12}^*}$ and simplification, we can conclude that (3.66) can be written as

$$\begin{aligned}&(\frac{\sin\alpha_1^*}{\sin\alpha_2^*} + \frac{\sin\alpha_1^*}{\sin\alpha_3^*} + \frac{\sin\alpha_3^*}{\sin\alpha_2^*} - \frac{\sin\alpha_2^*}{\sin\alpha_1^*} - \frac{\sin\alpha_2^*}{\sin\alpha_3^*} - \frac{\sin\alpha_3^*}{\sin\alpha_1^*})^2 \\ &+ 4(\frac{\sin\alpha_2^*}{\sin\alpha_3^*} - \frac{\sin\alpha_3^*}{\sin\alpha_2^*})(\frac{\sin\alpha_1^*}{\sin\alpha_3^*} - \frac{\sin\alpha_3^*}{\sin\alpha_1^*}) \geqslant 0.\end{aligned} \tag{3.67}$$

Similarly for agents 4 to N, to guarantee $\text{Im}(\lambda_{ij}) = 0, i = 4, \cdots, N, j = 1, 2$ for $\tilde{F}_i$ defined in (3.60), one has

$$\Delta_i^* = (\bar{\omega}_1^* - \bar{\omega}_2^*)^2 + 4\bar{r}_{12}^*\bar{r}_{21}^* \geqslant 0. \tag{3.68}$$

Multiplying $l_{ij_2}^{*2}$ at both sides of (3.68) and simplification yields

$$\begin{aligned}&[(\frac{\sin\alpha_{j_2j_1i}^*}{\sin\alpha_{ij_2j_1}^*} + 1)\sin\alpha_{j_1ij_2}^* - (\frac{\sin\alpha_{ij_3j_2}^*}{\sin\alpha_{ij_2j_3}^*} + 1)\sin\alpha_{j_2ij_3}^*]^2 \\ &+ 4(\frac{(\sin\alpha_{j_1ij_2}^* + \sin\alpha_{j_1ij_3}^*)\sin\alpha_{j_2j_1i}^*}{\sin\alpha_{ij_2j_1}^*} - \sin\alpha_{j_2ij_3}^*) \\ &\times (\frac{(\sin\alpha_{j_2ij_3}^* + \sin\alpha_{j_1ij_3}^*)\sin\alpha_{ij_3j_2}^*}{\sin\alpha_{ij_2j_3}^*} - \sin\alpha_{j_1ij_2}^*) \geqslant 0.\end{aligned} \tag{3.69}$$

• For the case of $\text{Im}(\lambda_{ij}) \neq 0$, since $\text{Im}(\lambda_{i1}) = -\text{Im}(\lambda_{i2})$ and $\text{Re}(\lambda_{i1}) = \text{Re}(\lambda_{i2}) < 0$, the stability condition (3.63) can be written as

$$\Delta_i^* < 0 \ \ and \ \ 4k_s^2\text{Re}(\lambda_{ij}) - \Delta_i^* < 0, \tag{3.70}$$

where $i = 1, 4, \cdots, N$, $j = 1, 2$, and $\text{Re}(\lambda_{ij}) = \frac{a_{11}^* + a_{22}^*}{2}$ when $i = 1$ and $\text{Re}(\lambda_{ij}) = \frac{\bar{\omega}_1^* + \bar{\omega}_2^*}{2}$ when $i \geqslant 4$. By combining the above two cases, one obtains the conditions such that all the eigenvalues of D_1^* have negative real parts, which implies the stability of the closed-loop system. In summary, we has the following result.

Theorem 3.14. *Consider that N agents of double-integrator dynamics (3.39) are governed by (3.40) with the identical gain k_s, the initial errors $X(0)$ are sufficiently small and the initial distances are bounded away from zero. The formation stabilization defined in (3.4)-(3.8) can be locally achieved if and only if (3.63) holds*

for $\forall i = 1, 4, \cdots, N$. *Moreover, (3.63) holds if and only if for each* $i = 1, 4, \cdots, N$, $\Delta_i^* \geqslant 0$ *or (3.70) holds.*

Proof. Note that since D_1^* is Hurwitz, $X = 0$ is the only equilibrium of (3.48), which is exponentially stable. We now analyze the evolution of the distance and angle errors among agents to guarantee that the nonlinear closed-loop dynamics (3.45) are well-defined because the collinearity case $\sin\alpha_{jik} = 0, (j, i, k) \in \mathcal{A}$ and collision case $l_{ij} = 0, l_{ik} = 0$ will make (3.41) and (3.42) invalid, respectively. For $t \in [0, T_1)$, since D_1^* is Hurwitz, for an arbitrary positive definite matrix $Q_1 \in \mathbb{R}^{(4N-4)\times(4N-4)}$, there always exists a unique positive definite matrix $P_1 \in \mathbb{R}^{(4N-4)\times(4N-4)}$ such that $D_1^{*T}P_1 + P_1D_1^* = -Q_1$. Now, for system (3.48), we design the Lyapunov function candidate as

$$V_1 = X^T P_1 X. \tag{3.71}$$

Taking the time-derivative of (3.71) yields

$$\dot{V}_1 = -X^T Q_1 X \leqslant -\frac{\lambda_{\min}(Q_1)}{\lambda_{\max}(P_1)} V_1. \tag{3.72}$$

Then, it follows that $\|X(t)\|^2 \leqslant \frac{V_1(t)}{\lambda_{\min}(P_1)} \leqslant \frac{V_1(0)}{\lambda_{\min}(P_1)} e^{-\frac{\lambda_{\min}(Q_1)}{\lambda_{\max}(P_1)}t}$. Since $\|X(t)\|^2 = e_1^2 + e_2^2 + e_{41}^2 + \cdots + e_{N1}^2 + e_{N2}^2 + \sum_{i=1}^N \|v_i\|^2$, one has that for $(j, i, k) \in \mathcal{A}$,

$$|\alpha_{jik}(t) - \alpha_{jik}^*| \leqslant \|X(t)\| \leqslant \sqrt{\frac{V_1(0)}{\lambda_{\min}(P_1)}} e^{-\frac{\lambda_{\min}(Q_1)}{2\lambda_{\max}(P_1)}t}, \tag{3.73}$$

Similarly, for the velocity of agent i, one has

$$\|v_i(t)\| \leqslant \|X(t)\| \leqslant \sqrt{\frac{V_1(0)}{\lambda_{\min}(P_1)}} e^{-\frac{\lambda_{\min}(Q_1)}{2\lambda_{\max}(P_1)}t}. \tag{3.74}$$

Note that (3.73) implies

$$\alpha_{jik}^* - \sqrt{\frac{V_1(0)}{\lambda_{\min}(P_1)}} \leqslant \alpha_{jik}(t) \leqslant \alpha_{jik}^* + \sqrt{\frac{V_1(0)}{\lambda_{\min}(P_1)}}. \tag{3.75}$$

According to (3.74), one has

$$\begin{aligned} l_{ij}(t) &= l_{ij}(0) + \int_0^t \dot{l}_{ij}(\tau)d\tau = l_{ij}(0) + \int_0^t z_{ij}^T(v_j - v_i)d\tau \\ &\geqslant l_{ij}(0) - \int_0^t (\|v_j\| + \|v_i\|)d\tau \\ &\geqslant l_{ij}(0) - 4\sqrt{\frac{V_1(0)}{\lambda_{\min}(P_1)}} \frac{\lambda_{\max}(P_1)}{\lambda_{\min}(Q_1)} (1 - e^{-\frac{\lambda_{\min}(Q_1)}{2\lambda_{\max}(P_1)}t}). \end{aligned} \tag{3.76}$$

Therefore, if

$$\alpha^*_{jik} > \sqrt{\frac{V_1(0)}{\lambda_{\min}(P_1)}} \text{ and } \alpha^*_{jik} + \sqrt{\frac{V_1(0)}{\lambda_{\min}(P_1)}} < \pi, \tag{3.77}$$

then no collinearity happens among j, i, k. If

$$l_{ij}(0) > 4\sqrt{\frac{V_1(0)}{\lambda_{\min}(P_1)}}\frac{\lambda_{\max}(P_1)}{\lambda_{\min}(Q_1)}, \tag{3.78}$$

no collision will happen between agents i and j. Because α^*_{jik} is bounded away from zero and π, and $l_{ij}(0)$ is bounded away from zero, and $X(0), V_1(0)$ are sufficiently small, (3.77) and (3.78) holds for $t \in [0, T_1)$. Assume that there exists a collision or collinearity in $[T_1, \infty)$ and denote the first time that it happens by T_2^-. Then, one has the following two cases.

• A collision between i and j happens at T_2^-. Since no collision and collinearity happens in $[0, T_2^-)$, the closed-loop system is well-defined in $[0, T_2^-)$. Following the calculations in (3.71)-(3.76), one has that $l_{ij}(T_2^-) \geqslant l_{ij}(0) - 4\sqrt{\frac{V_1(0)}{\lambda_{\min}(P_1)}}\frac{\lambda_{\max}(P_1)}{\lambda_{\min}(Q_1)} > 0$ which is bounded away from zero. This implies a contradiction with the assumption that collision happens at T_2^-. Thus, no collision between agents i and j happens at T_2^-.

•A collinearity among j, i, k happens at T_2^-. Then, one has that $\alpha_{jik}(T_2^-)$ will approach zero or π. Since no collinearity and collision happens in $[0, T_2^-)$, using (3.75), one has that $\alpha_{jik}(T_2^-)$ is bounded away from zero and π which implies a contradiction. Therefore, no collinearity will occur among j, i, k at T_2^-.

Since none of the above two cases is possible, no collision and collinearity will happen in $[0, \infty)$ given that the initial formation is sufficiently close to the desired formation. □

Remark 3.15. According to the parameters given in Example 1, we can check that $\tilde{F}^*_i, i = 1, 4, 5$ are Hurwitz which make the single-integrator dynamics stable in Fig. 3.4. However, $\Delta^*_i < 0$ but $4k_s^2 Re(\lambda_{ij}) - \Delta^*_i > 0, i = 4, 5, j = 1, 2$, i.e., (3.70) does not hold for $i = 4, 5$, which make the double-integrator dynamics unstable in Fig. 3.5.

3.3.2 The case of distinct control gains

The designed formation stabilization law (3.40) in the previous section requires all agents to have the identical velocity feedback gains k_s. To adapt for different actuator characteristics, e.g., energy consumption or speed constraints in different agents, in this subsection we design the formation stabilization law which allows each agent to have distinct control gain k_i, namely the control input for agent

$i, i = 1, \cdots, N$ is given by

$$u_i = -k_i v_i - \sum\nolimits_{(j,i,k)\in\mathcal{A}} (\alpha_{jik} - \alpha^*_{jik})(z_{ij} + z_{ik}), \tag{3.79}$$

where $k_i > 0$ and k_i can be different from k_j. By choosing the same system state variable X in (3.44), one has the close-loop dynamics of X

$$\dot{X} = \begin{bmatrix} 0_{(2N-4)\times(2N-4)} & R(X) \\ B(X) & -\text{diag}\{k_i\} \otimes I_2 \end{bmatrix} X = D_2(X)X, \tag{3.80}$$

where $\text{diag}\{k_i\} = \text{diag}\{k_1, \cdots, k_N\} \in \mathbb{R}^{N\times N}$. To prove the local stability of (3.80), we consider the characteristic polynomial of D_2^* again, that is

$$|\lambda I_{4N-4} - D_2^*| = \begin{vmatrix} \lambda I_{2N-4} & -R^* \\ -B^* & \text{diag}\{\lambda + k_i\} \otimes I_2 \end{vmatrix}, \tag{3.81}$$

where $\text{diag}\{\lambda + k_i\} = \text{diag}\{\lambda + k_1, \cdots, \lambda + k_N\}$. According to Schur complement theorem, one has

$$|\lambda I_{4N-4} - D_2^*| = \prod_{i=1}^{N} \{(\lambda + k_i)\text{det}[\lambda I_{2N-4} - R^*\text{diag}\{(\lambda + k_i)^{-1}\} \otimes I_2 B^*]\}.$$

By multiplying matrix B^* with $\text{diag}\{(\lambda + k_i)^{-1}\} \otimes I_2$ then with matrix R^*, it can be observed that

$$R^*\text{diag}\{(\lambda + k_i)^{-1}\} \otimes I_2 B^* = \begin{bmatrix} \bar{F}_1^* & 0 & 0 & \cdots & 0 \\ ** & \frac{\tilde{F}_4^*}{\lambda + k_4} & 0 & \cdots & 0 \\ ** & ** & \frac{\tilde{F}_5^*}{\lambda + k_5} & \cdots & 0 \\ \cdots & \cdots & \cdots & \ddots & \vdots \\ ** & ** & ** & ** & \frac{\tilde{F}_N^*}{\lambda + k_N} \end{bmatrix}, \tag{3.82}$$

where $\bar{F}_1^* = \bar{F}_1(X)|_{X=0}$, $\bar{F}_1(X) = \begin{bmatrix} \tilde{a}_{11} & \tilde{a}_{12} \\ \tilde{a}_{21} & \tilde{a}_{22} \end{bmatrix}$ and

$$\tilde{a}_{11} = \frac{(N_{213}+N_{312})(-z_{12}-z_{13})}{\lambda+k_1} + \frac{N_{213}(z_{31}+z_{32})}{\lambda+k_3},$$
$$\tilde{a}_{12} = \frac{N_{312}(z_{21}+z_{23})}{\lambda+k_2} + \frac{N_{213}(z_{31}+z_{32})}{\lambda+k_3},$$
$$\tilde{a}_{21} = \frac{(N_{321}+N_{123})(-z_{21}-z_{23})}{\lambda+k_2} + \frac{N_{123}(z_{31}+z_{32})}{\lambda+k_3},$$
$$\tilde{a}_{22} = \frac{(N_{321}+N_{123})(-z_{21}-z_{23})}{\lambda+k_2} + \frac{N_{123}(z_{31}+z_{32})}{\lambda+k_3}.$$

Then, it follows that

$$|\lambda I_{4N-4} - D_2^*| = \{\prod_{i=1}^{3}(\lambda+k_i)\}\det(\lambda I_2 - \bar{F}_1^*)\{\prod_{i=4}^{N}\det[\lambda(\lambda+k_i)I_2 - \tilde{F}_i^*]\}. \quad (3.83)$$

Note that the stability condition of $\{\prod_{i=4}^{N}\det[\lambda(\lambda+k_i)I_2 - \bar{F}_i^*]\}$ in (3.83) is the same as (3.62), which implies that there is no difference for the stability condition when agents 4 to N have identical or distinct velocity damping gains. Then, the stability condition for agents 4 to N can be described as

$$k_i^2\mathrm{Re}(\lambda_{ij}) + (\mathrm{Im}(\lambda_{ij}))^2 < 0, i = 4, \cdots, N, j = 1, 2, \quad (3.84)$$

which holds when (3.69) or (3.70) holds for $i = 4, \cdots, N$. But this is not the case for the first three agents. For the first three agents, the corresponding element in $\{\prod_{i=1}^{3}(\lambda+k_i)\}(\lambda I_2 - \bar{F}_1^*) = \begin{bmatrix} \bar{a}_{11}^* & \bar{a}_{12}^* \\ \bar{a}_{21}^* & \bar{a}_{22}^* \end{bmatrix}$ becomes that

$$\begin{aligned}
\bar{a}_{11}^* =& [\lambda(\lambda+k_1)(\lambda+k_2)(\lambda+k_3) \\
&- (N_{213}+N_{312})(-z_{12}-z_{13})(\lambda+k_2)(\lambda+k_3) \\
&- N_{213}(z_{31}+z_{32})(\lambda+k_1)(\lambda+k_2)]|_{X=0}, \\
\bar{a}_{22}^* =& [\lambda(\lambda+k_1)(\lambda+k_2)(\lambda+k_3) \\
&- (N_{321}+N_{123})(-z_{21}-z_{23})(\lambda+k_1)(\lambda+k_3) \\
&- N_{123}(z_{31}+z_{32})(\lambda+k_1)(\lambda+k_2)]|_{X=0}, \\
\bar{a}_{12}^* =& -[N_{312}(z_{21}+z_{23})(\lambda+k_1)(\lambda+k_3) \\
&- N_{213}(z_{31}+z_{32})(\lambda+k_1)(\lambda+k_2)]|_{X=0}, \\
\bar{a}_{21}^* =& -[(N_{321}+N_{123})(-z_{21}-z_{23})(\lambda+k_1)(\lambda+k_3) \\
&- N_{123}(z_{31}+z_{32})(\lambda+k_1)(\lambda+k_2)]|_{X=0}.
\end{aligned}$$

By letting $\{\prod_{i=1}^{3}(\lambda+k_i)\}\det(\lambda I_2 - \bar{F}_1^*) = 0$, the stability condition of the first

three agents becomes that the 8 solutions of the following algebraic equation all have negative real parts

$$\bar{a}_{11}^*\bar{a}_{22}^* - \bar{a}_{12}^*\bar{a}_{21}^* = b_8\lambda^8 + b_7\lambda^7 + \cdots + b_1\lambda + b_0 = 0 \tag{3.85}$$

which can be checked by Routh stability criterion [66, Theorem 40.1] or some numerical tools (e.g., Matlab). But the explicit solution of (3.85) is hard to be obtained due to the high order of the equation (3.85). The algebraic equation (3.85) is related to the desired triangular formation shape and the different velocity damping gains k_1, k_2, k_3, which implies that an inappropriate selection of first three agents' velocity damping gains may cause the system unstable.

Finally, we summarize the above discussion as the following result.

Theorem 3.16. *Consider that N agents of double-integrator dynamics (3.39) are governed by (3.79) with distinct gains k_i, the initial errors $X(0)$ are sufficient small and initial distances are bounded away from zero. The formation stabilization defined in (3.4)-(3.8) can be locally achieved if and only if all the solutions of (3.85) have negative real parts and (3.84) holds. Moreover, (3.84) holds if and only if for each $i = 4, \cdots, N$, (3.69) or (3.70) holds.*

The proof of theorem is followed by the above analysis. The analysis of collision and collinearity is similar to Theorem 1.

Remark 3.17. The formation stabilization laws (3.40) and (3.79) can be implemented in each agent's local coordinate frame, i.e., the alignment of all agents' local coordinate frames is not needed.

Remark 3.18. Note that in the stabilization of distance rigid formations with double-integrator dynamics [85], the fact that their control law is the gradient of a potential function helps their stability analysis, see e.g., the multiplication of rigidity matrix and its transpose being positive semi-definite, and symmetric structure in the Jacobian matrix of linearized system. However, for the control law (3.40) designed for the stabilization of angle rigid formations with double-integrator dynamics, it can be proved that it is not a gradient-based control law due to the asymmetric/directed direction measurements, which makes this work challenging and essential. The relationship between single-integrator and double-integrator dynamics for angle rigid formations is connected through the relationship $R(p)B(p) = A(e_a)$ obtained in (3.61).

Remark 3.19. Note that all the designed formation control algorithms in this chapter require the angle measurements to be noiseless. Now, suppose in 2D that all the angle measurements are subjected to an additional noise $\delta(t) \in \mathbb{R}$ which is bounded. According to the calculation of interior angle $\alpha_{jik} = (\phi_{ik} - \phi_{ij}) \bmod 2\pi$, one has that the interior angle remains the same under the noisy angle measurements

$\phi_{ik} + \delta(t), \phi_{ij} + \delta(t), j, k \in \mathcal{N}_i$. However, the direction of the bearing vector $b_{ij} = \begin{bmatrix} \cos(\phi_{ij} + \delta(t)) \\ \sin(\phi_{ij} + \delta(t)) \end{bmatrix}$ is influenced by the noise $\delta(t)$. Although the noise is bounded, it is still possible that the angle-only formation collides into one common point if the noise takes specific values. Thus, the general convergence analysis under the existence of noise is challenging and is left as future work.

3.4 Simulation examples

In this section, we first provide a simulation example to validate the effectiveness of the proposed angle rigidity-based control law (3.36). Then we compare the angle rigidity-based formation control law with bearing rigidity-based formation control law. To begin with, we give the desired formation shape in Fig. 3.6.

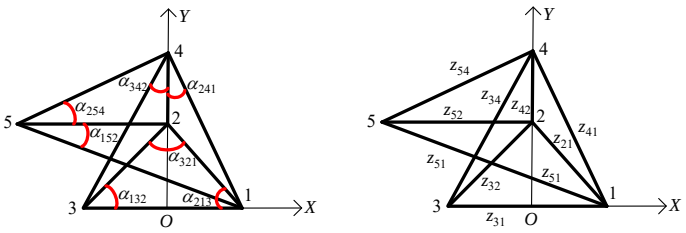

Figure 3.6: *Desired formation shape.*

3.4.1 Angle rigidity-based control law

Consider 5 agents in the plane with the following initial positions

$$p_1(0) = [0.8, 0.2]^{\mathrm{T}}, p_2(0) = [0.1, 1.4]^{\mathrm{T}}, p_3(0) = [-1.4, 0.3]^{\mathrm{T}},$$
$$p_4(0) = [0.1, 2.3]^{\mathrm{T}}, p_5(0) = [-1.7, 1.6]^{\mathrm{T}},$$

which are also used for other simulation examples. According to the form of $\mathcal{A}$ in (3.36), we consider the desired angles shown in Fig. 3.6(a) as

$$\alpha^*_{213} = \pi/4, \alpha^*_{132} = \pi/4, \alpha^*_{321} = \pi/2, \alpha^*_{342} = \arctan(0.5),$$
$$\alpha^*_{241} = \arctan(\frac{1}{2}), \alpha^*_{254} = \arctan(\frac{1}{2}), \alpha^*_{152} = \arctan(\frac{3}{\sqrt{10}}),$$

which leads to a globally infinitesimally angle rigid formation according to Proposition 2.12 and Theorem 2.17. To demonstrate the coordinate-independent property

illustrated in Remark 3.11, we introduce a misalignment $\theta_1 = 5^\circ$ in agent 1's coordinate frame $R_1(\theta) = \begin{bmatrix} \cos\theta_1 & -\sin\theta_1 \\ \sin\theta_1 & \cos\theta_1 \end{bmatrix}$, and the other agents' coordinate frames are the same as the XOY shown in Fig. 3.6.

Under the control law (3.36), the simulation results are given in Fig. 3.7-Fig. 3.8.

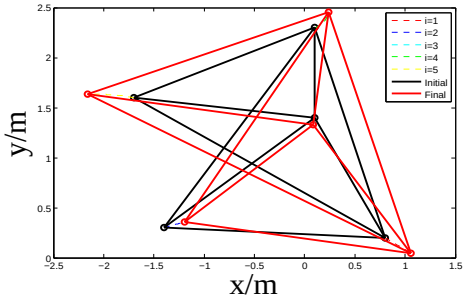

Figure 3.7: *Formation trajectories under angle rigidity-based control law with misalignment.*

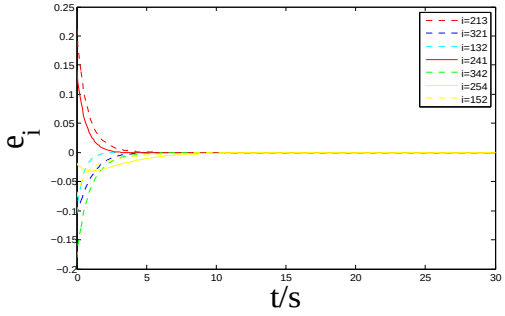

Figure 3.8: *Angle errors under angle rigidity-based control law with misalignment.*

3.4.2 Bearing rigidity-based control law

According to [101], a bearing rigidity-based control law is described by

$$\dot{p}_i = -\sum\nolimits_{j\in\mathcal{N}_i} P_{z_{ij}} z_{ij}^*, \tag{3.86}$$

where the desired bearing constraints in this simulation are defined as

$$z_{31}^* = [1,0]^{\mathrm{T}}, z_{21}^* = [\frac{\sqrt{2}}{2}, -\frac{\sqrt{2}}{2}]^{\mathrm{T}}, z_{32}^* = [\frac{\sqrt{2}}{2}, \frac{\sqrt{2}}{2}]^{\mathrm{T}},$$
$$z_{42}^* = [0,-1]^{\mathrm{T}} z_{41}^* = [\frac{\sqrt{5}}{5}, \frac{-2\sqrt{5}}{5}]^{\mathrm{T}}, z_{43}^* = [\frac{-\sqrt{5}}{5}, -\frac{2\sqrt{5}}{5}]^{\mathrm{T}},$$
$$z_{54}^* = [\frac{2\sqrt{5}}{5}, \frac{\sqrt{5}}{5}]^{\mathrm{T}}, z_{52}^* = [1,0]^{\mathrm{T}}, z_{51}^* = [\frac{3\sqrt{10}}{10}, \frac{-\sqrt{10}}{10}]^{\mathrm{T}}.$$

Then, we introduce the misalignment into agent 1's coordinate frame. By defining $\|z_{ij} - z_{ij}^*\|$ as bearing error, the simulation results are given in Fig. 3.9-Fig. 3.12.

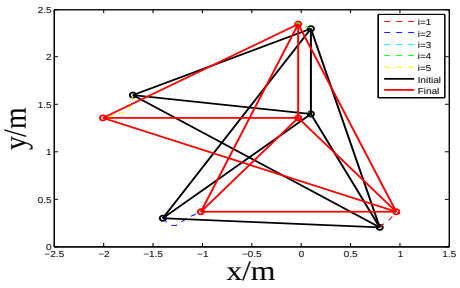

Figure 3.9: *Formation trajectories under bearing-based control without misalignment.*

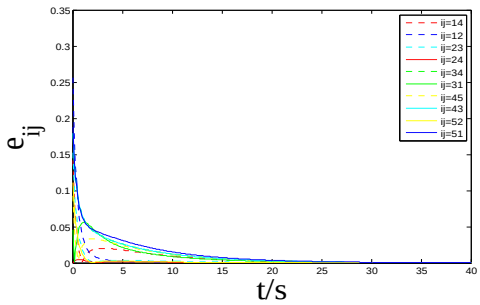

Figure 3.10: *Bearing errors under bearing-based control without misalignment.*

According to the above simulation results, one has that the angle rigidity-based formation control algorithms do not require the alignment of all agents' coordinate frames, while bearing rigidity-based control law in [101] does.

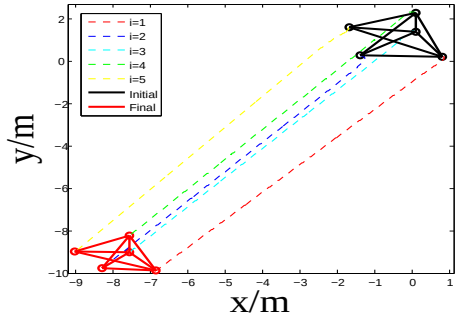

Figure 3.11: *Formation trajectories under bearing-based control with misalignment.*

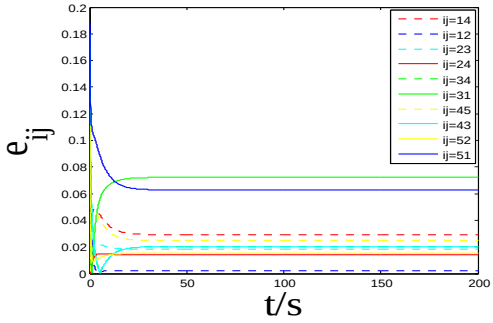

Figure 3.12: *Bearing errors under bearing-based control with misalignment.*

Appendix A

In view of (3.9), it follows

$$\begin{aligned}\dot{z}_{12} =& \frac{P_{z_{12}}}{l_{12}}(u_2 - u_1) \\ =& \frac{P_{z_{12}}}{l_{12}}[-(\alpha_2 - \alpha_2^*)(z_{23} + z_{21}) + (\alpha_1 - \alpha_1^*)(z_{13} + z_{12})].\end{aligned} \tag{3.87}$$

So

$$\begin{aligned}&\dot{z}_{12}^{\mathrm{T}} z_{13} \\ =&[(\alpha_1 - \alpha_1^*)(z_{13} + z_{12}) - (\alpha_2 - \alpha_2^*)(z_{23} + z_{21})]^{\mathrm{T}} \frac{P_{z_{12}}}{l_{12}} z_{13} \\ =& \frac{(\sin^2 \alpha_1)(\alpha_1 - \alpha_1^*) - (\cos \alpha_3 + \cos \alpha_1 \cos \alpha_2)(\alpha_2 - \alpha_2^*)}{l_{12}}.\end{aligned} \tag{3.88}$$

Since

$$\begin{aligned}\cos\alpha_3+\cos\alpha_1\cos\alpha_2 =&-\cos(\alpha_1+\alpha_2)+\cos\alpha_1\cos\alpha_2\\ =&\sin\alpha_2\sin\alpha_1,\end{aligned}\tag{3.89}$$

it follows

$$\dot{z}_{12}^{\mathrm{T}}z_{13}=\frac{\sin\alpha_1}{l_{12}}[(\alpha_1-\alpha_1^*)(\sin\alpha_1)-(\alpha_2-\alpha_2^*)\sin\alpha_2].$$

Similarly, one gets

$$z_{12}^{\mathrm{T}}\dot{z}_{13}=\frac{\sin\alpha_1}{l_{13}}[(\alpha_1-\alpha_1^*)(\sin\alpha_1)-(\alpha_3-\alpha_3^*)\sin\alpha_3].$$

By using (3.10), agent 1's closed-loop angle dynamics are

$$\begin{aligned}\dot{\alpha}_1=&-(\sin\alpha_1)(\frac{1}{l_{12}}+\frac{1}{l_{13}})(\alpha_1-\alpha_1^*)\\ &+\frac{\sin\alpha_2}{l_{12}}(\alpha_2-\alpha_2^*)+\frac{\sin\alpha_3}{l_{13}}(\alpha_3-\alpha_3^*).\end{aligned}\tag{3.90}$$

Similarly,

$$\begin{aligned}\dot{\alpha}_2=&-(\sin\alpha_2)(\frac{1}{l_{21}}+\frac{1}{l_{23}})(\alpha_2-\alpha_2^*)\\ &+\frac{\sin\alpha_1}{l_{21}}(\alpha_1-\alpha_1^*)+\frac{\sin\alpha_3}{l_{23}}(\alpha_3-\alpha_3^*),\end{aligned}\tag{3.91}$$

$$\begin{aligned}\dot{\alpha}_3=&-(\sin\alpha_3)(\frac{1}{l_{31}}+\frac{1}{l_{32}})(\alpha_3-\alpha_3^*)\\ &+\frac{\sin\alpha_1}{l_{31}}(\alpha_1-\alpha_1^*)+\frac{\sin\alpha_2}{l_{32}}(\alpha_2-\alpha_2^*).\end{aligned}\tag{3.92}$$

Writing (6.11)-(3.91) into a compact form, one has the closed-loop triangular formation dynamics given in (3.11).

Appendix B

Note that

$$\begin{aligned}\frac{\mathrm{d}(\cos\alpha_{241})}{\mathrm{d}t}=&-(\sin\alpha_{241})\dot{\alpha}_{241}=\frac{\mathrm{d}(z_{41}^{\mathrm{T}}z_{42})}{\mathrm{d}t}\\ =&(\dot{z}_{41})^{\mathrm{T}}z_{42}+(z_{41})^{\mathrm{T}}\dot{z}_{42},\end{aligned}\tag{3.93}$$

First, we calculate

$$\dot{z}_{41} = \frac{P_{z_{41}}}{l_{41}}(\dot{p}_1 - \dot{p}_4) = \frac{P_{z_{41}}}{l_{41}}u_1 - \frac{P_{z_{41}}}{l_{41}}u_4, \tag{3.94}$$

and

$$(\dot{z}_{41})^{\mathrm{T}} z_{42} = -\frac{u_4^{\mathrm{T}}}{l_{41}}(I_2 - z_{41}z_{41}^{\mathrm{T}})z_{42} + u_1^{\mathrm{T}}\frac{P_{z_{41}}}{l_{41}}z_{42} \tag{3.95}$$

By substituting the control law for agent 4, one has

$$\begin{aligned}
(\dot{z}_{41})^{\mathrm{T}} z_{42} =& -\frac{[(\alpha_{241} - \alpha_{241}^*)(\cos\alpha_{241} + \cos^2\alpha_{241})}{l_{41}}] \\
&- \frac{[(\alpha_{342} - \alpha_{342}^*)(\cos^2\alpha_{241} + \cos\alpha_{241}\cos\alpha_{341})]}{l_{41}} \\
&+ \frac{[(\alpha_{241} - \alpha_{241}^*)(\cos\alpha_{241} + 1)}{l_{41}}] \\
&+ \frac{[(\alpha_{342} - \alpha_{342}^*)(1 + \cos\alpha_{342})]}{l_{41}} - z_{42}^{\mathrm{T}}\frac{P_{z_{41}}}{l_{41}}(z_{12} + z_{13})e_1 \\
=& \frac{(\alpha_{241} - \alpha_{241}^*)\sin^2\alpha_{241}}{l_{41}} - z_{42}^{\mathrm{T}}\frac{P_{z_{41}}}{l_{41}}(z_{12} + z_{13})e_1 \\
&+ \frac{(\alpha_{342} - \alpha_{342}^*)(\sin^2\alpha_{241} + \sin^2\alpha_{241}\cos\alpha_{342})}{l_{41}} \\
&+ \frac{(\alpha_{342} - \alpha_{342}^*)\cos\alpha_{241}\sin\alpha_{241}\sin\alpha_{342}}{l_{41}},
\end{aligned} \tag{3.96}$$

and

$$\begin{aligned}
z_{41}^{\mathrm{T}}\dot{z}_{42} =& z_{41}^{\mathrm{T}}\frac{P_{z_{42}}}{l_{42}}u_2 - z_{41}^{\mathrm{T}}\frac{I_2 - z_{42}z_{42}^{\mathrm{T}}}{l_{42}}u_4 \\
=& -z_{41}^{\mathrm{T}}\frac{P_{z_{42}}}{l_{42}}(z_{21} + z_{23})e_2 + \frac{(\alpha_{241} - \alpha_{241}^*)\sin^2\alpha_{241}}{l_{42}} \\
&+ \frac{(\alpha_{342} - \alpha_{342}^*)(-\sin\alpha_{241}\sin\alpha_{342})}{l_{42}}.
\end{aligned} \tag{3.97}$$

Then, it follows

$$\begin{aligned}\dot{\alpha}_{241} =& -\frac{1}{\sin\alpha_{241}}\frac{\mathrm{d}(\cos\alpha_{241})}{\mathrm{d}t} = -\frac{\dot{z}_{41}^{\mathrm{T}} z_{42} + z_{41}^{\mathrm{T}}\dot{z}_{42}}{\sin\alpha_{241}} \\ =& -(\sin\alpha_{241})(\frac{1}{l_{41}} + \frac{1}{l_{42}})(\alpha_{241} - \alpha_{241}^*) \\ & - \frac{(\alpha_{342} - \alpha_{342}^*)(\sin\alpha_{241} + \sin\alpha_{341})}{l_{41}} \\ & + \frac{(\alpha_{342} - \alpha_{342}^*)\sin\alpha_{342}}{l_{42}} + \frac{z_{41}^{\mathrm{T}} P_{z_{42}}(z_{21} + z_{23})}{l_{42}\sin\alpha_{241}} e_2 \\ & + \frac{z_{42}^{\mathrm{T}} P_{z_{41}}(z_{12} + z_{13})}{l_{41}\sin\alpha_{241}} e_1. \end{aligned} \tag{3.98}$$

Analogously,

$$\begin{aligned}\dot{\alpha}_{342} =& -\frac{1}{\sin\alpha_{342}}\frac{\mathrm{d}(\cos\alpha_{342})}{\mathrm{d}t} = -\frac{\dot{z}_{42}^{\mathrm{T}} z_{43} + z_{42}^{\mathrm{T}}\dot{z}_{43}}{\sin\alpha_{342}} \\ =& -(\sin\alpha_{342})(\frac{1}{l_{43}} + \frac{1}{l_{42}})(\alpha_{342} - \alpha_{342}^*) \\ & - \frac{(\alpha_{241} - \alpha_{241}^*)(\sin\alpha_{342} + \sin\alpha_{341})}{l_{43}} \\ & + \frac{(\alpha_{241} - \alpha_{241}^*)\sin\alpha_{241}}{l_{42}} + \frac{z_{43}^{\mathrm{T}} P_{z_{42}}(z_{21} + z_{23})}{l_{42}\sin\alpha_{342}} e_2 \\ & - \frac{z_{42}^{\mathrm{T}} P_{z_{43}}(z_{31} + z_{32})}{l_{43}\sin\alpha_{342}}(e_1 + e_2). \end{aligned} \tag{3.99}$$

By combining (3.98) and (3.99), one has the compact form (3.25).

3.5 Concluding remarks

Based on the developed angle rigidity theory in 2D, we have also demonstrated in this chapter how to stabilize a multi-agent planar formation using only angle measurements, which can be realized in each agent's local coordinate frame. The exponential convergent rate of angle errors and no collision between specified agents have also been proved.

Chapter 4

Formation maneuvering in 2D

This chapter investigates how to maneuver a planar formation of mobile agents using designed mismatched angles. The desired formation shape is specified by a set of interior angle constraints. To realize the maneuver of translation, rotation and scaling of the formation as a whole, we intentionally force the agents to maintain mismatched desired angles by introducing a pair of mismatch parameters for each angle constraint. To allow different information requirements in the design and implementation stages, we consider both measurement-dependent and measurement-independent mismatches. Starting from a triangular formation, we consider generically angle rigid formations that can be constructed from the triangular formation by adding new agents in sequence, each having two angle constraints associated with some existing three agents. The control law for each newly added agent arises naturally from the angle constraints and makes full use of the angle mismatch parameters. We show that the control can effectively stabilize the formations while simultaneously realizing maneuvering.

4.1 Introduction

Two types of formation control problems, i.e., formation shape control and formation maneuvering control, have been extensively studied recently [7, 71]. The works in [17, 63, 101] realized the control of desired formation shapes by using the measurements of relative positions, distances and bearings between neighboring agents, respectively. At the same time, in many practical applications, formations are expected to be "maneuverable", e.g, capable of translating, scaling and rotating to adapt to complex environments. For instance, when a team of flying unmanned aerial vehicles aims at going through some areas containing obstacles, they need to change the velocity, orientation, and even the scale of the whole formation. Therefore, researchers have studied the formation maneuvering problem which requires the achievement of not only the desired formation shape but also simultaneously the translation, rotation or scaling of the formation [99].

To achieve formation maneuvering, some researchers have proposed several approaches given different types of formation shape descriptions and available sensing information. When a desired formation shape is described by relative positions,

formation translation was achieved in [75] requiring the measurements of relative positions. For rigid formations with distance constraints, the formation maneuvering algorithms were designed in [32, 85] by introducing a pair of mismatches per distance constraint, in which the rotational and translational maneuvering was achieved by using the measurement of relative positions in each agent's local coordinate frame. For a desired formation shape described by inter-agent bearings, based on the bearing rigidity developed in [101], the work in [99] achieved the scaling and translational formation maneuvering using relative positions. Note that these works [32, 75, 85, 99] cannot fully achieve the formation maneuvering of scaling, rotation and translation easily at the same time. The reason is that, because of the dependence of coordinate frames, displacement constraints vary during rotation and scaling, distance constraints vary during scaling, and bearing constraints vary during rotation. Note that for most of the proposed formation maneuvering algorithms [29, 31, 32, 41, 42, 61, 64, 75, 85, 99, 100], the measurements of relative positions are required. Compared with relative position measurements, angle measurements are cheaper, more reliable and accessible. With the rapid development of sensor technologies, angle information can be obtained from the locally equipped passive radars, sonar systems or cameras [89, 103].

Motivated by the facts that interior angle constraints are invariant during translation, rotation and scaling, this study aims at realizing the formation maneuvering enabling translation, rotation and scaling, under the conditions that the formation shape is described by interior angle constraints and the measurements are chosen angles. To be more specific, based on the angle-based formation stabilization law [11, 22], we employ the mismatches in prescribed angles, and propose to use "designed mismatched angles" after the angle mismatches are added to each agent's desired interior angles. This is a different approach than designing distance mismatches between two neighboring agents in the existing literature.

4.2 Problem Formulation

4.2.1 Angle measurements

Each agent i has its own fixed coordinate frame $\sum_i$ which may differ from $\sum_g$. Let p_j^i denote agent j's position in $\sum_i$. To simplify notation, whenever causing no confusion, we drop the superscript reference to $\sum_g$, e.g., $p_i = p_i^g$. Agent i measures the angle $\phi_{ij} \in [0, 2\pi), \forall j \in \mathcal{N}_i$ towards agent j evaluated counterclockwise from the X-axis of $\sum_i$, and here $\mathcal{N}_i$ denotes the set of the neighbours of agent i that do not coincide with i. We call the unit vector $z_{ij}^i := \frac{p_j^i - p_i^i}{\|p_j^i - p_i^i\|} = \begin{bmatrix} \cos\phi_{ij} \\ \sin\phi_{ij} \end{bmatrix}$ the bearing from i to j which starts from p_i^i, points towards p_j^i, and can be uniquely determined

by ϕ_{ij}. For the agents $i, i+1$, and $i-1$ shown in Fig. 4.1, the interior angle α_i can be calculated by

$$\alpha_i := \measuredangle(i-1)i(i+1) = \arccos(z_{i(i+1)}^{\mathrm{T}} z_{i(i-1)}). \tag{4.1}$$

Note that even when $\sum_i$ are chosen differently, α_i remains the same but $z_{ij}^g = R_i^g z_{ij}^i$, where z_{ij} is the bearing from p_i to p_j described in $\sum_g$, and $R_i^g \in SO(2)$ denotes the rotation matrix from $\sum_i$ to $\sum_g$.

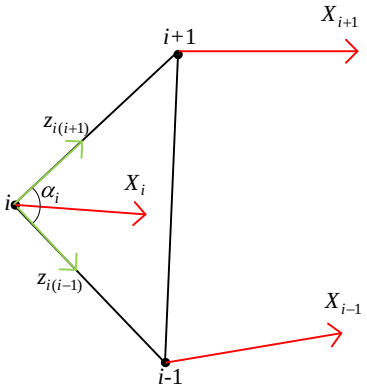

Figure 4.1: *The angle measurements.*

4.2.2 Problem formulation

The goal of this chapter is to design the control input for each agent i such that the N-agent system achieves a desired formation described by interior angles, and at the same time realizes desired maneuvering. First, we study the triangular case when $N = 3$, and then extend the obtained results to generically angle rigid formations when $N > 3$. For the triangular case, the objective stated separately is:

(i) to achieve the desired triangular formation shape, i.e.

$$\lim_{t\to\infty} e_i(t) = 0, \forall i = 1, 2, 3, \tag{4.2}$$

where the formation-shape error signal e_i are defined to be $e_i(t) = \alpha_i(t) - \alpha_i^*$, $\alpha_i^* \in (0, \pi)$ denotes agent i's desired interior angle, and naturally $\alpha_1^* + \alpha_2^* + \alpha_3^* = \pi$;
(ii) to achieve one of the following separately defined maneuvering:

(ii.A) translational formation maneuver

$$\lim_{t\to\infty}(\dot{p}_i(t) - v_c^*) = 0, \forall i = 1, 2, 3, \tag{4.3}$$

where $v_c^* \in \mathbb{R}^2$ is the desired translational velocity described in $\sum_g$.

(ii.B) rotational formation maneuver

$$\lim_{t\to\infty}(\dot{p}_i(t) - \omega^* E p_{ci}(t)) = 0, \tag{4.4}$$

where $E = \left[\begin{smallmatrix} 0 & -1 \\ 1 & 0 \end{smallmatrix}\right]$ is a skew-symmetric matrix, $p_{ci} = p_i - p_c$ denotes the vector from the maneuvering reference point p_c to agent i's position p_i (thus Ep_{ci} corresponding to rotating p_{ci} by $\pi/2$ counterclockwise), and $\omega^* \in \mathbb{R}$ is the desired rotational angular speed, with $\omega^* > 0$ corresponding to rotating counterclockwise. The formation reference point p_c can be chosen differently, e.g., the centroid $p_c = \frac{1}{N}\sum_{i=1}^N p_i$; in applications, it can be chosen to be the position of a well recognized landmark in the environment.

(ii.C) scaling formation maneuver

$$\lim_{t\to\infty}(\dot{p}_i(t) - s(t)p_{ci}(t)) = 0, \tag{4.5}$$

where $s(t) \in \mathbb{R}$ is the modulation factor for the scaling speed which can be typically chosen as $s(t) = k_s e^{-\gamma t}, \gamma > 0, k_s \in \mathbb{R}$. Note that $s(t) > 0$ or $k_s > 0$ corresponds to enlarging the formation, while $s(t) < 0$ or $k_s < 0$ shrinking the formation.

If the translation, rotation and scaling maneuverings are required to be achieved simultaneously, then by combining (4.3)-(4.5) together, the maneuvering control objective becomes

$$\lim_{t\to\infty}[\dot{p}_i(t) - (v_c^* + \omega^* E p_{ci}(t) + s(t)p_{ci}(t))] = 0. \tag{4.6}$$

When $N > 3$, we aim to control those multi-agent formations that are angle rigid. Here we briefly mention a few concepts from angle rigidity theory. The multi-point framework that we consider consists of a set of points and angle constraints, and it is said to be *angle rigid* if under appropriately chosen angle constraints, the framework can only translate, rotate or scale as a whole when one or more of its points are perturbed locally. An angle rigid multi-point framework with the configuration $p = [p_1^{\mathrm{T}}, \cdots, p_N^{\mathrm{T}}]^{\mathrm{T}} \in \mathbb{R}^{2N}$ being generic, e.g., no three points are collinear and no four points are on a circle, is said to be *generically angle rigid*. For more details about angle rigidity, readers can refer to [22].

To construct a generically angle rigid N-agent formation, according to [22], one can grow the formation by $N-2$ steps as introduced in Subsection 3.2. Then, for agents $i, i = 4, \ldots, N$, the formation control objective is to achieve

$$\lim_{t\to\infty} e_{i1}(t) = \lim_{t\to\infty}(\alpha_{j_1 i j_2}(t) - \alpha^*_{j_1 i j_2}) = 0, \tag{4.7}$$

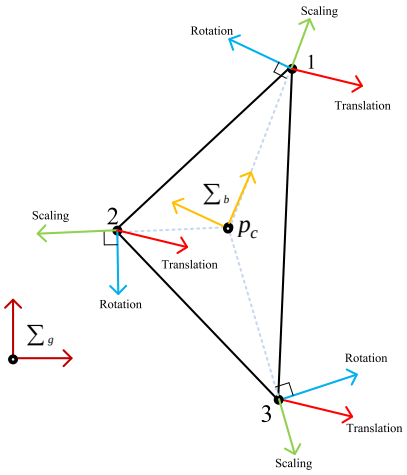

Figure 4.2: *Formation maneuver velocity vectors: translation, rotation and scaling.*

$$\lim_{t\to\infty} e_{i2}(t) = \lim_{t\to\infty}(\alpha_{j_2ij_3}(t) - \alpha^*_{j_2ij_3}) = 0, \tag{4.8}$$

where $j_1 < i, j_2 < i, j_3 < i$, and $\alpha^*_{j_1ij_2} \in (0,\pi), \alpha^*_{j_2ij_3} \in (0,\pi)$ denote agent i's two desired angles formed with agents $j_1, j_2, j_3 \in \{1, 2, ..., i-1\}$ respectively, and to achieve the maneuvering of translation, rotation and scaling as described in (4.3)-(4.6).

Therefore, the desired formation shape is described by a set of angle constraints $\alpha^* = \{\alpha^*_1, \alpha^*_2, \alpha^*_3, \alpha^*_{142}, \alpha^*_{243}, \cdots, \alpha^*_{j_1kj_2}, \alpha^*_{j_2kj_3}, \cdots, \alpha^*_{i_1Ni_2}, \alpha^*_{i_2Ni_3}\}$. The goal is to achieve these angles and the maneuvering objective (4.6) simultaneously.

4.3 Formation maneuvering for single-integrators

Consider in this section that for an N-agent system moving in the plane, the motion dynamics of its agent i are modeled by single-integrators

$$\dot{p}_i = u_i, i = 1, ..., N, \tag{4.9}$$

where $p_i \in \mathbb{R}^2$ denotes the position of agent i described in a fixed global coordinate frame $\sum_g$, and $u_i \in \mathbb{R}^2$ is the control input to be designed.

4.3.1 Triangular formation maneuver

In this section, we aim at achieving the triangular formation maneuvering for the first three agents. First, we will present a formation maneuver algorithm by introducing a pair of mismatches per angle constraint. Then, for the cases of measurement-dependent and measurement-independent mismatches, the formation maneuver control algorithms and the corresponding stability analysis will be given respectively.

A. Formation maneuver algorithm design

In [11], using bearing measurements, three agents achieved a triangular formation shape described by three interior angles $\alpha_i^*, i = 1, 2, 3$. The control algorithms designed in [11] can be equivalently written as

$$u_i = -k_i(\alpha_i - \alpha_i^*)\frac{z_{i(i+1)} + z_{i(i-1)}}{\|z_{i(i+1)} + z_{i(i-1)}\|}, \tag{4.10}$$

where $k_i > 0$, $z_{i(i+1)}$ is the unit vector starting from p_i and pointing towards p_{i+1}, and we assume $(i+1) = 1$ when $i = 3$, and $(i-1) = 3$ when $i = 1$ in this subsection. Now, we modify the control algorithm (4.10) into

$$u_i = -k_i(\alpha_i - \alpha_i^*)(z_{i(i+1)} + z_{i(i-1)}). \tag{4.11}$$

Now, we introduce a pair of designed-mismatches per angle constraint α_i^* into (4.11) such that the formation maneuvering with translation, rotation, and scaling can be realized. By following [21], we design the formation maneuvering law as

$$\begin{aligned} u_i =& -k_i(\alpha_i - \alpha_i^* - \frac{\mu_i}{k_i})z_{i(i+1)} - k_i(\alpha_i - \alpha_i^* - \frac{\tilde{\mu}_i}{k_i})z_{i(i-1)} \\ =& -k_i(\alpha_i - \alpha_i^*)[z_{i(i+1)} + z_{i(i-1)}] + [\mu_i z_{i(i+1)} + \tilde{\mu}_i z_{i(i-1)}] \\ =& u_{fi} + u_{mi}, \end{aligned} \tag{4.12}$$

where $\mu_i \in \mathbb{R}$ and $\tilde{\mu}_i \in \mathbb{R}$ are the designed-mismatches associated with agent i's desired angle α_i^*, u_{fi} is the formation shape control part and u_{mi} is the maneuver control part. From (4.12) and (4.6), the steady-state velocity $\dot{p}_i^*$ of agent i at the desired triangular formation shape ($\alpha_i = \alpha_i^*$) with the desired maneuver can be decomposed into three parts

$$\begin{aligned} \dot{p}_i^* =& \dot{p}_{i(translation)}^* + \dot{p}_{i(rotation)}^* + \dot{p}_{i(scaling)}^* \\ =& v_c^* + \omega^* E p_{ci} + s(t) p_{ci} = \mu_i z_{i(i+1)} + \tilde{\mu}_i z_{i(i-1)}, \end{aligned} \tag{4.13}$$

Note that in (4.13), $z_{i(i+1)}$ is determined by the bearing measurement $\phi_{i(i+1)}$,

but p_{ci} is the vector from the reference point p_c to agent i's position p_i which needs to be additionally measured. In the following two subsections, we introduce two techniques to design the mismatches to realize the desired maneuvering, which include the measurement-dependent mismatches $\mu_i(z_{ij}, p_{ci}), \tilde{\mu}_i(z_{ij}, p_{ci})$ or $\mu_i(t), \tilde{\mu}_i(t)$ for short that require the real-time measurements of $z_{ij}(t)$ and $p_{ci}(t)$, and the measurement-independent mismatches $\mu_i(\alpha^*), \tilde{\mu}_i(\alpha^*)$ or $\mu_i, \tilde{\mu}_i$ for short that are not related to the real-time measurements but calculated in the design stage based on the desired formation shape α^*.

B. Measurement-dependent mismatches

Now, we use the measurement-dependent mismatches to realize the desired maneuvering under the measurements of z_{ij} and p_{ci}, in which we assume that all the agents' coordinate frames $\sum_i$ have the same orientation as $\sum_g$. In the following, we first illustrate how to design $\mu_i(t)$ and $\tilde{\mu}_i(t)$, then analyze the stability of the closed-loop system. Note that the desired maneuvering velocity $\dot{p}_i^*$ in (4.13) is a linear combination of translation velocity v_c^*, rotation velocity $\omega^* E p_{ci}$ and scaling velocity $s(t)p_{ci}$. We first show in the following how to design μ_i and $\tilde{\mu}_i$ in (4.12) to achieve each maneuvering separately, then simultaneously.

(1) Translation

According to (4.13), only considering translation maneuvering with v_c^*, one requires

$$v_c^* = \mu_1(t) z_{12} + \tilde{\mu}_1(t) z_{13}, \tag{4.14}$$

$$v_c^* = \mu_2(t) z_{23} + \tilde{\mu}_2(t) z_{21}, \tag{4.15}$$

$$v_c^* = \mu_3(t) z_{31} + \tilde{\mu}_3(t) z_{32}, \tag{4.16}$$

where we assume that the three agents' positions are not collinear. Then, $\mu_i(t), \tilde{\mu}_i(t)$, $i = 1, 2, 3$ can be calculated by

$$\begin{bmatrix} \mu_i(t) \\ \tilde{\mu}_i(t) \end{bmatrix} = \begin{bmatrix} z_{i(i+1)}(1) & z_{i(i-1)}(1) \\ z_{i(i+1)}(2) & z_{i(i-1)}(2) \end{bmatrix}^{-1} \begin{bmatrix} v_c^*(1) \\ v_c^*(2) \end{bmatrix}, \tag{4.17}$$

where $z_{i(i+1)}(1)$ and $z_{i(i+1)}(2)$ denote the first and second elements of vector $z_{i(i+1)}$. Note that (4.14)-(4.16) are equivalent to adding the same v_c^* to all agents. To make (4.17) well-defined, the matrix $[z_{i(i+1)} \;\; z_{i(i-1)}]$ should always be invertible, which can be guaranteed if there is no collinearity among agents 1 to 3.

(2) Rotation

Only considering rotation around p_c in (4.13), one has

$$\omega^* E p_{c1} = \mu_1(t) z_{12} + \tilde{\mu}_1(t) z_{13}, \tag{4.18}$$
$$\omega^* E p_{c2} = \mu_2(t) z_{23} + \tilde{\mu}_2(t) z_{21}, \tag{4.19}$$
$$\omega^* E p_{c3} = \mu_3(t) z_{31} + \tilde{\mu}_3(t) z_{32}. \tag{4.20}$$

Similarly, $\mu_i(t), \tilde{\mu}_i(t), i = 1, 2, 3$ can be calculated by

$$\begin{bmatrix} \mu_i(t) \\ \tilde{\mu}_i(t) \end{bmatrix} = \begin{bmatrix} z_{i(i+1)}(1) & z_{i(i-1)}(1) \\ z_{i(i+1)}(2) & z_{i(i-1)}(2) \end{bmatrix}^{-1} \begin{bmatrix} -\omega^* p_{ci}(2) \\ \omega^* p_{ci}(1) \end{bmatrix}. \tag{4.21}$$

(3) Scaling

Only considering scaling with respect to p_c in (4.13), one has

$$s(t) p_{c1} = \mu_1(t) z_{12} + \tilde{\mu}_1(t) z_{13}, \tag{4.22}$$
$$s(t) p_{c2} = \mu_2(t) z_{23} + \tilde{\mu}_2(t) z_{21}, \tag{4.23}$$
$$s(t) p_{c3} = \mu_3(t) z_{31} + \tilde{\mu}_3(t) z_{32}. \tag{4.24}$$

Also, $\mu_i(t), \tilde{\mu}_i(t), i = 1, 2, 3$ can be calculated by

$$\begin{bmatrix} \mu_i(t) \\ \tilde{\mu}_i(t) \end{bmatrix} = \begin{bmatrix} z_{i(i+1)}(1) & z_{i(i-1)}(1) \\ z_{i(i+1)}(2) & z_{i(i-1)}(2) \end{bmatrix}^{-1} \begin{bmatrix} s(t) p_{ci}(1) \\ s(t) p_{ci}(2) \end{bmatrix}. \tag{4.25}$$

Then, by applying translation, rotation and scaling simultaneously, one has

$$\begin{aligned} \begin{bmatrix} \mu_i(t) \\ \tilde{\mu}_i(t) \end{bmatrix} =& [z_{i(i+1)}\ z_{i(i-1)}]^{-1} (v_c^* + \omega^* E p_{ci} + s(t) p_{ci}) \\ =& [z_{i(i+1)}\ z_{i(i-1)}]^{-1} \begin{bmatrix} v_c^*(1) - \omega^* p_{ci}(2) + s(t) p_{ci}(1) \\ v_c^*(2) + \omega^* p_{ci}(1) + s(t) p_{ci}(2) \end{bmatrix}, \end{aligned} \tag{4.26}$$

which is well-defined when $[z_{i(i+1)}\ z_{i(i-1)}]$ is invertible. By applying the designed mismatches (4.26) into control law (4.12), we are ready to give the following result.

Theorem 4.1. *Consider a 3-agent formation described by (4.9), with the control signal (4.12) and mismatches $\mu_i(t), \tilde{\mu}_i(t), i = 1, 2, 3$ as designed in (4.26). If the initial angle errors $e_i(0)$ are sufficiently small, $\alpha_i(0) \neq 0$, and $\|p_i(0) - p_j(0)\|, i \neq j$ are sufficiently away from zero, then the 3-agent formation converges exponentially to its desired shape and maneuvers with the combination of the prescribed translation*

(4.3), rotation (4.4) and scaling (4.5) .

Proof. Note that the angle error dynamics $\dot{e}_i$ are affected by the combination of formation shape control part $u_{fi} = -k_i(\alpha_i - \alpha_i^*)(z_{i(i+1)} + z_{i(i-1)})$ and maneuver control part $u_{mi} = \mu_i z_{i(i+1)} + \tilde{\mu}_i z_{i(i-1)}$. According to Appendix A, the angle error dynamics can be described by

$$\dot{e} = \begin{bmatrix} \dot{\alpha}_1 \\ \dot{\alpha}_2 \\ \dot{\alpha}_3 \end{bmatrix} = F_1(e)e = \begin{bmatrix} -g_1 & f_{12} & f_{13} \\ f_{21} & -g_2 & f_{23} \\ f_{31} & f_{32} & -g_3 \end{bmatrix} \begin{bmatrix} e_1 \\ e_2 \\ e_3 \end{bmatrix}, \tag{4.27}$$

where $f_{ij} = k_j(\sin\alpha_j)/l_{ij}$, $g_i = (\sin\alpha_i)(k_i/l_{i(i+1)} + k_i/l_{i(i-1)})$, and $l_{ij} = \|p_i - p_j\|$ denotes the distance between agents i and j. According to Appendix A and (4.27), the maneuver control part u_{mi} has no contribution to the angle error dynamics $\dot{e}_i$, which is reasonable since the whole formation's translation, rotation and scaling will not change its interior angles.

First, we prove that the 3-agent formation will not become collinear under (4.27) if it is not initially collinear. If for a fixed i, $\alpha_i \to \pi$, one has $\alpha_{i-1} \to 0$ and $\alpha_{i+1} \to 0$ because $\alpha_i + \alpha_{i-1} + \alpha_{i+1} = \pi$. Note that $\alpha_i^*, i = 1, 2, 3$ are bounded away from zero and π, which implies that $e_i > 0$ and $e_{i+1} < 0$, $e_{i-1} < 0$. Then, since $g_i > 0$ and $f_{ij} > 0, j = i-1, i+1$, from agent i's angle error dynamics $\dot{e}_i = -g_i e_i + f_{i(i+1)}e_{i+1} + f_{i(i-1)}e_{i-1}$, one has $\dot{e}_i < 0$, which implies that $\dot{\alpha}_i$ makes it impossible to achieve $\alpha_i = \pi$. Similarly should $\alpha_i \to 0$, one would obtain the contradicting result that α_i increases. Since α_i has to be 0 or π in the collinear situation, the contradictions we have constructed imply that the three agents will not become collinear if their initial positions are not collinear. Therefore, it follows that the calculation of (4.26) is well-defined.

Since $e_1 + e_2 + e_3 \equiv 0$, the angle error dynamics (4.27) can be reduced to

$$\dot{e}_s = \begin{bmatrix} \dot{e}_1 \\ \dot{e}_2 \end{bmatrix} = \begin{bmatrix} -(g_1 + f_{13}) & f_{12} - f_{13} \\ f_{21} - f_{23} & -(g_2 + f_{23}) \end{bmatrix} \begin{bmatrix} e_1 \\ e_2 \end{bmatrix} = F_{s1}(e_s)e_s. \tag{4.28}$$

Let $\mathbb{U} \in \mathbb{R}^2$ denote the neighborhood of the origin $\{e_1 = e_2 = 0\}$, in which we investigate the local stability of (6.15). Linearizing (6.15) at the origin, we obtain

$$\dot{e}_s = A_1 e_s, \tag{4.29}$$

where $A_1 = F_{s1}(e_s)|_{e_s=0}$. Then, under $e_s = 0$, i.e., $\alpha_i = \alpha_i^*$, one has

$$\text{tr}(A_1(\alpha^*)) = -g_1 - f_{13} - g_2 - f_{23} < 0, \tag{4.30}$$

$$\begin{aligned}\det(A_1(\alpha^*)) =&(g_1+f_{13})(g_2+f_{23})-(f_{21}-f_{23})(f_{12}-f_{13})\\ >&g_1f_{23}+g_2f_{13}+f_{21}f_{13}+f_{12}f_{23}>0,\end{aligned} \tag{4.31}$$

where we have used the fact that $g_1g_2 > f_{21}f_{12}$. According to (4.30) and (4.31), one has that A_1 is Hurwitz. By following the Lyapunov Theorem [54, Theorem 4.6], for an arbitrary positive definite matrix $Q_1 \in \mathbb{R}^{2\times 2}$, there always exists a positive definite matrix $P_1 \in \mathbb{R}^{2\times 2}$ such that $-Q_1 = P_1A_1 + A_1^{\mathrm{T}}P_1$. We then design the Lyapunov function candidate as

$$V_1 = e_s^{\mathrm{T}}P_1e_s,$$

whose time-derivative is

$$\dot{V}_1 = -e_s^{\mathrm{T}}Q_1e_s \leqslant -\frac{\lambda_{\min}(Q_1)}{\lambda_{\max}(P_1)}V_1. \tag{4.32}$$

where $\lambda_{\min}()$ and $\lambda_{\max}()$ denote the minimum and maximum eigenvalues of a square matrix, respectively. Then, one has

$$e_1^2+e_2^2 = \|e_s\|^2 \leqslant \frac{V_1}{\lambda_{\min}(P_1)} \leqslant \frac{V_1(0)}{\lambda_{\min}(P_1)}e^{-\frac{\lambda_{\min}(Q_1)}{\lambda_{\max}(P_1)}t}. \tag{4.33}$$

Also, one has

$$e_3^2 = e_1^2+e_2^2+2e_1e_2 \leqslant 2(e_1^2+e_2^2) \leqslant \frac{2V_1(0)}{\lambda_{\min}(P_1)}e^{-\frac{\lambda_{\min}(Q_1)}{\lambda_{\max}(P_1)}t},$$

which implies that e_i under the dynamics (4.27) is exponentially stable when the initial states lie in $\mathbb{U}$. Then, according to (4.9) and (4.12), one has $\lim_{t\to\infty}\dot{p}_i(t) = \mu_i(t)z_{i(i+1)}(t)+\tilde{\mu}_i(t)z_{i(i-1)}(t)$. Therefore, if (4.14)-(4.16), (4.18)-(4.20), or (4.22)-(4.24) are applied separately in (4.13), one has that the maneuvering defined in (4.3)-(4.5) is achieved separately. Meanwhile, if they are applied simultaneously by (4.26), the maneuverings consisting of translation, rotation and scaling are achieved simultaneously. □

C. Measurement-independent mismatches

Now, we consider that agent i can only measure $z_{i(i+1)}$ and $z_{i(i-1)}$ in (4.12). The mismatches μ_i and $\tilde{\mu}_i$ are calculated in the design stage by using the information of the desired formation shape. Towards this end, we first define a body frame $\sum_{b(t)}$ whose origin is fixed at the position $p_1(t)$ of agent 1, and X-axis points from the position $p_1(t)$ of agent 1 to the position $p_2(t)$ of agent 2, and Y-axis follows the direction under right-hand rule.

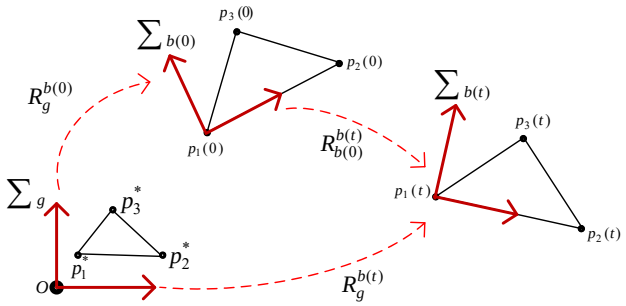

Figure 4.3: *Relationship between several coordinate frames.*

At the initial design stage $t = 0$, consider the static and reference formation configuration $p^{b*} = [(p_1^{b*})^{\mathrm{T}}, (p_2^{b*})^{\mathrm{T}}, \cdots, (p_N^{b*})^{\mathrm{T}}]^{\mathrm{T}} \in \mathbb{R}^{2N}$ described in $\sum_{b(0)}$, which satisfies all the desired angle constraints α^*. As shown in Fig. 4.3, according to the definition of $\sum_{b(0)}$, one has $p_1^{b*} = [0, 0]^{\mathrm{T}}$, $p_2^{b*} = [x_{p_2^*}, 0]^{\mathrm{T}}$ where $x_{p_2^*}$ can be chosen as an arbitrary positive number; then, one can calculate $p_3^{b*}, ..., p_N^{b*}$ using the angle constraints α^*. If one has a reference configuration $p^* = [(p_1^*)^{\mathrm{T}}, (p_2^*)^{\mathrm{T}}, \cdots, (p_N^*)^{\mathrm{T}}]^{\mathrm{T}}$ of the desired formation described in $\sum_g$ with $p_1^* = [0, 0]^{\mathrm{T}}$, $p_2^* = [x_{p_2^*}, 0]^{\mathrm{T}}$, then one directly has $p^{b*} = p^*$. Now, we use p^{b*} for the design of measurement-independent mismatches.

(1) Translation

Only considering translational maneuvering, similar to (4.14)-(4.16), one has

$$v_c^{b*} = R_g^{b(0)} v_c^* = \mu_i z_{i(i+1)}^{b*} + \tilde{\mu}_i z_{i(i-1)}^{b*}, i = 1, 2, 3 \tag{4.34}$$

where $z_{ij}^{b*} = \frac{p_j^{b*} - p_i^{b*}}{\|p_j^{b*} - p_i^{b*}\|}$ is the bearing calculated by p^{b*}. Then, $\mu_i, \tilde{\mu}_i, i = 1, 2, 3$ can be calculated by

$$\begin{bmatrix} \mu_i \\ \tilde{\mu}_i \end{bmatrix} = \begin{bmatrix} z_{i(i+1)}^{b*}(1) & z_{i(i-1)}^{b*}(1) \\ z_{i(i+1)}^{b*}(2) & z_{i(i-1)}^{b*}(2) \end{bmatrix}^{-1} \begin{bmatrix} v_c^{b*}(1) \\ v_c^{b*}(2) \end{bmatrix}. \tag{4.35}$$

Since the bearing vectors $z_{i(i+1)}^{b*}$, $z_{i(i-1)}^{b*}$ are not collinear in a generically angle rigid formation according to [22, Definition 4] and Assumption 3.1, the matrix $[z_{i(i+1)}^{b*} \;\; z_{i(i-1)}^{b*}]$ is invertible. Since the desired velocity v_c^{b*} is described in $\sum_{b(0)}$ in (4.34), the control objective (4.3) for translation maneuvering in this case is

modified to

$$\lim_{t\to\infty}(R_g^{b(t)}\dot{p}_i(t) - v_c^{b*}) = 0, \tag{4.36}$$

where $R_g^{b(t)}$ is the rotation matrix from $\sum_g$ to $\sum_{b(t)}$.

(2) Rotation

Considering rotation around the centroid in (4.13), one has

$$\omega^* E p_{ci}^{b*} = \mu_i z_{i(i+1)}^{b*} + \tilde{\mu}_i z_{i(i-1)}^{b*}, i = 1, 2, 3, \tag{4.37}$$

where $p_{ci}^{b*} = p_i^{b*} - p_c^{b*} = p_i^{b*} - \frac{1}{N}\sum_{j=1}^{N} p_j^{b*}$. Then, $\mu_i, \tilde{\mu}_i, i = 1, 2, 3$ can be similarly calculated as (4.25).

(3) Scaling

Only considering scaling with respect to the centroid in (4.13), one has

$$s(t)p_{ci}^{b*} = \mu_i z_{i(i+1)}^{b*} + \tilde{\mu}_i z_{i(i-1)}^{b*}. \tag{4.38}$$

Then, $\mu_i, \tilde{\mu}_i, i = 1, 2, 3$ can be calculated. Then, by applying translation, rotation and scaling simultaneously, one has

$$\begin{bmatrix}\mu_i \\ \tilde{\mu}_i\end{bmatrix} = [z_{i(i+1)}^{b*}\ z_{i(i-1)}^{b*}]^{-1}\left(v_c^{b*} + \omega^* E p_{ci}^{b*} + s(t)p_{ci}^{b*}\right) \tag{4.39}$$

which is well-defined since $[z_{i(i+1)}^{b*}\ z_{i(i-1)}^{b*}] \in \mathbb{R}^{2\times 2}$ is invertible. Now, we apply the constant mismatches designed in (4.39) into control law (4.12).

Theorem 4.2. *Consider the 3-agent formation described by (4.9), with the control inputs (4.12) and mismatches $\mu_i, \tilde{\mu}_i, i = 1, 2, 3$ as designed in (4.39). If the initial angle error $e_i(0)$, and the designed-mismatches are sufficiently small, $\alpha_i(0) \neq 0$ and $\|p_i(0) - p_j(0)\|, i \neq j$ are sufficiently away from zero, then the 3-agent formation converges exponentially to its desired shape and maneuvers with the prescribed translation (4.36), rotation (4.4) and scaling (4.5) simultaneously.*

Proof. To analyze the convergence of e_i, we first aim at obtaining the angle error dynamics $\dot{e}_i, i = 1, 2, 3$. Note that the analysis method of angle error dynamics given in [11] cannot be used in this case because of the part $\mu_i z_{i(i+1)} + \tilde{\mu}_i z_{i(i-1)}$ in control law (4.12). Instead, we derive the angle error dynamics by using the dot product of two bearings. According to Appendix B, one has the following angle

error dynamics

$$\dot{e} = [\dot{\alpha}_1 \;\; \dot{\alpha}_2 \;\; \dot{\alpha}_3]^{\mathrm{T}} = F_2(e)e + H_2(e,\mu,\tilde{\mu}) = \begin{bmatrix} -g_1 & f_{12} & f_{13} \\ f_{21} & -g_2 & f_{23} \\ f_{31} & f_{32} & -g_3 \end{bmatrix} \begin{bmatrix} \alpha_1 - \alpha_1^* \\ \alpha_2 - \alpha_2^* \\ \alpha_3 - \alpha_3^* \end{bmatrix} + \begin{bmatrix} h_1 \\ h_2 \\ h_3 \end{bmatrix}, \tag{4.40}$$

where g_i and f_{ij} have the same forms as (4.27), and

$$h_i = \frac{\tilde{\mu}_i \sin\alpha_i - \mu_{i+1}\sin\alpha_{i+1}}{l_{i(i+1)}} + \frac{\mu_i \sin\alpha_i - \tilde{\mu}_{i-1}\sin\alpha_{i-1}}{l_{i(i-1)}}.$$

Now, we analyze the local stability of (4.40). Since $e_1 + e_2 + e_3 = 0$, one has the following sub-dynamics

$$\begin{aligned} \dot{e}_s &= \begin{bmatrix} \dot{e}_1 \\ \dot{e}_2 \end{bmatrix} = F_{s2}(e_s)e_s + H_{s2}(e_s)U_2 \\ &= \begin{bmatrix} -(g_1+f_{13}) & f_{12}-f_{13} \\ f_{21}-f_{23} & -(g_2+f_{23}) \end{bmatrix} \begin{bmatrix} \alpha_1 - \alpha_1^* \\ \alpha_2 - \alpha_2^* \end{bmatrix} + \begin{bmatrix} h_{11} & h_{12} & h_{13} & h_{14} & h_{15} & h_{16} \\ h_{21} & h_{22} & h_{23} & h_{24} & h_{25} & h_{26} \end{bmatrix} U_2, \end{aligned} \tag{4.41}$$

where $U_2 = [\mu_1, \mu_2, \mu_3, \tilde{\mu}_1, \tilde{\mu}_2, \tilde{\mu}_3]^{\mathrm{T}}$, $h_{11} = \frac{\sin\alpha_1}{l_{13}}$, $h_{12} = -\frac{\sin\alpha_2}{l_{12}}$, $h_{13} = h_{15} = 0$, $h_{14} = \frac{\sin\alpha_1}{l_{12}}$, $h_{16} = -\frac{\sin\alpha_3}{l_{13}}$, $h_{21} = h_{26} = 0$, $h_{22} = \frac{\sin\alpha_2}{l_{21}}$, $h_{23} = -\frac{\sin\alpha_3}{l_{23}}$, $h_{24} = -\frac{\sin\alpha_1}{l_{21}}$, $h_{25} = -\frac{\sin\alpha_2}{l_{23}}$. It can be verified that $H_2(0,\mu,\tilde{\mu}) = 0$ which implies that $e = 0$ is an equilibrium of (4.40). To obtain the local stability of (4.41), we linearize the dynamics (4.41) at the origin. The linearized system of (4.41) at the origin can be written as

$$\dot{e}_s = A_1 e_s + B_1 e_s = (A_1 + B_1)e_s,$$

where $B_1 = \frac{\partial H_{s2}(e_s)U_2}{\partial e_s}|_{e_s=0} = [\frac{\partial H_{s2}(e_s)}{\partial e_1} \;\; \frac{\partial H_{s2}(e_s)}{\partial e_2}](I_2 \otimes U_2)|_{e_s=0}$, and $A_1 = F_{s2}(e_s)|_{e_s=0}$ which implies that for an arbitrary positive definite matrix $Q_2 \in \mathbb{R}^{2\times 2}$, there exists a positive definite matrix $P_2 \in \mathbb{R}^{2\times 2}$ such that $Q_2 = -(P_2 A_1 + A_1^{\mathrm{T}} P_2)$. Since $U_2(t)$ is bounded, we then check the stability of (4.41) when e_s lies in a neighborhood region $\mathbb{U}_2$ of the origin $e_s = 0$. Consider the Lyapunov function candidate

$$V_2 = e_s^{\mathrm{T}} P_2 e_s,$$

whose time-derivative is

$$\dot{V}_2 \leqslant -\lambda_{\min}(Q_2)\|e_s\|^2 + e_s^{\mathrm{T}}(B_1^{\mathrm{T}} P_2 + P_2 B_1)e_s \leqslant (-\lambda_{\min}(Q_2) + q_1)\|e_s\|^2, \tag{4.42}$$

where $q_1 = 2\|B_1\|\lambda_{\max}(P_2)$. For a neighborhood of the equilibrium, one can obtain $\lambda_{\min}(Q_2) \geqslant q_1$ by choosing

• *small designed-mismatches* $\mu_i, \tilde{\mu}_i$ since $\delta_2(\mu)$ in q_1 grows with μ continuously and $\delta_2(\mu) \geqslant \delta_2(0) = 0$, which in general require that the maneuvering speed $\|v_c^*\|, \omega^*, k_s$ should be small according to (4.39);
• *big feedback gain* k_i *when* $k_1 = k_2 = k_3$ which only makes $\lambda_{\max}(P_2)$ smaller but not $\lambda_{\min}(Q_2)$ because Q_2 is given and $\delta_2(\mu)$ is not related to k_i.

When $\lambda_{\min}(Q_2) \geqslant q_1$, the sub-dynamics (4.41) are locally exponentially stable. By following (4.32)-(4.33), one has

$$e_1^2 + e_2^2 = \|e_s\|^2 \leqslant \frac{V_2}{\lambda_{\min}(P_2)} \leqslant \frac{V_2(0)}{\lambda_{\min}(P_2)} e^{-\frac{\lambda_{\min}(Q_2)-q_1}{\lambda_{\max}(P_2)}t}. \tag{4.43}$$

Since $e_1 = e_2 = 0$ implies $e_3 = 0$, the overall dynamic system (4.40) is locally exponentially stable, i.e., $\lim_{t\to\infty} e_i = 0$, which implies that $\lim_{t\to\infty} \dot{p}_i(t) = \lim_{t\to\infty}(\mu_i z_{i(i+1)}(t) + \tilde{\mu}_i z_{i(i-1)}(t))$. Then, it follows that $\lim_{t\to\infty} R_g^{b(t)} \dot{p}_i(t) = \lim_{t\to\infty} R_g^{b(t)}(\mu_i z_{i(i+1)}(t) + \tilde{\mu}_i z_{i(i-1)}(t)) = \lim_{t\to\infty}(\mu_i z_{i(i+1)}^{b(t)}(t) + \tilde{\mu}_i z_{i(i-1)}^{b(t)}(t)) = v_c^{b*}$ where we have used the facts that $\sum_{b(t)}$ is rigidly attached at the real-time formation and $z_{ij}^{b(t)}(t) \to z_{ij}^{b*}$ when $\alpha_i \to \alpha_i^*$. For rotation and scaling, since $k_s p_{ci}^{b*} = \mu_i z_{i(i+1)}^{b*} + \tilde{\mu}_i z_{i(i-1)}^{b*}$ implies that $k_s p_{ci} = \mu_i z_{i(i+1)} + \tilde{\mu}_i z_{i(i-1)}$, one has that the rotation and scaling are also achieved. Therefore, the maneuvering defined in (4.36), and (4.4)-(4.5) is achieved. Note that the formation's eventual orientation $R_{b(\infty)}^g$ is not necessarily equal to $R_{b(0)}^g$ and the overall maneuvering velocity described in $\sum_g$ is $\lim_{t\to\infty} \dot{p}_i(t) = \lim_{t\to\infty}[R_{b(t)}^g v_c^{b*} + \omega^* E p_{ci}(t) + k_s p_{ci}(t)]$ where the formation's eventual orientation $R_{b(\infty)}^g$ depends on the initial states of the agents and the rotation maneuvering that the formation conducted. Finally, we analyze the non-collinearity in this case. Note that (4.43) implies that $\forall i = 1, 2, 3$

$$|e_i| = |\alpha_i - \alpha_i^*| \leqslant \sqrt{\frac{2V_2(0)}{\lambda_{\min}(P_2)}} e^{-\frac{\lambda_{\min}(Q_2)-q_1}{2\lambda_{\max}(P_2)}t} \leqslant \sqrt{\frac{2V_2(0)}{\lambda_{\min}(P_2)}},$$

If we choose initial formation errors $e_i(0)$ such that $V_2(0)$ is sufficiently small (corresponding to local stability), one has that $\alpha_i(t)$ will be bounded away from zero and π because $\alpha_i^*, i = 1, 2, 3$ are bounded away from zero and π. This implies that no collinearity will occur in this case. □

Remark 4.3. Each agent's position in (4.9) is described in the global coordinate frame, but it is not used in the maneuver control algorithm (4.12). For the case of measurement-independent mismatches, (4.12) can be realized in each agent's local coordinate frame which can have different orientation from $\sum_g$ since (4.12) can

be equivalently written as

$$\begin{aligned} R_i^g u_i^i = &- k_i(\alpha_i - \alpha_i^*) R_i^g (z_{i(i+1)}^i + z_{i(i-1)}^i) \\ &+ \mu_i R_i^g z_{i(i+1)}^i + \tilde{\mu}_i R_i^g z_{i(i-1)}^i, \end{aligned} \tag{4.44}$$

where $R_i^g \in SO(2)$ is the rotation matrix from agent i's local coordinate frame $\sum_i$ to the global coordinate frame $\sum_g$, u_i^i is the controller input applied in agent i's local coordinate frame $\sum_i$, and $z_{i(i+1)}^i, z_{i(i-1)}^i$ are the bearings measured in agent i's local coordinate frame. Since $(\alpha_i - \alpha_i^*)$ and $\mu_i, \tilde{\mu}_i$ are scalars, (4.44) can be reduced to

$$u_i^i = -k_i(\alpha_i - \alpha_i^*)(z_{i(i+1)}^i + z_{i(i-1)}^i) + \mu_i z_{i(i+1)}^i + \tilde{\mu}_i z_{i(i-1)}^i$$

which is equivalent to (4.12). Note that the measurement-independent mismatch design in (4.39) can be calculated in the design stage which uses the formation of the desired formation shape p^{b*} described in $\sum_{b(0)}$. However, the implementation of (4.12) is completely distributed, i.e., no aligned coordinate frames or global information is required to be shared among agents.

Remark 4.4. Note that the desired translation velocity in (4.14)-(4.16) is described in a global coordinate frame, but in (4.34) is described in $\sum_{b(0)}$. To achieve a desired translational velocity described in the global coordinate frame in the measurement-independent mismatch case, one can align one real-time bearing z_{ij} to the bearing z_{ij}^{b*} described in $\sum_{b(0)}$ [32]. However, the mismatch design for rotation and scaling in both time-varying and constant cases is not influenced by the global or local coordinate frame because the rotation and scaling is conducted with respect to the formation's reference point p_c instead of an external reference frame, see Fig. 4.2 and (4.3)-(4.5).

Remark 4.5. For the case of measurement-dependent mismatches, one can also add the desired maneuvering velocity $v_c^* + \omega^* E p_i^b + s(t) p_i^b$ directly into (4.11). The reasons for designing measurement-dependent mismatches are supported by two facts. The first is that the controllers for the cases of measurement-dependent and measurement-independent mismatches have the same form (4.12). Therefore, when the measurements of relative position are available, the formation maneuvering can be realized with measurement-dependent mismatches, but when they are unavailable, the formation maneuvering can be realized with measurement-independent mismatches whose control law has the same structure as measurement-dependent case. The second is that the analysis of angle error dynamics (4.40) in the case of measurement-independent mismatches is based on the angle error dynamics (4.27) in the case of measurement-dependent mismatches. We show that when the mismatches are measurement-dependent, the angle error dynamics (4.27) are not related with the mismatches anymore, which is reasonable since the

whole formation's maneuvering in terms of translation, rotation and scaling will not change the magnitude of agents' interior angles.

4.3.2 Collision analysis

Note that the bearing vector $z_{ij} = \frac{p_j - p_i}{\|p_j - p_i\|}, j \in \mathcal{N}_i$ used in the maneuver control law (4.12) is not well-defined if there exists collision between neighboring agents i and j. Therefore, the analysis on the collision among the three agents is needed. Since we are controlling interior angles, we would like to show that the distance $l_{ij} = \|p_i - p_j\|$ does not vary much, which is not obvious when maneuvering is conducted. Therefore we need to assess the order of magnitude of how much l_{ij} can grow or shrink from the initial conditions. Consequently, we provide the following analysis considering the cases of measurement-dependent and measurement-independent mismatches, respectively.

A. Measurement-dependent mismatches

Taking agents 1 and 2 as an example (the other cases can be similarly analyzed), one has

$$\begin{aligned} l_{12}(t) &= l_{12}(0) + \int_0^t \dot{l}_{12}(\tau)\mathrm{d}\tau \\ &= l_{12}(0) + \int_0^t \frac{(p_1 - p_2)^{\mathrm{T}}(\dot{p}_1 - \dot{p}_2)}{\|p_1 - p_2\|}\mathrm{d}\tau \\ &= l_{12}(0) + \int_0^t z_{21}^{\mathrm{T}}(u_{f1} - u_{f2} + u_{m1} - u_{m2})\mathrm{d}\tau. \end{aligned} \tag{4.45}$$

First, we consider the formation part $u_{f1} - u_{f2}$ in (4.45)

$$\begin{aligned} &\int_0^t z_{21}^{\mathrm{T}}(u_{f1} - u_{f2})\mathrm{d}\tau = \int_0^t k_2 e_2 z_{21}^{\mathrm{T}}(z_{21} + z_{23}) - k_1 e_1 z_{21}^{\mathrm{T}}(z_{12} + z_{13})\mathrm{d}\tau \\ \leqslant &\int_0^t (2k_1|e_1| + 2k_2|e_2|)\mathrm{d}\tau \leqslant 2\bar{k}_{12}\int_0^t \sqrt{e_1^2 + e_2^2 + 2|e_1||e_2|}\mathrm{d}\tau \\ \leqslant &2\sqrt{2}\bar{k}_{12}\int_0^t \sqrt{e_1^2 + e_2^2}\mathrm{d}\tau, \end{aligned} \tag{4.46}$$

where $\bar{k}_{12} = \max\{k_1, k_2\}$ and we have used the fact that $2|e_1||e_2| \leqslant e_1^2 + e_2^2$. By

using (4.33), one has

$$\begin{aligned}\int_0^t \sqrt{e_1^2+e_2^2}\mathrm{d}\tau &\leqslant \sqrt{\frac{V_1(0)}{\lambda_{\min}(P_1)}}\frac{2\lambda_{\max}(P_1)}{\lambda_{\min}(Q_1)}\left(1-e^{-\frac{\lambda_{\min}(Q_1)}{2\lambda_{\max}(P_1)}t}\right)\\ &\leqslant \frac{2\lambda_{\max}(P_1)}{\lambda_{\min}(Q_1)}\sqrt{\frac{V_1(0)}{\lambda_{\min}(P_1)}}.\end{aligned} \tag{4.47}$$

Then, we consider the maneuver part $u_{m1}-u_{m2}$ in (4.45). By using (4.12) and (4.26), one has

$$\int_0^t z_{21}^{\mathrm{T}}(u_{m1}-u_{m2})\mathrm{d}\tau=\int_0^t z_{21}^{\mathrm{T}}[\omega^* E+s(\tau)I_2](p_{c1}-p_{c2})\mathrm{d}\tau=\int_0^t s(\tau)l_{12}(\tau)\mathrm{d}\tau, \tag{4.48}$$

where we have used the fact that $z_{21}^{\mathrm{T}}Ez_{21}=0$ and $p_{c1}-p_{c2}=z_{21}l_{12}$. According to (4.54), the translational and rotational maneuvering has no impact on the change of $l_{12}(t)$, and only scaling has. Note that when modulation factor for the scaling speed $s(t)>0$, i.e., conducting formation enlargement, one always has $\int_0^t s(\tau)l_{12}(\tau)\mathrm{d}\tau\geqslant 0$. By substituting (4.46)-(4.54) into (4.45), when $s(t)>0$ one has

$$\begin{aligned}l_{12}(t)&\geqslant l_{12}(0)+\int_0^t s(\tau)l_{12}(\tau)\mathrm{d}\tau-\frac{4\bar{k}_{12}\lambda_{\max}(P_1)}{\lambda_{\min}(Q_1)}\sqrt{\frac{2V_1(0)}{\lambda_{\min}(P_1)}}\\ &\geqslant l_{12}(0)-\frac{4\bar{k}_{12}\lambda_{\max}(P_1)}{\lambda_{\min}(Q_1)}\sqrt{\frac{2V_1(0)}{\lambda_{\min}(P_1)}}.\end{aligned} \tag{4.49}$$

However, the case of $s(t)<0$ is also important in obstacle avoidance task because it corresponds to shrink the formation. To achieve the task of shrinking the formation, a typical form of $s(t)<0$ is $s(t)=-e^{-\gamma t}$. Now, we analyze the impact of this special case of shrinking formation on the change of $l_{12}(t)$. By using the integration by parts, one has

$$\begin{aligned}&\int_0^t s(\tau)l_{12}(\tau)\mathrm{d}\tau=\int_0^t \gamma^{-1}l_{12}(\tau)\mathrm{d}e^{-\gamma\tau}=\gamma^{-1}l_{12}e^{-\gamma t}-\gamma^{-1}\int_0^t e^{-\gamma\tau}\mathrm{d}l_{12}(\tau)\\ =&\gamma^{-1}l_{12}e^{-\gamma t}-\gamma^{-1}\int_0^t e^{-\gamma\tau}s(\tau)l_{12}(\tau)\mathrm{d}\tau-\gamma^{-1}\int_0^t e^{-\gamma\tau}[z_{21}^{\mathrm{T}}(u_{f1}-u_{f2})]\mathrm{d}\tau.\end{aligned} \tag{4.50}$$

Note that in (4.50), $\gamma^{-1}l_{12}e^{-\gamma t}\geqslant 0$ and $-\gamma^{-1}\int_0^t e^{-\gamma\tau}s(\tau)l_{12}(\tau)\mathrm{d}\tau\geqslant 0$ since

$s(t) < 0$. In addition, by using (4.46), one has

$$\begin{aligned}
&-\gamma^{-1}\int_0^t e^{-\gamma\tau}[z_{21}^{\mathrm{T}}(u_{f1}-u_{f2})]\mathrm{d}\tau \\
\leqslant&\gamma^{-1}2\sqrt{2}\bar{k}_{12}\int_0^t e^{-\gamma\tau}\sqrt{e_1^2+e_2^2}\,\mathrm{d}\tau \\
\leqslant&\gamma^{-1}2\sqrt{2}\bar{k}_{12}\sqrt{\frac{V_1(0)}{\lambda_{\min}(P_1)}}\int_0^t e^{-(\gamma+\frac{\lambda_{\min}(Q_1)}{2\lambda_{\max}(P_1)})\tau}\mathrm{d}\tau \\
\leqslant&\gamma^{-1}2\sqrt{2}\bar{k}_{12}\sqrt{\frac{V_1(0)}{\lambda_{\min}(P_1)}}\frac{2\lambda_{\max}(P_1)}{\lambda_{\min}(Q_1)+2\gamma\lambda_{\max}(P_1)}.
\end{aligned} \tag{4.51}$$

By substituting (4.46)-(4.54) and (4.50)-(4.51) into (4.45), when $s(t) = -e^{-\gamma t}$ one has

$$\begin{aligned}
l_{12}(t) \geqslant& l_{12}(0) - \frac{4\bar{k}_{12}\lambda_{\max}(P_1)}{\lambda_{\min}(Q_1)}\sqrt{\frac{2V_1(0)}{\lambda_{\min}(P_1)}} \\
&-\gamma^{-1}2\sqrt{2}\bar{k}_{12}\sqrt{\frac{V_1(0)}{\lambda_{\min}(P_1)}}\frac{2\lambda_{\max}(P_1)}{\lambda_{\min}(Q_1)+2\gamma\lambda_{\max}(P_1)}.
\end{aligned} \tag{4.52}$$

Finally, we summarize the above analysis into a proposition.

Proposition 4.6. *Consider a 3-agent formation described by (4.9), with the control signal (4.12) and mismatches $\mu_i(t), \tilde{\mu}_i(t), i = 1,2,3$ as designed in (4.26) and $\alpha_i(0) \neq 0$. For the case of $s(t) > 0$, if $l_{12}(0) > \frac{4\bar{k}_{12}\lambda_{\max}(P_1)}{\lambda_{\min}(Q_1)}\sqrt{\frac{2V_1(0)}{\lambda_{\min}(P_1)}}$, no collision will happen between agents 1 and 2. For the case of $s(t) = -e^{-\gamma t} < 0$, if $l_{12}(0) > \frac{4\bar{k}_{12}\lambda_{\max}(P_1)}{\lambda_{\min}(Q_1)}\sqrt{\frac{2V_1(0)}{\lambda_{\min}(P_1)}} + \gamma^{-1}2\sqrt{2}\bar{k}_{12}\sqrt{\frac{V_1(0)}{\lambda_{\min}(P_1)}}\frac{2\lambda_{\max}(P_1)}{\lambda_{\min}(Q_1)+2\gamma\lambda_{\max}(P_1)}$, then no collision will happen between agents 1 and 2.*

Proof. For the case of $s(t) > 0$, since $l_{12}(0) > 0$, $\exists T_2 > 0$ such that in $[0, T_2]$, no collision happens between agents 1 and 2. Assume that there exists a collision between agents 1 and 2 in $[T_2, \infty)$, then there must exist an escape time T_c such that $l_{12}(T_c) = 0$. Since no collision happens in $[T_2, T_c^-)$, the closed-loop system is well-defined in $[T_2, T_c^-)$. Following the calculations in (4.45)-(4.49), one has that $l_{12}(T_c^-) \geqslant l_{12}(0) - \frac{4\bar{k}_{12}\lambda_{\max}(P_1)}{\lambda_{\min}(Q_1)}\sqrt{\frac{2V_1(0)}{\lambda_{\min}(P_1)}} > 0$ which is bounded away from zero. This implies a contradiction with the assumption that collision happens at T_c. Thus, no collision happens in $[0, \infty)$. The case of $s(t) < 0$ can be similarly obtained. □

B. Measurement-independent mismatches

For the case of measurement-independent mismatches, the description of $l_{12}(t)$ in (4.45) still holds. By following the analysis from (4.45) to (4.47), one has the effect

of formation part $u_{f1}-u_{f2}$ on $l_{21}(t)$

$$\int_0^t z_{21}^{\mathrm{T}}(u_{f1}-u_{f2})\mathrm{d}\tau \leqslant \quad 2\sqrt{2}\bar{k}_{12}\int_0^t \sqrt{e_1^2+e_2^2}\mathrm{d}\tau \leqslant \frac{4\bar{k}_{12}\lambda_{\max}(P_2)}{\lambda_{\min}(Q_2)-q_1}\sqrt{\frac{2V_2(0)}{\lambda_{\min}(P_2)}}. \tag{4.53}$$

Then, we discuss the maneuver part $u_{m1}-u_{m2}$ in (4.45). By using (4.12) and (4.39), one has

$$\begin{aligned}&\int_0^t z_{21}^{\mathrm{T}}(u_{m1}-u_{m2})\mathrm{d}\tau = \int_0^t z_{21}^{\mathrm{T}}(\mu_1 z_{12}+\tilde{\mu}_1 z_{13}-\mu_2 z_{23}-\tilde{\mu}_2 z_{21})\mathrm{d}\tau\\ =&\int_0^t(-\mu_1-\tilde{\mu}_2-\tilde{\mu}_1\cos\alpha_1-\mu_2\cos\alpha_2)\mathrm{d}\tau.\end{aligned} \tag{4.54}$$

By using $\alpha_i=e_i+\alpha_i^*$, one has

$$\begin{aligned}&-\mu_1-\tilde{\mu}_2-\tilde{\mu}_1\cos\alpha_1-\mu_2\cos\alpha_2\\ =&-\mu_1-\tilde{\mu}_2-\tilde{\mu}_1(\cos e_1\cos\alpha_1^*-\sin e_1\sin\alpha_1^*)-\mu_2(\cos e_2\cos\alpha_2^*-\sin e_2\sin\alpha_2^*).\end{aligned}$$

Now, we use the Taylor series to describe $\cos e_i$ and $\sin e_i$

$$\cos e_i = 1-\frac{e_i^2}{2!}+\frac{e_i^4}{4!}+\cdots+\frac{(-1)^n e_i^{2n}}{(2n)!}, \tag{4.55}$$

$$\sin e_i = e_i-\frac{e_i^3}{3!}+\frac{e_i^5}{5!}+\cdots+\frac{(-1)^n e_i^{2n+1}}{(2n+1)!}, \tag{4.56}$$

where $n\to\infty$ and $n!$ denotes the factorial of n. Since $e_i(0)$ is sufficiently small and $e_i(t)$ converges to zero at an exponential speed, we only focus on the first main part in (4.55) and (4.56). Then, one has

$$\begin{aligned}&-\mu_1-\tilde{\mu}_2-\tilde{\mu}_1\cos\alpha_1-\mu_2\cos\alpha_2\\ \approx&-\mu_1-\tilde{\mu}_1\cos\alpha_1^*-\tilde{\mu}_2-\mu_2\cos\alpha_2^*+\tilde{\mu}_1 e_1\sin\alpha_1^*+\mu_2 e_2\sin\alpha_2^*.\end{aligned} \tag{4.57}$$

On the one hand, by using (4.39) for the first part of (4.57), one has

$$\begin{aligned}&-\mu_1-\tilde{\mu}_1\cos\alpha_1^*-\tilde{\mu}_2-\mu_2\cos\alpha_2^* = -\begin{bmatrix}1 & (z_{12}^{b*})^\top z_{13}^{b*}\end{bmatrix}\begin{bmatrix}\mu_1\\ \tilde{\mu}_1\end{bmatrix}-\begin{bmatrix}(z_{21}^{b*})^\top z_{23}^{*} & 1\end{bmatrix}\begin{bmatrix}\mu_2\\ \tilde{\mu}_2\end{bmatrix}\\ =&-(z_{12}^{b*})^\top\begin{bmatrix}z_{12}^{b*} & z_{13}^{b*}\end{bmatrix}[z_{12}^{b*}\ z_{13}^{b*}]^{-1}\left(v_c^{b*}+\omega^* E p_{c1}^{b*}+s(t)p_{c1}^{b*}\right)\\ &-(z_{21}^{b*})^\top\begin{bmatrix}z_{23}^{b*} & z_{21}^{b*}\end{bmatrix}[z_{23}^{b*}\ z_{21}^{b*}]^{-1}\left(v_c^{b*}+\omega^* E p_{c2}^{b*}+s(t)p_{c2}^{b*}\right)\\ =&(z_{12}^{b*})^\top[\omega^* E(p_2^{b*}-p_1^{b*})+s(t)(p_2^{b*}-p_1^{b*})]=s(t)l_{12}^{b*},\end{aligned} \tag{4.58}$$

where we have used the fact that $\cos\alpha_1^* = (z_{12}^{b*})^\top z_{13}^{b*}$. On the other hand, for the second part of (4.57), one has

$$\int_0^t (\tilde{\mu}_1 e_1 \sin\alpha_1^* + \mu_2 e_2 \sin\alpha_2^*)\mathrm{d}\tau \leqslant \int_0^t \mu_{\max 12}(|e_1| + |e_2|)\mathrm{d}\tau,$$

where $\mu_{\max 12} = \max\{|\tilde{\mu}_1|, |\mu_2|\}$ and we have used that fact that $|\sin\alpha_i^*| < 1$. By following (4.46) and (4.47), one has

$$\int_0^t (|e_1| + |e_2|)\mathrm{d}\tau \leqslant \sqrt{2}\int_0^t \sqrt{e_1^2 + e_2^2}\mathrm{d}\tau \leqslant \frac{2\lambda_{\max}(P_2)}{\lambda_{\min}(Q_2) - q_1}\sqrt{\frac{2V_2(0)}{\lambda_{\min}(P_2)}}. \tag{4.59}$$

By substituting (4.53) and (4.54)-(4.59), one has

$$\begin{aligned} l_{12}(t) \geqslant & l_{12}(0) + \int_0^t s(t) l_{12}^{b*}\mathrm{d}\tau - \frac{4\bar{k}_{12}\lambda_{\max}(P_2)}{\lambda_{\min}(Q_2) - q_1}\sqrt{\frac{2V_2(0)}{\lambda_{\min}(P_2)}} \\ & - \frac{2\mu_{\max 12}\lambda_{\max}(P_2)}{\lambda_{\min}(Q_2) - q_1}\sqrt{\frac{2V_2(0)}{\lambda_{\min}(P_2)}}, \end{aligned} \tag{4.60}$$

where $\int_0^t s(t) l_{12}^{b*}\mathrm{d}\tau > 0$ when $k_s > 0$. For the case of $k_s < 0$, the conclusion can be similarly analyzed by following (4.50)-(4.51). Finally, we summarize the above analysis into a proposition.

Proposition 4.7. *Consider the 3-agent formation described by (4.9), with the control inputs (4.12) and mismatches $\mu_i, \tilde{\mu}_i, i = 1, 2, 3$ as designed in (4.39), and the initial angle error $e_i(0)$, and the designed-mismatches are sufficiently small, $\alpha_i(0) \neq 0$ and $k_s > 0$. If $l_{12}(0) > \frac{4\bar{k}_{12}\lambda_{\max}(P_2)}{\lambda_{\min}(Q_2)-q_1}\sqrt{\frac{2V_2(0)}{\lambda_{\min}(P_2)}} + \frac{2\mu_{\max 12}\lambda_{\max}(P_2)}{\lambda_{\min}(Q_2)-q_1}\sqrt{\frac{2V_2(0)}{\lambda_{\min}(P_2)}}$, then no collision will happen between agents 1 and 2.*

The proof can be similarly obtained by following Proposition 4.6.

4.3.3 Extension to generically angle rigid formation

In this section, we aim at realizing N-agent formation maneuver control by using designed mismatches. Since the maneuvering for the first three agents is realized, we now consider how agent $i, i = 4, \cdots, N$ can be added to the formation by giving two desired angles $\alpha_{j_1 i j_2}^*$ and $\alpha_{j_2 i j_3}^*$, $j_1 < i, j_2 < i, j_3 < i$. As shown in Fig. 3.2, we first investigate how agent 4 can be merged with the first triangular formation, and then we illustrate how agents 5 to N can be similarly merged into the resulting formations.

We can design a similar stabilization control algorithm for agent 4 to achieve

the two desired angles α_{142}^* and α_{243}^*

$$u_4 = -k_{41}(\alpha_{142} - \alpha_{142}^*)(z_{41} + z_{42}) - k_{42}(\alpha_{243} - \alpha_{243}^*)(z_{42} + z_{43}), \tag{4.61}$$

where k_{41} and k_{42} are positive constants. To make agent 4 also maneuver with the desired translation, rotation and scaling, we modify the stabilization control algorithm (4.61) as the following formation maneuver control algorithm

$$\begin{aligned} u_4 =& -k_{41}(\alpha_{142} - \alpha_{142}^* - \frac{\mu_4}{k_{41}})(z_{41} + z_{42}) - k_{42}(\alpha_{243} - \alpha_{243}^* - \frac{\tilde{\mu}_4}{k_{42}})(z_{42} + z_{43}) \\ =& -k_{41}(\alpha_{142} - \alpha_{142}^*)(z_{41} + z_{42}) - k_{42}(\alpha_{243} - \alpha_{243}^*)(z_{42} + z_{43}) \\ &+ \mu_4 z_{41} + (\mu_4 + \tilde{\mu}_4) z_{42} + \tilde{\mu}_4 z_{43} \\ =& u_{f4} + u_{m4}, \end{aligned} \tag{4.62}$$

where $\mu_4 \in \mathbb{R}$ and $\tilde{\mu}_4 \in \mathbb{R}$ are the designed-mismatches associated with agent 4's desired angles α_{142}^* and α_{243}^*.

By following the similar steps given in Subsections. III. B and C, we give the following procedure for the measurement-dependent and measurement-independent mismatch cases, respectively.

A. Measurement-dependent mismatches

Similar to the design procedure (4.14)-(4.26), we use the measurement-dependent mismatches $\mu_4(t), \tilde{\mu}_4(t)$ to realize the desired maneuvering under the measurements of $z_{4i}, i = 1, 2, 3$ and $p_{c4} = p_4 - p_c$.

(1) Translation

According to (4.13), only considering translation maneuvering, one requires

$$v_c^* = \mu_4(t) z_{41} + (\mu_4(t) + \tilde{\mu}_4(t)) z_{42} + \tilde{\mu}_4(t) z_{43}, \tag{4.63}$$

Then, $\mu_4(t)$ and $\tilde{\mu}_4(t)$ can be calculated by

$$\begin{bmatrix} \mu_4(t) \\ \tilde{\mu}_4(t) \end{bmatrix} = \begin{bmatrix} (z_{41} + z_{42})(1) & (z_{42} + z_{43})(1) \\ (z_{41} + z_{42})(2) & (z_{42} + z_{43})(2) \end{bmatrix}^{-1} \begin{bmatrix} v_c^*(1) \\ v_c^*(2) \end{bmatrix}.$$

(2) Rotation

Based on (4.13), considering rotation maneuvering, one has

$$\omega^* E p_{c4} = \mu_4(t) z_{41} + (\mu_4(t) + \tilde{\mu}_4(t)) z_{42} + \tilde{\mu}_4(t) z_{43}. \tag{4.64}$$

Similarly, $\mu_4(t), \tilde{\mu}_4(t)$ can be calculated.

(3) Scaling

Only considering scaling maneuvering in (4.13), one has

$$s(t)p_{c4} = \mu_4(t)z_{41} + (\mu_4(t) + \tilde{\mu}_4(t))z_{42} + \tilde{\mu}_4(t)z_{43}. \tag{4.65}$$

Then, $\mu_4(t), \tilde{\mu}_4(t)$ can be calculated. By applying translation, rotation and scaling simultaneously, one has

$$\begin{bmatrix}\mu_4(t)\\ \tilde{\mu}_4(t)\end{bmatrix} = [z_{41} + z_{42}\ z_{42} + z_{43}]^{-1}(v_c^* + \omega^* E p_{c4} + s(t)p_{c4}). \tag{4.66}$$

Now, we give the result for the 4-agent case.

Theorem 4.8. *Consider a 4-agent formation described by (4.9), with the control (4.12) for agents 1 to 3, the control (4.62) for agent 4, and the mismatches $\mu_i(t), \tilde{\mu}_i(t), i = 1, 2, 3$ as designed in (4.26), and $\mu_4, \tilde{\mu}_4$ as designed in (4.66). If the initial angle errors $e_i(0), i = 1, 2, 3$ and $e_{41}(0), e_{42}(0)$ are sufficiently small, $\alpha_i(0) \neq 0$, $\sin\alpha_{124}^* > \sin\alpha_{214}^*$, $\sin\alpha_{423}^* > \sin\alpha_{234}^*$, and $\alpha_{143}^* = \alpha_{142}^* + \alpha_{243}^*$ and $\|p_i(0) - p_j(0)\|, i \neq j$ are sufficiently away from zero, then the 4-agent formation converges exponentially to its desired shape and maneuvers with the prescribed translation, rotation and scaling simultaneously.*

Proof. According to Appendix C, one has agent 4's angle error dynamics

$$\begin{aligned}\dot{e}_4 &= \begin{bmatrix}\dot{e}_{41}\\ \dot{e}_{42}\end{bmatrix} = F_4(e_4)e_4 + W(e_4)e_s \\ &= \begin{bmatrix}-\bar{g}_1 & \bar{f}_{12}\\ \bar{f}_{21} & -\bar{g}_2\end{bmatrix}\begin{bmatrix}\alpha_{142} - \alpha_{142}^*\\ \alpha_{243} - \alpha_{243}^*\end{bmatrix} + \begin{bmatrix}w_{11} & w_{12}\\ w_{21} & w_{22}\end{bmatrix}\begin{bmatrix}e_1\\ e_2\end{bmatrix},\end{aligned} \tag{4.67}$$

where $\bar{g}_1 = k_{41}\sin\alpha_{142}(1/l_{41} + 1/l_{42}), \bar{g}_2 = k_{42}\sin\alpha_{243}(1/l_{43} + 1/l_{42})$, $\bar{f}_{12} = -\frac{k_{42}(\sin\alpha_{142}+\sin\alpha_{143})}{l_{41}} + \frac{k_{42}\sin\alpha_{243}}{l_{42}}, \bar{f}_{21} = -\frac{k_{41}(\sin\alpha_{243}+\sin\alpha_{143})}{l_{43}} + \frac{k_{41}\sin\alpha_{142}}{l_{42}}, w_{11} = \frac{z_{42}^{\mathrm{T}}P_{z_{41}}(z_{12}+z_{13})}{l_{41}\sin\alpha_{142}}, w_{12} = \frac{z_{41}^{\mathrm{T}}P_{z_{42}}(z_{21}+z_{23})}{l_{42}\sin\alpha_{142}}, w_{21} = -\frac{z_{42}^{\mathrm{T}}P_{z_{43}}(z_{31}+z_{32})}{l_{43}\sin\alpha_{243}}, w_{22} = \frac{z_{43}^{\mathrm{T}}P_{z_{42}}(z_{21}+z_{23})}{l_{42}\sin\alpha_{243}} - \frac{z_{42}^{\mathrm{T}}P_{z_{43}}(z_{31}+z_{32})}{l_{43}\sin\alpha_{243}}$.

By considering a small neighborhood of the origin $\{e_1 = 0, e_2 = 0, e_{41} = 0, e_{42} = 0\}$, (4.67) can be linearized to

$$\dot{e}_4 = A_2 e_4 + B_2 e_s, \tag{4.68}$$

where $A_2 = F_4(e_4)|_{e_4=0,e_s=0}$, and $B_2 = W(e_4)|_{e_4=0,e_s=0}$. Then, one has

$$\text{tr}(A_2) = (-\bar{g}_1 - \bar{g}_2)|_{e_4=0,e_s=0} < 0,$$

$$\begin{aligned}
&\frac{\det(A_2)}{k_{41}k_{42}}|_{e_4=0,e_s=0} = \frac{\bar{g}_1\bar{g}_2 - \bar{f}_{12}\bar{f}_{21}}{k_{41}k_{42}}|_{e_4=0,e_s=0} \\
&= \frac{l_{41}^*(\sin\alpha_{241}^*\sin\alpha_{342}^* + \sin^2\alpha_{342}^* + \sin\alpha_{342}^*\sin\alpha_{341}^*)}{l_{41}^*l_{42}^*l_{43}^*} \\
&+ \frac{l_{43}^*(\sin\alpha_{241}^*\sin\alpha_{342}^* + \sin^2\alpha_{241}^* + \sin\alpha_{241}^*\sin\alpha_{341}^*)}{l_{42}^*l_{41}^*l_{43}^*} \\
&- \frac{l_{42}^*(\sin\alpha_{241}^*\sin\alpha_{341}^* + \sin\alpha_{341}^*\sin\alpha_{342}^* + \sin^2\alpha_{341}^*)}{l_{41}^*l_{42}^*l_{43}^*}.
\end{aligned}$$

Then, if $\det(A_2) > 0$, one has that A_2 is Hurwitz. It can be observed that $\det(A_2) > 0$ if $l_{41}^* > l_{42}^*$ and $l_{43}^* > l_{42}^*$ hold because on the one hand

$$l_{43}^*\sin\alpha_{241}^*\sin\alpha_{341}^* > l_{42}^*\sin\alpha_{241}^*\sin\alpha_{341}^*, \;\; l_{41}^*\sin\alpha_{341}^*\sin\alpha_{342}^* > l_{42}^*\sin\alpha_{341}^*\sin\alpha_{342}^*,$$

since $\sin\alpha_{341}^*\sin\alpha_{342}^* > 0$. On the other hand,

$$\begin{aligned}
&\sin^2\alpha_{341}^* = [\sin\alpha_{241}^*\cos\alpha_{342}^* + \cos\alpha_{241}^*\sin\alpha_{342}^*]^2 \\
&= \sin^2\alpha_{241}^*\cos^2\alpha_{342}^* + \cos^2\alpha_{241}^*\sin^2\alpha_{342}^* + 2\sin\alpha_{241}^*\cos\alpha_{342}^*\cos\alpha_{241}^*\sin\alpha_{342}^*,
\end{aligned}$$

and

$$l_{41}^*\sin^2\alpha_{342}^* > l_{42}^*\sin^2\alpha_{342}^*\cos^2\alpha_{241}^*, \;\; l_{43}^*\sin^2\alpha_{241}^* > l_{42}^*\sin^2\alpha_{241}^*\cos^2\alpha_{342}^*,$$

since $\cos^2\alpha_{241}^* < 0$, $\cos^2\alpha_{342}^* < 1$, and

$$\begin{aligned}
&l_{41}^*\sin\alpha_{241}^*\sin\alpha_{342}^* + l_{43}^*\sin\alpha_{241}^*\sin\alpha_{342}^* > 2l_{42}^*\sin\alpha_{241}^*\sin\alpha_{342}^* \\
&> 2l_{42}^*\sin\alpha_{241}^*\cos\alpha_{342}^*\cos\alpha_{241}^*\sin\alpha_{342}^*.
\end{aligned}$$

since $\sin\alpha_{241}^*\sin\alpha_{342}^* > 0$ and $\cos\alpha_{342}^*\cos\alpha_{241}^* < 1$. Based on law of sines, the conditions $l_{41}^* > l_{42}^*$ and $l_{43}^* > l_{42}^*$ are equivalent to $\sin\alpha_{124}^* > \sin\alpha_{214}^*$ and $\sin\alpha_{423}^* > \sin\alpha_{234}^*$, respectively.

Combining (4.29) and (4.68), one has the linearized 4-agent angle error dynamics

$$\dot{\bar{e}}_4 = \begin{bmatrix} \dot{e}_s \\ \dot{e}_4 \end{bmatrix} = A_4\bar{e}_4 = \begin{bmatrix} A_1 & 0 \\ B_2 & A_2 \end{bmatrix}\begin{bmatrix} e_s \\ e_4 \end{bmatrix}. \tag{4.69}$$

When A_1 and A_2 are Hurwitz, one has that A_4 is also Hurwitz. Then, for an arbitrary positive definite matrix $Q_3 \in \mathbb{R}^{4\times4}$, there always exists a positive definite

matrix $P_3 \in \mathbb{R}^{4\times 4}$ such that $-Q_3 = P_3 A_4 + A_4^{\mathrm{T}} P_3$. Design the Lyapunov function candidate as

$$V_3 = \bar{e}_4^{\mathrm{T}} P_3 \bar{e}_4,$$

whose time-derivative is

$$\dot{V}_3 = -\bar{e}_4^{\mathrm{T}} Q_3 \bar{e}_4 \leqslant -\lambda_{\min}(Q_3)\|\bar{e}_4\|^2 \leqslant -\frac{\lambda_{\min}(Q_3)}{\lambda_{\max}(P_3)} V_3.$$

Then, one has

$$\|e_4\|^2 \leqslant \|\bar{e}_4\|^2 \leqslant \frac{V_3}{\lambda_{\min}(P_3)} \leqslant \frac{V_3(0)}{\lambda_{\min}(P_3)} e^{-\frac{\lambda_{\min}(Q_3)}{\lambda_{\max}(P_3)}t}, \tag{4.70}$$

which implies that $\|e_4\|$ also exponentially converges to zero when the four agents' initial angle errors are in a small neighborhood of the origin $\{e_1 = 0, e_2 = 0, e_{41} = 0, e_{42} = 0\}$. To make the calculation of (4.66) valid and $W(e_4)$ well-defined, one has to guarantee that $z_{41}(t) \neq \pm z_{42}(t), z_{42}(t) \neq \pm z_{43}(t), \forall t > 0$, which are equivalent to $\alpha_{142}(t) \neq 0, \pi$ and $\alpha_{243}(t) \neq 0, \pi, \forall t > 0$, respectively. From (4.70), one has $|e_{41}(t)| \leqslant \sqrt{\frac{V_3(0)}{\lambda_{\min}(P_3)}}$, which implies

$$-\sqrt{\frac{V_3(0)}{\lambda_{\min}(P_3)}} + \alpha_{142}^* \leqslant \alpha_{142}(t) \leqslant \sqrt{\frac{V_3(0)}{\lambda_{\min}(P_3)}} + \alpha_{142}^*.$$

Therefore, if

$$\sqrt{V_3(0)} < \sqrt{\lambda_{\min}(P_3)} * \min\{\pi - \alpha_{142}^*, \alpha_{142}^*, \pi - \alpha_{243}^*, \alpha_{243}^*\},$$

one obtains $0 < \alpha_{142}(t) < \pi, 0 < \alpha_{243}(t) < \pi, \forall t > 0$, which guarantee the validness of the calculation of (4.66) since the first three agents are not collinear for $\forall t > 0$. Then, according to (4.9) and (4.62), one has $\lim_{t\to\infty} \dot{p}_4(t) = \lim_{t\to\infty} u_{m4}(t) = \lim_{t\to\infty}[\mu_4(t) z_{41} + (\mu_4(t) + \tilde{\mu}_4(t)) z_{42} + \tilde{\mu}_4(t) z_{43}] = \lim_{t\to\infty} \dot{p}_4^*(t)$. By using (4.63)-(4.65), one has that the maneuvering defined in (4.13) is achieved. □

To guarantee that $\|W(e_4)\|$ is bounded and control law (4.62) is well-defined, the collision between agent 4 and agents 1 to 3 needs to be avoided. Similar to the 3-agent formation case, we conduct the collision analysis by considering $l_{41}(t)$ which takes agent 1 as an example

$$l_{41}(t) = l_{41}(0) + \int_0^t z_{41}^{\mathrm{T}}(u_{f1} - u_{f4} + u_{m1} - u_{m4})\mathrm{d}\tau. \tag{4.71}$$

On the one hand, by using (4.33) and (4.70), one has

$$\begin{aligned}
&\int_0^t z_{41}^{\mathrm{T}}(u_{f1}-u_{f4})\mathrm{d}\tau \leqslant \int_0^t 2(k_1|e_1|+k_{41}|e_{41}|+k_{42}|e_{42}|)d\tau\\
&\leqslant \int_0^t 2(k_1\sqrt{e_1^2+e_2^2}+\sqrt{2}\bar{k}_4\sqrt{e_{41}^2+e_{42}^2})d\tau\\
&\leqslant \frac{4k_1\lambda_{\max}(P_1)}{\lambda_{\min}(Q_1)}\sqrt{\frac{V_1(0)}{\lambda_{\min}(P_1)}}+\frac{4\bar{k}_4\lambda_{\max}(P_3)}{\lambda_{\min}(Q_3)}\sqrt{\frac{2V_3(0)}{\lambda_{\min}(P_3)}},
\end{aligned}$$

where $\bar{k}_4=\max\{k_{41},k_{42}\}$. On the other hand, by using (4.26) and (4.66), one has

$$\begin{aligned}
&\int_0^t z_{41}^{\mathrm{T}}(u_{m1}-u_{m4})\mathrm{d}\tau=\int_0^t z_{41}^{\mathrm{T}}\left(\omega^* E+s(\tau)I_2\right)(p_{c1}-p_{c4})\mathrm{d}\tau\\
&=\int_0^t s(\tau)l_{41}(\tau)\mathrm{d}\tau\geqslant 0
\end{aligned}\tag{4.72}$$

when $s(t)>0$. For the case of $s(t)<0$, the conclusion can be similarly analyzed by following (4.50)-(4.51). Similarly, one has the following proposition.

Proposition 4.9. *Consider a 4-agent formation described by (4.9), with the control (4.12) for agents 1 to 3, the control (4.62) for agent 4, and the mismatches $\mu_i(t),\tilde{\mu}_i(t),i=1,2,3$ as designed in (4.26), and $\mu_4(t),\tilde{\mu}_4(t)$ as designed in (4.66) and $s(t)>0$. If the initial angle errors $e_i(0),i=1,2,3$ and $e_{41}(0),e_{42}(0)$ are sufficiently small, $\alpha_i(0)\neq 0$, $\sin\alpha_{124}^*>\sin\alpha_{214}^*$, $\sin\alpha_{423}^*>\sin\alpha_{234}^*$, and $\alpha_{143}^*=\alpha_{142}^*+\alpha_{243}^*$. If $l_{41}(0)>\frac{4k_1\lambda_{\max}(P_1)}{\lambda_{\min}(Q_1)}\sqrt{\frac{V_1(0)}{\lambda_{\min}(P_1)}}+\frac{4\bar{k}_4\lambda_{\max}(P_3)}{\lambda_{\min}(Q_3)}\sqrt{\frac{2V_3(0)}{\lambda_{\min}(P_3)}}$, then no collision will happen between agents 4 and 1.*

Now, we design a general formation maneuver control algorithm for arbitrary agent $i,4\leqslant i\leqslant N$

$$\begin{aligned}
u_i=&-k_{i1}(\alpha_{j_1ij_2}-\alpha_{j_2ij_3}^*-\frac{\mu_i}{k_{i1}})(z_{ij_1}+z_{ij_2})-k_{i2}(\alpha_{j_2ij_3}-\alpha_{j_2ij_3}^*-\frac{\tilde{\mu}_i}{k_{i2}})(z_{ij_2}+z_{ij_3})\\
=&-k_{i1}(\alpha_{j_1ij_2}-\alpha_{j_1ij_2}^*)(z_{ij_1}+z_{ij_2})-k_{i2}(\alpha_{j_2ij_3}-\alpha_{j_2ij_3}^*)(z_{ij_2}+z_{ij_3})\\
&+\mu_i z_{ij_1}+(\mu_i+\tilde{\mu}_i)z_{ij_2}+\tilde{\mu}_i z_{ij_3}\\
=&u_{fi}+u_{mi},
\end{aligned}\tag{4.73}$$

where $\mu_i(t),\tilde{\mu}_i(t)$ can be similarly designed according to (4.63)-(4.66), and $j_1,j_2,j_3<i$. Under the fact that 4-agent formation achieves the desired shape exponentially, we suppose for a $4<k<N$, the k-agent formation converges to the desired shape exponentially. We need to prove that for $(k+1)$-agent formation, the angle errors $e_{(k+1)1}=\alpha_{j_1(k+1)j_2}-\alpha_{j_1(k+1)j_2}^*$ and $e_{(k+1)2}=\alpha_{j_2(k+1)j_3}-\alpha_{j_2(k+1)j_3}^*$ converges to zero exponentially. Similar to the proof from (4.61) to (4.70), one has that the an-

gle errors $e_{(k+1)1}$ and $e_{(k+1)2}$ exponentially converge to zero. Therefore, the control algorithm (4.73) can locally stabilize agent $k+1$, i.e., the $(k+1)$-agent formation converges to the desired shape exponentially. So, by using induction, N-agent formation converges to the desired formation shape exponentially. Similarly, the formation maneuvering is achieved since $\lim_{t\to\infty}\dot{p}_i(t)=\lim_{t\to\infty}u_{mi}(t)=\lim_{t\to\infty}\dot{p}_i^*(t)$.

B. Measurement-independent mismatches

Similar to the design procedure (4.63)-(4.66), we use the measurement-independent mismatches to realize the desired maneuvering under the measurements of $z_{4i}, i=1,2,3$, and the information of desired formation shape p^{b*} described in $\sum_{b(0)}$ is required to be known in the mismatch design stage.

By applying translation, rotation and scaling simultaneously, one has

$$\mu_4 z_{41}^{b*}+(\mu_4+\tilde{\mu}_4)z_{42}^{b*}+\tilde{\mu}_4 z_{43}^{b*}=v_c^{b*}+\omega^* E p_{c4}^{b*}+s(t)p_{c4}^{b*}, \tag{4.74}$$

where $z_{4j}^{b*}=\frac{p_j^{b*}-p_4^{b*}}{\|p_j^{b*}-p_4^{b*}\|}$. Then, mismatches $\mu_4,\tilde{\mu}_4$ can be calculated by

$$\begin{bmatrix}\mu_4\\ \tilde{\mu}_4\end{bmatrix}=[z_{41}^{b*}+z_{42}^{b*}\ z_{42}^{b*}+z_{43}^{b*}]^{-1}(v_c^{b*}+\omega^* E p_{c4}^{b*}+s(t)p_{c4}^{b*}) \tag{4.75}$$

which is well-defined when $[z_{41}^{b*}+z_{42}^{b*}\ z_{42}^{b*}+z_{43}^{b*}]^{-1}$ is invertible. Since no three points are collinear in the desired generically angle rigid formation[22, Definition 4], the matrix $[z_{41}^{b*}+z_{42}^{b*}\ z_{42}^{b*}+z_{43}^{b*}]$ is invertible. Now, we present the main result.

Theorem 4.10. *Consider a 4-agent formation described by (4.9), with the control (4.12) for agents 1 to 3, the control (4.62) for agent 4, and the mismatches $\mu_i,\tilde{\mu}_i, i=1,2,3$ as designed in (4.39), and $\mu_4,\tilde{\mu}_4$ as designed in (4.75). If the initial angle error $e_i(0), i=1,...,3$, $e_{41}(0), e_{42}(0)$ and the designed-mismatches are sufficiently small, $\alpha_i(0)\neq 0$ and $\|p_i(0)-p_j(0)\|, i\neq j$ are sufficiently away from zero and $\sin\alpha_{124}^*>\sin\alpha_{214}^*$, $\sin\alpha_{423}^*>\sin\alpha_{234}^*$, and $\alpha_{143}^*=\alpha_{142}^*+\alpha_{243}^*$, then the 4-agent formation converges exponentially to its desired shape and maneuvers with the prescribed translation (4.36), rotation (4.4) and scaling (4.5) simultaneously.*

Proof. According to Appendix D, one has agent 4's angle error dynamics

$$\begin{aligned}\dot{e}_4&=F_4(e_4)e_4+W(e_4)e_s+H_4(e_4)U_4 \\ &=\begin{bmatrix}-\bar{g}_1 & \bar{f}_{12}\\ \bar{f}_{21} & -\bar{g}_2\end{bmatrix}\begin{bmatrix}\alpha_{142}-\alpha_{142}^*\\ \alpha_{243}-\alpha_{243}^*\end{bmatrix}+\begin{bmatrix}w_{11} & w_{12}\\ w_{21} & w_{22}\end{bmatrix}\begin{bmatrix}e_1\\ e_2\end{bmatrix}\\ &\quad+\begin{bmatrix}h_{11} & h_{12} & h_{13} & h_{14} & h_{15} & h_{16} & h_{17} & h_{18}\\ h_{21} & h_{22} & h_{23} & h_{24} & h_{25} & h_{26} & h_{27} & h_{28}\end{bmatrix}U_4,\end{aligned} \tag{4.76}$$

where $F_4(e_4)$, $W(e_4)$ have the same definitions as (4.67), $h_{11} = -z_{42}^{\mathrm{T}} \frac{P_{z_{41}}}{l_{41}\sin\alpha_{142}} z_{12}$, $h_{12} = -z_{41}^{\mathrm{T}} \frac{P_{z_{42}}}{l_{42}\sin\alpha_{142}} z_{23}$, $h_{13} = 0$, $h_{14} = z_{42}^{\mathrm{T}} \frac{P_{z_{41}}}{l_{41}\sin\alpha_{142}} z_{42} + z_{41}^{\mathrm{T}} \frac{P_{z_{42}}}{l_{42}\sin\alpha_{142}} z_{41}$, $h_{15} = -z_{42}^{\mathrm{T}} \frac{P_{z_{41}}}{l_{41}\sin\alpha_{142}} z_{13}$, $h_{16} = -z_{41}^{\mathrm{T}} \frac{P_{z_{42}}}{l_{42}\sin\alpha_{142}} z_{21}$, $h_{17} = 0$, $h_{18} = z_{42}^{\mathrm{T}} \frac{P_{z_{41}}}{l_{41}\sin\alpha_{142}} (z_{42} + z_{43}) + z_{41}^{\mathrm{T}} \frac{P_{z_{42}}}{l_{42}\sin\alpha_{142}} z_{43}$, $h_{21} = 0$, $h_{22} = -z_{43}^{\mathrm{T}} \frac{P_{z_{42}}}{l_{42}\sin\alpha_{243}} z_{23}$, $h_{23} = -z_{42}^{\mathrm{T}} \frac{P_{z_{43}}}{l_{43}\sin\alpha_{243}} z_{31}$, $h_{24} = z_{42}^{\mathrm{T}} \frac{P_{z_{43}}}{l_{43}\sin\alpha_{243}} (z_{41} + z_{42}) + z_{43}^{\mathrm{T}} \frac{P_{z_{42}}}{l_{42}\sin\alpha_{243}} z_{41}$, $h_{25} = 0$, $h_{26} = -z_{43}^{\mathrm{T}} \frac{P_{z_{42}}}{l_{42}\sin\alpha_{243}} z_{21}$, $h_{27} = -z_{42}^{\mathrm{T}} \frac{P_{z_{43}}}{l_{43}\sin\alpha_{243}} z_{32}$, $h_{28} = z_{42}^{\mathrm{T}} \frac{P_{z_{43}}}{l_{43}\sin\alpha_{243}} z_{42} + z_{43}^{\mathrm{T}} \frac{P_{z_{42}}}{l_{42}\sin\alpha_{243}} z_{43}$,
$U_4 = [\mu_1, \mu_2, \mu_3, \mu_4, \tilde{\mu}_1, \tilde{\mu}_2, \tilde{\mu}_3, \tilde{\mu}_4]^{\mathrm{T}}$.

Note that $\|e_s\|$ and $\|U_4\|$ are sufficiently small. Therefore, the angle error dynamics (4.76) are locally stable when $F_4(e_4)|_{e_4=0}$ is Hurwitz. To obtain the local stability of (4.76), by using the similar analysis steps from (4.68) to (4.72), one has the local stability of angle error dynamics (4.76). Also, when the initial angle errors are sufficiently small and the initial distances are sufficiently away from zero, no collision will happen. Similarly, it can be proved that the prescribed formation maneuvering in terms of translation, rotation and scaling can be achieved. For agents $4 < i \leqslant N$, under the formation maneuver algorithm (4.73) with constant mismatches which are similarly designed according to (4.66), one can also prove that the formation shape and maneuvering can be achieved simultaneously. □

Remark 4.11. Note that the formation shape given in Fig. 3.2 is described by the angles $\measuredangle ijk$, which will be maintained by agent j under the bearing measurements of z_{ji} and z_{jk}. Therefore, the bearing measurements among the first three agents are undirected, while for agents from 4 to N, the bearing measurements are directed. In addition, since $p_i^b - p_j^b = p_i - p_c - (p_j - p_c) = p_i - p_j$, the maneuvering reference point p_c can be set as other well-selected point of interest, which is not necessary the centroid of the formation. Although the results in Theorems 1-4 and Propositions 1-3 are local, this work first realizes formation maneuvering by controlling interior angles and using bearing measurements.

4.4 Formation maneuvering for double-integrators

Consider in this section that for an N-agent system moving in the plane, the motion dynamics of its agent i are modeled by double-integrators

$$\begin{aligned} \dot{p}_i &= v_i, \\ \dot{v}_i &= u_i, i = 1, ..., N, \end{aligned} \tag{4.77}$$

where $v_i \in \mathbb{R}^2$ denotes the velocity of agent i. Note that the maneuvering reference point p_c used in rotation (4.4) and scaling (4.5) is usually set as the formation centroid or a leader agent's position in practical tasks. Considering the cascading construction of desired angle rigid formation in section 2.3, we assume in this

section that agent 1's position is the maneuvering reference point of the rotational and scaling motions, i.e., $p_c = p_1$. Then, the desired maneuvering velocity for agent $i, \forall i \in \mathcal{V}$ can be described by

$$v_{mi}(t) = v_c^* + \gamma_c^* e^{-t} p_{i1} + \omega_c^* E p_{i1}, \tag{4.78}$$

where $p_{i1} = p_1 - p_i$. Therefore, the objective of this section is to design control input u_i under the available information of $z_{ij}, j \in \mathcal{N}_i$ and $v_i - v_{mi}$ such that the formation maneuvering defined in (4.3)-(4.5) can be achieved. In the following, we consider two cases that the relative velocity $v_1 - v_i$ can or cannot be measured by agent $i, i = 2, \cdots, N$, respectively.

4.4.1 The case with relative velocity measurement

Now, we design the maneuvering control algorithm as

$$u_i = \dot{v}_{mi} - k_s(v_i - v_{mi}) - \sum\nolimits_{(j,i,k)\in\mathcal{A}} (\alpha_{jik} - \alpha_{jik}^*)(z_{ij} + z_{ik}), \tag{4.79}$$

where $\dot{v}_{mi}$ is the feedforward term for the agent's double-integrator dynamics which can be calculated by

$$\begin{aligned} \dot{v}_{mi} =& (\gamma_c^* I_2 + \omega_c^* E)\dot{p}_{i1} - \gamma_c^* e^{-t} p_{i1} \\ =& (\gamma_c^* I_2 + \omega_c^* E)(v_1 - v_i) - \gamma_c^* e^{-t} p_{i1}. \end{aligned} \tag{4.80}$$

Note that the relative velocity information $v_1 - v_i$ is included in (4.80).

Theorem 4.12. *Consider that N agents of double-integrator dynamics (4.77) are governed by (4.79), the initial angle and velocity errors are sufficiently small, and the initial distances are bounded away from zero. The formation maneuvering defined in (4.2), and (4.6)-*(4.8) *can be locally achieved if and only if (3.63) holds for $\forall i = 1, 4, \cdots, N$.*

Proof. First, we analyze the angle error dynamics and velocity error dynamics of the closed-loop system under the designed maneuvering control algorithm. In this maneuvering case, we define the following system state variables

$$Y = [e_1, e_2, e_{41}, e_{42}, \cdots, e_{N1}, e_{N2}, v_1^T - v_{m1}^T, \cdots, v_N^T - v_{mN}^T]^T. \tag{4.81}$$

Our objective is to prove that $Y = 0$ is a locally stable equilibrium under (4.79). Similar to the formation stabilization case, $\ddot{p}_i(0)$ is bounded if the initial velocity $v_i(0)$ is bounded and $l_{ij}(0), l_{ik}(0), \sin\alpha_{jik}(0)$ are bounded away from zero. Therefore, $\exists T_2 > 0$ such that $l_{ij}(t), l_{ik}(t), \sin\alpha_{jik}(t), \forall (j,i,k) \in \mathcal{A}$ are bounded away from zero for $t \in [0, T_2)$. We first analyze angle error and velocity error dynamics

for $t \in [0, T_2)$. According to (3.43), one has

$$\begin{aligned}\dot{\alpha}_{jik} =& - z_{ik}^T \frac{P_{z_{ij}}}{l_{ij}\sin\alpha_{jik}} v_j - z_{ij}^T \frac{P_{z_{ik}}}{l_{ik}\sin\alpha_{jik}} v_k \\ &+ (z_{ik}^T \frac{P_{z_{ij}}}{l_{ij}\sin\alpha_{jik}} + z_{ij}^T \frac{P_{z_{ik}}}{l_{ik}\sin\alpha_{jik}}) v_i. \end{aligned} \tag{4.82}$$

Note that the velocity error variable in this case is $v_i - v_{mi}$ instead of v_i. Therefore, we rewrite (4.82) into

$$\begin{aligned}\dot{\alpha}_{jik} =& - z_{ik}^T \frac{P_{z_{ij}}}{l_{ij}\sin\alpha_{jik}} v_j - z_{ij}^T \frac{P_{z_{ik}}}{l_{ik}\sin\alpha_{jik}} v_k + (z_{ik}^T \frac{P_{z_{ij}}}{l_{ij}\sin\alpha_{jik}} + z_{ij}^T \frac{P_{z_{ik}}}{l_{ik}\sin\alpha_{jik}}) v_i \\ =& - z_{ik}^T \frac{P_{z_{ij}}}{l_{ij}\sin\alpha_{jik}} (v_j - v_{mj}) - z_{ij}^T \frac{P_{z_{ik}}}{l_{ik}\sin\alpha_{jik}} (v_k - v_{mk}) \\ &+ (z_{ik}^T \frac{P_{z_{ij}}}{l_{ij}\sin\alpha_{jik}} + z_{ij}^T \frac{P_{z_{ik}}}{l_{ik}\sin\alpha_{jik}}) (v_i - v_{mi}) \\ &- z_{ik}^T \frac{P_{z_{ij}}}{l_{ij}\sin\alpha_{jik}} v_{mj} - z_{ij}^T \frac{P_{z_{ik}}}{l_{ik}\sin\alpha_{jik}} v_{mk} \\ &+ (z_{ik}^T \frac{P_{z_{ij}}}{l_{ij}\sin\alpha_{jik}} + z_{ij}^T \frac{P_{z_{ik}}}{l_{ik}\sin\alpha_{jik}}) v_{mi}. \end{aligned} \tag{4.83}$$

In the following, we investigate the effect of the maneuverings in the last three components of (4.83) on the angle dynamics $\dot{\alpha}_{jik}$. For translational maneuvering $v_{mi} = v_c^*, \forall i \in \mathcal{V}$, one has

$$- z_{ik}^T \frac{P_{z_{ij}}}{l_{ij}\sin\alpha_{jik}} v_c^* - z_{ij}^T \frac{P_{z_{ik}}}{l_{ik}\sin\alpha_{jik}} v_c^* + (z_{ik}^T \frac{P_{z_{ij}}}{l_{ij}\sin\alpha_{jik}} + z_{ij}^T \frac{P_{z_{ik}}}{l_{ik}\sin\alpha_{jik}}) v_c^* = 0. \tag{4.84}$$

For scaling maneuvering, one has

$$\begin{aligned}&- \gamma_c^* z_{ik}^T \frac{P_{z_{ij}}}{l_{ij}\sin\alpha_{jik}} p_{j1} - \gamma_c^* z_{ij}^T \frac{P_{z_{ik}}}{l_{ik}\sin\alpha_{jik}} p_{k1} \\ &+ \gamma_c^* (z_{ik}^T \frac{P_{z_{ij}}}{l_{ij}\sin\alpha_{jik}} + z_{ij}^T \frac{P_{z_{ik}}}{l_{ik}\sin\alpha_{jik}}) p_{i1} = 0. \end{aligned} \tag{4.85}$$

For rotational maneuvering, one has

$$- \frac{\omega_c^* z_{ik}^T P_{z_{ij}} E p_{j1}}{l_{ij}\sin\alpha_{jik}} - \frac{\omega_c^* z_{ij}^T P_{z_{ik}} E p_{k1}}{l_{ik}\sin\alpha_{jik}} + \omega_c^* (\frac{z_{ik}^T P_{z_{ij}}}{l_{ij}\sin\alpha_{jik}} + \frac{z_{ij}^T P_{z_{ik}}}{l_{ik}\sin\alpha_{jik}}) E p_{i1} = 0, \tag{4.86}$$

where we have used the fact that $P_{z_{ij}} z_{ij} = 0$.

Therefore, (4.84)-(4.86) imply that the maneuvering in terms of translation, rotation and scaling has no effect on the angle dynamics $\dot{\alpha}_{jik}, (j,i,k) \in \mathcal{A}$ in (4.83). This is because the whole formation's translation, rotation and scaling will not change the interior angle α_{jik}. Therefore, one still has the similar angle dynamics $\dot{\alpha}_{jik}$ in (4.83) as the case of formation stabilization (3.42).

Then, we analyze the velocity error dynamics of $v_i - v_{mi}$. By using (4.79), one has

$$\dot{v}_i - \dot{v}_{mi} = -k_s(v_i - v_{mi}) - \sum\nolimits_{(j,i,k)\in\mathcal{A}} (\alpha_{jik} - \alpha^*_{jik})(z_{ij} + z_{ik})$$

which is also similar to the velocity dynamics of formation stabilization due to the usage of the feedforward term $\dot{v}_{mi}$ in (4.79). Therefore, we obtain the following overall dynamics

$$\dot{Y} = \begin{bmatrix} 0_{(2N-4)\times(2N-4)} & R(Y) \\ B(Y) & -k_s \otimes I_{2N} \end{bmatrix} Y = D_3(Y)Y, \tag{4.87}$$

where $R(Y)$ and $B(Y)$ have the same definitions as (3.46) and (3.47). Therefore, using linearization for (4.87) around $Y = 0$, one can obtain the local and exponential convergence of the closed-loop dynamics (4.87) around the desired equilibrium $Y = 0$, which is the same as the local and exponential convergence of (3.48) around $X = 0$. Now, we extend T_2 to infinity to establish the stability for (4.87). Similar to (3.71)-(3.77), by constructing $V_2 = Y^T P_1 Y$, one has that no collinearity will happen since (3.73) and (3.77) still hold. The analysis for the distance change l_{ij} is slightly different. Note that (3.74) is changed to

$$\|v_i - v_{mi}\| \leqslant \|Y(t)\| \leqslant \sqrt{\frac{V_2(0)}{\lambda_{\min}(P_1)}} e^{-\frac{\lambda_{\min}(Q_1)}{2\lambda_{\max}(P_1)}t}, \tag{4.88}$$

Also, (3.76) is changed to

$$\begin{aligned} l_{ij}(t) &= l_{ij}(0) + \int_0^t z_{ij}^T (v_j - v_i) d\tau \\ &\geqslant l_{ij}(0) - \int_0^t (\|v_j - v_{mj}\| + \|v_i - v_{mi}\| + z_{ij}^T (v_{mi} - v_{mj})) d\tau \\ &\geqslant l_{ij}(0) - 4\sqrt{\frac{V_2(0)}{\lambda_{\min}(P_1)}} \frac{\lambda_{\max}(P_1)}{\lambda_{\min}(Q_1)} (1 - e^{-\frac{\lambda_{\min}(Q_1)}{2\lambda_{\max}(P_1)}t}) + \gamma_c^* \int_0^t e^{-\tau} l_{ij}(\tau) \mathrm{d}\tau, \end{aligned} \tag{4.89}$$

where the last part $\gamma_c^* \int_0^t e^{-\tau} l_{ij}(\tau) d\tau$ describes the distance change under scaling maneuvering. Therefore, when $\gamma_c^* > 0$, i.e., enlarging the formation, the satisfied condition (3.78) is enough to guarantee $l_{ij}(t) > 0$ in this case. When $\gamma_c^* < 0$, i.e., shrinking the formation, we need to further analyze how much the shrinking will

conduct in the last part of (4.89). By using the integration by parts, one has

$$\begin{aligned}
&\gamma_c^* \int_0^t e^{-\tau} l_{ij}(\tau)\mathrm{d}\tau = -\gamma_c^* e^{-t} l_{ij} + \gamma_c^* \int_0^t e^{-t}\mathrm{d}l_{ij} \\
&= -\gamma_c^* e^{-t} l_{ij} + \gamma_c^{*2} \int_0^t e^{-2\tau} l_{ij}(\tau)\mathrm{d}\tau \\
&\quad + \gamma_c^* \int_0^t e^{-t} z_{ij}^T (v_j - v_{mj} - v_i + v_{mi})\mathrm{d}\tau,
\end{aligned} \tag{4.90}$$

where $-\gamma_c^* e^{-t} l_{ij} + \gamma_c^{*2} \int_0^t e^{-2\tau} l_{ij}(\tau)\mathrm{d}\tau > 0$. For the last part of (4.90), one has

$$\begin{aligned}
&\gamma_c^* \int_0^t e^{-t} z_{ij}^T (v_j - v_{mj} - v_i + v_{mi})\mathrm{d}\tau \\
\leqslant &|\gamma_c^*| \int_0^t (\|v_j - v_{mj}\| + \|v_i - v_{mi}\|)\mathrm{d}\tau \\
\leqslant &4|\gamma_c^*| \sqrt{\frac{V_2(0)}{\lambda_{\min}(P_1)}} \frac{\lambda_{\max}(P_1)}{\lambda_{\min}(Q_1)} (1 - e^{-\frac{\lambda_{\min}(Q_1)}{2\lambda_{\max}(P_1)} t}).
\end{aligned} \tag{4.91}$$

By summing up (4.89)-(4.91), one has that if

$$l_{ij}(0) > 4(|\gamma_c^*| + 1) \sqrt{\frac{V_2(0)}{\lambda_{\min}(P_1)}} \frac{\lambda_{\max}(P_1)}{\lambda_{\min}(Q_1)}, \tag{4.92}$$

then $l_{ij}(t) > 0$. Since $V_2(0)$ is sufficiently small, the right side of (4.92) is also sufficiently small. Therefore (4.92) holds and T_2 can be extended to infinity. Then, it follows that $\lim_{t\to\infty} Y(t) = 0$, which implies that e_1, e_2 and $e_{i1}, e_{i2}, i = 4, ..., N$ are locally and exponentially achieved. By summarizing the above analysis, we come to the conclusion that the formation maneuvering in terms of translation, rotation and scaling can be achieved under (4.79). □

4.4.2 The case without relative velocity measurement

Now, we consider that the relative velocity information $v_1 - v_i$ is unavailable for agent $i, i = 2, \cdots, N$. First, we rewrite (4.80) into

$$\begin{aligned}
\dot{v}_{mi} =&(\gamma_c^* I_2 + \omega_c^* E)(v_1 - v_i) - \gamma_c^* e^{-t} p_{i1} \\
=&(\gamma_c^* I_2 + \omega_c^* E)[(v_1 - v_{m1}) - (v_i - v_{mi})] \\
&- (\gamma_c^* I_2 + \omega_c^* E + \gamma_c^* e^{-t} I_2) p_{i1}.
\end{aligned} \tag{4.93}$$

Note that if the formation achieves the desired collective motion, then $(v_1 - v_{m1})$ and $(v_i - v_{mi})$ converge to zero. This motivate us to investigate whether the

following control law

$$\begin{aligned} u_i = &-(\gamma_c^* I_2 + \gamma_c^* e^{-t} I_2 + \omega_c^* E) p_{i1} - k_s(v_i - v_{mi}) \\ &- \sum\nolimits_{(j,i,k)\in\mathcal{A}} (\alpha_{jik} - \alpha_{jik}^*)(z_{ij} + z_{ik}), i \in \mathcal{V} \end{aligned} \tag{4.94}$$

is sufficient to achieve the desired formation shape together with the desired collective motion. In comparison to the maneuvering control law (4.79), no relative velocity measurement $(v_1 - v_i)$ is needed in (4.94).

Theorem 4.13. *Consider that N agents of double-integrator dynamics (4.77) are governed by (4.94), the initial angle and velocity errors are sufficiently small, and the initial distances are bounded away from zero. The formation maneuvering defined in (4.2), and (4.6)-(4.8) can be locally achieved if (3.63) holds for $\forall i = 1, 4, \cdots, N$ and the rotational ω_c^* and scaling speed γ_c^* are sufficiently small.*

Proof. By following steps from (4.82)-(4.87), the linearized closed-loop dynamics under (4.94) will become

$$\dot{Y} = (D_1^* + D_3)Y = (D_1^* + \begin{bmatrix} 0_{(2N-4)\times(2N-4)} & 0 \\ 0 & D_4 \end{bmatrix})Y, \tag{4.95}$$

where $D_4 = \begin{bmatrix} 0 & 0 & 0 & \cdots & 0 \\ -\bar{B} & \bar{B} & 0 & \cdots & 0 \\ -\bar{B} & 0 & \bar{B} & \cdots & 0 \\ -\bar{B} & 0 & 0 & \cdots & \bar{B} \end{bmatrix}$ and $\bar{B} = \gamma_c^* I_2 + \omega_c^* E + \gamma_c^* e^{-t} I_2$. According to the conclusion in Theorem 1, under condition (3.63), D_1^* is Hurwitz. Now, we design the Lyapunov function candidate

$$V_3 = \frac{1}{2} Y^T P_1 Y. \tag{4.96}$$

Taking the time-derivative of (4.96) yields

$$\begin{aligned} \dot{V}_3 &= -Y^T Q_1 Y + Y^T (D_3 P_1 + P_1 D_3^T) Y \\ &\leqslant -\lambda_{\min}(Q_1) Y^T Y + 2\|P_1\|\|D_3\| Y^T Y \\ &\leqslant -\left[\lambda_{\min}(Q_1) - 16(N-1)(|\gamma_c^*| + |\omega_c^*|)\|P_1\|\right] Y^T Y, \end{aligned} \tag{4.97}$$

where we used the fact that $\|D_3\|_2 \leqslant (4N-4)\|D_3\|_{\max} = 8(N-1)(2|\gamma_c^*| + |\omega_c^*|)$. Because Q_1 is an arbitrary given matrix, one can select sufficiently small $\|P_1\|$ and $2|\gamma_c^*| + |\omega_c^*|$ such that $\lambda_{\min}(Q_1) > 16(N-1)(2|\gamma_c^*| + |\omega_c^*|)\|P_1\|$ holds. According to (3.71), one has $P_1 = \int_0^\infty e^{D_1^{*T} t} Q_1 e^{D_1^* t} \mathrm{d}t$ where $\mathrm{Re}(\lambda(D_1^*)) < 0$ since D_1^* is Hurwitz. According to (3.50), one can select proper k_s to obtain smaller $\|P_1\|$. Therefore, by properly choosing $k_s, \gamma_c^*, \omega_c^*$, one obtains that $\dot{V}_3 < 0$. Since (4.97) implies

exponential stability, the convergence analysis of the closed-loop dynamics can be extended to infinity, which implies that $\lim_{t\to\infty} Y(t) = 0$. By following similar steps as Theorem 4.12, one also obtains that the formation maneuvering in terms of translation, rotation and scaling can be achieved under (4.94). □

Remark 4.14. To make the formation maneuvering laws (4.79) and (4.94) implement in all agents' local coordinate frame, the desired translational maneuvering velocity v_c^* needs to be described in each agent's local coordinate frame in the design stage. But this is not required for rotation and scaling maneuverings since ω_c^* and γ_c^* are scalars which are independent on the orientation of coordinate frames.

4.5 Simulation examples

In this section, to verify the effectiveness of the proposed formation maneuver control algorithms, we present numerical simulation examples by conducting the 4-agent obstacle avoidance task. The desired angles describing the formation shape are set as $\alpha_1^* = \pi/4,\ \alpha_2^* = \pi/2,\ \alpha_3^* = \pi/4,\ \alpha_{142} = \arctan 0.5,\ \alpha_{243} = \arctan 0.5$. The initial positions of all agents are $p_1(0) = [0.8; -3.2],\ p_2(0) = [0.1; -4.4],\ p_3(0) = [-1.4; -3.3],\ p_4(0) = [0.1; -5.3]$. The positions described in $\sum_{b*}$ are $p_1^{b*} = [0.9619; 4.6234],\ p_2^{b*} = [-0.1706; 3.1289],\ p_3^{b*} = [-1.6666; 4.2629],$ $p_4^{b*} = [0.0134; 1.8154]$, which satisfy all the desired angle constraints. The control gains are set to be $k_i = 1, i = 1, 2, 3,\ k_{41} = k_{42} = 1$. For the case of time-varying mismatches, the maneuvering command velocity is $v_c^* = [0; 1.2], t \in [0, 9];\ v_c^* = [1; 0], t \in [11, 20];\ \omega^* = -\frac{\pi}{8}, t \in [7, 11];\ s(t) = -0.8e^{-0.4(t-12)}, t \in [12, 13];\ s(t) = 0.8e^{-0.4(t-16)}, t \in [16.5, 17]$. The corresponding simulation results are shown in Fig. 4-5.

For the case of constant mismatches, the maneuvering command velocity is $v_c^{b*} = [0.5795; 0.9933], t \in [0, 9];\ v_c^{b*} = [[1.2957; 0.7558], t \in [13, 20];\ \omega^* = -\frac{\pi}{8}, t \in [9, 13];\ s(t) = -0.4e^{-0.4(t-12)}, t \in [14, 15];\ s(t) = 0.4e^{-0.4(t-12)}, t \in [16.5, 17]$.

The corresponding simulation results are shown in Fig. 6-7.

From the above simulation results, it is clear that in both the constant and time-varying mismatch cases, the translation, rotation and scaling maneuvering can be conducted simultaneously. The angle errors converge at an exponential speed in both cases.

4.6 appendices

Appendix A: For Section III. B, we use the dot product of two bearings to obtain the angle error dynamics. In the following, we consider the maneuvering of translation,

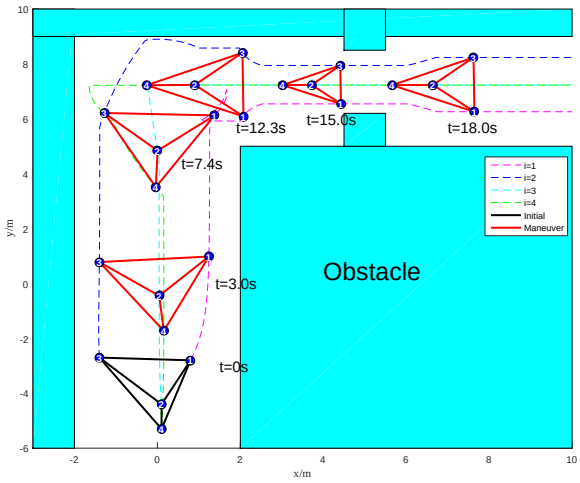

Figure 4.4: *The formation maneuvering trajectories under measurement-dependent mismatches.*

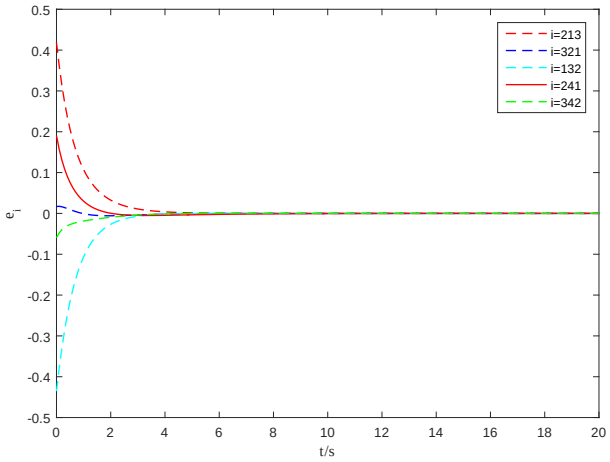

Figure 4.5: *The evolution of angle errors under measurement-dependent mismatches.*

rotation and scaling simultaneously. Take agent 1 as an example,

$$\frac{\mathrm{d}(\cos\alpha_1)}{\mathrm{d}t} = -\sin(\alpha_1)\dot{\alpha}_1 = \frac{\mathrm{d}(z_{12}^{\mathrm{T}} z_{13})}{\mathrm{d}t} = (\dot{z}_{12})^{\mathrm{T}} z_{13} + (z_{12})^{\mathrm{T}} \dot{z}_{13}. \tag{4.98}$$

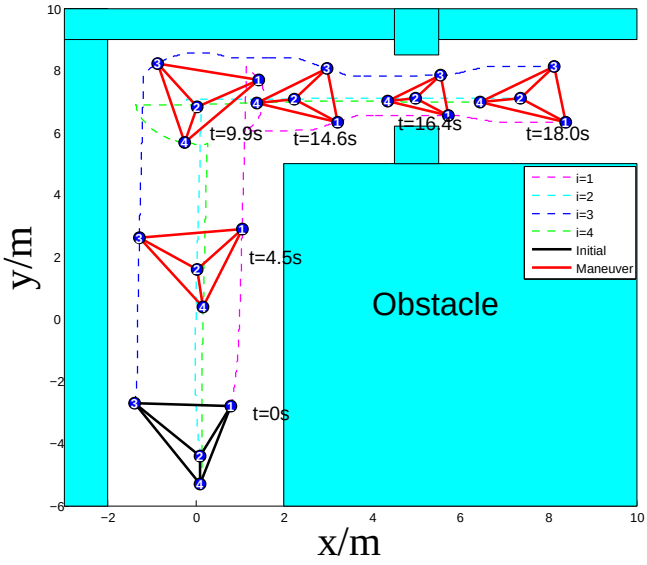

Figure 4.6: *The formation maneuvering trajectories under measurement-independent mismatches.*

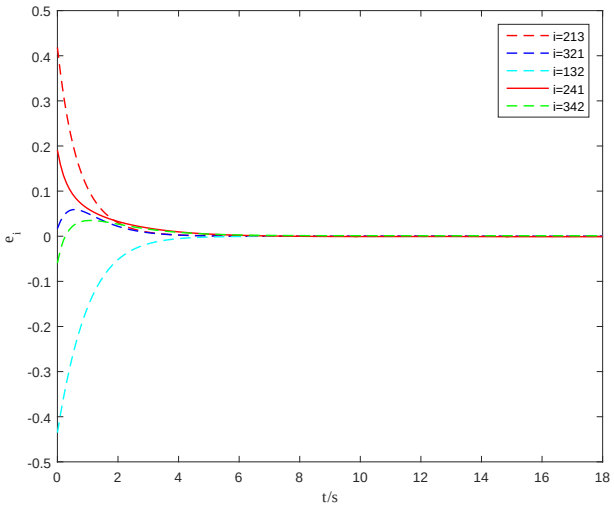

Figure 4.7: *The evolution of angle errors under measurement-independent mismatches.*

Considering that for $x \in \mathbb{R}^2, x \neq 0$, $\frac{\mathrm{d}}{\mathrm{d}t}(\frac{x}{\|x\|}) = \frac{I_2 - \frac{x}{\|x\|}\frac{x^{\mathrm{T}}}{\|x\|}}{\|x\|}\dot{x}$ and denoting $P_{x/\|x\|} = I_2 - \frac{x}{\|x\|}\frac{x^{\mathrm{T}}}{\|x\|}$, one has

$$\dot{z}_{12} = \frac{P_{z_{12}}}{l_{12}}(\dot{p}_2 - \dot{p}_1). \tag{4.99}$$

By using (4.12), one has

$$\begin{aligned}\dot{z}_{12} =&\frac{P_{z_{12}}}{l_{12}}(u_2-u_1) \\ =&\frac{P_{z_{12}}}{l_{12}}[-k_2(\alpha_2-\alpha_2^*)(z_{23}+z_{21})+\mu_2(t)z_{23}+\tilde{\mu}_2(t)z_{21} \\ &+k_1(\alpha_1-\alpha_1^*)(z_{13}+z_{12})-\mu_1(t)z_{12}-\tilde{\mu}_1(t)z_{13}].\end{aligned} \tag{4.100}$$

According to (4.26), one has

$$\begin{aligned}&\mu_2(t)z_{23}+\tilde{\mu}_2(t)z_{21}-\mu_1(t)z_{12}-\tilde{\mu}_1(t)z_{13} \\ =&v_c^*+(\omega^*E+s(t)I_2)p_{c2}-v_c^*-(\omega^*E+s(t)I_2)p_{c1} \\ =&\left(\omega^*E+s(t)I_2\right)(p_{c2}-p_{c1}).\end{aligned} \tag{4.101}$$

Substituting (4.101) into (4.100) yields

$$\begin{aligned}(\dot{z}_{12})^{\mathrm{T}}z_{13} =&[k_1(\alpha_1-\alpha_1^*)(z_{13}+z_{12})-k_2(\alpha_2-\alpha_2^*)(z_{23}+z_{21}) \\ &+(\omega^*E+s(t)I_2)(p_{c2}-p_{c1})]^{\mathrm{T}}\frac{P_{z_{12}}}{l_{12}}z_{13} \\ =&\frac{1}{l_{12}}[k_1(\sin^2\alpha_1)(\alpha_1-\alpha_1^*)-k_2(\sin\alpha_1\sin\alpha_2)(\alpha_2-\alpha_2^*)]-\omega^*z_{12}^{\mathrm{T}}EP_{z_{21}}z_{13},\end{aligned} \tag{4.102}$$

where we have used the fact that $P_x x=0$ for all $x\in\mathbb{R}^2$ and $s(t)l_{12}z_{12}^{\mathrm{T}}P_{z_{21}}z_{13}=0$. Since $x^{\mathrm{T}}Ex=0$ for all $x\in\mathbb{R}^2$, one has

$$-\omega^*z_{12}^{\mathrm{T}}EP_{z_{21}}z_{13}=-\omega^*z_{12}^{\mathrm{T}}Ez_{13}.$$

Similarly, one can get

$$\begin{aligned}(z_{12})^{\mathrm{T}}\dot{z}_{13} =&\omega^*z_{12}^{\mathrm{T}}Ez_{13}+\frac{1}{l_{13}}[k_1(\sin^2\alpha_1)(\alpha_1-\alpha_1^*) \\ &-k_3(\cos\alpha_2+\cos\alpha_1\cos\alpha_3)(\alpha_3-\alpha_3^*)].\end{aligned} \tag{4.103}$$

Substituting (4.102) and (4.103) into (4.98), one has the angle error dynamics of agent 1

$$\dot{\alpha}_1=-(\sin\alpha_1)(\frac{k_1}{l_{12}}+\frac{k_1}{l_{13}})(\alpha_1-\alpha_1^*)+k_2\frac{\sin\alpha_2}{l_{12}}(\alpha_2-\alpha_2^*)+k_3\frac{\sin\alpha_3}{l_{13}}(\alpha_3-\alpha_3^*). \tag{4.104}$$

By using the same analysis steps, one has

$$\dot{\alpha}_2 = -(\sin\alpha_2)(\frac{k_2}{l_{21}} + \frac{k_2}{l_{23}})(\alpha_2 - \alpha_2^*) + k_1\frac{\sin\alpha_1}{l_{21}}(\alpha_1 - \alpha_1^*) + k_3\frac{\sin\alpha_3}{l_{23}}(\alpha_3 - \alpha_3^*), \tag{4.105}$$

$$\dot{\alpha}_3 = -(\sin\alpha_3)(\frac{k_3}{l_{31}} + \frac{k_3}{l_{32}})(\alpha_3 - \alpha_3^*) + k_1\frac{\sin\alpha_1}{l_{31}}(\alpha_1 - \alpha_1^*) + k_2\frac{\sin\alpha_2}{l_{32}}(\alpha_2 - \alpha_2^*). \tag{4.106}$$

Writing (4.104), (4.105) and (4.106) into a compact form, one has the overall angle error dynamics (4.27), which are independent of the time-varying mismatches $\mu_i(t)$ and $\tilde{\mu}_i(t)$.

Appendix B: For Section III. C, to obtain the angle error dynamics of agent 1 under constant mismatches, by using (4.99) and (4.12), one has

$$\begin{aligned}\dot{z}_{12} =& \frac{P_{z_{12}}}{l_{12}}[-k_2(\alpha_2 - \alpha_2^*)(z_{23} + z_{21}) + \mu_2 z_{23} + \tilde{\mu}_2 z_{21} \\ &+ k_1(\alpha_1 - \alpha_1^*)(z_{13} + z_{12}) - \mu_1 z_{12} - \tilde{\mu}_1 z_{13}].\end{aligned}$$

Then, one has

$$\begin{aligned}(\dot{z}_{12})^{\mathrm{T}} z_{13} =& \frac{1}{l_{12}}[k_1(\sin^2\alpha_1)(\alpha_1 - \alpha_1^*) - k_2(\cos\alpha_3 + \cos\alpha_1\cos\alpha_2)\times \\ &(\alpha_2 - \alpha_2^*) - \tilde{\mu}_1\sin^2(\alpha_1) + \mu_2(\cos\alpha_3 + \cos\alpha_1\cos\alpha_2)].\end{aligned}$$

Similarly, one can get

$$\begin{aligned}(z_{12})^{\mathrm{T}} \dot{z}_{13} =& \frac{1}{l_{13}}[k_1(\sin^2\alpha_1)(\alpha_1 - \alpha_1^*) - k_3(\cos\alpha_2 + \cos\alpha_1\cos\alpha_3)\times \\ &(\alpha_3 - \alpha_3^*) - \mu_1\sin^2(\alpha_1) + \tilde{\mu}_3(\cos\alpha_2 + \cos\alpha_1\cos\alpha_3)].\end{aligned}$$

Using (4.98), one has

$$\begin{aligned}\dot{\alpha}_1 =& -(\sin\alpha_1)(\frac{k_1}{l_{12}} + \frac{k_1}{l_{13}})(\alpha_1 - \alpha_1^*) + k_2\frac{\sin\alpha_2}{l_{12}}(\alpha_2 - \alpha_2^*) \\ &+ k_3\frac{\sin\alpha_3}{l_{13}}(\alpha_3 - \alpha_3^*) + \frac{\tilde{\mu}_1\sin\alpha_1 - \mu_2\sin\alpha_2}{l_{12}} + \frac{\mu_1\sin\alpha_1 - \tilde{\mu}_3\sin\alpha_3}{l_{13}}.\end{aligned} \tag{4.107}$$

Similarly, we can also get

$$\begin{aligned}\dot{\alpha}_2 =& -(\sin\alpha_2)(\frac{k_2}{l_{21}}+\frac{k_2}{l_{23}})(\alpha_2-\alpha_2^*)+k_1\frac{\sin\alpha_1}{l_{21}}(\alpha_1-\alpha_1^*)\\ &+k_3\frac{\sin\alpha_3}{l_{23}}(\alpha_3-\alpha_3^*)+\frac{\tilde{\mu}_2\sin\alpha_2-\mu_1\sin\alpha_1}{l_{21}}+(\mu_2\sin\alpha_2-\tilde{\mu}_3\sin\alpha_3)/l_{23}\end{aligned}$$

$$\begin{aligned}\dot{\alpha}_3 =& -(\sin\alpha_3)(\frac{k_3}{l_{31}}+\frac{k_3}{l_{32}})(\alpha_3-\alpha_3^*)+k_1\frac{\sin\alpha_1}{l_{31}}(\alpha_1-\alpha_1^*)\\ &+k_2\frac{\sin\alpha_2}{l_{32}}(\alpha_2-\alpha_2^*)+\frac{\tilde{\mu}_3\sin\alpha_3-\mu_1\sin\alpha_1}{l_{31}}+\frac{\mu_3\sin\alpha_3-\tilde{\mu}_2\sin\alpha_2}{l_{32}}.\end{aligned} \tag{4.108}$$

Writing (4.107)-(4.108) in a compact form, one has the angle error dynamics given in (4.40).

Appendix C: For Section IV. A, we use a similar approach to obtain the angle error dynamics of e_{41} and e_{42} for agent 4 under the control algorithm (4.62). In the following, we consider the maneuvering of translation, rotation and scaling simultaneously. According to (4.98), one has

$$\dot{\alpha}_{142}=\frac{z_{42}^{\mathrm{T}}\dot{z}_{41}+z_{41}^{\mathrm{T}}\dot{z}_{42}}{-\sin\alpha_{142}}. \tag{4.109}$$

By using (4.12) and (4.62), one has

$$\dot{z}_{41}=\frac{P_{z_{41}}}{l_{41}}(\dot{p}_1-\dot{p}_4)=\frac{P_{z_{41}}}{l_{41}}(u_{f1}-u_{f4}+u_{m1}-u_{m4}).$$

By substituting the definitions of u_{fi} and u_{mi}, one has

$$\begin{aligned}z_{42}^{\mathrm{T}}\frac{P_{z_{41}}}{l_{41}}(u_{f1}-u_{f4})=&\frac{-z_{42}^{\mathrm{T}}P_{z_{41}}(z_{12}+z_{13})e_1+k_{41}(\alpha_{142}-\alpha_{142}^*)\sin^2\alpha_{142}}{l_{41}}\\ &+\frac{k_{42}(\alpha_{243}-\alpha_{243}^*)(\sin\alpha_{142})(\sin\alpha_{142}+\sin\alpha_{143})}{l_{41}}.\end{aligned} \tag{4.110}$$

On the other hand, one has

$$z_{42}^{\mathrm{T}}\frac{P_{z_{41}}}{l_{41}}(u_{m1}-u_{m4})=\frac{z_{42}^{\mathrm{T}}P_{z_{41}}(\omega^*E+s(t)I_2)(p_1-p_4)}{l_{41}}=\omega^*z_{42}^{\mathrm{T}}Ez_{41}, \tag{4.111}$$

where we have used the fact that $P_{z_{41}}z_{41}=0$ and $z_{41}^{\mathrm{T}}Ez_{41}=0$. Similarly, one also

has

$$\begin{aligned} z_{41}^{\mathrm{T}}\dot{z}_{42} =& z_{41}^{\mathrm{T}}\frac{P_{z_{42}}}{l_{42}}(u_{f2}-u_{f4}+u_{m2}-u_{m4}) \\ =& \frac{-z_{41}^{\mathrm{T}}P_{z_{42}}(z_{21}+z_{23})e_2+k_{41}(\alpha_{142}-\alpha_{142}^*)\sin^2\alpha_{142}}{l_{42}} \\ &+\frac{k_{42}(\alpha_{243}-\alpha_{243}^*)(-\sin\alpha_{142}\sin\alpha_{243})}{l_{42}}+\omega^* z_{41}^{\mathrm{T}}Ez_{42}. \end{aligned} \tag{4.112}$$

By substituting (4.110), (4.111) and (4.112) into (4.109), one has the dynamics of α_{142}

$$\begin{aligned} \dot{\alpha}_{142} =& -(\sin\alpha_{142})(\frac{k_{41}}{l_{41}}+\frac{k_{41}}{l_{42}})(\alpha_{142}-\alpha_{142}^*)-\frac{k_{42}(\alpha_{243}-\alpha_{243}^*)(\sin\alpha_{142}+\sin\alpha_{143})}{l_{41}} \\ &+\frac{k_{42}(\alpha_{243}-\alpha_{243}^*)\sin\alpha_{243}}{l_{42}}+\frac{z_{41}^{\mathrm{T}}P_{z_{42}}(z_{21}+z_{23})e_2}{l_{42}\sin\alpha_{142}}+\frac{z_{42}^{\mathrm{T}}P_{z_{41}}(z_{12}+z_{13})e_1}{l_{41}\sin\alpha_{142}}. \end{aligned} \tag{4.113}$$

$$\begin{aligned} \dot{\alpha}_{243} =& -(\sin\alpha_{243})(\frac{k_{42}}{l_{43}}+\frac{k_{42}}{l_{42}})(\alpha_{243}-\alpha_{243}^*)-\frac{u_{f2}^{\mathrm{T}}P_{z_{42}}z_{43}}{l_{42}\sin\alpha_{243}} \\ &-\frac{k_{41}(\alpha_{142}-\alpha_{142}^*)(\sin\alpha_{243}+\sin\alpha_{143})}{l_{43}} \\ &+\frac{k_{41}(\alpha_{142}-\alpha_{142}^*)\sin\alpha_{142}}{l_{42}}-\frac{u_{f3}^{\mathrm{T}}P_{z_{43}}z_{42}}{l_{43}\sin\alpha_{243}}. \end{aligned} \tag{4.114}$$

By combining (4.113) and (4.114), one has the angle error dynamics given in (4.67), which are independent of the time-varying mismatches $\mu_i(t), \tilde{\mu}_i, i = 1, \cdots, 4$.

Appendix D: For Section IV. B, by using the same approach, one has

$$\dot{z}_{41}=\frac{P_{z_{41}}}{l_{41}}(\dot{p}_1-\dot{p}_4)=\frac{P_{z_{41}}}{l_{41}}(u_{f1}-u_{f4})+\frac{P_{z_{41}}}{l_{41}}(u_{m1}-u_{m4}).$$

Then, one obtains

$$\begin{aligned} (\dot{z}_{41})^{\mathrm{T}}z_{42} =& \frac{u_{f1}^{\mathrm{T}}P_{z_{41}}z_{42}}{l_{41}}+\frac{k_{41}(\alpha_{142}-\alpha_{142}^*)\sin^2\alpha_{142}}{l_{41}}+z_{42}^{\mathrm{T}}\frac{P_{z_{41}}}{l_{41}}(u_{m1}-u_{m4}) \\ &+\frac{k_{42}(\alpha_{243}-\alpha_{243}^*)(\sin^2\alpha_{142}+\sin^2\alpha_{142}\cos\alpha_{243}+\cos\alpha_{142}\sin\alpha_{142}\sin\alpha_{243})}{l_{41}}. \end{aligned}$$

By using the same approach, one can also has

$$\begin{aligned} z_{41}^{\mathrm{T}}\dot{z}_{42} =& \frac{z_{41}^{\mathrm{T}}P_{z_{42}}u_{f2}}{l_{42}} - z_{41}^{\mathrm{T}}\frac{P_{z_{42}}}{l_{42}}u_4 + z_{41}^{\mathrm{T}}\frac{P_{z_{42}}}{l_{42}}(u_{m2}-u_{m4}) \\ =& \frac{k_{41}(\alpha_{142}-\alpha_{142}^*)\sin^2\alpha_{142}}{l_{42}} + z_{41}^{\mathrm{T}}\frac{P_{z_{42}}}{l_{42}}(u_{m2}-u_{m4}) \\ &+ \frac{k_{42}(\alpha_{243}-\alpha_{243}^*)(-\sin\alpha_{142}\sin\alpha_{243})}{l_{42}} + \frac{u_{f2}^{\mathrm{T}}P_{z_{42}}z_{41}}{l_{42}}. \end{aligned} \tag{4.115}$$

Using (4.109), one has the dynamics of α_{142} and α_{243}

$$\begin{aligned} \dot{\alpha}_{142} =& -(\sin\alpha_{142})(\frac{k_{41}}{l_{41}}+\frac{k_{41}}{l_{42}})(\alpha_{142}-\alpha_{142}^*) - \frac{k_{42}(\alpha_{243}-\alpha_{243}^*)(\sin\alpha_{142}+\sin\alpha_{143})}{l_{41}} \\ &+ \frac{k_{42}(\alpha_{243}-\alpha_{243}^*)\sin\alpha_{243}}{l_{42}} - \frac{u_{f2}^{\mathrm{T}}P_{z_{42}}z_{41}}{l_{42}\sin\alpha_{142}} - \frac{u_{f1}^{\mathrm{T}}P_{z_{41}}z_{42}}{l_{41}\sin\alpha_{142}} \\ &- z_{42}^{\mathrm{T}}\frac{P_{z_{41}}}{l_{41}\sin\alpha_{142}}(u_{m1}-u_{m4}) - z_{41}^{\mathrm{T}}\frac{P_{z_{42}}}{l_{42}\sin\alpha_{142}}(u_{m2}-u_{m4}). \end{aligned} \tag{4.116}$$

$$\begin{aligned} \dot{\alpha}_{243} =& -(\sin\alpha_{243})(\frac{k_{42}}{l_{43}}+\frac{k_{42}}{l_{42}})(\alpha_{243}-\alpha_{243}^*) - \frac{k_{41}(\alpha_{142}-\alpha_{142}^*)(\sin\alpha_{243}+\sin\alpha_{143})}{l_{43}} \\ &+ \frac{k_{41}(\alpha_{142}-\alpha_{142}^*)\sin\alpha_{142}}{l_{42}} - \frac{u_{f3}^{\mathrm{T}}P_{z_{43}}z_{42}}{l_{43}\sin\alpha_{243}} - z_{42}^{\mathrm{T}}\frac{P_{z_{43}}}{l_{43}\sin\alpha_{243}}(u_{m3}-u_{m4}) \\ &- \frac{u_{f2}^{\mathrm{T}}P_{z_{42}}z_{43}}{l_{42}\sin\alpha_{243}} - z_{43}^{\mathrm{T}}\frac{P_{z_{42}}}{l_{42}\sin\alpha_{243}}(u_{m2}-u_{m4}). \end{aligned} \tag{4.117}$$

By substituting $u_{mi}, i = 1,\cdots,4$ from (4.12) and (4.62) into (4.116) and (4.117), one has the angle error dynamics given in (4.76).

4.7 Concluding remarks

This chapter has realized the formation maneuver control in 2D by using the designed-mismatch angle approach. The formation has been described by angles and constructed from a triangular shape and grown with two angle constraints for each newly added agent. Two types of designed-mismatches have been investigated: measurement-dependent case and measurement-independent case. For both cases, the formation maneuver control algorithms have been proposed to realize the desired maneuvering. To analyze the stability of the angle errors, the angle error dynamics have been derived by using the dot product of two bearings.

Part II

Angle rigidity and formation control in 3D

Chapter 5

Angle rigidity in 3D

This chapter establishes the notion and properties of 3D angle rigidity for multi-point frameworks, and then designs control laws to stabilize angle rigid formations of mobile agents in 3D. Angles are defined using the interior angles of triangles within the given framework, which are independent of the choice of coordinate frames, can be conveniently measured using monocular cameras, and thus are fundamentally different from the bearings, which depend on the choice of coordinate systems. We show that 3D angle rigidity is a local property, which is in contrast to the 3D bearing rigidity as has been proved to be a global property in the literature. We show how to construct some classes of 3D angle rigid frameworks by adding repeatedly new points to the original small angle rigid framework with carefully chosen angle constraints. Furthermore, we also investigate how to merge two 3D angle rigid frameworks. We pay special attention to angle rigidity of convex polyhedra.

5.1 Introduction

Distance rigidity has been first defined for frameworks in a d-dimensional space whose only allowed smooth motions are those that preserve the distance between every pair of its points [9]. The necessary and sufficient condition for a generic framework's rigidity is closely associated with the dimension d [9]. For the necessary and sufficient condition for global rigidity, it has been proven that Hendrickson's conjecture is true for $d = 1, 2$ but false for $d \geqslant 3$ [26, 50]. Bearing rigidity has been established by using bearing constraints [101]. When all bearings are described in the coordinate frames in $\mathbb{R}^d$ with the same orientation, it has been shown that local bearing rigidity implies global bearing rigidity for an arbitrary d. However, this is not the case for angle rigidity, which has been developed in 2D in Chapter 2. When signed angles are employed in 2D, it has been shown in Chapter 2 that the resulting angle rigidity is in fact not a global property. Note that angle rigidity in 3D is more complicated and its related properties have not been adequately studied before in the literature.

5.2 Angularity and its rigidity in 3D

The notion of "angularity" has been introduced in Chapter 2 to study angle rigidity in 2D. We now extend it to 3D. All the discussions in this chapter are confined to 3D and the right-hand rule applies to all rotation operations of vectors.

5.2.1 Angularity

The definitions of vertex set $\mathcal{V}$, *angle set* $\mathcal{A}$ in 3D have the same definitions as in 2D. Now consider the embedding of the vertex set $\mathcal{V}$ in $\mathbb{R}^3$ through which each vertex i is associated with a *distinct* position $p_i \in \mathbb{R}^3$ and let $p = [p_1^{\mathrm{T}}, \cdots, p_N^{\mathrm{T}}]^{\mathrm{T}} \in \mathbb{R}^{3N}$ be the configuration of all the vertices. Then the combination of the vertex set $\mathcal{V}$, the angle set $\mathcal{A}$ and the position vector p is an *angularity* $\mathbb{A}(\mathcal{V}, \mathcal{A}, p)$ in 3D. As shown in Fig. 5.1, an element (j, i, k) in $\mathcal{A}$, when p_i, p_j and p_k are distinct, corresponds to the interior angle formed by the rays $\overrightarrow{ij}$ and $\overrightarrow{ik}$; more specifically, using the position vector p, the angle $\measuredangle jik \in [0, \pi]$ corresponding to the triplet (j, i, k) in $\mathcal{A}$ can be calculated by

$$\measuredangle jik = \arccos\left(\frac{(p_j - p_i)^{\mathrm{T}}(p_k - p_i)}{\|p_j - p_i\|\|p_k - p_i\|}\right). \tag{5.1}$$

where $\measuredangle jik = \measuredangle kij$ which is different from the 2D case. In 3D, we define the direction vector $b_{ij} = \frac{p_j - p_i}{\|p_j - p_i\|}$ starting from p_i and pointing towards a different position p_j.

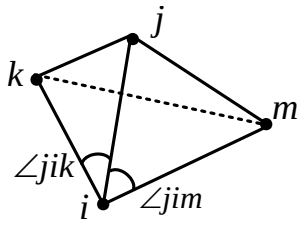

Figure 5.1: *Angles used in defining 3D angle rigidity*

5.2.2 Angle rigidity

Before defining angle rigidity, we give the definitions of equivalence and congruence for two angularities in 3D.

Definition 5.1. *[22] We say two angularities $\mathbb{A}(\mathcal{V},\mathcal{A},p)$ and $\mathbb{A}'(\mathcal{V},\mathcal{A},p')$ in 3D with the same $\mathcal{V}$ and $\mathcal{A}$ are* equivalent *if*

$$\measuredangle jik(p_j,p_i,p_k)=\measuredangle jik(p'_j,p'_i,p'_k) \text{ for all } (j,i,k)\in\mathcal{A}.$$

We say that $\mathbb{A}$ and $\mathbb{A}'$ are congruent *if*

$$\measuredangle jik(p_j,p_i,p_k)=\measuredangle jik(p'_j,p'_i,p'_k) \text{ for all } j,i,k\in\mathcal{V}.$$

Although Definitions 5.1 is similar to Definition 2.1, they are inherently different because the angle in 2D is defined with direction but not in 3D. Then, we have the same definitions for global angle rigidity and angle rigidity in 3D as Definitions 2.2 and 2.3. Note that global angle rigidity always implies angle rigidity in 3D; however, the inverse is not necessarily true. Note that this is different from bearing rigidity for which global bearing rigidity and bearing rigidity are equivalent [36, 101].

Theorem 5.2. *An angle rigid angularity $\mathbb{A}(\mathcal{V},\mathcal{A},p)$ in 3D is not necessarily globally angle rigid.*

We prove this theorem by constructing an angularity that is angle rigid but not globally angle rigid. Consider the angularity $\mathbb{A}(\mathcal{V},\mathcal{A},p)$ in Fig. 5.2 with

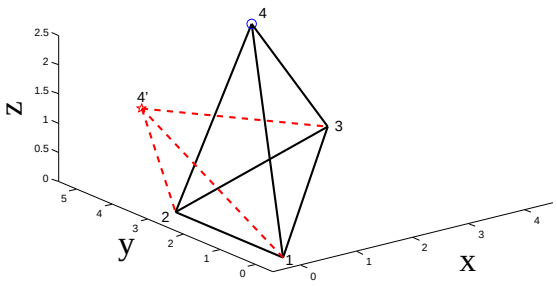

Figure 5.2: *Flex ambiguity in angle rigid angularity*

$\mathcal{V}=\{1,2,3,4\}$, $\mathcal{A}=\{(1,3,2),(3,1,2),(1,4,2),(1,4,3),(2,4,3)\}$, and the embedding $p_1=[0,0,0]^{\mathrm{T}}, p_2=[0,3,0]^{\mathrm{T}}, p_3=[4,5,0]^{\mathrm{T}}, p_4=[2,4,2.5]^{\mathrm{T}}$. Then, the corresponding angles $\measuredangle 132, \measuredangle 312, \measuredangle 142, \measuredangle 341, \measuredangle 243$ can be calculated by using (5.1).

We first check that $\mathbb{A}(\mathcal{V},\mathcal{A},p)$ is angle rigid. In $\triangle 123$, one can uniquely determine $\measuredangle 123=\pi-\measuredangle 132-\measuredangle 312$, which implies that the interior angles in $\triangle 123$ are uniquely determined. Should point 4's position be uniquely determined by $\measuredangle 142, \measuredangle 143, \measuredangle 243$, the other angles formed by 4 and 1,2,3 would also be uniquely determined. To check the uniqueness of point 4 under $\measuredangle 142, \measuredangle 143, \measuredangle 243$, we first show the surface which satisfies the angle constraint of $\measuredangle 142$ given points 1 and

2. The angle constraint of $\measuredangle 142$ in 3D gives rise to a closed surface (Fig.5.3 (b)) formed by rotating the major arc $\overset{\frown}{12}$ along the line $\overline{12}$ in Fig.5.3 (a). Given points 1,

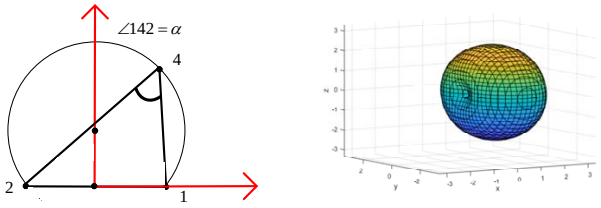

(a) Angle in 2D (b) Angle in 3D

Figure 5.3: *Angle in 2D and 3D*

2 and 3 and angles $\measuredangle 142, \measuredangle 143, \measuredangle 243$, point 4 can be determined by three surfaces. By numerically checking the intersections of these three surfaces in Fig. 5.4, one

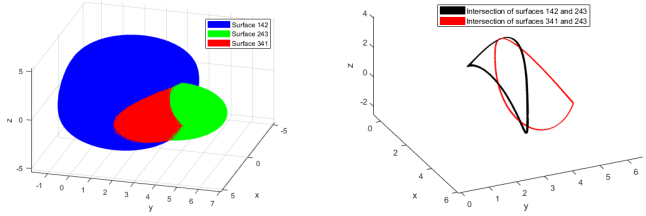

Figure 5.4: *Intersection of three surfaces*

can see that there are four separate intersection points on these three surfaces. Therefore, when p_1, p_2, p_3, p_4 are locally perturbed, there is only one unique position for 4 in the neighborhood of its current position because these four intersection points are separate. So, the angularity is angle rigid.

We now show that $\mathbb{A}(\mathcal{V}, \mathcal{A}, p)$ is not globally angle rigid. By perturbing p_4 in $\mathbb{R}^3$, one finds another point $p_4' = [0.0802, 4.0778, 1.4765]^{\mathrm{T}}$ which satisfies all the angle constraints associated with $\mathcal{A}$ together with p_1, p_2, p_3. This flex ambiguity implies that $\mathbb{A}$ is not globally angle rigid. □

Note that non-generic embeddings of p in $\mathbb{R}^3$ may change the rigidity of an angularity. Consider the three different embeddings of the following 4-vertex angularity.

When $\measuredangle 213 = 0, \measuredangle 143 = 0$ as shown in Fig 4.(a), the angularity is angle rigid but not globally angle rigid since if 2 and 3 swap their positions, $\measuredangle 213, \measuredangle 143$ remain the same but $\measuredangle 234$ changes by π. On the other hand, Fig. 4(b) shows that when the

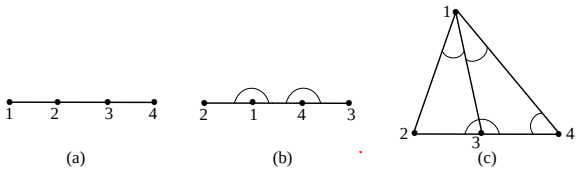

Figure 5.5: *Non-generic p changes rigidity*

same two angles are assigned to be $\measuredangle 213 = \pi, \measuredangle 143 = \pi$, the angularity becomes globally angle rigid according to Definition 2.2. Note that in the above two cases, all the four points are collinear. When only three points are collinear as in Fig 4(c), this angularity is in general flexible if fewer than 4 angle constraints are given according to 2D angle rigidity in Chapter 2 since points 1,2,3,4 are in a plane in this case. By giving three generic angles (e.g., not 0 or π) for $\measuredangle 213, \measuredangle 143, \measuredangle 413$ and one non-generic angle $\measuredangle 234 = \pi$ in Fig. 4(c), the angularity becomes globally angle rigid because $\measuredangle 124 = \pi - \measuredangle 213 - \measuredangle 143 - \measuredangle 413$, $\measuredangle 132 = \measuredangle 413 + \measuredangle 143$ and $\measuredangle 134 = \pi - \measuredangle 132$ are all uniquely determined. However, 4 vertices in general form a tetrahedron in 3D. To rule out non-generic situations for p, the notion of generic positions can be utilized [22, 28].

When p is generic, e.g., no three points are collinear and no four points are on a circle, angle rigidity only depends on $\mathcal{V}$ and $\mathcal{A}$, which is also called *generic rigidity* of $\mathbb{A}(\mathcal{V}, \mathcal{A}, p)$. Now we provide some sufficient conditions for an angularity to be angle rigid or globally angle rigid. First, for two angularities $\mathbb{A}(\mathcal{V}, \mathcal{A}, p)$ and $\mathbb{A}'(\mathcal{V}', \mathcal{A}', p')$, we say $\mathbb{A}$ is a *sub-angularity* of $\mathbb{A}'$ if $\mathcal{V} \subset \mathcal{V}'$, $\mathcal{A} \subset \mathcal{A}'$ and p is the corresponding sub-vector of p'. For the smallest angularities with only three vertices, there is no difference between generic angle rigidity and generic global angle rigidity.

Lemma 5.3. *For a 3-vertex angularity in 3D, if it is generically angle rigid, it is also generically globally angle rigid.*

Proof. This is straightforward by following the proof in 2D angle rigidity in Chapter 2. □

Now, we develop the vertex addition operations for 3D angle rigidity to construct an angle rigid angularity from the smallest 3-vertex angularity. Towards this end, we first define some related notions.

Definition 5.4. *For a given angularity $\mathbb{A}(\mathcal{V}, \mathcal{A}, p)$, we say that a new vertex i positioned at p_i is* linearly constrained *with respect to $\mathbb{A}$ if there is $j \in \mathcal{V}$ such that $p_i \neq p_j$ and p_i is constrained to be on a ray, which is fixed once p_j is fixed, starting from p_j; we also say i is* conically constrained *with respect to $\mathbb{A}$ if there are $j, k \in \mathcal{V}$ such that $\{p_i, p_j, p_k\}$ is generic and p_i is constrained to be on a cone, which is fixed once*

p_j and p_k are fixed, with p_j as the cone's apex and $\overrightarrow{jk}$ as the cone's axis; finally we say i is near-spherically constrained *with respect to $\mathbb{A}$ if there are $j, k \in \mathcal{V}$ such that $\{p_i, p_j, p_k\}$ is generic and p_i is constrained to be on a near-spherical surface, which is fixed once p_j and p_k are fixed, with $\overline{jk}$ in the surface's rotation axis. For convenience, we also simply say i's angle constraint is linear, conic and near-spherical in the above three cases, respectively.*

Definition 5.5. *For four generic points p_i, p_j, p_k, p_m, we say i, j, k are in a counterclockwise (resp. clockwise) direction with respect to m if the signed volume of the tetrahedron formed by p_m and p_i, p_j, p_k is positive (resp. negative), i.e., $V_{m-ijk} = \frac{(p_i - p_m)^{\mathrm{T}}[(p_j - p_m) \times (p_k - p_m)]}{6} > 0$ where $\times$ denotes the cross product. Correspondingly, when the sign of the tetrahedron is fixed to be positive (resp. negative), we say the four points are under a counterclockwise (resp. clockwise) constraint.*

Remark 5.6. Two non-coincident conic constraints sharing the same apex p_j will lead to two cones intersecting at no more than two rays, denoted by $\overrightarrow{ji_1}$ and $\overrightarrow{ji_2}$. Since $\overrightarrow{ji_1}$ and $\overrightarrow{ji_2}$ are symmetric with respect to the plane formed by the two cones' rotation axes $\overrightarrow{jk_1}$ and $\overrightarrow{jk_2}$, one has that $V_{i_1-jk_1k_2}$ and $V_{i_2-jk_1k_2}$ have different signs. Therefore, each linear constraint can be obtained by two conic constraints with a common apex and an associated counterclockwise constraint.

Definition 5.7 (Type-I vertex addition)**.** *For a given angularity $\mathbb{A}(\mathcal{V}, \mathcal{A}, p)$, we say the angularity $\mathbb{A}'$ with the augmented vertex set $\{\mathcal{V} \cup \{i\}\}$ is obtained from $\mathbb{A}$ through a* Type-I vertex addition *if the new vertex i's constraints with respect to $\mathbb{A}$ contain at least one of the following:*
Case 1: two linear constraints, not aligned but intersecting, each of which is associated with three vertices in $\mathcal{V}$, e.g., $\overrightarrow{j_1i}$ and $\overrightarrow{j_2i}$ in Fig. 5.6.(a);
Case 2: one linear constraint $\overrightarrow{j_1i}$ and one conic constraint whose rotation axis $\overline{j_1j_2}$ passes through the linear constraint ray's starting point p_{j_1}.

Definition 5.8 (Type-II vertex addition)**.** *For a given angularity $\mathbb{A}(\mathcal{V}, \mathcal{A}, p)$, we say the angularity $\mathbb{A}'$ with the augmented vertex set $\{\mathcal{V} \cup \{i\}\}$ is obtained from $\mathbb{A}$ through a* Type-II vertex addition *if the new vertex i's constraints with respect to $\mathbb{A}$ contain at least one of the following:*
Case 1: three near-spherical constraints associated with three vertices $\{j_1, j_2, k_1\}$ in $\mathcal{V}$, and $\{p_i, p_{j_1}, p_{j_2}, p_{k_1}\}$ are generic;
Case 2: two near-spherical constraints and one conic constraint associated with three vertices $\{j_1, j_2, k_1\}$ in $\mathcal{V}$, and $\{p_i, p_{j_1}, p_{j_2}, p_{k_1}\}$ are generic.

Now we are ready to present a sufficient condition for global angle rigidity using Type-I vertex addition.

Proposition 5.9. *An angularity in 3D is globally angle rigid if it can be obtained through a sequence of Type-I vertex additions starting from a generically angle rigid 3-vertex angularity.*

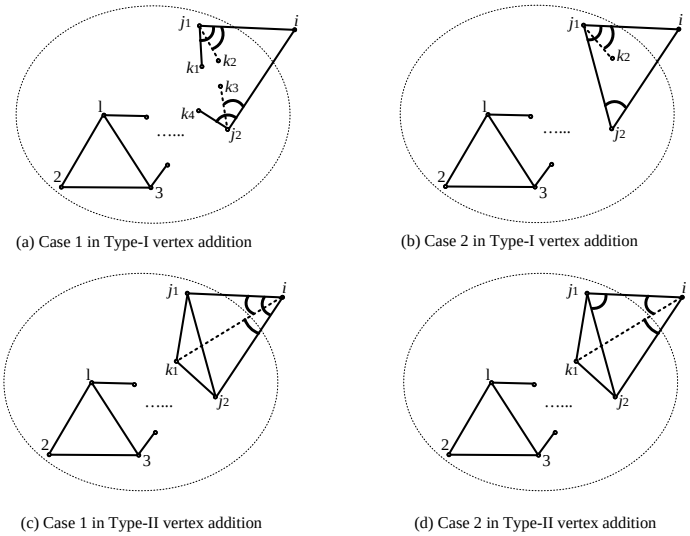

(a) Case 1 in Type-I vertex addition

(b) Case 2 in Type-I vertex addition

(c) Case 1 in Type-II vertex addition

(d) Case 2 in Type-II vertex addition

Figure 5.6: *Type-I vertex addition and Type-II vertex addition*

Proof. According to Lemma 5.3, a generically angle rigid 3-vertex angularity is globally angle rigid. Consider the two cases in the Type-I vertex addition. If case 1 applies, each linear constraint corresponds to a ray according to Definition 5.5. Then the position p_i of the newly added vertex i is unique since two rays, not aligned, starting from two different points may intersect only at one point; if case 2 applies, p_i is again unique since a ray starting from the axis of a cone can have only one intersection with the cone. Therefore, p_i is always globally uniquely determined, after which all the involved angles are also globally uniquely determined. Then, iteratively, after a sequence of type-I vertex additions, the obtained angularity is globally angle rigid. □

In comparison, type-II vertex additions can only guarantee angle rigidity instead of global angle rigidity.

Proposition 5.10. *An angularity in 3D is angle rigid if it can be obtained through a sequence of Type-II vertex additions starting from a generically angle rigid 3-vertex angularity.*

The proof can be easily constructed following similar arguments as those for Proposition 5.9 and Theorem 5.2. The only difference is that p_i now may have multiple isolated solutions and is only unique locally. Also note that only two types of constraints are defined in Type-II vertex addition operation in Definition 5.8, but there are more possible combinations of constraints which can also guarantee a

locally unique point p_i.

Remark 5.11. Note that in Type-II vertex addition, we further require the positions of the three associated vertices in $\mathbb{A}$ to be generic. Otherwise, the position of the added vertex i is not locally unique. For example, in Fig. 5.6(c), if j_1, j_2, k_1 are collinear, then the solution of p_i under the given three near-spherical constraints will be a circle which can be obtained by rotating i in the triangle $\triangle ij_1j_2$ along $\overline{j_1j_2}$.

Corollary 5.12. *For an angularity $\mathbb{A}(\mathcal{V}, \mathcal{A}, p)$, if there exists an angle rigid (resp. globally angle rigid) sub-angularity $\mathbb{A}'(\mathcal{V}, \mathcal{A}', p)$ with $\mathcal{A}' \subset \mathcal{A}$, then $\mathbb{A}(\mathcal{V}, \mathcal{A}, p)$ is also angle rigid (resp. globally angle rigid).*

Proof. Since the vertex set in the sub-angularity $\mathbb{A}'$ is the same as $\mathbb{A}$, it is straightforward from Definitions 2.2 and 2.3 that angle rigidity of the sub-angularity $\mathbb{A}'$ implies angle rigidity of $\mathbb{A}$. □

Remark 5.13. The associated counterclockwise direction constraint introduced in Definition 5.5 can be used to remove the reflection ambiguity such that the position of the added vertex i in the Type-I vertex addition operation (Definition 5.7) can be globally uniquely determined. But this constraint is not sufficient to make the position of the added point in Type-II vertex addition operation (Definition 5.8) globally uniquely determined. An example is given in Fig. 5.2, where points 1,2,3 are in the clockwise direction with respect to both points 4 and 4'. In other words, not only reflection ambiguity but also flex ambiguity may exist in Type-II vertex addition operation.

5.2.3 Merging two angle rigid angularities

After introducing how to add one vertex to an angularity in Propositions 5.9 and 5.10, we now investigate how to add 3 vertices to an angularity, which becomes useful later for merging two angle rigid angularities.

Definition 5.14 (3-vertex addition operation)**.** *For a given angularity $\mathbb{A}(\mathcal{V}, \mathcal{A}, p)$ and three new vertices $\{i_1, i_2, i_3\}$, we say that the angularity $\mathbb{A}'$ with the augmented vertex set $\{\mathcal{V} \cup \{i_1, i_2, i_3\}\}$ is obtained from $\mathbb{A}$ through a* 3-vertex addition operation *if the new vertices' constraints with respect to $\mathbb{A}$ contain: two unaligned linear constraints for i_1, two unaligned linear constraints for i_2, and one conic constraint and one associated counterclockwise constraint $V_{i_3-i_2i_1k_1}$ for i_3 with i_1 or i_2 being the cone's apex and k_1 in the cone's rotation axis. We further denote the angle set corresponding to these added angle constraints by $\mathcal{A}^{\{i_1,i_2,i_3\}}$.*

Now we merge a 3-vertex generically angle rigid angularity to a globally angle rigid angularity by the 3-vertex addition operation.

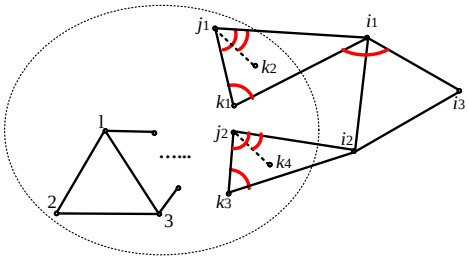

Figure 5.7: *The 3-vertex addition operation*

Proposition 5.15. *For a globally angle rigid angularity $\mathbb{A}(\mathcal{V}, \mathcal{A}, p)$ and a 3-vertex generically angle rigid angularity $\mathbb{A}_3(\{i_1, i_2, i_3\}, \mathcal{A}_3, [p_{i_1}^{\mathrm{T}}, p_{i_2}^{\mathrm{T}}, p_{i_3}^{\mathrm{T}}]^{\mathrm{T}})$, if one merges $\mathbb{A}$ and $\mathbb{A}_3$ by adding the vertices i_1, i_2, i_3 to $\mathbb{A}$ through the 3-vertex addition operation, then the merged angularity $\mathbb{A}'(\mathcal{V} \cup \{i_1, i_2, i_3\}, \mathcal{A} \cup \mathcal{A}_3 \cup \mathcal{A}^{\{i_1, i_2, i_3\}}, [p^{\mathrm{T}}, p_{i_1}^{\mathrm{T}}, p_{i_2}^{\mathrm{T}}, p_{i_3}^{\mathrm{T}}]^{\mathrm{T}})$ is globally angle rigid.*

Proof. Note that the positions of the added vertices i_1 and i_2 are globally unique according to Proposition 5.9 (case 1 of Type I vertex addition). After p_{i_1} and p_{i_2} are fixed, the vertex i_3 is constrained on the intersection of two cones with $\overline{i_1 i_2}$ as those two cones' rotation axis because $\mathbb{A}_3$ is generically angle rigid and $\measuredangle i_3 i_1 i_2$ and $\measuredangle i_3 i_2 i_1$ are fixed. By further using the given conic constraint for i_3 together with the associated counterclockwise constraint, one has that the position of the added vertex i_3 is also globally unique according to Proposition 5.9 (case 2 of Type-I vertex addition). □

Fig. 5.7 also shows the original angle constraints to realize the 3-vertex addition operation. Note that the number of these angle constraints in Fig. 5.7 is 7. This is because the total degrees of freedoms for vertices i_1, i_2, i_3 in 3D is 9, and at least 2 angle constraints are needed to make $\mathbb{A}_3$ generically angle rigid. Thus, at least 9-2=7 angle constraints related to i_1, i_2, i_3 are needed to merge $\mathbb{A}_3$ with $\mathbb{A}$. Now we are ready to discuss how to merge two angle rigid angularities as shown in Fig. 5.8.

Proposition 5.16. *Suppose that the angularity $\mathbb{A}_1(\mathcal{V}_1, \mathcal{A}_1, p)$ is globally angle rigid and $\mathbb{A}_2(\mathcal{V}_2, \mathcal{A}_2, p')$ with $\mathcal{V}_1 \cap \mathcal{V}_2 = \varnothing$ has a sub-angularity $\mathbb{A}_2'(\mathcal{V}_2, \mathcal{A}_2', p')$ which can be obtained through a sequence of Type-I vertex additions from a generically angle rigid 3-vertex angularity $\mathbb{A}_3(\{i_1, i_2, i_3\}, \mathcal{A}_3, [p_{i_1}^{\mathrm{T}}, p_{i_2}^{\mathrm{T}}, p_{i_3}^{\mathrm{T}}]^{\mathrm{T}})$. If one merges $\mathbb{A}_1$ and $\mathbb{A}_2$ by adding the vertices i_1, i_2, i_3 to $\mathbb{A}_1$ through the 3-vertex addition operation, then the merged angularity $\mathbb{A}''(\mathcal{V}_1 \cup \mathcal{V}_2, \mathcal{A}_1 \cup \mathcal{A}_2 \cup \mathcal{A}^{\{i_1, i_2, i_3\}}, [p^{\mathrm{T}}, p'^{\mathrm{T}}]^{\mathrm{T}})$ is globally angle rigid.*

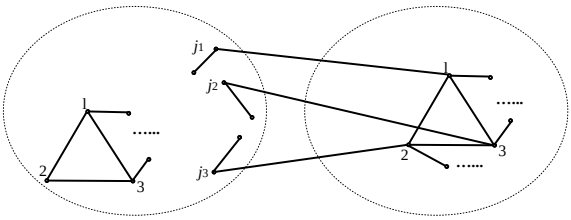

Figure 5.8: *Merging two angle rigid angularities*

Proof. First, by adding the vertices i_1, i_2, i_3 to $\mathbb{A}_1$ through the 3-vertex addition operation, one has global angle rigidity of the merged angularity with augmented vertex set $\{\mathcal{V}_1 \cup \{i_1, i_2, i_3\}\}$ according to Proposition 5.15. Since $\mathbb{A}'_2$ can be obtained through a sequence of Type-I vertex additions from $\mathbb{A}_3$, one has global angle rigidity of the angularity $\mathbb{A}'_{1-2}(\mathcal{V}_1 \cup \mathcal{V}_2, \mathcal{A}_1 \cup \mathcal{A}'_2 \cup \mathcal{A}^{\{i_1,i_2,i_3\}}, [p^{\mathrm{T}}, p'^{\mathrm{T}}]^{\mathrm{T}})$ after merging $\mathbb{A}_1$ and $\mathbb{A}'_2$ according to Proposition 5.9. Because the angularity $\mathbb{A}'_{1-2}$ is a sub-angularity of $\mathbb{A}''$, the merged angularity $\mathbb{A}''$ is globally angle rigid according to Corollary 5.12. □

5.2.4 Angle rigidity of convex polyhedron

Note that Type-I, Type-II and 3-vertex addition operations are developed in Subsections 5.2.2, 5.2.3 to check angle rigidity of the angularity which can be sequentially constructed from a triangle. However, not all angularities can be constructed through such sequential operations, e.g., a convex polyhedron[1] with angle constraints[2] all on its surfaces. As is well known, distance rigidity of convex polyhedra is one of the oldest geometric problems and has been studied by Euler [38], Cauchy [18], and Gluck [40], to name a few. Although many distance rigidity-related results have been obtained for convex polyhedra, the problem of angle rigidity of convex polyhedra has not been investigated so far. In this subsection, we discuss angle rigidity of convex polyhedra. Before presenting the results, we first define the angularity corresponding to a convex polyhedron and provide some related lemmas.

For a convex polyhedron $\mathbb{P}$, we define the corresponding angularity $\mathbb{A}(\mathcal{V}, \mathcal{A}, p)$, where $\mathcal{V}$ is the vertex set consisting of all the vertices of $\mathbb{P}$, $\mathcal{A}$ is the angle set consisting of all the angles of the faces of $\mathbb{P}$, and p is the position vector of the 3D embedding of the vertices in $\mathcal{V}$. Define the *angle function* $f_{\mathcal{A}}(p) := [f_1, \cdots, f_M]^{\mathrm{T}} \in$

[1] We only consider closed polyhedra in this thesis.

[2] Note that for a closed polyhedron, one can easily distinguish the inside that its surfaces enclose from its outside, so it is possible to define the positive directions of the faces to be the normals pointing outwards. Therefore, the angle constraints on the surfaces of such a polyhedron can be associated with the clockwise or counterclockwise directions.

$\mathbb{R}^M$ for the angularity $\mathbb{A}(\mathcal{V}, \mathcal{A}, p)$ where $M = |\mathcal{A}|$, $f_m : \mathbb{R}^9 \to [0, \pi]$, $m = 1, \cdots, M$, is the mapping from the position vector $[p_i^{\mathrm{T}}, p_j^{\mathrm{T}}, p_k^{\mathrm{T}}]^{\mathrm{T}}$ of the mth element (i, j, k) in $\mathcal{A}$ to the angle $\measuredangle ijk \in [0, \pi]$.

Lemma 5.17 ([6], Section 10.3.2, Theorem 1)**.** *If all angles on the faces of a convex polyhedron $\mathbb{P}$ remain constant when $\mathbb{A}$ is perturbed, then all dihedral angles of $\mathbb{P}$ remain constant as well.*

Lemma 5.18 ([6], Section 10.4.1, Theorem 1)**.** *If all edge lengths, angles in faces and dihedral angles of a convex polyhedron $\mathbb{P}$ remain constant under a perturbation of $\mathbb{A}$, then the perturbation must be a translation or rotation of $\mathbb{A}$.*

Now, we have the following result.

Theorem 5.19. *The angularity $\mathbb{A}(\mathcal{V}, \mathcal{A}, p)$ obtained from a convex polyhedron $\mathbb{P}$ with all faces being triangles is angle rigid.*

Proof. Following Definition 2.3, we consider $\mathbb{A}$'s equivalent angularity $\mathbb{A}'(\mathcal{V}, \mathcal{A}, p')$ with $\|p' - p\| < \epsilon, \epsilon > 0$, and denote by $\mathbb{P}'$ the corresponding polyhedron. Since $\mathbb{A}$ and $\mathbb{A}'$ are equivalent, each two corresponding face angles in $\mathbb{A}$ and $\mathbb{A}'$ have the same value (i.e., $f_{\mathcal{A}}(p) = f_{\mathcal{A}}(p')$). According to Lemma 5.17, one has that each two corresponding dihedral angles formed by two adjacent faces in $\mathbb{P}$ and $\mathbb{P}'$ have the same value.

Considering an arbitrary face triangle $\triangle ijk, i, j, k \in \mathcal{V}$, one has $\triangle ijk(p_i, p_j, p_k) \sim \triangle ijk(p'_i, p'_j, p'_k)$. Now, we scale $\mathbb{A}'$ to obtain $\mathbb{A}''$ which satisfies $\|p_i - p_j\| = \|p''_i - p''_j\|$, $\|p_i - p_k\| = \|p''_i - p''_k\|$ and $\|p_k - p_j\| = \|p''_k - p''_j\|$. We denote the scaled polyhedron by $\mathbb{P}''$. Since the scaling will not change all (face or dihedral) angles of a polyhedron, one has $f_{\mathcal{A}^* - \mathcal{A}}(p') = f_{\mathcal{A}^* - \mathcal{A}}(p'')$ and $f_{\mathcal{A}}(p') = f_{\mathcal{A}}(p'')$, where $\mathcal{A}^* = \{(i, j, k) | \forall i, j, k \in \mathcal{A}, i \neq j \neq k\}$ is the complete angle set. Now, we check $\mathbb{A}$ and $\mathbb{A}''$. First, all the face angles have the same values in $\mathbb{A}$ and $\mathbb{A}''$ because $f_{\mathcal{A}}(p) = f_{\mathcal{A}}(p') = f_{\mathcal{A}}(p'')$. Secondly, all the dihedral angles in $\mathbb{P}$ and $\mathbb{P}''$ have the same values because $\mathbb{P}$ and $\mathbb{P}'$ have the same dihedral angles and $\mathbb{A}''$ is a scaling of $\mathbb{A}'$. Thirdly, because $\triangle ijk(p_i, p_j, p_k) \simeq \triangle ijk(p''_i, p''_j, p''_k)$, the lengths of the edges in $\mathbb{P}$ have the same values as the lengths of the corresponding edges in $\mathbb{P}''$ which can be obtained by using the law of sines iteratively for the face triangles in $\mathbb{P}$ and $\mathbb{P}''$. From the above three facts and using Lemma 5.18 for $\mathbb{A}$ and $\mathbb{A}''$, one has that $\mathbb{A}''$ is the translation or rotation of $\mathbb{A}$, under which the values of all triple-vertex angles remain unchanged. It follows that $f_{\mathcal{A}^* - \mathcal{A}}(p) = f_{\mathcal{A}^* - \mathcal{A}}(p'') = f_{\mathcal{A}^* - \mathcal{A}}(p')$. Therefore, $\mathbb{A}$ and $\mathbb{A}'$ are congruent, and $\mathbb{A}$ is angle rigid. □

However, the above result about convex polyhedra with triangular faces is restrictive. We now study the case of convex polyhedra whose faces are not necessarily triangles by using the operations of the polygonal triangulation and surface triangulation.

Definition 5.20 (Polygonal triangulation [27]). *Polygonal triangulation is the decomposition of a polygon into a set of triangles where any two of these triangles intersect at a common vertex, edge, or empty set.*

Definition 5.21 (Surface triangulation). *Surface triangulation for a polyhedron $\mathbb{P}$ is the decomposition of the surface of $\mathbb{P}$ using polygonal triangulation for each face of $\mathbb{P}$ and at the same time any two decomposed triangles from two faces of $\mathbb{P}$ only intersect at a common vertex, edge, or empty set.*

Then, we define the corresponding triangulated angularity.

Definition 5.22 (Triangulated polyhedral angularity). *Let $\mathcal{K}$ be a surface triangulation of a polyhedron $\mathbb{P}$ with the vertex set $\mathcal{V} = \{1, 2, ..., N\}$ and embedding $p = [p_1^T, ..., p_N^T]^T$. Then we call $\mathbb{A}(\mathcal{V} \cup \mathcal{V}', \mathcal{A}, [p^T, p'^T]^T)$ a* triangulated polyhedral angularity, *where $\mathcal{V}'$ is the vertex set consisting of the vertices added in the surface triangulation $\mathcal{K}$, p' is the corresponding embedding of the vertices in $\mathcal{V}'$, and $\mathcal{A}$ denotes the angle set consisting of the interior angles of all polygonal faces of the polyhedron with vertices $\mathcal{V} \cup \mathcal{V}'$ and embedding $[p^T, p'^T]^T$ and all the interior angles of triangles obtained by $\mathcal{K}$ for the surface of $\mathbb{P}$. Then, the polyhedron corresponding to $\mathcal{K}$ is called a triangulated polyhedron $\tilde{\mathbb{P}}$.*

Note that if $\mathbb{P}$ is convex, we say its corresponding $\mathbb{A}$ is a convex triangulated polyhedral angularity. Then, we present the result about the convex triangulated polyhedral angularity.

Theorem 5.23. *A convex triangulated polyhedral angularity $\mathbb{A}(\mathcal{V} \cup \mathcal{V}', \mathcal{A}, [p^T, p'^T]^T)$ without any vertex of $\mathcal{V}'$ lying in the interior of a face of $\mathbb{P}$ is angle rigid.*

We first give two lemmas which will be used in the proof of Theorem 5.23.

Lemma 5.24. *When locally perturbing the convex triangulated polyhedral angularity $\mathbb{A}(\mathcal{V} \cup \mathcal{V}', \mathcal{A}, [p^T, p'^T]^T)$, the vertices of $\mathcal{V} \cup \mathcal{V}'$ that are on a face of $\tilde{\mathbb{P}}$ are always coplanar under the angle constraints given in $\mathcal{A}$.*

Proof. We first prove that under the given angle constraints all the triangles in a face of $\tilde{\mathbb{P}}$ will be coplanar under the local perturbation. Consider an arbitrary face $\mathbb{S}$ of $\tilde{\mathbb{P}}$ whose vertices consist of $\mathcal{I} = \{i_1, ..., i_m\}$ where $m \geqslant 3$. Suppose that $i_k, 1 \leqslant k \leqslant m$ is one of the vertices in $\mathbb{S}$ and is involved in face triangles $\triangle j_1 i_k j_2, \triangle j_2 i_k j_3, ..., \triangle j_{n-1} i_k j_n$ where $j_1, ..., j_n \in \mathcal{I}$ and $j_1, ..., j_n \neq i_k$. Note that if $j_1 = j_{n-1}$ and $j_2 = j_n$, i.e., i_k is only involved in one triangle $\triangle j_1 i_k j_2$ in $\mathbb{S}$, then one has that j_1, i_k, j_2 are coplanar since three arbitrary points in 3D are coplanar. When i_k is involved in more than one triangle in $\mathbb{S}$, one has $\{(j_1, i_k, j_2), (j_2, i_k, j_3), ..., (j_{n-1}, i_k, j_n)\} \in \mathcal{A}$, $(j_1, i_k, j_n) \in \mathcal{A}$ and $\measuredangle j_1 i_k j_2 + \measuredangle j_2 i_k j_3 + ... \measuredangle j_{n-1} i_k j_n = \measuredangle j_1 i_k j_n$. Therefore, under the local perturbation, $i_k, j_1, j_2, ..., j_n$ must be coplanar; otherwise $\measuredangle j_1 i_k j_2 + \measuredangle j_2 i_k j_3 + ... \measuredangle j_{n-1} i_k j_n >$

$\measuredangle j_1 i_k j_n$ which violates the given angle constraint. Note that for each triangle $\triangle ijk$ in face $\mathbb{S}$, there always exists another triangle in face $\mathbb{S}$ which shares a common edge with $\triangle ijk$. Without loss of generality, assume that the another triangle is $\triangle ij\tilde{k}$ and the intersected edge is ij. Consider the first case that i is only involved in these two triangles in face $\mathbb{S}$. Then $\{(j,i,k),(j,i,\tilde{k})\} \in \mathcal{A}$, $(k,i,\tilde{k}) \in \mathcal{A}$ and $\measuredangle jik + \measuredangle ji\tilde{k} = \measuredangle ki\tilde{k}$. Under local perturbation, these two triangles are coplanar. The second case is that i is involved in multiple triangles, using the same argument for the shared vertex as i_k, one has that these triangles are coplanar.

Now, consider that vertex i_k is involved in $n-1$ coplanar triangles in face $\mathbb{S}$ and its neighboring vertex i_{k+1} is involved in $\tilde{n}$ coplanar triangles in $\mathbb{S}$. Note that those $n-1$ triangles from i_k and $\tilde{n}$ triangles from i_{k+1} must share at least common triangle because of the existence of edge $i_k i_{k+1}$. Then, those $n+\tilde{n}-2$ triangles of i_k and i_{k+1} should be coplanar, and thus all the these triangles' vertices are coplanar. Next, if i_k+1 has a different neighboring vertex than i_k, we consider this vertex and label it i_{k+2}. Using the previous argument again, one has that all triangles of i_k, i_{k+1}, i_{k+2} are coplanar. Using this argument repeatedly for new neighboring vertices until one reaches all vertices in $\mathcal{I}$, one has that all the triangles in $\mathbb{S} \cap \mathcal{K}$ are coplanar since the vertices of each triangle in $\mathbb{S} \cap \mathcal{K}$ lie in $\mathcal{I}$. Because all the triangles in $\mathbb{S} \cap \mathcal{K}$ cover all the vertices in $\mathcal{I}$, one has that the vertices of $\mathcal{V} \cup \mathcal{V}'$ that is in $\mathbb{S}$ are coplanar under the perturbation. The same holds for the other faces of $\tilde{\mathbb{P}}$. □

Lemma 5.25. *When locally perturbing the convex triangulated polyhedral angularity $\mathbb{A}(\mathcal{V} \cup \mathcal{V}', \mathcal{A}, [p^T, p'^T]^T)$, if the scale of a triangle in a face of $\tilde{\mathbb{P}}$ remains constant, then all the edge lengths of $\tilde{\mathbb{P}}$ remain constant.*

Proof. Note that after triangulating the faces of the polyhedron $\mathbb{P}$, the surface of $\tilde{\mathbb{P}}$ becomes $\mathcal{K}$, in which each triangle $\triangle ijk \in \mathcal{K}$ has three neighboring triangles and each of them shares a different edge with the triangle $\triangle ijk$. When the scale of this arbitrary triangle $\triangle ijk$ in $\mathcal{K}$ is fixed, its three neighboring triangles also have the same fixed scale using the law of sines. Now, we show why the scales of all the other triangles in $\mathcal{K}$ are fixed as well. Let the face where $\triangle ijk$ lies be $\mathbb{S}_1$ and the total number of triangles in $\mathbb{S}_1$ is m. Then, after fixing the scale of the three neighboring triangles of $\triangle ijk$, one can fix $\triangle ijk$'s neighboring triangles' neighboring triangle; such a propagating fixing process will fix the scales of all the triangles in $\mathbb{S}_1$. Now consider $\mathbb{S}_1$'s neighbouring face $\mathbb{S}_2$ which shares at least one edge with $\mathbb{S}_1$. Since the scales of all triangles in $\mathbb{S}_1$ are fixed, the length of this shared edge is fixed and the scale of the triangle containing this edge in $\mathbb{S}_2$ is also fixed. Apply for $\mathbb{S}_2$ the same argument for $\mathbb{S}_1$, all the triangles in $\mathbb{S}_2$ can be fixed. Because the polyhedron $\mathbb{P}$ is closed, under the triangulation $\mathcal{K}$, one can always fix the neighboring triangles from those triangles with fixed scale until all

the triangles in $\mathcal{K}$ are fixed. Therefore, all the edge lengths are constant provided that one triangle's scale is constant. □

Proof of Theorem 5.23 We prove Theorem 5.23 following the proof of Theorem 5.19. According to Lemma 5.24, one has that the vertices of $\mathcal{V} \cup \mathcal{V}'$ that are involved in a face of $\tilde{\mathbb{P}}$ will be coplanar under the perturbation. Therefore, using Lemma 5.17, each corresponding dihedral angle formed by two adjacent faces keep constant under the perturbation. On the other hand, Lemma 5.25 implies that all the edge lengths of $\tilde{\mathbb{P}}$ keep constant under the given conditions. Based on these two facts and the proof of Theorem 5.19, one has that $\mathbb{A}$ is angle rigid. □

Instead of triangulating the surface of convex polyhedra, we now give the result when each face of the convex polyhedron is infinitesimally angle rigid. A face in a convex polyhedron is said to be infinitesimally angle rigid if it can only translate, rotate and scale as a whole under any local perturbation of the polyhedron.

Corollary 5.26. *A convex polyhedron with infinitesimally angle rigid faces is angle rigid.*

The proof of this corollary follows the proof of Theorem 5.19. On the one hand, all angles in each face will remain constant under a perturbation according to the definition of infinitesimally angle rigid face. On the other hand, translation and rotation of a face will not change the lengths of its edges. When one edge length is fixed under the perturbation, the scale of the infinitesimally angle rigid face is also fixed which implies that the lengths of the other edges of the face are fixed. Note that each face of the convex polyhedron has at least three neighboring faces and each pair of them share a different edge with the original face. Therefore, by fixing edge length iteratively, all the edge lengths of the polyhedron will be fixed given one fixed edge length in the polyhedron. From the above two facts and Lemma 5.18, one has that the convex polyhedron is angle rigid.

5.2.5 Angle rigidity matrix

Note that the above proposed checking conditions do not work when the angularity cannot be constructed by Type-I, Type-II, merging operations or is not a convex polyhedron. To develop a general checking condition, taking an angle $\beta = \measuredangle ijk \in (0, \pi)$ in $f_{\mathcal{A}}(p)$ as an example, one has

$$\dot{\beta} = N_{kji}\dot{p}_i - (N_{kji} + N_{ijk})\dot{p}_j + N_{ijk}\dot{p}_k, \tag{5.2}$$

where $N_{kji} = -\frac{b_{jk}^{\mathrm{T}} P_{b_{ji}}}{l_{ji} \sin\beta} \in \mathbb{R}^{1\times 3}, i, j, k \in \mathcal{V}$. Then, one will have the angle rigidity matrix $R(p) = \frac{\partial f_{\mathcal{A}}(p)}{\partial p} \in \mathbb{R}^{M\times 3N}$, which has the same structure as it in the 2D case.

Now, we study the null space of the angle rigidity matrix $R(p)$. First, we introduce

$$q_1 = 1_N \otimes \begin{bmatrix}1\\0\\0\end{bmatrix}, q_2 = 1_N \otimes \begin{bmatrix}0\\1\\0\end{bmatrix}, q_3 = 1_N \otimes \begin{bmatrix}0\\0\\1\end{bmatrix}, \tag{5.3}$$

$$q_4 = \begin{bmatrix}(Q_1 p_1)^{\mathrm{T}}, & (Q_1 p_2)^{\mathrm{T}}, & \cdots, & (Q_1 p_N)^{\mathrm{T}}\end{bmatrix}^{\mathrm{T}}, \tag{5.4}$$

$$q_5 = \begin{bmatrix}(Q_2 p_1)^{\mathrm{T}}, & (Q_2 p_2)^{\mathrm{T}}, & \cdots, & (Q_2 p_N)^{\mathrm{T}}\end{bmatrix}^{\mathrm{T}}, \tag{5.5}$$

$$q_6 = \begin{bmatrix}(Q_3 p_1)^{\mathrm{T}}, & (Q_3 p_2)^{\mathrm{T}}, & \cdots, & (Q_3 p_N)^{\mathrm{T}}\end{bmatrix}^{\mathrm{T}}, \tag{5.6}$$

$$q_7 = \begin{bmatrix}p_1^{\mathrm{T}}, & p_2^{\mathrm{T}}, & \cdots, & p_N^{\mathrm{T}}\end{bmatrix}^{\mathrm{T}}, \tag{5.7}$$

where $\otimes$ represents Kronecker product, $Q_1 = \begin{bmatrix}0 & 1 & 0\\-1 & 0 & 0\\0 & 0 & 0\end{bmatrix}$, $Q_2 = \begin{bmatrix}0 & 0 & 1\\0 & 0 & 0\\-1 & 0 & 0\end{bmatrix}$, $Q_3 = \begin{bmatrix}0 & 0 & 0\\0 & 0 & 1\\0 & -1 & 0\end{bmatrix}$ and 1_N denotes the $N \times 1$ column vector of all ones. Note that q_1, q_2 and q_3 correspond to translation, q_4, q_5, q_6 rotation, and q_7 scaling. Now we present the theorem.

Theorem 5.27. *For an angle rigidity matrix $R(p)$, it always holds that*

$$\text{Span}\{q_1, q_2, q_3, q_4, q_5, q_6, q_7\} \subseteq \text{Null}(R(p))$$

and correspondingly $\text{Rank}(R(p)) \leqslant 3N - 7$.

Proof. Because each row sum of $R(p)$ equals zero, one has $R(p)q_1 = 0$, $R(p)q_2 = 0$ and $R(p)q_3 = 0$. Taking an arbitrary row $\measuredangle ijk$ in $R(p)$ as an example, one has the corresponding row in $R(p)q_4$

$$\begin{aligned}&N_{kji}Q_1(p_i - p_j) + N_{ijk}Q_1(p_k - p_j)\\ =&\frac{b_{jk}^{\mathrm{T}} P_{b_{ji}} Q_1 b_{ji} + b_{ji}^{\mathrm{T}} P_{b_{jk}} Q_1 b_{jk}}{-\sin\beta} = \frac{b_{jk}^{\mathrm{T}} Q_1 b_{ji} + b_{ji}^{\mathrm{T}} Q_1 b_{jk}}{-\sin\beta}\\ =&0,\end{aligned}$$

where we have used $Q_1^{\mathrm{T}} = -Q_1$ and $b_{ji}^{\mathrm{T}} Q_1 b_{ji} = 0$. The case for Q_2, Q_3 can be similarly obtained. Then, for $R(p)q_7$, one has $N_{kji}(p_i - p_j) + N_{ijk}(p_k - p_j) = \frac{b_{jk}^{\mathrm{T}} P_{b_{ji}} b_{ji} + b_{ji}^{\mathrm{T}} P_{b_{jk}} b_{jk}}{-\sin\beta} = 0$, where we have used the fact that $P_{b_{ji}} b_{ji} = 0$. Therefore,

Span$\{q_1, q_2, q_3, q_4, q_5, q_6, q_7\} \subseteq$ Null$(R(p))$.

Because each vertex $i, \forall i \in \mathcal{V}$ has a distinct position p_i, one has that q_4, q_5, q_6, q_7 are linearly independent from q_1, q_2 and q_3; otherwise the linear combination of q_1, q_2 and q_3, i.e., $\gamma_1 q_1 + \gamma_2 q_2 + \gamma_3 q_3, \gamma_i \in \mathbb{R}, i = 1, 2, 3$ will give the same coordinate components $p_1 = p_2 = \cdots = p_N$. Since $q_1^{\mathrm{T}} q_2 = 0$, $q_1^{\mathrm{T}} q_3 = 0$ and $q_2^{\mathrm{T}} q_3 = 0$, one has that q_1, q_2, q_3 are linearly independent from each other. Since the Z-coordinate of the vector $Q_1 p_i, i = 1, \cdots, N$ is always zero and the Y-coordinate of the vector $Q_2 p_i, i = 1, \cdots, N$ is zero, one has that q_4 and q_5 are linearly independent, which is similar to the cases of q_4 and q_6, and q_5 and q_6. Then, q_4, q_5, q_6 are linearly independent. Also, $q_4^{\mathrm{T}} q_7 = 0$, $q_5^{\mathrm{T}} q_7 = 0$ and $q_6^{\mathrm{T}} q_7 = 0$ imply that q_4, q_5, q_6 are linearly independent from q_7. Therefore, one has that $q_1, q_2, q_3, q_4, q_5, q_6, q_7$ are linearly independent, which implies Rank$(R(p)) \leqslant 3N - 7$. □

Based on Theorem 5.27 and Chapter 2, one can also define infinitesimal angle rigidity in 3D and its checking condition using the rank of angle rigidity matrix. The main purpose of defining angle rigidity matrix and infinitesimal angle rigidity is to check angle rigidity of angularity which cannot be explicitly constructed by type-I or type-II vertex additions.

Remark 5.28. In 2D angle rigidity in Chapter 2, several combinatoral necessary conditions are developed for infinitesimal angle rigidity (including cyclic angles, angles with the same middle vertex and over constrained angle subset), which are not necessary anymore in 3D angle rigidity. However, to check the generic rigidity of $\mathbb{A}(\mathcal{V}, \mathcal{A}, p)$, one can use the rank condition by a random realization of p [43].

5.3 Concluding remarks

In this Chapter, we have studied angle rigidity in 3D case. First, we have shown that angle rigidity in 3D is a local property because of the existence of flex ambiguity. Two types of vertex addition operations have been developed to construct a globally angle rigid angularity or an angle rigid angularity, respectively. We have also shown how to merge two globally angle rigid angularities into one globally angle rigid angularity. Angle rigidity of convex polyhedra has been studied.

Chapter 6

Formation stabilization in 3D

Using the developed 3D angle rigidity theory in Chapter 5, we propose formation control algorithms in this chapter for a team of mobile agents to achieve a desired angle rigid formation in 3D, in which only local direction measurements are needed. The formation is constructed based on the proposed vertex-addition operations which start from a triangular formation and then add each new vertex into the existing formation by three new angle constraints. We will also show how to achieve convex polyhedral formations in which angles constraints are in the surfaces of the formations.

6.1 Introduction

Different from the 2D formations for ground robots in chapters 3 and 4, in the applications of autonomous aerial refueling [91], drone swarm's group display [3] and satellite formation keeping [90], a desired spatial formation is usually required to be formed by those teams of vehicles. Similar to the motivation of 2D formations, to make full use of low-cost, lightweight, and low-power onboard sensors [22, 102] and avoid the requirement on the alignment of coordinate frames [52, 55, 72, 85], there is a great need to further study multi-agent formations in 3D. In this chapter we design a control algorithm to stabilize a multi-agent formation by only using direction measurements with the help of 3D angle rigidity theory that we have developed in Chapter 5.

6.2 Multi-agent sequential formations

Consider a group of N agents, labeled by $1, 2, \cdots, N$, in 3D, each of which is governed by single-integrator dynamics

$$\dot{p}_i = u_i, i = 1, \cdots, N, \tag{6.1}$$

where $p_i \in \mathbb{R}^3$ denotes agent i's position, and u_i is the control input to be designed. Each agent i can only measure the direction $\overrightarrow{ij}, j \in \mathcal{N}_i$, where $\mathcal{N}_i$ denotes agent

i's neighbor set. We consider that the desired formation is constructed through a sequence of Type-I or Type-II vertex additions from a generically angle rigid triangular formation, which is globally angle rigid or angle rigid according to Propositions 5.9 and 5.10, respectively. Correspondingly, we propose to control the first three agents to form the desired triangular formation and then control the remaining agents following the sequence of Type-I or Type-II vertex additions.

6.2.1 Formation control for the first three agents

In this subsection, we show how to achieve a desired triangular formation for the first three agents. The control objectives for agents 1 to 3 are

$$\lim_{t\to\infty} e_1(t) = \lim_{t\to\infty}(\alpha_{312}(t) - \alpha^*_{312}) = 0, \tag{6.2}$$
$$\lim_{t\to\infty} e_2(t) = \lim_{t\to\infty}(\alpha_{123}(t) - \alpha^*_{123}) = 0, \tag{6.3}$$
$$\lim_{t\to\infty} e_3(t) = \lim_{t\to\infty}(\alpha_{231}(t) - \alpha^*_{231}) = 0, \tag{6.4}$$

where $\alpha^*_{jik} \in (0,\pi), i,j,k \in \{1,2,3\}$ denotes agent i's desired angle formed with agents j,k. Motivated by [16], we design the following cyclic pursuing rule

$$u_1 = -(\alpha_{312} - \alpha^*_{312})b_{12}, \tag{6.5}$$
$$u_2 = -(\alpha_{123} - \alpha^*_{123})b_{23}, \tag{6.6}$$
$$u_3 = -(\alpha_{231} - \alpha^*_{231})b_{31}, \tag{6.7}$$

where $\alpha_{jik} = \arccos(b_{ij}^{\mathrm{T}} b_{ik})$ and each agent $i, i = 1,2,3$ only needs to measure the directions $\overrightarrow{ij}$ and $\overrightarrow{ik}$ in its own coordinate frame to implement (6.5)-(6.7). Note that the direction $\overrightarrow{ij}$ in 3D has a unique correspondence to azimuth and altitude angles described in agent i's coordinate frame. Now, we study the angle error dynamics.

Suppose $l_{ij}(0) \neq 0$ and $\sin\alpha_{jik}(0) \neq 0, i,j,k = 1,2,3$, then $\exists T_1 > 0$ such that for $t \in [0,T_1)$, $l_{ij}(t) \neq 0$ and $\sin\alpha_{jik}(t) \neq 0$. Then for $t \in [0,T_1)$, taking e_1 as an example, according to (5.2), one has

$$\begin{aligned}\dot{e}_1 = \dot{\alpha}_{312} &= -\frac{\dot{b}_{13}^{\mathrm{T}} b_{12} + b_{13}^{\mathrm{T}}\dot{b}_{12}}{\sin\alpha_{312}} \\ &= -[\frac{P_{b_{13}}(\dot{p}_3 - \dot{p}_1)}{l_{13}\sin\alpha_{312}}]^{\mathrm{T}} b_{12} - b_{13}^{\mathrm{T}}\frac{P_{b_{12}}}{l_{12}\sin\alpha_{312}}(\dot{p}_2 - \dot{p}_1).\end{aligned} \tag{6.8}$$

By substituting (6.5)-(6.7) into (6.8), it follows

$$\begin{aligned} b_{13}^{\mathrm{T}}\dot{b}_{12} =& \frac{b_{13}^{\mathrm{T}}P_{b_{12}}}{l_{12}}[(\alpha_{312}-\alpha_{312}^{*})b_{12}-(\alpha_{123}-\alpha_{123}^{*})b_{23}] \\ =& -\frac{\sin\alpha_{312}\sin\alpha_{123}}{l_{12}}(\alpha_{123}-\alpha_{123}^{*}). \end{aligned} \tag{6.9}$$

Similarly,

$$\begin{aligned} \dot{b}_{13}^{\mathrm{T}}b_{12} =& \frac{b_{12}^{\mathrm{T}}P_{b_{13}}}{l_{13}}[(\alpha_{312}-\alpha_{312}^{*})b_{12}-(\alpha_{231}-\alpha_{231}^{*})b_{31}] \\ =& \frac{\sin^2\alpha_{312}}{l_{13}}(\alpha_{312}-\alpha_{312}^{*}). \end{aligned} \tag{6.10}$$

By substituting (6.9) and (6.10) into (6.8), one obtains

$$\dot{e}_1 = -\frac{\sin\alpha_{312}}{l_{13}}e_1+\frac{\sin\alpha_{123}}{l_{12}}e_2. \tag{6.11}$$

By following the steps similar to (6.8)-(6.11), one has

$$\dot{e}_2 = -\frac{\sin\alpha_{123}}{l_{21}}e_2+\frac{\sin\alpha_{231}}{l_{23}}e_3, \tag{6.12}$$

$$\dot{e}_3 = -\frac{\sin\alpha_{231}}{l_{32}}e_3+\frac{\sin\alpha_{312}}{l_{31}}e_1. \tag{6.13}$$

Writing (6.11)-(6.13) into the matrix form, one has the overall angle error dynamics of the first three agents

$$\begin{aligned} \dot{e}_f =& [\dot{e}_1 \;\; \dot{e}_2 \;\; \dot{e}_3]^{\mathrm{T}} = F_1(e_f)e_f \\ =& \begin{bmatrix} -g_{312} & g_{123} & 0 \\ 0 & -g_{123} & g_{231} \\ g_{312} & 0 & -g_{231} \end{bmatrix} \begin{bmatrix} \alpha_{312}-\alpha_{312}^{*} \\ \alpha_{123}-\alpha_{123}^{*} \\ \alpha_{231}-\alpha_{231}^{*} \end{bmatrix}, \end{aligned} \tag{6.14}$$

where $g_{jik}=\frac{\sin\alpha_{jik}}{l_{ji}}, i,j,k\in\{1,2,3\}$. Since $e_1+e_2+e_3\equiv 0$, (6.14) is equivalent to

$$\dot{e}_s = \begin{bmatrix} \dot{e}_1 \\ \dot{e}_2 \end{bmatrix} = \begin{bmatrix} -g_{312} & g_{123} \\ -g_{231} & -(g_{123}+g_{231}) \end{bmatrix} \begin{bmatrix} e_1 \\ e_2 \end{bmatrix} = F_s(e_s)e_s. \tag{6.15}$$

Although (6.15) is derived for $t\in[0,T_1)$, we now show that T_1 can be extended to infinity.

Lemma 6.1 (Non-collinearity)**.** *For the 3-agent formation under the control law* (6.5)-(6.7)*, if the formation is not initially collinear, it will not become collinear for*

$\forall t > 0$, and thus (6.15) applies for any $t > 0$.

Proof. We prove by contradiction. Suppose collinearity may occur for $t > T_1$, and let T_s be the first time at which the three agents approach being collinear. Then at T_s^-, it must be true that for the triangular formation formed by these three agents, two interior angles approach zero and the third approaches π. Without loss of generality, assume that agent 1 is the agent associated with the interior angle approaching π, and thus $\alpha_1(T_s^-) = \pi - \epsilon_1$, $\alpha_2(T_s^-) = \epsilon_2$ and $\alpha_3(T_s^-) = \epsilon_3$ for some infinitesimally small positive numbers ϵ_1, ϵ_2 and ϵ_3 satisfying $\epsilon_1 = \epsilon_2 + \epsilon_3$. For $t \in [0, T_s)$, one has

$$\dot{e}_1 = -g_{312}e_1 + g_{123}e_2. \tag{6.16}$$

Since α_1^* is bounded away from π, $e_1(T_s^-) > 0$; since α_2^* is bounded away from zero, $e_2(T_s^-) < 0$. In addition, one can further check that at T_s^-, $g_{312} > 0$ and $g_{123} > 0$. Hence, $\dot{e}_1(T_s^-) < 0$, which implies that at T_s^-, if time further evolves, α_1 decreases away from π, which contradicts the assumption that at T_s, the three agents become collinear and thus α_1 becomes π. So we have reached the contradiction and the proof is complete. □

Now we present the convergence result for the first three agents.

Theorem 6.2. *For the three-agent formation under the control law (6.5)-(6.7), if $\alpha_{312}(0), \alpha_{123}(0), \alpha_{231}(0)$ are not zero, the initial angle errors $e_i(0), i = 1, 2, 3$ are sufficiently small and the initial distances $l_{12}(0), l_{23}(0), l_{31}(0)$ are bounded away from zero, then the angle errors $e_i(t)$ converge exponentially to zero.*

Proof. To show the local convergence of e_i, we use linearization to analyze the angle error dynamics (6.15). By taking e_1 as an example, the linearized dynamics around the desired equilibrium $e_s = 0$ are

$$\begin{aligned}
\dot{e}_1 &= \left[\frac{\partial(-g_{312}e_1 + g_{123}e_2)}{\partial e_1}|_{e_s=0}\right] e_1 + \left[\frac{\partial(-g_{312}e_1 + g_{123}e_2)}{\partial e_2}|_{e_s=0}\right] e_2 \\
&= \left[\left(-g_{312} - \frac{\partial g_{312}}{\partial e_1}e_1 + \frac{\partial g_{123}}{\partial e_1}e_2\right)|_{e_s=0}\right] e_1 \\
&\quad + \left[\left(g_{123} + \frac{\partial g_{123}}{\partial e_2}e_2 - \frac{\partial g_{312}}{\partial e_2}e_1\right)|_{e_s=0}\right] e_2 \\
&= -g_{312}^* e_1 + g_{123}^* e_2,
\end{aligned} \tag{6.17}$$

where $g_{jik}^* = g_{jik}|_{e_s=0}, j \neq i \neq k$ and $j, i, k \in \{1, 2, 3\}$. Then, by following the same step as (6.17) for e_2, the linearized dynamics of (6.15) can be written as

$$\dot{e}_s = A_1 e_s, \tag{6.18}$$

where $A_1 = F_s(e_s)|_{e_s=0}$ is a 2×2 constant matrix. Then, it is obvious that

$\text{tr}(A_1) = -g^*_{312} - g^*_{123} - g^*_{231} < 0$, $\det(A_1) = g^*_{312}(g^*_{123} + g^*_{231}) + g^*_{123}g^*_{231} > 0$, where tr() and det() represent the trace and determinant of a square matrix, respectively. It follows that A_1 is Hurwitz. Then, for the 2×2 identity matrix $I_2 \in \mathbb{R}^{2\times 2}$, there always exists a positive definite matrix $P_1 \in \mathbb{R}^{2\times 2}$ such that $-I_2 = P_1 A_1 + A_1^{\mathrm{T}} P_1$ [54, Theorem 4.6]. Consider the Lyapunov function candidate

$$V_1 = e_s^{\mathrm{T}} P_1 e_s. \tag{6.19}$$

Taking the time-derivative of (6.19) yields

$$\dot{V}_1 = -e_s^{\mathrm{T}} e_s \leqslant -\frac{V_1}{\lambda_{\max}(P_1)}, \tag{6.20}$$

where $\lambda_{\max}()$ denote the maximum eigenvalue of a real symmetric matrix. Then one has that $V_1(t) \leqslant V_1(0) e^{-\frac{t}{\lambda_{\max}(P_1)}}$. Because P_1 is positive definite, one has

$$e_1^2 + e_2^2 = \|e_s\|^2 \leqslant \frac{V_1}{\lambda_{\min}(P_1)} \leqslant \frac{V_1(0)}{\lambda_{\min}(P_1)} e^{-\frac{t}{\lambda_{\max}(P_1)}}. \tag{6.21}$$

where $\lambda_{\min}()$ denote the minimum eigenvalue of a real symmetric matrix. Since $e_1 + e_2 + e_3 \equiv 0$, one has

$$e_3^2 = e_1^2 + e_2^2 + 2e_1e_2 \leqslant 2(e_1^2 + e_2^2) \leqslant \frac{2V_1(0)}{\lambda_{\min}(P_1)} e^{-\frac{t}{\lambda_{\max}(P_1)}}$$

which implies that $e_i, i = 1, 2, 3$, under the dynamics (6.14) is locally exponentially stable. □

In the following subsections, we study the control of the overall formation.

6.2.2 Formation control for the remaining agents by Type-I vertex addition

In this subsection, we show how to control the remaining agents to the formation by Type-I vertex addition (case 2) developed in Definition 5.7. To be specific, the control objectives for agent $i, 4 \leqslant i \leqslant N$, are

$$\lim_{t\to\infty} e_{i1}(t) = \lim_{t\to\infty}(\alpha_{ij_1j_2}(t) - \alpha^*_{ij_1j_2}) = 0, \tag{6.22}$$

$$\lim_{t\to\infty} e_{i2}(t) = \lim_{t\to\infty}(\alpha_{ij_2j_1}(t) - \alpha^*_{ij_2j_1}) = 0, \tag{6.23}$$

$$\lim_{t\to\infty} e_{i3}(t) = \lim_{t\to\infty}(\alpha_{ij_2j_3}(t) - \alpha^*_{ij_2j_3}) = 0, \tag{6.24}$$

where $i = 4, \cdots, N$, $j_1 \neq j_2 \neq j_3$ $j_1 < i, j_2 < i, j_3 < i$, and $\alpha^*_{ij_1j_2} \in (0, \pi), \alpha^*_{ij_2j_1} \in (0, \pi), \alpha^*_{ij_2j_3} \in (0, \pi)$ denote three desired angles that agent i aims at maintaining

with its neighboring agents j_1, j_2, j_3.

We first illustrate how to control agent 4, and then extend the result to the N-agent case. We propose the following control law for agent 4

$$u_4 =(\alpha_{412} - \alpha^*_{412})b_{42} + (\alpha_{421} - \alpha^*_{421})b_{41} + (\alpha_{423} - \alpha^*_{423})b_{43}. \tag{6.25}$$

Note that in (6.25), the real-time angle information $\alpha_{412} = \arccos(b_{14}^{\mathrm{T}} b_{12})$ cannot be calculated by agent 4's own direction measurements, but can be calculated via agent 1's direction measurements $\overrightarrow{14}, \overrightarrow{12}$. Therefore, the implementation of control law (6.25) relies on not only agent 4's direction measurements $\overrightarrow{41}, \overrightarrow{42}, \overrightarrow{43}$, but also the real-time angle information $\alpha_{412}(t), \alpha_{421}(t), \alpha_{423}(t)$ which can be sent to agent 4 through wireless communication. Now we present the convergence of agent 4.

Theorem 6.3. *For the four-agent formation under the control law (6.5)-(6.7) and* (6.25)*, if* $\alpha_{123}(0)$*,*$\alpha_{231}(0)$*,*$\alpha_{312}(0)$*,* $\alpha_{412}(0)$*,*$\alpha_{421}(0)$*,*$\alpha_{423}(0)$ *are not zero or* π*, the initial angle errors* $e_i(0), e_{4i}(0), i = 1, 2, 3$ *are sufficiently small, the initial distances* $l_{jk}(0), j \neq k, j, k \in \{1, 2, 3, 4\}$ *are bounded away from zero and* $p_4(0)$ *is sufficiently away from the plane formed by* $p_1(0), p_2(0), p_3(0)$*, then the angle errors* $e_{4i}(t)$ *converge exponentially to zero.*

Proof. Since $l_{jk}(0) \neq 0$ and $\sin\alpha_{412}(0),\ \sin\alpha_{421}(0), \sin\alpha_{423}(0)$ are not zero, $\exists T_2 > 0$ such that for $t \in [0, T_2)$, $l_{jk}(t) \neq 0$ and $\sin\alpha_{412}(t),\ \sin\alpha_{421}(t),\ \sin\alpha_{423}(t)$ are not zero. Now we study the dynamics of angle errors $e_{41} = \alpha_{412} - \alpha^*_{412}$, $e_{42} = \alpha_{421} - \alpha^*_{421}$, $e_{43} = \alpha_{423} - \alpha^*_{423}$. Taking e_{41} as an example, by using (5.2), one has

$$\dot{e}_{41} = \dot{\alpha}_{412} = -\,[\frac{P_{b_{14}}}{l_{14}\sin\alpha_{412}}(\dot{p}_4 - \dot{p}_1)]^{\mathrm{T}} b_{12} - b_{14}^{\mathrm{T}} \frac{P_{b_{12}}}{l_{12}\sin\alpha_{412}}(\dot{p}_2 - \dot{p}_1). \tag{6.26}$$

Substituting (6.25) and (6.5)-(6.7) into (6.26) yields

$$\begin{aligned}\dot{e}_{41} =& -\frac{\sin\alpha_{142}}{l_{14}}(\alpha_{412} - \alpha^*_{412}) - \frac{b_{12}^{\mathrm{T}} P_{b_{14}} b_{43}}{l_{14}\sin\alpha_{412}}(\alpha_{423} - \alpha^*_{423}) \\ & - \frac{b_{12}^{\mathrm{T}} P_{b_{14}} b_{12}}{l_{14}\sin\alpha_{412}} e_1 + \frac{b_{14}^{\mathrm{T}} P_{b_{12}} b_{23}}{l_{12}\sin\alpha_{412}} e_2.\end{aligned} \tag{6.27}$$

Similarly, one can compute $\dot{e}_{42}$ and $\dot{e}_{43}$ to obtain

$$\begin{aligned}\dot{e}_4 &= \begin{bmatrix}\dot{e}_{41} & \dot{e}_{42} & \dot{e}_{43}\end{bmatrix}^{\mathrm{T}} = F_4(e_s, e_4)e_4 + G_4(e_s, e_4)e_s \\ &= \begin{bmatrix} -\frac{\sin\alpha_{142}}{l_{14}} & 0 & -\frac{b_{12}^{\mathrm{T}} P_{b_{14}} b_{43}}{l_{14}\sin\alpha_{412}} \\ 0 & -\frac{\sin\alpha_{142}}{l_{24}} & -\frac{b_{21}^{\mathrm{T}} P_{b_{24}} b_{43}}{l_{24}\sin\alpha_{421}} \\ 0 & -\frac{b_{23}^{\mathrm{T}} P_{b_{24}} b_{41}}{l_{24}\sin\alpha_{423}} & -\frac{\sin\alpha_{243}}{l_{24}} \end{bmatrix} \begin{bmatrix} e_{41} \\ e_{42} \\ e_{43} \end{bmatrix} + \begin{bmatrix} G_{11} & G_{12} \\ G_{21} & G_{22} \\ G_{31} & G_{32} \end{bmatrix} \begin{bmatrix} e_1 \\ e_2 \end{bmatrix},\end{aligned} \tag{6.28}$$

where $G_{11} = -\frac{b_{12}^{\mathrm{T}} P_{b_{14}} b_{12}}{l_{41}\sin\alpha_{412}}$, $G_{12} = \frac{b_{14}^{\mathrm{T}} P_{b_{12}} b_{23}}{l_{12}\sin\alpha_{412}}$, $G_{21} = 0$, $G_{22} = -(\frac{b_{21}^{\mathrm{T}} P_{b_{24}} b_{23}}{l_{24}\sin\alpha_{421}} + \frac{b_{24}^{\mathrm{T}} P_{b_{21}} b_{23}}{l_{21}\sin\alpha_{421}})$, $G_{31} = -\frac{b_{24}^{\mathrm{T}} P_{b_{23}} b_{31}}{l_{23}\sin\alpha_{423}}$, $G_{32} = -(\frac{b_{23}^{\mathrm{T}} P_{b_{24}} b_{23}}{l_{24}\sin\alpha_{423}} + \frac{b_{24}^{\mathrm{T}} P_{b_{23}} b_{31}}{l_{23}\sin\alpha_{423}})$. Now, we check the local stability of the 4-agent formation for the region close to the desired equilibrium $\{e_s = 0, e_4 = 0\}$. Linearizing (6.28) around $\{e_s = 0, e_4 = 0\}$ by following (6.17), one has the linearized dynamics

$$\dot{e}_4 = A_4 e_4 + B_4 e_s, \tag{6.29}$$

where $A_4 = F_4(e_s, e_4)|_{e_s=0,e_4=0}$, $B_4 = G_4(e_s, e_4)|_{e_s=0,e_4=0}$ are constant matrices. Now, we check whether A_4 is Hurwitz.

$$\begin{aligned}\det(\lambda I_3 - A_4) =&(\lambda + \frac{\sin\alpha_{142}^*}{l_{14}^*})(\lambda + \frac{\sin\alpha_{142}^*}{l_{24}^*})(\lambda + \frac{\sin\alpha_{243}^*}{l_{24}^*})\\ &- (\lambda + \frac{\sin\alpha_{142}^*}{l_{14}^*})\frac{(b_{21}^{*\mathrm{T}} P_{b_{24}^*} b_{43}^*)}{l_{24}^*\sin\alpha_{421}^*}\frac{(b_{23}^{*\mathrm{T}} P_{b_{24}^*} b_{41}^*)}{l_{24}^*\sin\alpha_{423}^*},\end{aligned}$$

where $\lambda \in \mathbb{C}$ denotes the eigenvalue of A_4, l_{ji}^* and b_{ji}^*, $j, i \in \mathcal{V}$ are the distance and bearing evaluated at $\{e_s = 0, e_4 = 0\}$, respectively. Checking the eigenvalues of A_4 by letting $\det(\lambda I_3 - A_4) = 0$, one has that A_4 always has an eigenvalue $-\frac{\sin\alpha_{142}^*}{l_{14}^*} < 0$. However, it is quite challenging to check the sign of the real parts of the remaining two eigenvalues of A_4. Here, we first calculate

$$\begin{aligned}&(b_{21}^{*\mathrm{T}} P_{b_{24}^*} b_{43}^*)(b_{23}^{*\mathrm{T}} P_{b_{24}^*} b_{41}^*) \\ =&\frac{l_{23}^*(b_{21}^{*\mathrm{T}} P_{b_{24}^*} b_{23}^*)}{l_{43}^*}\frac{l_{43}^*(b_{43}^{*\mathrm{T}} P_{b_{24}^*} b_{41}^*)}{l_{23}^*} \\ =&[\cos\alpha_{123}^* - \cos\alpha_{423}^*\cos\alpha_{421}^*][\cos\alpha_{143}^* - \cos\alpha_{142}^*\cos\alpha_{243}^*],\end{aligned} \tag{6.30}$$

where we have used the facts that $b_{43} = \frac{(p_3 - p_2) + (p_2 - p_4)}{l_{43}}$, $P_{b_{24}}(p_2 - p_4) = 0$, and $b_{23} = \frac{(p_3 - p_4) + (p_4 - p_2)}{l_{23}}$. Then, the other two eigenvalues of A_4 satisfy

$$\lambda^2 + (\frac{\sin\alpha_{142}^*}{l_{24}^*} + \frac{\sin\alpha_{243}^*}{l_{24}^*})\lambda + \varepsilon_1 = 0, \tag{6.31}$$

where $\varepsilon_1 = -\frac{[\cos\alpha_{123}^* - \cos\alpha_{423}^*\cos\alpha_{421}^*]}{l_{24}^*\sin\alpha_{421}^*}\frac{[\cos\alpha_{143}^* - \cos\alpha_{142}^*\cos\alpha_{243}^*]}{l_{24}^*\sin\alpha_{423}^*}$ $+ \frac{\sin\alpha_{142}^*}{l_{24}^*}\frac{\sin\alpha_{243}^*}{l_{24}^*}$. If $\varepsilon_1 > 0$, then the remaining two eigenvalues of A_4 have negative real parts, which implies that A_4 is Hurwitz. Note that $\varepsilon_1 > 0$ is equivalent to

$$\begin{aligned}&\sin\alpha_{421}^*\sin\alpha_{423}^*\sin\alpha_{142}^*\sin\alpha_{243}^* > \\ &[\cos\alpha_{123}^* - \cos\alpha_{423}^*\cos\alpha_{421}^*][\cos\alpha_{143}^* - \cos\alpha_{142}^*\cos\alpha_{243}^*].\end{aligned} \tag{6.32}$$

Now, we prove that (6.32) holds for arbitrary tetrahedron formations formed by

agents 1-4. Splitting (6.32) into two inequalities $\sin\alpha^*_{421}\sin\alpha^*_{423} > |\cos\alpha^*_{123} - \cos\alpha^*_{423}\cos\alpha^*_{421}|$ and $\sin\alpha^*_{142}\sin\alpha^*_{243} > |\cos\alpha^*_{143} - \cos\alpha^*_{142}\cos\alpha^*_{243}|$, we first illustrate how to prove the first inequality by using the facts that $\alpha^*_{123} \in (0,\pi), \alpha^*_{423} \in (0,\pi), \alpha^*_{421} \in (0,\pi)$, and $\alpha^*_{123} + \alpha^*_{423} + \alpha^*_{421} < 2\pi$, $2\pi > \alpha^*_{ijk} + \alpha^*_{ijm} > \alpha^*_{kjm} > 0, i,j,k,m \in \{1,2,3,4\}$.

• Case 1: $\cos\alpha^*_{123} > \cos\alpha^*_{423}\cos\alpha^*_{421}$. When $0 < \alpha^*_{421} - \alpha^*_{423} < \pi$, by using $0 < \alpha^*_{421} < \alpha^*_{123} + \alpha^*_{423} < \pi$, one has that $0 < \alpha^*_{421} - \alpha^*_{423} < \alpha^*_{123} < \pi$. It follows that $\cos(\alpha^*_{421} - \alpha^*_{423}) > \cos\alpha^*_{123}$, which gives $\sin\alpha^*_{421}\sin\alpha^*_{423} > \cos\alpha^*_{123} - \cos\alpha^*_{423}\cos\alpha^*_{421}$. When $-\pi < \alpha^*_{421} - \alpha^*_{423} < 0$, by using $\alpha^*_{423} < \alpha^*_{421} + \alpha^*_{123}$, one has $-\pi < -\alpha^*_{123} < \alpha^*_{421} - \alpha^*_{423} < 0$. It follows that $\cos(\alpha^*_{421} - \alpha^*_{423}) > \cos(-\alpha^*_{123}) = \cos(\alpha^*_{123})$, which also gives $\sin\alpha^*_{421}\sin\alpha^*_{423} > \cos\alpha^*_{123} - \cos\alpha^*_{423}\cos\alpha^*_{421}$.

• Case 2: $\cos\alpha^*_{123} < \cos\alpha^*_{423}\cos\alpha^*_{421}$. When $\pi < \alpha^*_{421} + \alpha^*_{423} < 2\pi$, by using $\alpha^*_{123} \in (0,\pi)$, $(2\pi - (\alpha^*_{421} + \alpha^*_{243})) \in (0,\pi)$ and $\alpha^*_{123} < 2\pi - (\alpha^*_{421} + \alpha^*_{423})$, one has $\cos\alpha^*_{123} > \cos(2\pi - (\alpha^*_{421} + \alpha^*_{423})) = \cos(\alpha^*_{421} + \alpha^*_{423})$. It follows $\sin\alpha^*_{421}\sin\alpha^*_{423} > \cos\alpha^*_{423}\cos\alpha^*_{421} - \cos\alpha^*_{123}$. When $0 < \alpha^*_{421} + \alpha^*_{423} < \pi$, by using $0 < \alpha^*_{123} < \alpha^*_{421} + \alpha^*_{423} < \pi$, one also has $\sin\alpha^*_{421}\sin\alpha^*_{423} > \cos\alpha^*_{423}\cos\alpha^*_{421} - \cos\alpha^*_{123}$.

Combining the above two cases together, one has that $\sin\alpha^*_{421}\sin\alpha^*_{423} > |\cos\alpha^*_{123} - \cos\alpha^*_{423}\cos\alpha^*_{421}|$ holds for an arbitrary tetrahedron formation. The same analysis can be conducted for the second inequality, which proves (6.32).

By combining (6.30)-(6.32), one has that A_4 is alway Hurwitz for arbitrary tetrahedron formation formed by agents 1-4. Writing (6.18) and (6.29) into a compact form yields

$$\dot{\bar{e}}_4 = \begin{bmatrix} \dot{e}_s \\ \dot{e}_4 \end{bmatrix} = H_4\bar{e}_4 = \begin{bmatrix} A_1 & 0 \\ B_4 & A_4 \end{bmatrix} \begin{bmatrix} e_s \\ e_4 \end{bmatrix}. \tag{6.33}$$

Because A_1 and A_4 are Hurwitz, one has that H_4 is also Hurwitz [13, Proposition 5.5.13]. Then, for the 5×5 identity matrix $I_5 \in \mathbb{R}^{5\times 5}$, there exists a positive definite matrix $P_2 \in \mathbb{R}^{5\times 5}$ such that $P_2H_4 + H_4^{\mathrm{T}}P_2 = -I_5$. Construct the Lyapunov function

$$V_2 = \bar{e}_4^{\mathrm{T}}P_2\bar{e}_4. \tag{6.34}$$

Taking the time-derivative of (6.34) yields

$$\dot{V}_2 = -\bar{e}_4^{\mathrm{T}}\bar{e}_4 \leqslant -\frac{V_2}{\lambda_{\max}(P_2)}. \tag{6.35}$$

Then, it follows that

$$\|e_4\|^2 \leqslant \|\bar{e}_4\|^2 \leqslant \frac{V_2}{\lambda_{\min}(P_2)} \leqslant \frac{V_2(0)}{\lambda_{\min}(P_2)} e^{-\frac{t}{\lambda_{\max}(P_2)}}, \tag{6.36}$$

which implies the exponential stability of $\|e_4(t)\|$ for $\forall t \in [0, T_2)$. Note that

$\|\dot{p}_4\| \leqslant |e_{41}| + |e_{42}| + |e_{43}| \leqslant \sqrt{3}\|e_4\| \leqslant \sqrt{\frac{3V_2(0)}{\lambda_{\min}(P_2)}} e^{-\frac{t}{2\lambda_{\max}(P_2)}}$ which implies $\|p_4(t) - p_4(0)\| \leqslant \int_0^t \|\dot{p}_4(\tau)\| d\tau \leqslant 2\lambda_{\max}(P_2)\sqrt{\frac{3V_2(0)}{\lambda_{\min}(P_2)}}\left(1 - e^{-\frac{t}{2\lambda_{\max}(P_2)}}\right)$ for $\forall t \in [0, T_2)$. Since $V_2(0)$ is sufficiently small, $\|p_4(t) - p_4(0)\|$ is also sufficiently small for $\forall t \in [0, T_2)$. Since $p_4(0)$ is sufficiently away from the plane formed by $p_1(0), p_2(0), p_3(0)$, one has that $p_4(T_2^-)$ is also sufficiently away from the plane formed by $p_1(0), p_2(0), p_3(0)$ which implies that $l_{4i}(T_2^-) \neq 0, i = 1, 2, 3,$ and $\sin\alpha_{412}(T_2^-)$, $\sin\alpha_{421}(T_2^-)$, $\sin\alpha_{423}(T_2^-)$ are not zero. Then, one can extend T_2^- to T_3, $T_3 > T_2$. In fact one can check that when $T_3 \to \infty$, $\|p_4(t) - p_4(0)\|$ is still sufficiently small for $\forall t \in [0, \infty)$ which implies that (6.28) is always well-defined and $\|e_4(t)\|$ is exponentially stable for $\forall t \in [0, \infty)$. □

Remark 6.4. Note that the first three agents always lie in the plane formed by $p_1(0), p_2(0), p_3(0)$ since the control actions (6.5)-(6.7) are confined in this plane. If $\exists T_3$ such that $p_4(T_3)$ lies in that plane, then $p_4(t), \forall t > T_3$ will always be in that plane according to the control law (6.25). Then the angle error in (6.28) will not converge to zero because in this case $F_4(e_s, e_4)$ becomes singular. Therefore, Theorem 6.3 requires that $p_4(0)$ is sufficiently away from the plane formed by $p_1(0), p_2(0), p_3(0)$.

Now, we precisely describe the requirements on $l_{4i}(0), i = 1, 2, 3$, $e_{4i}(0)$ and the initial distance $h_{4-123}(0)$ between $p_4(0)$ and the plane formed by $p_1(0), p_2(0), p_3(0)$, respectively such that (6.28) is well-defined. Taking l_{41} as an example, one has

$$\begin{aligned} l_{41}(t) &= l_{41}(0) + \int_0^t \dot{l}_{41}(\tau) d\tau \\ &\geqslant l_{41}(0) - \int_0^t |b_{41}^{\mathrm{T}}(\dot{p}_1 - \dot{p}_4)| d\tau \\ &\geqslant l_{41}(0) - \int_0^t (|e_1| + |e_{41}| + |e_{42}| + |e_{43}|) d\tau \\ &\geqslant l_{41}(0) - 2\int_0^t \sqrt{e_1^2 + e_{41}^2 + e_{42}^2 + e_{43}^2} d\tau \\ &\geqslant l_{41}(0) - 4\sqrt{\frac{V_2(0)}{\lambda_{\min}(P_2)}}\lambda_{\max}(P_2)(1 - e^{-\frac{t}{2\lambda_{\max}(P_2)}}). \end{aligned} \tag{6.37}$$

To guarantee that $1/\sin\alpha_{412}$ is well-defined in (6.26), one requires $0 < \alpha_{412}(t) < \pi$. According to (6.36), one has

$$|e_{41}| = |\alpha_{412} - \alpha_{412}^*| \leqslant \|e_4\| \leqslant \sqrt{\frac{V_2(0)}{\lambda_{\min}(P_2)}}. \tag{6.38}$$

It follows that

$$\alpha_{412}^* - \sqrt{\frac{V_2(0)}{\lambda_{\min}(P_2)}} \leqslant \alpha_{412}(t) \leqslant \alpha_{412}^* + \sqrt{\frac{V_2(0)}{\lambda_{\min}(P_2)}}.$$

Therefore, if

$$\sqrt{V_2(0)} < \sqrt{\lambda_{\min}(P_2)} * \min\{\pi - \alpha_{412}^*, \alpha_{412}^*\}, \tag{6.39}$$

one always has $0 < \alpha_{412}(t) < \pi$.

The distance $h_{4-123}(t)$ between $p_4(t)$ and the plane formed by $p_1(0), p_2(0), p_3(0)$ can be calculated by

$$h_{4-123}(t) = \frac{V_{4-123}}{S_{123}(0)} = \frac{p_{4\bar{1}}^{\mathrm{T}}(t)\,(p_{4\bar{2}}(t) \times p_{4\bar{3}}(t))}{3l_{12}(0)l_{13}(0)\sin\alpha_{213}(0)}, \tag{6.40}$$

where $p_{4\bar{i}}(t) = p_i(0) - p_4(t), i = 1, 2, 3$. Then, one has

$$\begin{aligned}\dot{V}_{4-123} =& \frac{1}{6}\dot{p}_4^{\mathrm{T}}\,(p_{4\bar{2}} \times p_{4\bar{3}}) + p_{4\bar{1}}^{\mathrm{T}}\,[\dot{p}_4 \times (p_3(0) - p_2(0))] \\ \leqslant& \frac{1}{6}(|e_{41}| + |e_{42}| + |e_{43}|)[l_{42(max)}l_{43(max)} \\ &+ l_{32}(0)l_{41(max)}],\end{aligned} \tag{6.41}$$

where $l_{4i(max)} = \max\{\|p_{4\bar{i}}(t)\|, \forall t > 0\} = l_{4i}(0) + 4\sqrt{\frac{V_2(0)}{\lambda_{\min}(P_2)}}\lambda_{\max}(P_2)$, and we have used the fact that $\|p_{4\bar{i}}(t)\| \leqslant l_{4i}(0) + \int_0^t \|\dot{p}_4(\tau)\|d\tau \leqslant l_{4i}(0) + \int_0^t (|e_{41}| + |e_{42}| + |e_{43}|)\|d\tau \leqslant l_{4i}(0) + 4\sqrt{\frac{V_2(0)}{\lambda_{\min}(P_2)}}\lambda_{\max}(P_2)$. Therefore, one has

$$\begin{aligned}h_{4-123}(t) &\geqslant h_{4-123}(0) - \int_0^t |\dot{h}_{4-123}(\tau)|d\tau \\ &\geqslant h_{4-123}(0) - \int_0^t \frac{|\dot{V}_{4-123}(\tau)|}{S_{123}(0)}d\tau \\ &\geqslant h_{4-123}(0) - \varepsilon_2(1 - e^{-\frac{t}{2\lambda_{\max}(P_2)}}),\end{aligned} \tag{6.42}$$

where $\varepsilon_2 = \frac{4[l_{42(max)}l_{43(max)} + l_{32}(0)l_{41(max)}]}{3l_{12}(0)l_{13}(0)\sin\alpha_{213}(0)}\lambda_{\max}(P_2)\sqrt{\frac{V_2(0)}{\lambda_{\min}(P_2)}}$. Now, we summarize the results from (6.37) to (6.42).

Corollary 6.5. *Consider that the four-agent formation under the control law (6.5)-(6.7) and* (6.25)*,* $\sin\alpha_{jik}(0) \neq 0, j, i, k \in \{1, 2, 3, 4\}$ *and* $e_i(0)$ *are sufficiently small. If* $l_{41}(0) > 4\sqrt{\frac{V_2(0)}{\lambda_{\min}(P_2)}}\lambda_{\max}(P_2)$*, then no collision between agents 1 and 4 will occur for* $t > 0$*; if* $\sqrt{V_2(0)} < \sqrt{\lambda_{\min}(P_2)} * \min\{\pi - \alpha_{412}^*, \alpha_{412}^*\}$*, then no collinearity will happen among agents 1, 2, 4; if* $h_{4-123}(0) > \varepsilon_2$*, then agent 4 will never reach the plane formed by agents 1, 2, 3.*

The proof of Corollary 6.5 is straightforward using proof of contradiction. Now, we extend the results to the N-agent case by designing the following control law for agent $i, 4 \leqslant i \leqslant N$

$$\begin{aligned} u_i =&(\alpha_{ij_1j_2} - \alpha^*_{ij_1j_2})b_{ij_2} + (\alpha_{ij_2j_1} - \alpha^*_{ij_2j_1})b_{ij_1} \\ &+ (\alpha_{ij_2j_3} - \alpha^*_{ij_2j_3})b_{ij_3}. \end{aligned} \tag{6.43}$$

Theorem 6.6. *For the N-agent formation under the control law (6.5)-(6.7) and* (6.43)*, if $\sin\alpha_{jik}(0) \neq 0, j, i, k \in \{1, ..., N\}$, the initial angle errors $e_m(0), e_{im}, m = 1, 2, 3$ are sufficiently small, the initial distances $l_{ji}(0)$ are bounded away from zero and $p_i(0)$ is sufficiently away from the plane formed by $p_{j_1}(0), p_{j_2}(0), p_{j_3}(0), j_1, j_2, j_3 \in \mathcal{N}_i$, then the angle errors $e_{im}(t)$ converge exponentially to zero.*

The proof of Theorem 6.6 can be obtained by combining Theorems 6.2 and 6.3.

6.2.3 Formation control for the remaining agents by Type-II vertex addition

Now, we investigate how to add the remaining agents by Type-II vertex addition (case 1) developed in Definition 5.7. We design the following control law for agent 4

$$\begin{aligned} u_4 =& -(\alpha_{142} - \alpha^*_{142})(b_{41} + b_{42}) - (\alpha_{243} - \alpha^*_{243})(b_{42} + b_{43}) \\ &- (\alpha_{341} - \alpha^*_{341})(b_{43} + b_{41}), \end{aligned} \tag{6.44}$$

where $\alpha^*_{142} \in (0, \pi), \alpha^*_{243} \in (0, \pi), \alpha^*_{341} \in (0, \pi)$ are three desired angles that agent 4 aims at achieving with agents 1, 2, 3. The implementation of (6.44) only relies on agent 4's direction measurements $\overrightarrow{41}$, $\overrightarrow{42}$, and $\overrightarrow{43}$. To obtain the convergence of $\tilde{e}_{41} = \alpha_{142} - \alpha^*_{142}, \tilde{e}_{42} = \alpha_{243} - \alpha^*_{243}, \tilde{e}_{43} = \alpha_{341} - \alpha^*_{341}$, we first aim at obtaining the dynamics of $\tilde{e}_{41}, \tilde{e}_{42}, \tilde{e}_{43}$. Since the three components in (6.44) are similar, we first analyze the dynamics of $\alpha_{i4k}, i, k \in \{1, 2, 3\}$ by taking its time-derivative with respect to time

$$\begin{aligned} \dot{\alpha}_{i4k} =&N_{k4i}\dot{p}_i - (N_{i4k} + N_{k4i})\dot{p}_4 + N_{i4k}\dot{p}_k \\ =&N_{k4i}\dot{p}_i + N_{i4k}\dot{p}_k + (N_{i4k} + N_{k4i})[e_{4i}(b_{4i} + b_{4k}) \\ &+ e_{4k}(b_{4k} + b_{4m}) + e_{4m}(b_{4m} + b_{4i})] \\ =&N_{k4i}\dot{p}_i + N_{i4k}\dot{p}_k + e_{4i}(N_{i4k}b_{4i} + N_{k4i}b_{4k}) \\ &+ e_{4k}(N_{k4i}b_{4k} + N_{i4k}b_{4m} + N_{k4i}b_{4m}) \\ &+ e_{4m}(N_{i4k}b_{4m} + N_{k4i}b_{4m} + N_{i4k}b_{4i}), \end{aligned} \tag{6.45}$$

where $N_{kji} \in \mathbb{R}^{1\times 3}$ is defined in (5.2) and $m = \{1,2,3\}/\{i,k\}$. By defining $f_{ijk} = -N_{ijk}b_{ji} = \frac{\sin\alpha_{ijk}}{l_{jk}} > 0$ and using $i = 1, k = 2, m = 3$ in (6.45), one has

$$\begin{aligned}\dot{\tilde{e}}_{41} =& -N_{142}(b_{21}+b_{23})e_2 - N_{241}(b_{12}+b_{13})e_1\\ &-\tilde{e}_{41}(f_{142}+f_{241})\\ &+\tilde{e}_{42}(-f_{241}+N_{142}b_{43}+N_{241}b_{43})\\ &+\tilde{e}_{43}(-f_{142}+N_{241}b_{43}+N_{142}b_{43}).\end{aligned} \tag{6.46}$$

Following the similar steps for $\tilde{e}_{42}$ and $\tilde{e}_{43}$, one has the overall angle error dynamics

$$\begin{aligned}\dot{\tilde{e}}_4 &= \begin{bmatrix}\dot{\tilde{e}}_{41} & \dot{\tilde{e}}_{42} & \dot{\tilde{e}}_{43}\end{bmatrix} = \tilde{F}_4(e_s,\tilde{e}_4)\tilde{e}_4 + \tilde{G}_4(e_s,\tilde{e}_4)e_s\\ &= \begin{bmatrix}-f_{142}-f_{241} & -f_{241}+h_{(142,3)} & -f_{142}+h_{(142,3)}\\ -f_{243}+h_{(243,1)} & -f_{243}-f_{342} & -f_{342}+h_{(243,1)}\\ -f_{143}+h_{(143,2)} & -f_{341}+h_{(143,2)} & -f_{341}-f_{143}\end{bmatrix}\begin{bmatrix}\tilde{e}_{41}\\ \tilde{e}_{42}\\ \tilde{e}_{43}\end{bmatrix}\\ &+ \begin{bmatrix}\tilde{G}_{11} & \tilde{G}_{12}\\ \tilde{G}_{22} & \tilde{G}_{22}\\ \tilde{G}_{31} & \tilde{G}_{32}\end{bmatrix}\begin{bmatrix}e_1\\ e_2\end{bmatrix},\end{aligned} \tag{6.47}$$

where $h_{(ijk,m)} = (N_{ijk}+N_{kji})b_{jm}$, and $\tilde{G}_{11} = -N_{241}(b_{12}+b_{13})$, $\tilde{G}_{22} = -N_{142}(b_{21}+b_{23})$, $\tilde{G}_{21} = -N_{342}(b_{21}+b_{23})$, $\tilde{G}_{22} = -[N_{243}(b_{31}+b_{32}) + N_{342}(b_{21}+b_{23})]$, $\tilde{G}_{31} = -N_{341}(b_{31}+b_{32}) - N_{143}(b_{31}+b_{32})$, $\tilde{G}_{32} = -N_{143}(b_{31}+b_{32})$. Now, we present the convergence result.

Theorem 6.7. *For the four-agent formation under the control law (6.5)-(6.7) and* (6.44)*, if*

$$0 < h^*_{(i4k,j)} < 2\min\{f^*_{k4i}, f^*_{i4k}\}, \tag{6.48}$$

$i,j,k \in \{1,2,3\}, i \neq j \neq k$, $\sin\alpha_{j4k}(0) \neq 0$*, the initial angle errors* $\tilde{e}_{4i}(0)$ *are sufficiently small, the initial distances* $l_{4i}(0)$ *are bounded away from zero and* $p_4(0)$ *is sufficiently away from the plane formed by* $p_1(0), p_2(0), p_3(0)$*, then the angle errors* $\tilde{e}_4(t)$ *converge exponentially to zero.*

Proof. Linearizing (6.47) around $\{e_s = 0, e_4 = 0\}$ by following (6.17), one has the linearized dynamics

$$\dot{\tilde{e}}_4 = \tilde{A}_4\tilde{e}_4 + \tilde{B}_4 e_s, \tag{6.49}$$

where $\tilde{A}_4 = \tilde{F}_4(e_s,\tilde{e}_4)|_{e_s=0,\tilde{e}_4=0}$, $B_4 = G_4(e_s,e_4)|_{e_s=0,e_4=0}$ are constant matrices. Now, we check whether $\tilde{A}_4$ is Hurwitz. To obtain the stability of the linearized system (6.49), we aim at proving that $\tilde{A}_4$ is Hurwitz. By using the Gershgorin circle theorem [46, Theorem 6.1.1], one has that the three eigenvalues of matrix $\tilde{A}_4$ must

lie within the union of the following three Gershgorin discs

$$|\lambda + f^*_{142} + f^*_{241}| \leqslant | - f^*_{241} + h^*_{(142,3)}| + | - f^*_{142} + h^*_{(142,3)}|, \tag{6.50}$$
$$|\lambda + f^*_{243} + f^*_{342}| \leqslant | - f^*_{243} + h^*_{(243,1)}| + | - f^*_{342} + h^*_{(243,1)}|, \tag{6.51}$$
$$|\lambda + f^*_{341} + f^*_{143}| \leqslant | - f^*_{143} + h^*_{(143,2)}| + | - f^*_{341} + h^*_{(143,2)}|. \tag{6.52}$$

where $\lambda \in \mathbb{C}$ denotes the eigenvalue of $\tilde{A}_4$. Note that $f^*_{i4k} > 0$ for all $i, k = 1, 2, 3$. Therefore, by using (6.48), one has

$$0 < | - f^*_{241} + h^*_{(142,3)}| + | - f^*_{142} + h^*_{(142,3)}| < f^*_{142} + f^*_{241}, \tag{6.53}$$
$$0 < | - f^*_{241} + h^*_{(142,3)}| + | - f^*_{142} + h^*_{(142,3)}| < f^*_{243} + f^*_{342}, \tag{6.54}$$
$$0 < | - f^*_{143} + h^*_{(143,2)}| + | - f^*_{341} + h^*_{(143,2)}| < f^*_{341} + f^*_{143}. \tag{6.55}$$

By combining (6.50)-(6.52) with (6.53)-(6.55), one has that the union of the three Gershgorin discs in (6.50)-(6.52) always lies in the left half of the complex plane, which implies that the three eigenvalues of $\tilde{A}_4$ have negative real parts. Therefore, (6.48) is a sufficient condition to guarantee that matrix $\tilde{A}_4$ is Hurwitz which implies the exponential convergence of $\tilde{e}_4$ by following (6.33)-(6.36). □

Also, by following (6.37)-(6.42), one can precisely describe the requirements on $l_{ji}(0)$, $\tilde{e}_{4i}(0)$ and the initial distance $h_{4-123}(0)$ in this case. Similarly, we can extend the results to N-agent case by designing the following control law for agent $i, 4 \leqslant i \leqslant N$

$$\begin{aligned} u_i = &- (\alpha_{j_1ij_2} - \alpha^*_{j_1ij_2})(b_{ij_1} + b_{ij_2}) \\ &- (\alpha_{j_2ij_3} - \alpha^*_{j_2ij_3})(b_{ij_2} + b_{ij_3}) \\ &- (\alpha_{j_3ij_1} - \alpha^*_{j_3ij_1})(b_{ij_3} + b_{ij_1}), \end{aligned} \tag{6.56}$$

where $\alpha^*_{j_1ij_2} \in (0, \pi), \alpha^*_{j_2ij_3} \in (0, \pi), \alpha^*_{j_3ij_1} \in (0, \pi)$. Then, the result similar to Theorem 6.6 can also be obtained.

Remark 6.8. It can be checked that to implement the proposed formation control laws in Section IV, each agent is allowed to have its own local coordinate frame [22]. In subsections IV. B and C, two types of formation control algorithm are designed for the remaining agents from 4 to N by following the Type-I and Type-II vertex addition operations developed in 3D angle rigidity theory, respectively. Note that the control law (6.56) can be implemented by only using the local measured bearing information, while the control law (6.43) needs additional communication. However, (6.43) can be used to stabilize an arbitrary tetrahedron formation, and (6.56) can stabilize tetrahedron formation satisfying (6.48).

Remark 6.9. Although the presentation structure of this 3D case is similar to the 2D case [22], the employed methodologies are different due to the different performing

forms of angles as shown in Fig. 5.3. In the 3-D angle rigidity part, we develop Type-I and Type-II vertex additions, which are more challenging than 2-D case since each angle constraint is unsigned and shows a complicated surface. Also, the merging operation towards two angle rigid angularities is investigated.

6.3 Convex polyhedral formations

In this section, we assume that the angle constraints are only in the faces of a convex polyhedral formation. According to Theorem 5.19, a convex polyhedron with all faces being triangles is angle rigid. In the following, we first show how to stabilize a convex polyhedral formation with 4 triangular faces and 12 angle constraints. Then, we show how to extend it to more general cases. Assume that

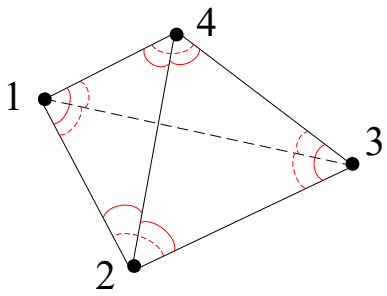

Figure 6.1: *Convex polyhedral formation with 12 face angle constraints*

four agents are governed by single-integrator dynamics (6.1). The aim is to design $u_i, i = 1, 2, 3, 4$, such that those 12 desired angles in the four triangular faces of the tetrahedron formation can be achieved. Towards this end, the control laws are designed as

$$\begin{aligned} u_1 &= -e_{312}b_{12} - e_{214}b_{14} - e_{413}b_{13} \\ u_2 &= -e_{321}b_{21} - e_{423}b_{23} - e_{124}b_{24} \\ u_3 &= -e_{231}b_{31} - e_{432}b_{32} - e_{134}b_{34} \\ u_4 &= -e_{341}b_{41} - e_{243}b_{43} - e_{142}b_{42} \end{aligned} \tag{6.57}$$

where $e_{ijk} = \alpha_{ijk} - \alpha^*_{ijk}$, and $i \neq j \neq k$, $i, j, k \in \{1, 2, 3, 4\}$, and $\alpha^*_{ijk} \in (0, \pi)$ is the desired angle between $\overrightarrow{ji}$ and $\overrightarrow{jk}$,. Following the calculations and analysis in

Section 6.2, one has the angle error dynamics

$$\begin{aligned}\dot{e}_{ijk} =&N_{ijk}(\dot{p}_k - \dot{p}_j) + N_{kji}(\dot{p}_i - \dot{p}_j)\\ =&N_{ijk}(-e_{ikm}b_{km} - e_{jki}b_{ki} + e_{ijm}b_{jm} + e_{kji}b_{ji})\\ &+ N_{kji}(-e_{jik}b_{ik} - e_{kim}b_{im} + e_{ijm}b_{jm} + e_{mjk}b_{jk})\end{aligned} \tag{6.58}$$

where N_{ijk} is defined in (5.2), and $m = \{1,2,3,4\}/\{i,j,k\}$. For example, when $i = 4, j = 2, k = 3$, (6.58) becomes

$$\begin{aligned}\dot{e}_{423} =&N_{423}(-e_{431}b_{31} - e_{234}b_{34} + e_{421}b_{21} + e_{324}b_{24})\\ &+ N_{324}(-e_{243}b_{43} - e_{341}b_{41} + e_{421}b_{21} + e_{123}b_{23})\end{aligned} \tag{6.59}$$

where $N_{423}b_{24} = -\frac{\sin\alpha_{423}}{l_{23}}$, $N_{423}b_{34} = -\frac{\sin\alpha_{234}}{l_{23}}$ and $N_{324}b_{43} = -\frac{\sin\alpha_{342}}{l_{24}}$. By specifying all possible i, j, k and using (6.58), one will have the error dynamics of the 12 face angles. However, the three angles in each face of the tetrahedron is linearly dependent, e.g., $e_{123} + e_{231} + e_{312} = 0$. Therefore, we choose in each face two interior angles to form the state variable $e_s = [e_{123}, e_{231}, e_{234}, e_{243}, e_{214}, e_{241}, e_{341}, e_{314}]^T$ and take $\mathcal{A}_1 = \{(1,2,3),(2,3,1),(2,3,4),(2,4,3),(2,1,4),(2,4,1),(3,4,1),(3,1,4)\}$. Then, one has the closed-loop angle error dynamics

$$\dot{e}_s = A(e_s)e_s \tag{6.60}$$

Following the linearization steps in Section 6.2, (6.60) can be linearized as $\dot{e}_s = A_s^* e_s$ where $A_s^* = A(e_s)|_{e_s=0}$. Then, one has the result.

Theorem 6.10. *For the four-agent convex polyhedral formation under the control (6.57), if*

$$\begin{aligned}\frac{\sin\alpha_{ijk}^* + \sin\alpha_{jki}^*}{l_{jk}^*} >&|\frac{\sin\alpha_{kij}^*}{l_{ji}^*} - \frac{\sin\alpha_{jki}}{l_{jk}^*}| + |N_{ijk}^* b_{km}^*| + |N_{ijk}^* b_{jm}^*|\\ &+ |N_{kji}^* b_{im}^*| + |N_{kji}^* b_{jm}^*| + |N_{kji}^* b_{jk}^*|,\end{aligned} \tag{6.61}$$

where $(i,j,k) \in \mathcal{A}_1$, $m = \{1,2,3,4\}/\{i,j,k\}$, $\sin\alpha_{ijk}(0) \neq 0$, *the initial angle errors* $e_{ijk}(0)$ *are sufficiently small, and the initial distances* $l_{ij}(0)$ *are bounded away from zero, then the angle errors* $e_{ijk}(t)$ *converge exponentially to zero.*

Proof. To check the local stability of (6.60), one needs to analyze the eigenvalue distribution of matrix $A_s^* \in \mathbb{R}^{8\times 8}$. Using Gershgorin circle theorem [46, Theorem 6.1.1], for each row of A_s^*, if the sum of the absolute values of the off-diagonal entries is less than the absolute value of the negative diagonal entry, all the eigenvalues of the matrix lie in left half-plane. Now, take the angle dynamics (6.62) as an example. Because $e_{423} + e_{234} + e_{243} = 0$, the linearized dynamics of (6.62) can

be written as

$$\begin{aligned}\dot{e}_{423} =& -(\frac{\sin\alpha^*_{423}}{l^*_{23}}+\frac{\sin\alpha^*_{234}}{l^*_{23}})e_{423}+(\frac{\sin\alpha^*_{342}}{l^*_{24}}-\frac{\sin\alpha^*_{234}}{l^*_{23}})e_{243}\\ &-N^*_{423}b^*_{31}e_{431}+N^*_{423}b^*_{21}e_{421}\\ &-N^*_{324}b^*_{41}e_{341}+N^*_{324}b^*_{21}e_{421}+N^*_{324}b^*_{23}e_{123}\end{aligned} \tag{6.62}$$

Therefore, one requires

$$\begin{aligned}\frac{\sin\alpha^*_{423}}{l^*_{23}}+\frac{\sin\alpha^*_{234}}{l^*_{23}} >& |\frac{\sin\alpha^*_{342}}{l^*_{24}}-\frac{\sin\alpha^*_{234}}{l^*_{23}}|+|N^*_{423}b^*_{31}|+|N^*_{423}b^*_{21}|\\ &+|N^*_{324}b^*_{41}|+|N^*_{324}b^*_{21}|+|N^*_{324}b^*_{23}|\end{aligned} \tag{6.63}$$

which is one case of condition (6.61). For the other 5 angles, using the same analysis steps, one obtains the similar condition as described in (6.61). Therefore, if the condition (6.61) holds for all the six angles defined in $\mathcal{A}_1$, one has that A^*_s is Hurwitz. Following similar analysis steps in Section 6.2, one has the local stability of (6.60). □

For an N-agent convex polyhedral formation, the control law for agent $i \leqslant N$ can be designed as

$$u_i = -\sum\nolimits_{(j,i,k)\in\mathcal{A}} e_{jik}b_{ik} \tag{6.64}$$

where $\mathcal{A}$ is the angle set containing all the angles from the triangular faces of the convex polyhedral formation. Using similar steps as (6.58)-(6.63), a stability condition can be obtained to guarantee the local stability of the convex polyhedral formation with triangular faces.

6.4 Simulation

In this section, we use numerical examples with 4 agents to validate the effectiveness of the proposed formation control algorithms. The desired angles among agents are calculated using the embedding $[p_1, p_2, p_3, p_4]$ given in Theorem 5.2. We initialize all agents' positions around the embedding:

$$\begin{aligned}&p_1(0) = [0.2, -0.3, -0.1]^T, p_2(0) = [0.3, 2.7, 0.1]^T,\\ &p_3(0) = [4.2, 4.9, -0.2]^T, p_4(0) = [2.3, 4.1, 2.2]^T.\end{aligned}$$

When agent 4 is governed by (6.25), i.e., Type-I vertex addition, Fig. 6.2 gives the formation trajectories and the evolution of angle errors. When agent 4 is governed by (6.44), i.e., Type-II vertex addition, Fig. 6.3 gives the formation trajectories and the evolution of angle errors.

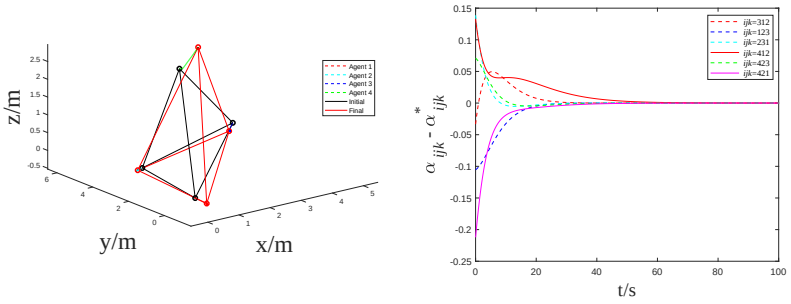

Figure 6.2: *Formation trajectories and angle errors under* (6.25)

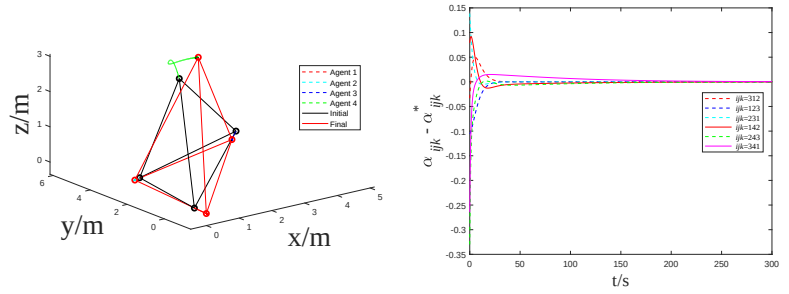

Figure 6.3: *Formation trajectories and angle errors under* (6.44)

According to Figs. 6.2 and 6.3, agent 4 under the control of (6.25) moves more directly to the desired position than the control of (6.44). The convergence speed of angle errors under (6.25) is faster than (6.44). This illustrates the better performance of (6.25) which owes to the availability of communication from agents 1, 2 to agent 4. Next, we simulate the case when agent 4 is controlled by (6.44) but its initial position is close to the ambiguity position, i.e., $p_4(0) = [0.08, 4.07, 1.47]^T$.

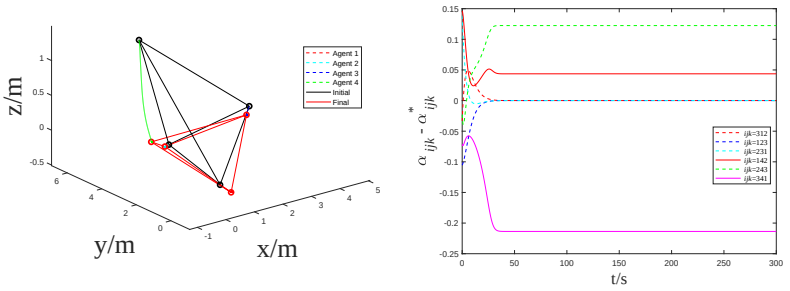

Figure 6.4: *Formation trajectories and angle errors under* (6.44) *when initial states are closed to the ambiguity formation*

According to Fig. 6.4, agent 4 finally converges to an undesired position in the plane formed by $p_1(0), p_2(0), p_3(0)$, and the angle errors do not converge to zero but nonzero constants finally. This illustrates that the formation under the control of (6.44) is unstable when its initial formation is close to the ambiguity formation.

When the four agents are governed by (6.57), Figure 6.5 shows the formation trajectories of the four agents and the evolution of angle errors which imply that the desired polyhedral formation is achieved. Note that in this case, the agents 1, 2 and 3 are no longer coplanar at all the time.

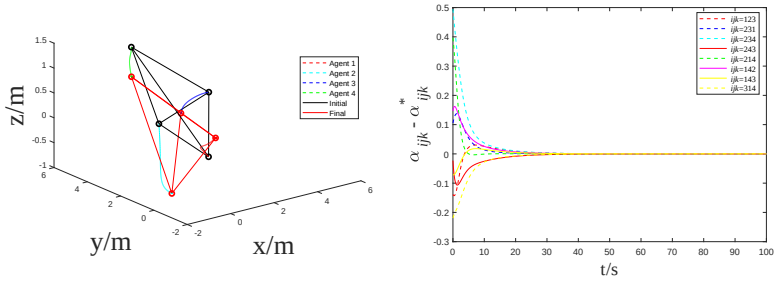

Figure 6.5: *Formation trajectories and angle errors under control law* (6.57)

6.5 Concluding remarks

In this chapter, using the developed angle rigidity theory in 3D, we have investigated how to stabilize a multi-agent formation in 3D. First, using the two types of construction approaches, multi-agent formations from sequential operations have been achieved. Then, using angle constraints only in the faces of a convex polyhedron, multi-agent polyhedral formations can also be stabilized.

Chapter 7

Conclusions and future work

This chapter summarizes the main results of this thesis and indicates the possible future research directions.

7.1 Conclusions

This thesis has proposed angle rigidity graph theory in both 2D and 3D which has been used to achieve multi-agent formations using only angle measurements. We have defined a new multi-point framework, i.e., angularity, to describe the angle constraints. We have shown the non-equivalence between global angle rigidity and angle rigidity. Then we have developed the construction methods to obtain a globally angle rigid angularity and angle rigid angularity, respectively. To check whether a given angularity is angle rigid, we have also defined infinitesimal angle rigidity. Using the developed angle rigidity theory, we have proposed angle-only formation control algorithms to stabilize and maneuver a group of vehicles with desired shape in collective motion, respectively. Now, we provide specific conclusions for each technical chapter.

Chapter 2 has developed the notion of angle rigidity for a multi-point framework, named angularity, consisting of a set of nodes embedded in a Euclidean space and a set of angle constraints among them. Different from bearings or angles defined in a global coordinate frame, the angles we use do not rely on the knowledge of a global coordinate frame and are with the positive sign in the counterclockwise direction. We have demonstrated that this angle rigidity property, in sharp comparison to bearing rigidity or other reported rigidity related to angles of frameworks in the literature, is not a global property since an angle rigid angularity may allow flex ambiguity. We then have defined two types of vertex addition operations to construct an angle rigid or globally angle rigid angularities. Further, we have provided necessary and sufficient conditions for infinitesimal angle rigidity by checking the rank of an angularity's rigidity matrix. A combinatorial necessary condition has also been developed for infinitesimal minimal angle rigidity.

Using the developed angle rigidity theory in Chapter 2, Chapter 3 has demonstrated how to stabilize a multi-agent planar formation using only angle measurements, which can be realized in each agent's local coordinate frame. The desired

angle rigid formation is constructed through the Type-I vertex addition operation developed in Chapter 2. By following this vertex addition operation, we have first designed the triangular formation control algorithm for the first three agents. Then, we have proposed the formation control algorithm for the remaining agents to add them into the existing formation step by step. The exponential convergence rate of angle errors and collision-free property between specified agents have also been proved. We have investigated the multi-agent formations with the single-integrator and double-integrator dynamics, respectively.

Chapter 4 has realized how to maneuver a planar formation of mobile agents using designed mismatched angles. The desired formation shape is still constructed through the Type-I vertex addition operation and is specified by a set of interior angle constraints. To realize the maneuver of translation, rotation and scaling of the formation with single-integrator dynamics, we have intentionally forced the agents to maintain mismatched desired angles by introducing a pair of mismatch parameters for each angle constraint. To allow different information requirements in the design and implementation stages, we have considered both measurement-dependent and measurement-independent mismatches. Starting from a triangular formation, we have considered generically angle rigid formations that can be constructed from the triangular formation by adding new agents in sequence, each having two angle constraints associated with some existing three agents. The control law for each newly added agent arises naturally from the angle constraints and makes full use of the angle mismatch parameters. We have also shown that the control can effectively stabilize the formations while simultaneously realizing maneuvering. When the formation is governed by double-integrator dynamics, we have also achieved the formation maneuvering. Simulations have been conducted to validate the theoretical results.

Chapter 5 has discussed angle rigidity for an angularity in 3D. The angles have been defined using interior angles of triangles, which are independent from coordinate frames and can be measured by using monocular cameras. We have shown that the resulting angle rigidity is not a global property in comparison to the case of 3D bearing rigidity. We have demonstrated that such angle rigid frameworks can be constructed through adding repeatedly new points to the original small angle rigid framework if one chooses angle constraints carefully. Based on the classic distance rigidity results on convex polyhedra, we have also studied the angle rigidity of convex polyhedral angularity. Finally, we have defined the angle rigidity matrix of an angularity in 3D.

In Chapter 6, by using the developed 3D angle rigidity theory in Chapter 5, formation stabilization algorithms have been designed for a team of vehicles in 3D to achieve an angle rigid formation, in which only local angle measurements are needed. Different from the formation stabilization in 2D, we have proposed a formation controller with a simpler structure, in which both Type-I and Type-II

vertex addition operations have been employed to add the new agents, respectively. Also, convex polyhedral formations have been achieved using the proposed control law.

7.2 Future work

In this thesis we have proposed the angle rigidity graph theory and applied it to achieve multi-agent formations. Several directions are of interest to be considered in future research. In this section, we identify some future topics.

• Global angle rigidity: This thesis has proposed the sufficient conditions for global angle rigidity, but they are not necessary. The necessary and sufficient conditions for global distance rigidity have been studied for decades, and the conditions for global distance rigidity in 3D or higher dimensions are still unknown. A first future step in this direction can be to study the necessary and sufficient conditions for 2D global angle rigidity.

• Infinitesimal rigidity: This thesis has proposed the necessary condition for minimal and infinitesimal angle rigidity, but it is not sufficient. A well-known necessary and sufficient condition was developed by Laman for minimal and infinitesimal distance rigidity. Therefore, future study can concentrate on the necessary and sufficient conditions for minimal and infinitesimal angle rigidity.

• Formation maneuvering in 3D: The formation stabilization task has been achieved in 3D by using only angle measurements. However, the formation maneuvering has not been investigated yet, which will be useful to maneuver a team of drones or satellites.

• Angle-only formation control with more complicated dynamics and noisy measurements: Only single-integrator and double-integrator dynamics have been considered in this thesis, and the more complicated dynamics have not been considered. One may want to consider as a starter in this line of research the unicycle model and nonlinear Euler-Lagrange dynamics. Also, the measurements of angles are assumed to be noiseless in this thesis, and future work may take the measurement noise into consideration.

• The other related applications: Besides multi-agent formations, there are also other application scenarios which can benefit from the developed angle rigidity theory in this thesis, e.g., flocking, circumnavigation and vehicle platooning.

Bibliography

[1] https://www.whoi.edu/news-insights/content/underwater-robots-swarm-the-ocean/.

[2] Ahmad Afzal, Walter Viktor, Petracek Pavel, Petrlik Matej, Baca Tomas, Zaitlik David, and Martin Saska. Autonomous aerial swarm in a complex environment without gnss and without communication. https://www.youtube.com/watch?v=HH78AheC-DMt=4s.

[3] Hyo-Sung Ahn. *Formation Control: Approaches for Distributed Agents*, volume 205. Springer, 2019.

[4] Martin Aigner and Günter M Ziegler. Cauchy's rigidity theorem. In *Proofs from THE BOOK*, pages 71–74. Springer, 2004.

[5] Aleksandr Danilovich Aleksandrov. *Konvexe Polyeder:(originalens tit.: Vypuklye mnogogranniki)*, volume 8. Akademie-Verlag, 1958.

[6] Alexandr D Alexandrov. *Convex polyhedra*. Springer Science & Business Media, 2005.

[7] Brian DO Anderson, Changbin Yu, Baris Fidan, and Julien M Hendrickx. Rigid graph control architectures for autonomous formations. *IEEE Control Systems Magazine*, 28(6):48–63, 2008.

[8] Brian DO Anderson, Zhiyong Sun, Toshiharu Sugie, Shun-ichi Azuma, and Kazunori Sakurama. Formation shape control with distance and area constraints. *IFAC Journal of Systems and Control*, 1:2–12, 2017.

[9] Leonard Asimow and Ben Roth. The rigidity of graphs. *Transactions of the American Mathematical Society*, 245:279–289, 1978.

[10] Leonard Asimow and Ben Roth. The rigidity of graphs, II. *Journal of Mathematical Analysis and Applications*, 68(1):171–190, 1979.

[11] Meysam Basiri, Adrian N Bishop, and Patric Jensfelt. Distributed control of triangular formations with angle-only constraints. *Systems and Control Letters*, 59(2):147–154, 2010.

[12] Randal W Beard, Jonathan Lawton, and Fred Y Hadaegh. A coordination architecture for spacecraft formation control. *IEEE Transactions on Control Systems Technology*, 9(6):777–790, 2001.

[13] Dennis S Bernstein. *Matrix mathematics: theory, facts, and formulas*. Princeton university press, 2009.

[14] Adrian N Bishop, Iman Shames, and Brian DO Anderson. Stabilization of rigid formations with direction-only constraints. In *2011 50th IEEE Conference on Decision and Control and European Control Conference*, pages 746–752. IEEE, 2011.

[15] Adrian N Bishop, Mohammad Deghat, Brian Anderson, and Yiguang Hong. Distributed formation control with relaxed motion requirements. *International Journal of Robust and Nonlinear Control*, 25(17):3210–3230, 2015.

[16] Ming Cao, A Stephen Morse, C Yu, Brian DO Anderson, and S Dasguvta. Controlling a triangular formation of mobile autonomous agents. In *2007 46th IEEE Conference on Decision and Control*, pages 3603–3608. IEEE, 2007.

[17] Ming Cao, Changbin Yu, and Brian DO Anderson. Formation control using range-only measurements. *Automatica*, 47(4):776–781, 2011.

[18] A Cauchy. Deuxieme memoire sur les polygones et les polydres. *Journal de l'École Polytechnique*, 1813, 1813.

[19] Nelson PK Chan, Bayu Jayawardhana, and Jacquelien MA Scherpen. Distributed formation with diffusive obstacle avoidance control in coordinated mobile robots. In *2018 IEEE Conference on Decision and Control (CDC)*, pages 4571–4576. IEEE, 2018.

[20] Nelson PK Chan, Bayu Jayawardhana, and Hector Garcia de Marina. Angle-constrained formation control for circular mobile robots. *arXiv preprint arXiv:2005.04694*, 2020.

[21] Liangming Chen, Ming Cao, Hector Garcia de Marina, Yanning Guo, and Yuri Kapitanyuk. Triangular formation maneuver using designed mismatched angles. In *2019 18th European Control Conference (ECC)*, pages 1544–1549. IEEE, 2019.

[22] Liangming Chen, Ming Cao, and Chuanjiang Li. Angle rigidity and its usage to stabilize multi-agent formations in 2D. *IEEE Transactions on Automatic Control*, 2020.

[23] R Connelly and SD Guest. Frameworks, tensegrities and symmetry: understanding stable structures. *Cornell University, College of Arts and Sciences*, 2015.

[24] Robert Connelly. The rigidity of certain cabled frameworks and the second-order rigidity of arbitrarily triangulated convex surfaces. *Advances in Mathematics*, 37(3):272–299, 1980.

[25] Robert Connelly. Rigidity and energy. *Inventiones mathematicae*, 66(1): 11–33, 1982.

[26] Robert Connelly. On generic global rigidity, applied geometry and discrete mathematics, 147–155. *DIMACS Ser. Discrete Math. Theoret. Comput. Sci*, 4, 1991.

[27] Robert Connelly. Rigidity. In *Handbook of convex geometry*, pages 223–271. Elsevier, 1993.

[28] Robert Connelly. Generic global rigidity. *Discrete & Computational Geometry*, 33(4):549–563, 2005.

[29] Samuel Coogan and Murat Arcak. Scaling the size of a formation using relative position feedback. *Automatica*, 48(10):2677–2685, 2012.

[30] Aveek K Das, Rafael Fierro, Vijay Kumar, James P Ostrowski, John Spletzer, and Camillo J Taylor. A vision-based formation control framework. *IEEE Transactions on Robotics and Automation*, 18(5):813–825, 2002.

[31] Hector Garcia De Marina, Ming Cao, and Bayu Jayawardhana. Controlling rigid formations of mobile agents under inconsistent measurements. *IEEE Transactions on Robotics*, 31(1):31–39, 2014.

[32] Hector Jesús Garcia de Marina Peinado. *Distributed formation control for autonomous robots*. PhD thesis, University of Groningen Groningen, 2016.

[33] Mohammad Deghat, Iman Shames, Brian DO Anderson, and Changbin Yu. Localization and circumnavigation of a slowly moving target using bearing measurements. *IEEE Transactions on Automatic Control*, 59(8):2182–2188, 2014.

[34] Max Dehn. Über die starrheit konvexer polyeder. *Mathematische Annalen*, 77(4):466–473, 1916.

[35] Xiwang Dong, Bocheng Yu, Zongying Shi, and Yisheng Zhong. Time-varying formation control for unmanned aerial vehicles: Theories and applications. *IEEE Transactions on Control Systems Technology*, 23(1):340–348, 2015.

[36] Tolga Eren. Formation shape control based on bearing rigidity. *International Journal of Control*, 85(9):1361–1379, 2012.

[37] Tolga Eren, Walter Whiteley, A Stephen Morse, Peter N Belhumeur, and Brian DO Anderson. Sensor and network topologies of formations with direction, bearing, and angle information between agents. In *2003 42nd IEEE Conference on Decision and Control*, volume 3, pages 3064–3069, 2003.

[38] L. Euler. Opera postuma. *Euler Archive index number E819*, 1:494–496, 1862.

[39] Antonio Franchi and Paolo Robuffo Giordano. Decentralized control of parallel rigid formations with direction constraints and bearing measurements. In *2012 IEEE 51st IEEE Conference on Decision and Control (CDC)*, pages 5310–5317. IEEE, 2012.

[40] Herman Gluck. Almost all simply connected closed surfaces are rigid. In *Geometric topology*, pages 225–239. Springer, 1975.

[41] Tingrui Han, Zhiyun Lin, Ronghao Zheng, and Minyue Fu. A barycentric coordinate-based approach to formation control under directed and switching sensing graphs. *IEEE Transactions on Cybernetics*, 48(4):1202–1215, 2018.

[42] Zhimin Han, Lili Wang, Zhiyun Lin, and Ronghao Zheng. Formation control with size scaling via a complex Laplacian-based approach. *IEEE Transactions on Cybernetics*, 46(10):2348–2359, 2016.

[43] Bruce Hendrickson. Conditions for unique graph realizations. *SIAM Journal on Computing*, 21(1):65–84, 1992.

[44] L. Henneberg. *Die graphische Statik der starren Systeme*. Leipzig: Teubner, 1911.

[45] Lebrecht Henneberg. *Die graphische Statik der starren Systeme*, volume 31. BG Teubner, 1911.

[46] Roger A Horn and Charles R Johnson. *Matrix analysis*. Cambridge university press, 2012.

[47] https:// mms. gsfc.nasa.gov/.

[48] Youfang Huang, Wen Liu, Bo Li, Yongsheng Yang, and Bing Xiao. Finite-time formation tracking control with collision avoidance for quadrotor uavs. *Journal of the Franklin Institute*, 2020.

[49] Benoît Ildefonse, Dimitrios Sokoutis, and Neil S Mancktelow. Mechanical interactions between rigid particles in a deforming ductile matrix. analogue experiments in simple shear flow. *Journal of Structural Geology*, 14(10): 1253–1266, 1992.

[50] Bill Jackson and Tibor Jordán. Connected rigidity matroids and unique realizations of graphs. *Journal of Combinatorial Theory, Series B*, 94(1):1–29, 2005.

[51] James S Jennings, Greg Whelan, and William F Evans. Cooperative search and rescue with a team of mobile robots. In *1997 8th International Conference on Advanced Robotics. Proceedings. ICAR'97*, pages 193–200. IEEE, 1997.

[52] Gangshan Jing, Guofeng Zhang, Heung Wing Joseph Lee, and Long Wang. Angle-based shape determination theory of planar graphs with application to formation stabilization. *Automatica*, 105:117–129, 2019.

[53] Vikram Kapila, Andrew G Sparks, James M Buffington, and Qiguo Yan. Spacecraft formation flying: Dynamics and control. *Journal of Guidance, Control, and Dynamics*, 23(3):561–564, 2000.

[54] Hassan K Khalil. *Nonlinear systems*, volume 3. Prentice hall Upper Saddle River, NJ, 2002.

[55] Laura Krick, Mireille E Broucke, and Bruce A Francis. Stabilisation of infinitesimally rigid formations of multi-robot networks. *International Journal of control*, 82(3):423–439, 2009.

[56] Seong-Ho Kwon, Minh Hoang Trinh, Koog-Hwan Oh, Shiyu Zhao, and Hyo-Sung Ahn. Infinitesimal weak rigidity, formation control of three agents, and extension to 3-dimensional space. *arXiv preprint arXiv:1803.09545*, 2018.

[57] Seong-Ho Kwon, Minh Hoang Trinh, Koog-Hwan Oh, Shiyu Zhao, and Hyo-Sung Ahn. Infinitesimal Weak rigidity and stability analysis on three-agent formations. In *2018 57th Annual Conference of the Society of Instrument and Control Engineers of Japan (SICE)*, pages 266–271. IEEE, 2018.

[58] Gerard Laman. On graphs and rigidity of plane skeletal structures. *Journal of Engineering mathematics*, 4(4):331–340, 1970.

[59] Byung-Hun Lee and Hyo-Sung Ahn. Distributed formation control via global orientation estimation. *Automatica*, 73:125–129, 2016.

[60] M Anthony Lewis and Kar-Han Tan. High precision formation control of mobile robots using virtual structures. *Autonomous robots*, 4(4):387–403, 1997.

[61] Xiuxian Li and Lihua Xie. Dynamic formation control over directed networks using graphical laplacian approach. *IEEE Transactions on Automatic Control*, 63(11):3761–3774, 2018.

[62] Heinrich Liebmann. Über die verbiegung der geschlossenen flächen positiver krümmung. *Mathematische Annalen*, 53(1-2):81–112, 1900.

[63] Zhiyun Lin, Bruce Francis, and Manfredi Maggiore. Necessary and sufficient graphical conditions for formation control of unicycles. *IEEE Transactions on Automatic Control*, 50(1):121–127, 2005.

[64] Zhiyun Lin, Wei Ding, Gangfeng Yan, Changbin Yu, and Alessandro Giua. Leader–follower formation via complex laplacian. *Automatica*, 49(6):1900–1906, 2013.

[65] Xiaoyuan Luo, Xianluo Li, Xiaolei Li, and Xinping Guan. Bearing-only formation control of multi-agent systems in local reference frames. *International Journal of Control*, pages 1–12, 2019.

[66] Morris Marden. *Geometry of polynomials*. Number 3. American Mathematical Soc., 1949.

[67] George Mayer and Mehmet Sarikaya. Rigid biological composite materials: structural examples for biomimetic design. *Experimental Mechanics*, 42(4): 395–403, 2002.

[68] Giulia Michieletto, Angelo Cenedese, and Antonio Franchi. Bearing rigidity theory in SE (3). In *2016 55th IEEE Conference on Decision and Control*, pages 5950–5955. IEEE, 2016.

[69] Pablo Millán, Luis Orihuela, Isabel Jurado, and Francisco Rodriguez Rubio. Formation control of autonomous underwater vehicles subject to communication delays. *IEEE Transactions on Control Systems Technology*, 22(2): 770–777, 2014.

[70] Alexandros Nikou, Christos K Verginis, and Dimos V Dimarogonas. Robust distance-based formation control of multiple rigid bodies with orientation alignment. *IFAC-PapersOnLine*, 50(1):15458–15463, 2017.

[71] Kwang-Kyo Oh, Myoung-Chul Park, and Hyo-Sung Ahn. A survey of multi-agent formation control. *Automatica*, 53:424–440, 2015.

[72] Reza Olfati-Saber and Richard M Murray. Graph rigidity and distributed formation stabilization of multi-vehicle systems. In *Proceedings of the 41st IEEE Conference on Decision and Control, 2002.*, volume 3, pages 2965–2971. IEEE, 2002.

[73] Myoung-Chul Park, Hong-Kyong Kim, and Hyo-Sung Ahn. Rigidity of distance-based formations with additional subtended-angle constraints. In *2017 17th International Conference on Control, Automation and Systems (ICCAS)*, pages 111–116. IEEE, 2017.

[74] W. Ren and N. Sorensen. Distributed coordination architecture for multi-robot formation control. *Robotics and Autonomous Systems*, 56(4):324–333, 2008.

[75] Wei Ren. Multi-vehicle consensus with a time-varying reference state. *Systems & Control Letters*, 56(7-8):474–483, 2007.

[76] David S Richeson. *Euler's gem: the polyhedron formula and the birth of topology*. Princeton University Press, 2019.

[77] Ben Roth. Rigid and flexible frameworks. *The American Mathematical Monthly*, 88(1):6–21, 1981.

[78] Iman Shames, Baris Fidan, and Brian DO Anderson. Close target reconnaissance using autonomous uav formations. In *2008 47th IEEE Conference on Decision and Control*, pages 1729–1734. IEEE, 2008.

[79] Iman Shames, Barış Fidan, and Brian DO Anderson. Minimization of the effect of noisy measurements on localization of multi-agent autonomous formations. *Automatica*, 45(4):1058–1065, 2009.

[80] Iman Shames et al. *Formation control and coordination of autonomous agents*. PhD thesis, The Australian National University, 2010.

[81] Khoshnam Shojaei. Neural network formation control of underactuated autonomous underwater vehicles with saturating actuators. *Neurocomputing*, 194:372–384, 2016.

[82] Zhiyong Sun. *Cooperative coordination and formation control for multi-agent systems*. Springer, 2018.

[83] Zhiyong Sun, Shaoshuai Mou, Brian DO Anderson, and A Stephen Morse. Formation movements in minimally rigid formation control with mismatched mutual distances. In *53rd IEEE Conference on Decision and Control*, pages 6161–6166. IEEE, 2014.

[84] Zhiyong Sun, Uwe Helmke, and Brian DO Anderson. Rigid formation shape control in general dimensions: an invariance principle and open problems. In *2015 54th IEEE Conference on Decision and Control (CDC)*, pages 6095–6100. IEEE, 2015.

[85] Zhiyong Sun, Brian DO Anderson, Mohammad Deghat, and Hyo-Sung Ahn. Rigid formation control of double-integrator systems. *International Journal of Control*, 90(7):1403–1419, 2017.

[86] Zhiyong Sun, Qingchen Liu, Na Huang, Changbin Yu, and Brian DO Anderson. Cooperative event-based rigid formation control. *IEEE Transactions on Systems, Man, and Cybernetics: Systems*, 2019.

[87] Tiong-Seng Tay and Walter Whiteley. Generating isostatic frameworks. *Structural Topology 1985 Núm 11*, 1985.

[88] Minh Hoang Trinh, Kwang-Kyo Oh, and Hyo-Sung Ahn. Angle-based control of directed acyclic formations with three-leaders. In *International conference on mechatronics and control*, pages 2268–2271, 2014.

[89] Minh Hoang Trinh, Shiyu Zhao, Zhiyong Sun, Daniel Zelazo, Brian DO Anderson, and Hyo-Sung Ahn. Bearing-based formation control of a group of agents with leader-first follower structure. *IEEE Transactions on Automatic Control*, 64(2):598–613, 2019.

[90] Yuri Ulybyshev. Long-term formation keeping of satellite constellation using linear-quadratic controller. *Journal of Guidance, Control, and Dynamics*, 21 (1):109–115, 1998.

[91] John Valasek, Kiran Gunnam, Jennifer Kimmett, Monish D Tandale, John L Junkins, and Declan Hughes. Vision-based sensor and navigation system for autonomous air refueling. *Journal of Guidance, Control, and Dynamics*, 28 (5):979–989, 2005.

[92] Walter Whiteley. Some matroids from discrete applied geometry. *Contemporary Mathematics*, 197:171–312, 1996.

[93] Walter Whiteley. Rigidity and scene analysis. 2004.

[94] Qingkai Yang. *Constructing tensegrity frameworks and related applications in multi-agent formation control*. PhD thesis, University of Groningen Groningen, 2019.

[95] Qingkai Yang, Ming Cao, Hao Fang, and Jie Chen. Constructing universally rigid tensegrity frameworks with application in multiagent formation control. *IEEE Transactions on Automatic Control*, 64(1):381–388, 2018.

[96] Qingkai Yang, Zhiyong Sun, Ming Cao, Hao Fang, and Jie Chen. Stress-matrix-based formation scaling control. *Automatica*, 101:120–127, 2019.

[97] Daniel Zelazo, Paolo Robuffo Giordano, and Antonio Franchi. Bearing-only formation control using an SE (2) rigidity theory. In *2015 54th IEEE Conference on Decision and Control*, pages 6121–6126. IEEE, 2015.

[98] S. Zhao and D. Zelazo. Translational and scaling formation maneuver control via a bearing-based approach. *IEEE Transactions on Control of Network Systems*, 4(3):429–438, 2017.

[99] S Zhao and Daniel Zelazo. Translational and scaling formation maneuver control via a bearing-based approach. *IEEE Transactions on Control of Network Systems*, 4(3):429–438, 2017.

[100] Shiyu Zhao. Affine formation maneuver control of multi-agent systems. *IEEE Transactions on Automatic Control*, 63(12):4140–4155, 2018.

[101] Shiyu Zhao and Daniel Zelazo. Bearing rigidity and almost global bearing-only formation stabilization. *IEEE Transactions on Automatic Control*, 61(5): 1255–1268, 2016.

[102] Shiyu Zhao and Daniel Zelazo. Bearing rigidity theory and its applications for control and estimation of network systems: Life beyond distance rigidity. *IEEE Control Systems Magazine*, 39(2):66–83, 2019.

[103] Shiyu Zhao and Daniel Zelazo. Bearing rigidity theory and its applications for control and estimation of network systems: Life beyond distance rigidity. *IEEE Control Systems Magazine*, 39(2):66–83, 2019.

[104] Shiyu Zhao, Feng Lin, Kemao Peng, Ben M Chen, and Tong H Lee. Distributed control of angle-constrained cyclic formations using bearing-only measurements. *Systems & Control Letters*, 63:12–24, 2014.

[105] Shiyu Zhao, Feng Lin, Kemao Peng, Ben M Chen, and Tong H Lee. Finite-time stabilisation of cyclic formations using bearing-only measurements. *International Journal of Control*, 87(4):715–727, 2014.

Summary

Rigidity theory has been studied for centuries, dating back to the works of Euler and Cauchy. Motivated by the challenging formation problem where a vehicle cannot measure positions or relative positions but some angles, this thesis proposes angle rigidity graph theory in 2D and 3D and uses them to develop angle-only formation control algorithms. We first develop the notion of 2D angle rigidity for a multi-point framework, named "angularity", consisting of a set of nodes embedded in a Euclidean space and a set of angle constraints among them. Different from bearings or angles defined in a global frame, the angles we use do not rely on the knowledge of a global frame and are with a positive sign in the counter-clockwise direction. Angle rigidity refers to the property specifying that under appropriate angle constraints, the angularity can only translate, rotate or scale as a whole when one or more of its nodes are perturbed locally. We demonstrate that this angle rigidity property, in sharp contrast to bearing rigidity or other reported rigidity related to angles of frameworks in the literature, is not a global property since an angle rigid angularity may allow flex ambiguity. We then construct necessary and sufficient conditions for infinitesimal angle rigidity by checking the rank of an angularity's rigidity matrix. We also develop a combinatorial necessary condition for infinitesimal minimal angle rigidity.

Using the developed 2D angle rigidity theory, we demonstrate how to stabilize a multi-agent planar formation using only angle measurements, which can be realized in each agent's local coordinate frame. The desired angle rigid formation is constructed by the Type-I vertex addition operation defined in 2D angle rigidity theory. By following this vertex addition operation, we first design the triangular formation control algorithm for the first three agents. Then, we propose the formation control algorithm for the remaining agents to add the remaining agents into the existing formation step by step. We have also proved the exponential convergence rate of angle errors and the collision-free property between specified agents.

Besides the stabilization of angle rigid formations, we also study how to maneuver a planar formation of mobile agents with collective motions using designed mismatched angles. To realize the maneuver of translation, rotation and scaling of the formation as a whole, we intentionally force the agents to maintain mismatched desired angles by introducing a pair of mismatch parameters for each angle constraint. To allow different information requirements in the design and implementation stages, we consider both measurement-dependent and measurement-independent mismatches. The control law for each newly added agent arises naturally from the angle constraints and makes full use of the angle mismatch parameters. We show that the control law can effectively stabilize the formations while simultaneously realizing maneuvering. Simulations are conducted to validate the theoretical results.

Then, we develop 3D angle rigidity theory. We show that the resulting angle rigidity is not a global property in comparison to the case of 3D bearing rigidity. We demonstrate that such angle rigid frameworks can be constructed through adding repeatedly new points to the original small angle rigid framework if one chooses angle constraints carefully. Based on the classic distance rigidity results on convex polyhedra, we investigate the angle rigidity of convex polyhedral angularities. The angle rigidity matrix of an angularity in 3D is also defined. By using the developed 3D angle rigidity theory, the formation stabilization algorithms are designed for a 3D team of vehicles to achieve angle rigid formations, in which only local angle measurements are needed.

Samenvatting

Stijfheidstheorie wordt al eeuwenlang bestudeerd en dateert uit de werken van Euler en Cauchy. Gemotiveerd door het uitdagende formatieprobleem waarbij enkel en alleen hoekmetingen gemeten wordt en niet de gebruikelijke posities of relatieve posities, stelt dit proefschrift de theorie van hoekstijfheidsgrafen voor in twee- en driedimensionale ruimten om algoritmen voor formatieregeling te ontwikkelen met alleen hoeken. We ontwikkelen eerst het idee van 2D hoekstijfheid voor een meerpuntsraamwerk, genaamd “angulariteit”; bestaande uit een reeks knooppunten ingebed in een Euclidische ruimte en een reeks hoekbeperkingen daartussen. Verschillend van normaal-vectoren of hoeken gedefinieerd in een globaal coördinatenstelsel, gebruiken we hoeken die niet afhankelijk zijn van de kennis van een globaal coördinatenstelsel, maar waarbij de positieve richting tegen de klok in is gedefineerd. Hoekstijfheid verwijst naar de eigenschap die specificeert dat onder de juiste hoekbeperkingen, de angulariteit alleen als geheel kan transleren, roteren, of op- en afschalen wanneer een of meerdere knooppunten lokaal worden verstoord. We demonstreren dat deze hoekstijfheidseigenschap gebaseerd is op normale vectoren of andere bestaande hoekstijfheidstheorieën en niet een globale eigenschap aangezien een starre hoekstijfheid buigambiguïteit mogelijk maakt. Vervolgens construeren we noodzakelijke en voldoende voorwaarden voor oneindig kleine hoekstijfheid door de rang van de stijfheidsmatrix van een angulariteit te controleren. We ontwikkelen ook een combinatorische noodzakelijke voorwaarde voor oneindig kleine minimale hoekstijfheid.

Met behulp van de ontwikkelde 2D-hoekstijfheidstheorie laten we zien hoe een multi-agent planaire formatie in het vlakke plaat kan worden gestabiliseerd met behulp van alleen hoekmetingen, die kunnen worden gerealiseerd in het lokale coördinatenstelsel van elke agent. De gewenste starre hoekformatie wordt geconstrueerd door de Type-I knooppunt-optelbewerking gedefinieerd in de 2D-hoekstijfheidstheorie. Door deze knooppunt-optelbewerking te volgen, ontwerpen we eerst het algoritme voor het regelen van de driehoekige formatie voor de

eerste drie agenten. Vervolgens stellen we het formatieregeling-algoritme voor de resterende agenten om deze stap-voor-stap aan de bestaande formatie toe te voegen. We hebben ook de exponentiële convergentiesnelheid van hoekfouten en botsingsvrije eigenschap tussen gespecificeerde agenten bewezen.

Naast de stabilisatie van starre hoekformaties, bestuderen we ook hoe een formatie van mobiele agenten met collectieve bewegingen kan worden gemanoeuvreerd met behulp van ontworpen niet-overeenkomende hoeken. Om de manoeuvre van translatie, rotatie en op- of afschaling van de formatie als geheel te realiseren, dwingen we de agenten opzettelijk om niet-overeenkomende gewenste hoeken te handhaven door een paar niet-overeenkomende parameters in te voeren voor elke hoekbeperking. Om verschillende informatie-eisen in de ontwerp-en implementatiefase mogelijk te maken, houden we rekening met zowel meetafhankelijke als meetonafhankelijke verschillen. De regelaar voor elk nieuw toegevoegde agent komt op natuurlijke wijze voort uit de hoekbeperkingen en maakt volledig gebruik van de parameters voor niet-overeenkomende hoeken. We laten zien dat de regelaar de formaties effectief kan stabiliseren en tegelijkertijd ook manoeuvreren. Er zijn simulaties uitgevoerd om de theoretische resultaten te valideren.

Vervolgens ontwikkelen we de 3D-hoekstijfheidstheorie. We laten zien dat de resulterende hoekstijfheid geen globale eigenschap is in vergelijking met stijfheid gebaseerd op normale vectoren. We demonstreren dat een dergelijke starre hoekformaties kunnen worden geconstrueerd door herhaaldelijk nieuwe knooppunten aan de bestaande starre hoekformatie toe te voegen met de bijbehorende hoekbeperkingen. Gebaseerd op de klassieke resultaten van afstandsstijfheid op convexe veelvlakken, onderzoeken we de hoekstijfheid van convexe veelvlakken. De stijfheidsmatrix van een angulariteit in 3D wordt ook gedefinieerd. Door gebruik te maken van de ontwikkelde 3D-hoekstijfheidstheorie, zijn de formatiestabilisatie-algoritmen ontworpen voor een 3D-team van voertuigen om starre hoekformaties te bereiken, waarbij alleen lokale hoekmetingen nodig zijn.